The small GTPase Arf1p from *Saccaromyces cerevisiae* goes new ways

- Novel roles in mRNA transport

and in the formation of specialized vesicles from the Golgi -

Die kleine GTPase Arf1p aus *Saccharomyces cerevisiae* geht neue Wege

- Neue Funktionen im mRNA Transport

und bei der Bildung von spezialisierten Golgi-Vesikeln -

D I S S E R T A T I O N

der Fakultät für Chemie und Pharmazie
der Eberhard-Karls-Universität Tübingen

zur Erlangung des Grades eines Doktors
der Naturwissenschaften

2004

vorgelegt von

Mark Trautwein

Tag der mündlichen Prüfung:	16. November 2004
Dekan:	Prof. Dr. Stefan Laufer
Erster Berichterstatter:	Prof. Dr. Hans-Georg Rammensee
Zweiter Berichterstatter:	Prof. Dr. Frank Madeo

Die vorliegende Arbeit wurde angefertigt unter der Anleitung von Dr. Anne Spang in der Arbeitsgruppe „Hefen und Würmer: Modellsysteme für intrazellulären Transport“ am Friedrich-Miescher-Laboratorium der Max-Planck-Gesellschaft, Tübingen.
Prof. Dr. Hans-Georg Rammensee vom Interfakultären Institut für Zellbiologie, Abteilung Immunologie, Universität Tübingen, übernahm die Vertretung der Arbeit vor der Fakultät.

"Previous generations have been absolutely convinced that their scientific theories were well-nigh perfect, only for it to turn out that they had missed the point entirely. Why should it be any different for our generation? Beware of scientific fundamentalists who try to tell you everything is pretty much worked out, and only a few routine details are left to do. It is just when the majority of scientists believe such things that the next revolution in our world-view creeps into being, its feeble birth-squeaks all but drowned by the earsplitting roar of orthodoxy." (Pratchett *et al.*, 2002)

Table of Contents

1 Introduction

1.1 Intracellular protein sorting: Vesicular traffic, secretion and endocytosis

A typical mammalian cell contains up to 10,000 different proteins at a given time point. A yeast cell in comparison contains 5,000 different kinds of proteins, which is only slightly less impressive. Most proteins reside in the cytosol. However, as many as up to half of the proteins produced in a typical cell are delivered to a particular cellular membrane, to the lumen of cellular organelles, or are secreted out of the cell. The intracellular protein sorting can be subdivided in two major pathways (Palade, 1975; Lodish *et al.*, 2003): the cytoplasmic and the secretory pathway.

In the cytoplasmic pathway, the protein translation is initiated and completed on cytosolic ribosomes. Those proteins that contain no protein targeting sequence are released into the cytosol and remain there. Proteins with an organelle-specific targeting sequence are first released into the cytosol but are subsequently imported into mitochondria, peroxisomes or the nucleus.

In contrast, all proteins carrying an endoplasmic reticulcum (ER)-signal sequence are initially targeted to the ER membrane and enter the secretory pathway. These proteins not only include soluble and membrane proteins of the ER, but also resident proteins of the Golgi apparatus, of the endosomal system, of the lysosomes/vacuoles, plasma membrane proteins and proteins which are secreted from the cell (for simplicity collectively referred to as secretory proteins). The transport of the proteins from the ER to their final destinations along the secretory pathway is accomplished by small vesicles that bud from the membrane of one organelle and fuse with the membrane of the next organelle in the pathway (Fig. 1). The secretory pathway is essentially conserved from yeast to man and a hallmark of eukaryotic cells. This process is of major significance for the cellular protein metabolism. For example, 70% of the proteins synthesized by hepatocytes are secreted into the blood. Like pancreatic cells and glandular cells, these cells are specialized for secretion. However, every cell uses the secretory pathway to some extent. Extracellular matrix proteins constitute about 5% of the protein made by most cultured cells. Moreover, MHC class I-peptides, although generated in the cytosol, are moving with their receptor along the secretory pathway to reach the cell surface. The unicellular eukaryote *Saccharomyces cerevisiae* has been used now for more than two decades to elucidate

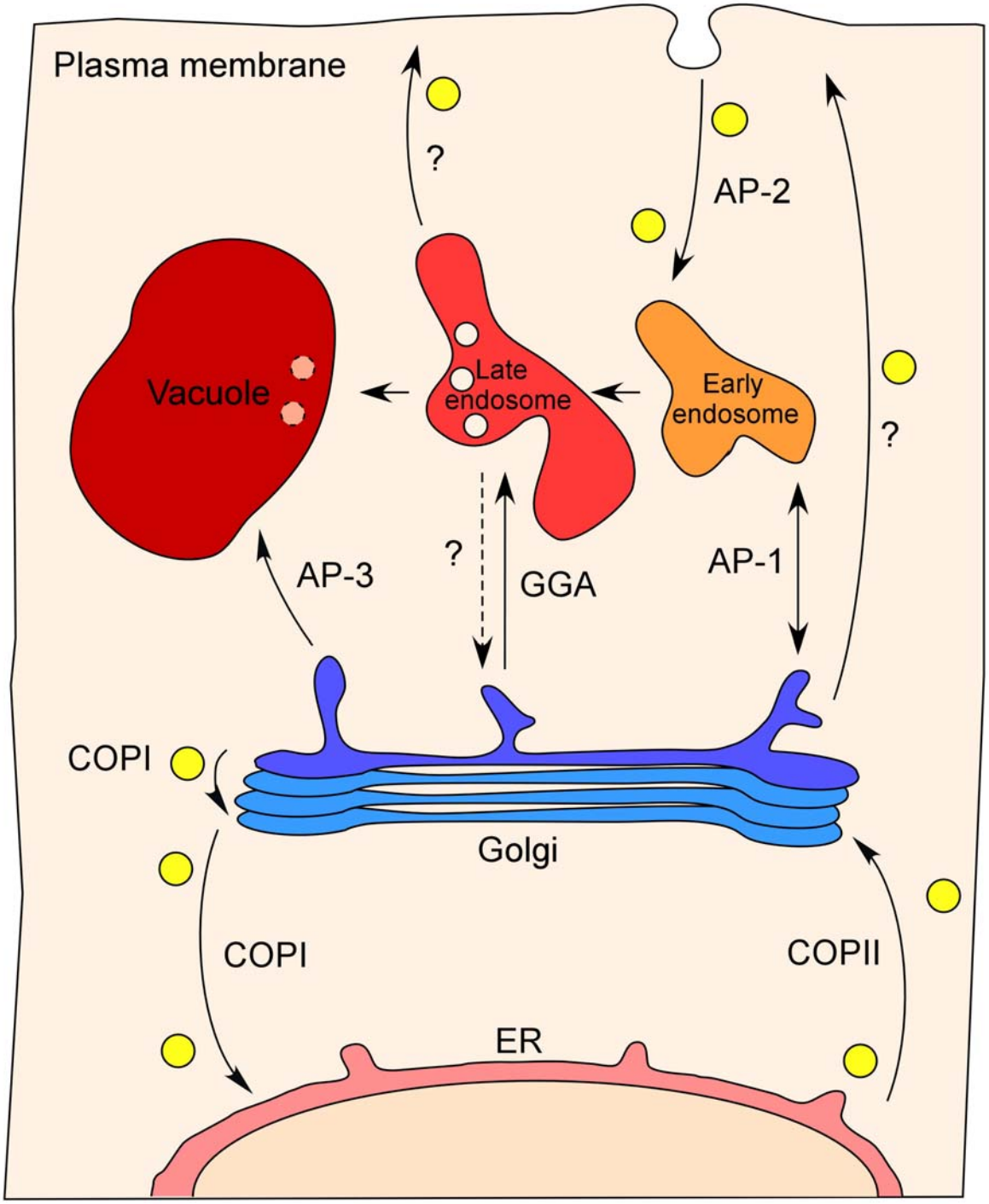

Figure 1: Overview of the most important vesicular traffic routes in a cell. The protein coat of the vesicular trafficking steps is indicated. COPII-coated vesicles mediate anterograde ER-Golgi transport, whereas COPI-coated vesicles mediate retrograde Golgi-ER as well as intra-Golgi transport. Clathrin/adaptor protein-coated vesicles travel from the trans-Golgi network to early and late endosomes as well as the vacuole/lysosome. Endocytosis is mediated by clathrin/AP-2-coated vesicles. The nature of the vesicle coat of secreted vesicles derived from the late endosome and the trans-Golgi network is not known. It has been proposed that the retromer complex is a vesicle coat involved in the retrieval pathway from late endosome to trans-Golgi network (dashed arrow; Pfeffer, 2001). Internal vesicles are depicted in the late endosome and represent multi-vesicular bodies. These internal vesicles are destined to the vacuole/lysosome for degradation.

protein and membrane traffic. *Saccharomyces cerevisiae* was the organism of choice because of its excellent genetic and biochemical amenability. It is particularly evident from landmark studies using *Saccharomyces cerevisiae* that secretion, which is protein *and* membrane flux, is an essential process to accomplish the vast expansion of the cell membrane surface that is needed for cell growth (Novick *et al.*, 1980). Many bacterial toxins and viruses (e. g. cholera toxin, influenza virus A, simian virus 40) use the secretory pathway in the opposite direction to travel from the plasma membrane to the cytosol (Sandvig and van Deurs, 2002; Smith and Helenius, 2004).

In most eukaryotes, secretory proteins enter the ER by co-translational translocation through the Sec61 translocon complex. In yeast, however, some secretory proteins enter the ER lumen post-translationally. Glycosylation as well as formation of disulfide bonds, protein folding and assembly, and proteolytic cleavages occur in the ER before proteins leave the ER again. Secretory proteins are transported by anterograde COPII-coated vesicles to the Golgi apparatus where further processing of the proteins takes place. To balance this forward movement of cargo, organelle homeostasis requires the retrieval of transport machinery components and escaped ER-resident proteins by the action of vesicular transport carriers. Retrograde COPI-coated vesicles retrieve proteins and lipids from the Golgi back the ER. All of these steps are tightly regulated and balanced so that a large amount of cargo can flow through the secretory pathway without compromising the integrity and steady-state composition of the constituent organelles.

The secretory proteins eventually reach the trans-Golgi network by cisternal progression of the Golgi stacks (Pelham, 2001). The trans-Golgi network represents a major branch point of the secretory pathway and serves as sorting station. Thus, a protein can be loaded into different kinds of vesicles and thereby reach the plasma membrane, the endodomal system or the lysosome/vacuole. The endosomes also function in the endocytic pathway (hence the name) in which vesicles bud from the plasma membrane bringing membrane proteins and their bound ligands into the cell. Some proteins are transported to the lysosome/vacuole while others are recycled back to the cell surface. The membrane fluxes along these pathways are very large and rapid. A fibroblast kept in resting conditions in a tissue culture plate internalizes an amount of membrane equivalent to the whole surface area of the cell within one hour (Kirchhausen, 2000). Inside the cell, it often takes only seconds for a carrier vesicle to move from a donor membrane to an acceptor organelle. Despite these rapid and large fluxes, only a subset of the proteins and lipids in the donor membrane are taken up into the transport vesicle, effectively preventing the homogenization of the

membrane components and permitting membranous organelles to maintain distinct identities throughout the life of the cell.

1.2 Molecular mechanism of vesicular traffic

A common element of the secretory and endocytic pathway is the existence of many different small membrane-bounded and protein-coated vesicles that transport proteins and lipids from one organelle to another. These vesicles bud from the membrane of a donor organelle and eventually fuse with the membrane of an acceptor organelle. Despite the fact that most steps in the secretory and endocytic pathways employ different types of vesicles, the basic principles of vesicle formation and fusion are essentially conserved. Considerable progress has been made in understanding the molecular basis for membrane traffic (reviewed by Kirchhausen, 2000; Bonifacino and Glick, 2004). The best-studied vesicles are those that are clearly identifiable by their protein coats, namely COPII-, COPI-, and clathrin-coated vesicles. During the formation of a vesicle, a limited set of coat proteins carries out a programmed set of sequential interactions that lead to budding from the donor membrane, uncoating, fusion with the target membrane and recycling of the coat components (Fig. 2).

Budding is initiated by recruitment of a small GTPase of the Sar1/Arf family to a patch of donor membrane. Coat components from the cytosol are then able to bind to the membrane. Polymerization of the coat protein on the membrane leads to a curved lattice that drives the formation of a vesicle bud by adhering to the cytosolic face of the membrane. At the same time, coat proteins participate directly and indirectly to recruit soluble and membrane cargo proteins to the forming vesicle. Vesicle budding and cargo selection at different stages of the exocytic and endocytic pathways are meditated by different coats and different sorting signals. The coat components not only recruit cargo but also deform the membrane to form a bud. When the bud has reached a charateristic size (detemined by the coat), the vesicle is released by scission of the neck connecting the deeply invaginated membrane to the donor surface. Finally, during uncoating, the coat components are released so that membrane fusion can occur between the naked vesicle and the target organelle. It is believed that Rab GTPases control the docking of the vesicles on target membranes (reviewed by Zerial and McBride, 2001). Vesicle fusion is mediated by a complex process involving the pairing of cognate v- and t-SNARE proteins (reviewed by Jahn *et al.*, 2003). In the following sections, the formation of different vesicles is discussed in more detail.

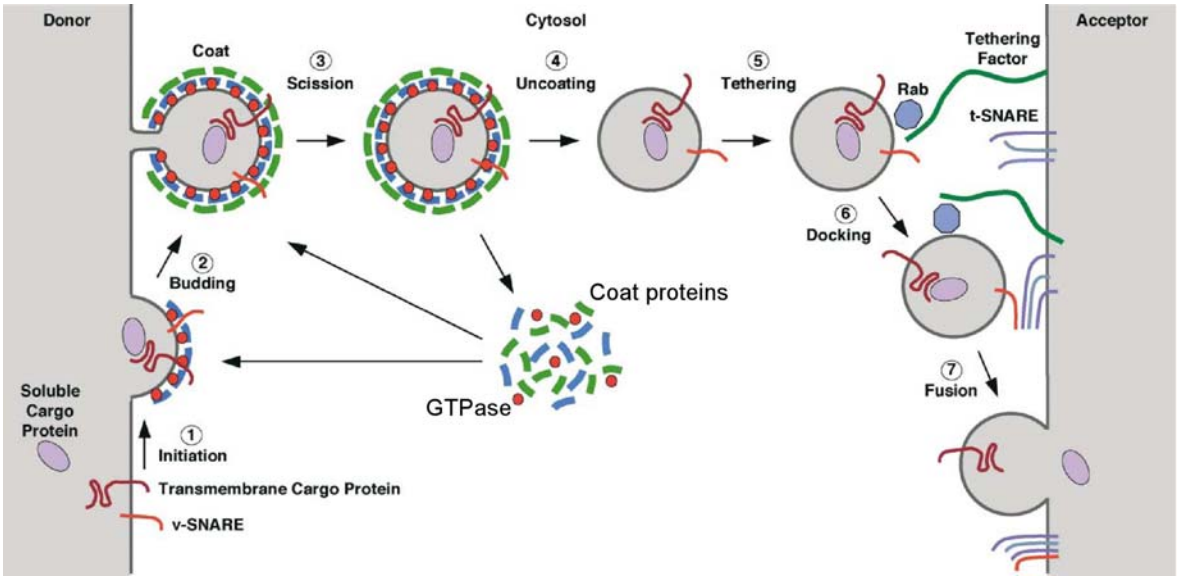

Figure 2: The common mechanism of vesicle budding and fusion (adapted from Bonifacino and Glick, 2004). Small GTPases of the Arf/Sar1 family become associated with a donor membrane. In turn, they are able to recruit soluble coat components from the cytosol. Polymerization of coat proteins leads to membrane deformation and cargo incorporation. After scission of the vesicle from the donor membrane and shedding of the protein coat, the vesicle is ready to dock and fuse with an acceptor membrane (mediated by Rab GTPases and SNARE proteins).

1.3 Early stages of the secretory pathway

1.3.1 COPII-coated vesicles

COPII components and COPII-coated vesicles were originally discovered in the yeast *Saccharomyces cerevisiae* using genetic approaches coupled with cell-free assays (reviewed by Springer *et al.*, 1999; Barlowe, 2000). These vesicles, which also have mammalian counterparts, transport newly synthesized proteins destined for secretion from the ER to the Golgi apparatus (Fig. 1). Although clathrin-coated vesicles have been discovered first, the molecular understanding of vesicle formation is most advanced for COPII-coated vesicles. COPII vesicles (50 – 90 nm in diameter) can be reconstituted *in vitro* using a minimal system consisting of chemically defined liposomes, GMP-PNP (a non-hydrolyzable GTP analog) and the purified components Sar1p, Sec23p, Sec24p, Sec13p and Sec31p (Matsuoka *et al.*, 1998). Furthermore, it has been shown that some COPII components have the ability to self-assemble into spherical particles in solution (Antonny *et al.*, 2003). For some COPII proteins, structural details are known from crystal structures and/or electron microscopic studies (Lederkremer *et al.*, 2001; Bi *et al.*, 2002).

Formation of COPII-coated vesicles is triggered when Sec12p, a guanine nucleotide exchange factor (GEF), catalyzes the exchange of bound GDP to GTP on the small GTPase Sar1p (Fig. 3). This exchange induces binding of Sar1p to the ER membrane followed by binding of the Sec23p/Sec24p complex forming a membrane-proximal layer (Barlowe *et al.*, 1993; Barlowe and Schekman, 1993). ER membranes with Sec23p/Sec24p and Sar1p-GTP can then recruit the Sec13p/Sec31p complex to complete the coat structure (Barlowe *et al.*, 1994). The large protein Sec16p which is bound to the cytosolic side of the ER membrane interacts with Sec13p/Sec31p and Sec23p/Sec24p and organizes the other coat proteins, increasing the efficiency of coat polymerization (Espenshade *et al.*, 1995; Supek *et al.*, 2002). Completing the cycle, Sec23p acts as a GTPase activating protein (GAP) for Sar1p (Yoshihisa *et al.*, 1993). It is thought, that after GTP hydrolysis, Sar1p-GDP is released, leading to uncoating of the vesicle before fusion. In this model, the kinetics of GTP hydrolysis would have to be slower than the kinetics of vesicle budding. Alternatively, the polymeric nature of the coat could provide kinetic stability even in the absence of Sar1p-GTP.

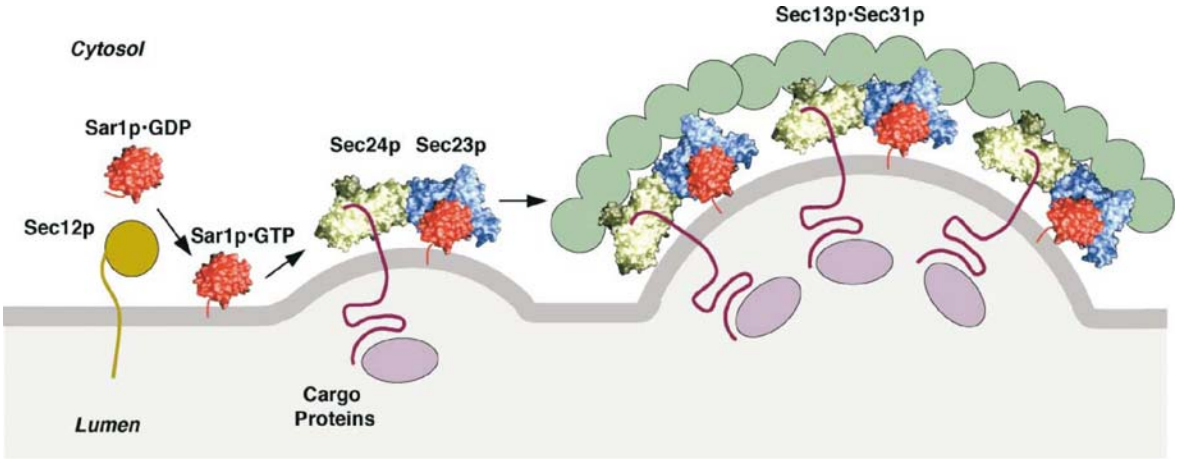

Figure 3: The formation of COPII-coated vesicles (from Bonifacino and Glick, 2004). Sar1p is activated by the Sec12p and becomes membrane-associated at the ER. Sar1p-GTP is able to recruit the Sec23p/Sec24p complex from the cytosol. This trimeric complex binds the Sec13p/Sec31p complex. Polymerization of the coat induces membrane deformation. Cargo is incorporated into the vesicle by direct and indirect binding to the coat components.

Most transmembrane cargo proteins bind directly to the COPII coat, whereas other transmembrane cargo proteins and most soluble cargo proteins bind indirectly via transmembrane export cargo receptors. The Sec23p/Sec24p complex is the component responsible for cargo recognition but the sorting signals recognized are quite complex (Springer and Schekman, 1998; Barlowe, 2003). Among the sorting signals recognized are

di-acidic, di-basic and short hydrophobic sequences. Members of the p24 transmembrane family of export cargo receptors bind to Sec23p through a di-phenylalanine motif (Dominguez *et al.*, 1998). Export cargo receptors leave the ER together with their ligands, unload their cargo and recycle back to the ER. The p24 family members Emp24p and Erv25p have been shown to recruit the GPI-anchored proteins Gas1p into COPII-coated vesicles (Muniz *et al.*, 2000). There are two paralogs of Sec24p in *Saccharomyces cerevisiae* (Lst1p and Iss1p). This diversification of COPII subunits probably endows the coat with the ability to sort different cargo proteins and to be differentially regulated (Roberg *et al.*, 1999; Shimoni *et al.*, 2000). In addition to recruiting the Sec23p/Sec24p complex, the GTP-bound form of Sar1p activates Sec23p/sec24p complex to bind SNARE proteins involved in the specificity of targeting and in the fusion of vesicles with acceptor membranes (Springer and Schekman, 1998). Sec24p has three different binding sites for ER-Golgi SNARE proteins: the A-site, the B-site and the Arg342-site, each recognizing different signals on different proteins (Miller *et al.*, 2003; Mossessova *et al.*, 2003). Apparently, Sec24p cannot bind assembled SNARE complexes but instead selects for the uncomplexed, fusion-competent forms of the SNAREs (Mossessova *et al.*, 2003). Thus, vesicle fusion is mechanistically linked with vesicle budding.

1.3.2 COPI-coated vesicles

Proteins can be recycled to the ER from the cis-Golgi via a retrograde route. Such proteins include ER resident proteins that have escaped the ER retention and functional components of anterograde COPII vesicles like ER-Golgi SNARE proteins that return to participate in another round of COPII vesicle formation. Retrograde vesicles are coated with the COPI coat, which consists of the small GTPase Arf1 and the heptameric coatomer complex (reviewed by Wieland and Harter, 1999; Spang, 2002). Arf1 is closely related to Sar1 but unlike Sar1, which functions exclusively in COPII vesicle formation, Arf1 proteins have many effectors, including COPI and other coats. However, currently maybe best understood is the role of Arf1 in the formation of COPI vesicles, which mediate retrograde Golgi-ER as well as intra-Golgi transport (Fig. 1). Like for COPII vesicles, COPI vesicle formation can be reconstituted *in vitro*. It has been shown that Arf1p, coatomer and GTPγS are sufficient to bud coated vesicles (40 – 70 nm in diameter) from chemically defined liposomes (Spang *et al.*, 1998).

Similar to all members of the Ras protein superfamily, Arf1 undergoes cycles of activation and inactivation mediated by GEFs and GAPs. Upon Arf1-GEF mediated nucleotide

exchange from GDP to GTP (Chardin *et al.*, 1996; Morinaga *et al.*, 1996; Peyroche *et al.*, 1996), Arf1 is recruited to and tightly associated with Golgi-membranes (Fig. 4). In turn, activated Arf1 recruits the large heptameric coatomer complex from the cytosol to the membrane via the β- and γ-subunit (Zhao *et al.*, 1999). Unlike in COPII vesicle formation, the membrane-proximal (βγδζ) and membrane-distal (αβ'ε) subcomplexes bind simultaneously (Hara-Kuge *et al.*, 1994). Binding of the coatomer complex to Arf1 and subsequent polymerization induces deformation of the membrane and finally vesicle budding.

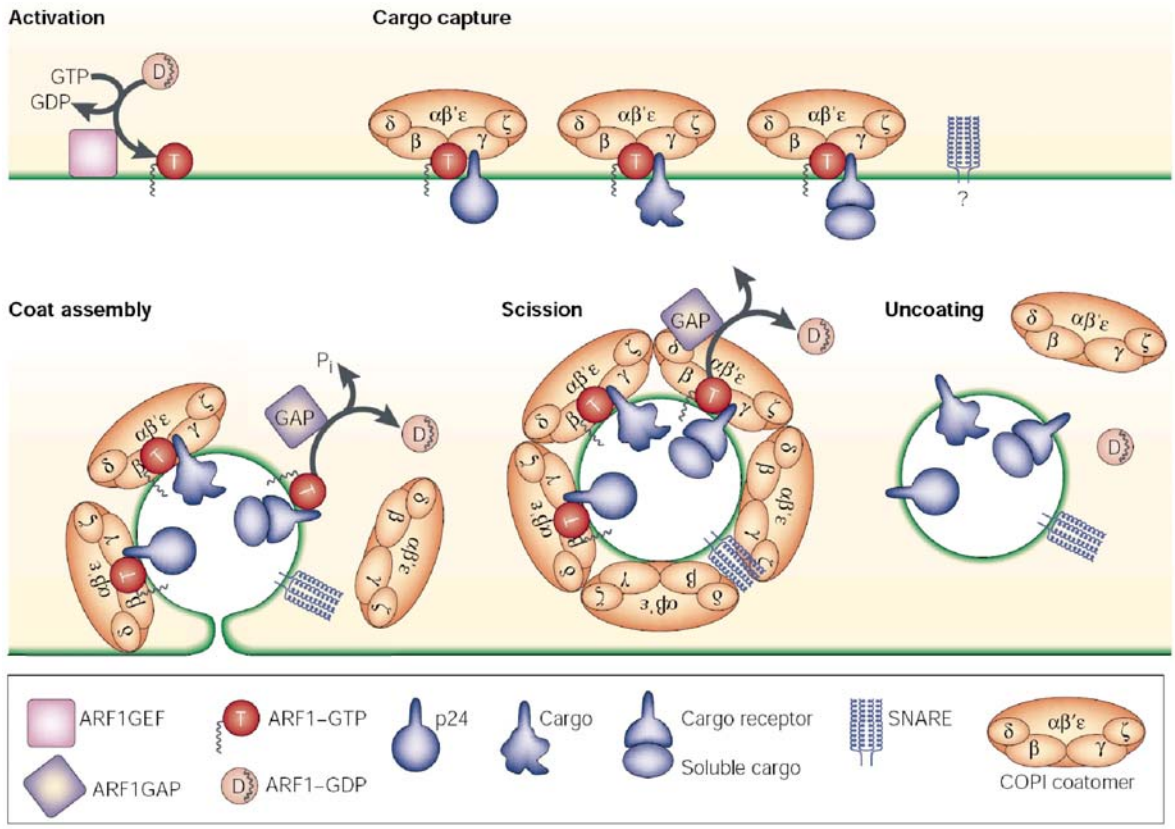

Figure 4: The formation of COPI-coated vesicles (from Kirchhausen, 2000). Membrane-association of activated Arf1 promotes recruitment of the coatomer complex from the cytosol. Polymerization of the coat induces membrane deformation and vesicle budding. Cargo proteins are incorporated into the vesicle by direct and indirect interactions with COPI components. After uncoating, the vesicle is ready to dock and fuse with a target membrane.

In a simple model, prior to fusion of vesicles with a target membrane, the coat dissociates in response to the Arf1-GAP stimulated GTP hydrolysis on Arf1 (Tanigawa *et al.*, 1993). In this case Arf1 would act like a timer for vesicle formation similar to Sar1. Structural studies extended this idea with respect to cargo recruitment (Goldberg, 1999, 2000). The rate of GTP hydrolysis depends on association of Arf1 with both Arf1-GAP and coatomer.

It was shown that the GTP hydrolsis was inhibited by a peptide derived from a p24 cargo receptor protein. This lead to the speculation that in the absence of cargo, the rate of GTP hydrolysis is too rapid to allow for vesicle formation because coatomer dissociates prematurely. In contrast, when bound to cargo, p24 will inhibit the GAP activity. The slower rate of GTP hydrolysis on Arf1 would provide time for a vesicle to be formed. In this way, vesicle formation would be coupled to cargo incorporation.

Problems associated with the kinetic model and the structural data (obtained from a truncated version of human ARF1-GTP) provoked re-examination of the role of GTP hydrolysis (Szafer *et al.*, 2000). Apparently, the GTPase cycle of controlled binding and hydrolysis of GTP is critical for Arf1 function. In contrast to the proposal that sorting is accomplished by cargo-dendent inhibition of Arf1-mediated GTP hydrolysis, some studies suggested that GTP is hydrolyzed in order to concentrate cargo before the vesicle is completely formed (Nickel *et al.*, 1998; Lanoix *et al.*, 1999; Malsam *et al.*, 1999). A kinetic proof-reading mechanism for protein sorting has been proposed (Weiss and Nilsson, 2003). Support for this idea comes from two studies showing that Arf1-GAP is required for vesicle formation and is becoming an intrinsic part of the vesicle (Yang *et al.*, 2002; Lewis *et al.*, 2004), although also a conflicting study exists (Reinhard *et al.*, 2003). Furthermore, it has been shown that Arf1-GAP activity is controlled by membrane curvature and therefore by the size of the vesicle (Bigay *et al.*, 2003).

Although the precise mechanism of cargo sorting remains a matter of debate, the cargo sorting process happens concomitant with vesicle budding. The γ-subunit of coatomer has been shown to interact with membrane cargo proteins carrying the ER-retrieval motif K(X)KXX in their cytoplasmic domains (Cosson and Letourneur, 1994; Harter *et al.*, 1996). The KDEL-receptor binds to soluble cargo bearing the ER-retrieval sequence KDEL in the lumenal part of the forming vesicles at the Golgi and binds to ARF-GAP (Aoe *et al.*, 1999). Other examples for proteins that are sorted into the COPI vesicles are v-SNAREs, which are part of the targeting and fusion machinery. Their incorporation is ensured by interaction with Arf1p-GAP (Rein *et al.*, 2002). The p24-family of cargo receptor proteins bind to both COPII and COPI through di-phenylalanine and di-basic motifs and cycle between ER and Golgi (Schimmoller *et al.*, 1995; Stamnes *et al.*, 1995; Sohn *et al.*, 1996; reviewed by Kaiser, 2000). Whether they are essential for the vesicle formation itself remains to be shown (Bremser *et al.*, 1999): At least in yeast, a knockout of the entire p24 family (eight members) does not have a severe consequence on the viability of the cell (Springer *et al.*, 2000). Most importantly, p24 protein family members

form hetero- and homo-oligomeric complexes with each other (Dominguez *et al.*, 1998; Fullekrug *et al.*, 1999; Marzioch *et al.*, 1999; Jenne *et al.*, 2002). It has been suggested that the state of oligomerization regulates the interaction of the supposed cargo receptors with coat proteins and/or cargo proteins (Gommel *et al.*, 1999). Multimerization of cargo receptors for transport seems to be a common theme: the COPI-binding putative cargo receptors Mst27p and Mst28p form at least dimeric complexes (Sandmann *et al.*, 2003).

1.4 Later stages of the secretory pathway, endocytosis and sorting of internalized proteins

1.4.1 Clathrin-coated and related vesicles

Clathrin-coated vesicles (50 – 150 nm in diameter) are the most prominent carrier vesicles and were the first to be discovered (Roth and Porter, 1964; Pearse, 1975). The low-density lipoprotein receptor and many other plasma membrane proteins and their ligands are internalized by a clathrin-dependent pathway leading to endosomes (Fig. 1). In addition, clathrin-coated vesicles also bud from the trans-Golgi network and fuse with endosomes or lysosomes (Kirchhausen, 2000).

Clathrin coats are considerably more complex than COPII and COPI. Arf1-GTP and/or specific phosphoinositides (e. g. phosphatidylinositol 4,5-bisphosphate and phosphatidyl-inositol 4-phosphate) recruit a variety of clathrin "adaptors" from the cytosol to membranes (Fig. 5). Examples of clathrin adaptors are the heterotetrameric AP-1, AP-2, AP-3, AP-4 complexes and the monomeric GGA proteins. Adaptor proteins form a heterogenous membrane-proximal layer onto which clathrin is subsequently deposited as membrane-distal layer. Clathrin and clathrin-adaptor complexes can polymerize into spherical, cage-like structures *in vitro* indicating that these proteins have an intrinsic ability to deform membranes (Kirchhausen and Harrison, 1981; Ungewickell and Branton, 1981). However, clathrin-coated vesicle formation requires the additional action of regulatory and accessory proteins. Clathrin vesicle scission depends on dynamins (reviewed by Sever, 2002) and shedding of the coat requires the cytosolic chaperones Hsc70 and auxilin (Rothman and Schmid, 1986; Ungewickell *et al.*, 1995). The reason for the need of a whole accessory machinery might be the involvement of clathrin in multiple post-Golgi sorting events, each requiring a specific set of adaptors and regulators.

Although it was shown that ARF1-GTP, tyrosine-based signals and phosphatidyl-inositol 4,5-bisphosphate constitute a minimal machinery to recruit the AP-1 complex to the membrane (Crottet *et al.*, 2002), the complex process of clathrin-coated vesicle formation

prevented reconstitution *in vitro* from purified components. An exception are AP-3/clathrin-coated vesicles which were reconstituted from liposomes *in vitro* using a minimal machinery consisting of purified AP-3 complex, clathrin, ARF1 and GTPγS (Drake *et al.*, 2000).

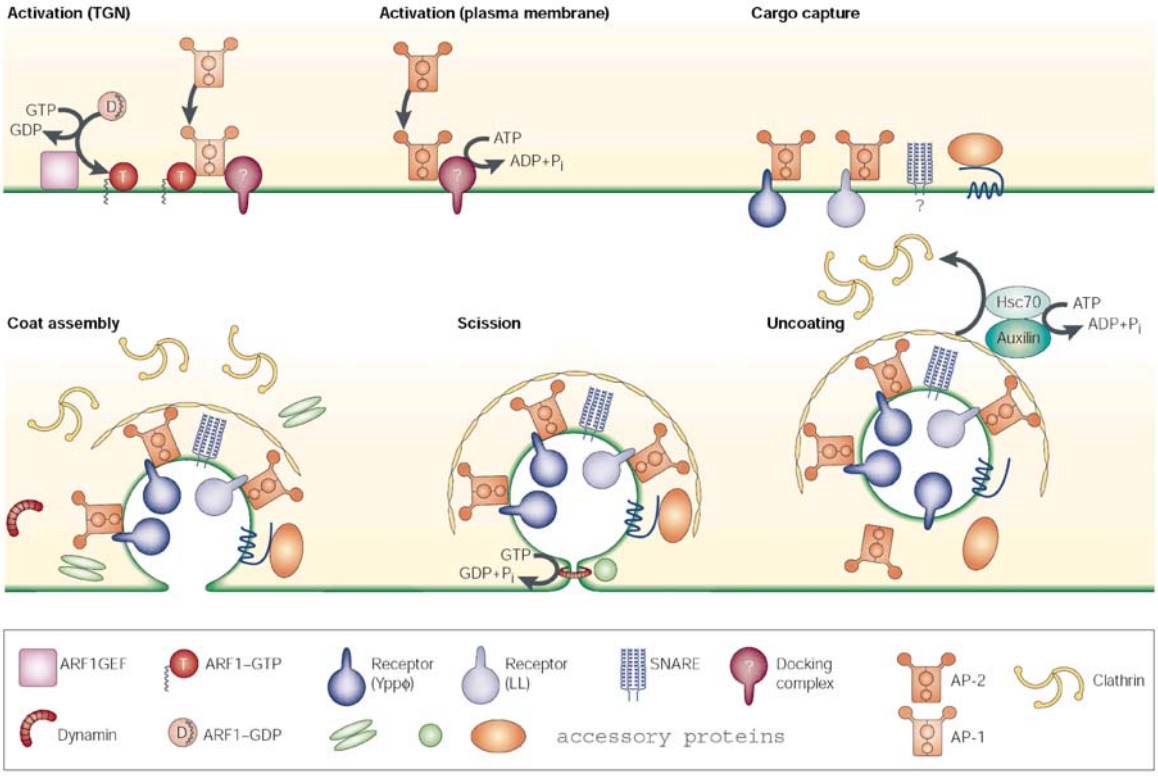

Figure 5: The key steps in formation of clathrin-coated vesicles (adapted from Kirchhausen, 2000). Arf1-GTP and/or specific phosphoinositides recruit a variety of clathrin "adaptors" complexes (AP-1 or AP-2) from the cytosol to membranes. Clathrin and clathrin-adaptor complexes can polymerize into spherical, cage-like structures. Cargo recruitment is accomplished by direct and indirect binding to clathrin adaptor complexes. Vesicle scission depends on dynamins and shedding of the coat requires the cytosolic chaperones Hsc70 and auxilin.

AP-1 complexes and GGA proteins participate in clathrin-recruitment to the TGN and endosomes (reviewed by Boman, 2001; Boehm and Bonifacino, 2002; Bonifacino, 2004) (Fig. 1). In mammalian cells, ARF1 is required for both of these trafficking events and it physically interacts with AP-1 and the GGA proteins. In yeast, however, this view has been challenged. Although Arf1p can interact with the GGA protein, it seems not to be essential for GGA mediated trafficking steps (Boman *et al.*, 2002). AP-2 complexes are involved in receptor-mediated endocytosis at the plasma membrane (Fig. 1). Yeast cells use clathrin for endocytosis but attempts to implicate AP-2 in yeast endocytosis failed so far (Payne *et al.*, 1988; Tan *et al.*, 1993; Rad *et al.*, 1995; reviewed by Baggett and

Wendland, 2001). In addition, clathrin-independent endocytosis exists in yeast. Although ARF1 has been reported to be involved in the recruitment of AP-2 to the endosomal membrane (West *et al.*, 1997), this view has recently been challenged (Jones *et al.*, 1999a) and the effects reported previously were probably indirect. AP-3 complexes mediate traffic from the TGN directly to the lysosome/vacuole bypassing the endodomal system (reviewed by Robinson and Bonifacino, 2001) (Fig. 1). Whether this step is dependent on clathrin in yeast remains unclear (Cowles *et al.*, 1997). AP-4 complexes, which are absent in organisms such as *Saccharomyces cerevisiae*, *Caenorhabditis elegans*, and *Drosophila melanogaster* have not been extensively studied so far (Dell'Angelica *et al.*, 1999; Hirst *et al.*, 1999). Indirect evidence in mammalian cells suggests that they might be involved in a special trafficking pathway in the endosomal/lysosomal system (Aguilar *et al.*, 2001).

The adaptor protein complexes bind to transmembrane cargo proteins by recognizing cytosolic sorting signals that contain either critical tyrosine, di-leucine residues or conjugated ubiquitin (Bonifacino and Traub, 2003). The tyrosine-based signal present in the LDL-receptor was indeed the first cytosolic sorting signal to be identified (Davis *et al.*, 1986). Acidic clusters present in the transmembrane mannose-6-phosphate receptor ensure its incorporation in a forming vesicle. The mannose-6-phophate receptor itself binds soluble cargo proteins modified by mannose-6-phosphate which is a sorting signal for proteins destined to the lysosome. Thus, clathrin/adaptor protein coats, COPII-, and COPI-coats serve the same basic functions: cytosolic signal recognition and membrane deformation.

1.4.2 Endocytosis and endosomal sorting

All eukaryotic cells continually engage in endocytosis. The most well-understood endocytic process - receptor-mediated endocytosis – involves the internalization of receptors and their ligands by clathrin-coated pits. Many of the ligands are subsequently degraded in late endosomes or lysosomes, whereas many of the receptors are re-used up to several hundred times. Endosomes have a crucial role in coordinating vesicular transport between the TGN, the plasma membrane and the lysosomal/vacuolar organelles (Fig. 1). Collectively, endosomes comprise a system of heterogeneous compartments that have generally been characterized as ‘early’ or ‘late’ depending on the kinetics with which the compartments are loaded with endocytosed material. Furthermore, early endosomes and late endosomes can be distinguished on the basis of their morphological appearance (reviewed by Gruenberg, 2001; Pelham, 2002). For example, a subset of late endosomes

typically has a multivesicular appearance and is referred to as multi-vesicular body (MVB). Studies in multicellular organisms have revealed crucial roles for MVBs in seemingly distinct processes like growth-factor-receptor downregulation, antigen-presentation and retroviral budding (reviewed by Katzmann *et al.*, 2002). However, *Saccharomyces cerevisiae* has been most crucial in the discovery of molecular players in the MVB-sorting pathway. It has been appreciated that endocytosed receptor proteins targeted to the vacuole for degradation were primarily associated with membrane fragments and small vesicles *within* the interior of the vacuole rather than the vacuole surface membrane. These observations suggested that endocytosed membrane proteins can be incorporated into specialized vesicles that form at the endosomal membrane. Although these vesicles are similar in size and appearance to transport vesicles, they differ in their topology. Transport vesicles bud outward from the surface of a donor membrane (into the cytosol) whereas vesicles within the endosome bud inward from the surface into the lumen (away from the cytosol). Eventually, the surface membrane of a MVB fuses with the membrane of the vacuole/lysosome and delivers its internal vesicles and the membrane proteins they contain into the interior of the vacuole/lysosome for degradation. Thus, the sorting of proteins in the endosomal membranes determines which ones will remain on the vacuole/lysosome surface (protected from degradation) and which ones will be incorporated into internal vesicles (and ultimately be degraded).

A particularly interesting example for the role of MVBs is the MHC class II-peptide presentation during immune response (Fig. 6). Immature dendritic cells package MHC class II molecules into lumenal vesicles of MVB-like compartments that are known as MHC class II compartments (MIICs). When the cell receives a maturation stimulus, the lumenal vesicles fuse with the limiting MIIC membrane, the MCH class II molecules are loaded with antigenic peptide and the MHC class II-peptide complexes are transported via secretory vesicles to the plasma membrane for presentation to naïve T cells (Kleijmeer *et al.*, 2001). Surprisingly, the stimulation of dendritic cells can also cause the limiting membranes of MIICs to dock and fuse with the plasma membrane, which releases the lumenal vesicles of MIICs from the cell. These secreted vesicles, now termed exosomes, contain MHC molecules and co-stimulatory factors for T cells, but their precise physiological targets have yet to be elucidated (Zitvogel *et al.*, 1998).

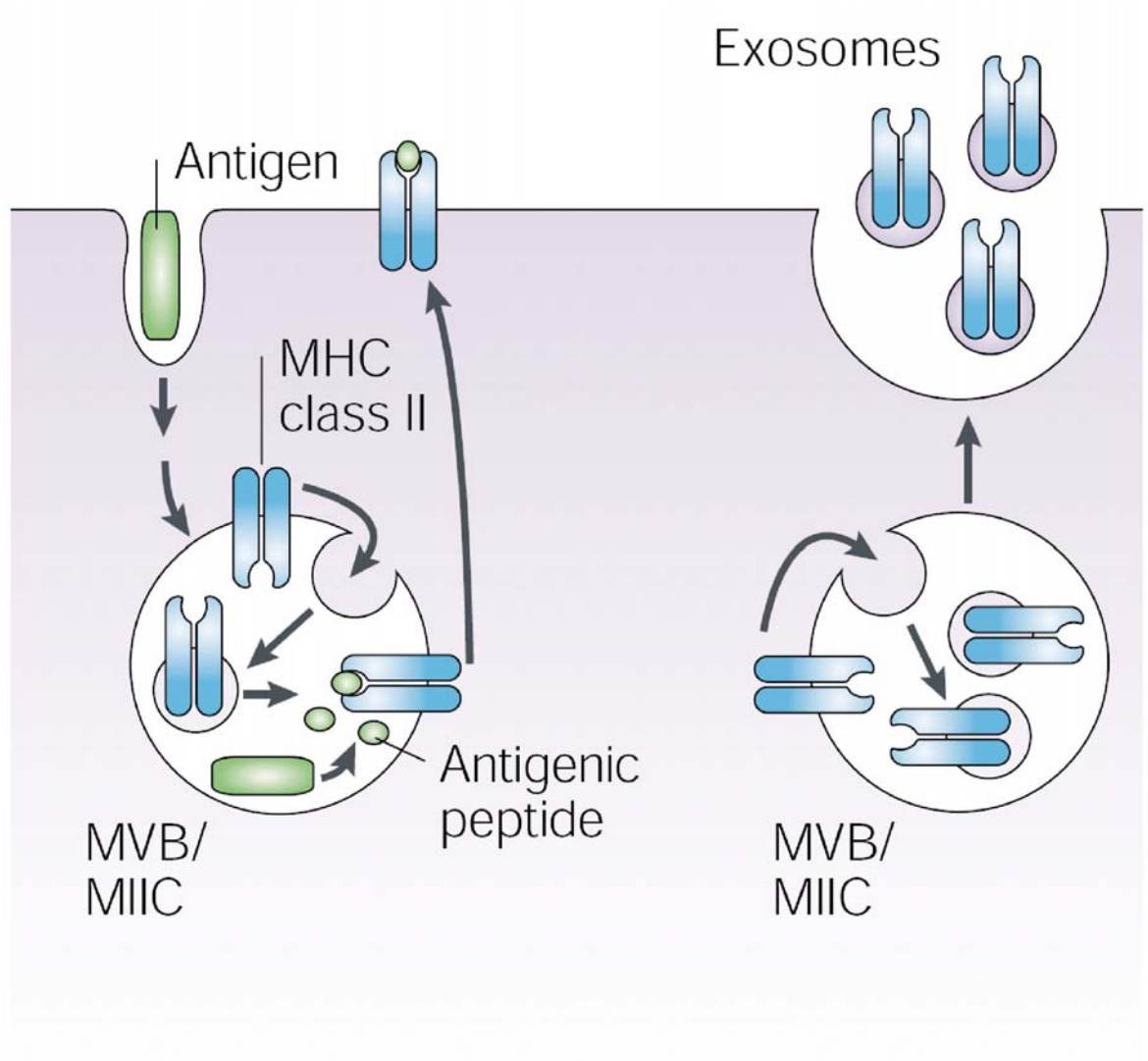

Figure 6: The role of multi-vesicular bodies in MHC class II-mediated immune response (adapted from Katzmann *et al.*, 2002). MHC class II molecules in MIICs are loaded with antigenic peptides generated in the endosomal system. After fusion of internal vesicles with the MIIC membrane, traffic of MHC class II-peptide comlexes in secretory vesicles leads to peptide presentation at the cell surface. Alternatively, the antigenic stimulation of dendritic cells can cause the limiting membranes of MIICs to dock and fuse with the plasma membrane, which releases the lumenal vesicles of MIICs from the cell. These external vesicles are now termed exosomes.

1.5 The Arf GTPases: Structure and function

ADP-ribosylation factors (Arfs) are well-conserved, multi-functional small GTPases found in all eukaryotes. They constitute a major branch of the Ras superfamily of small GTPases. The prototypic member, Arf1, was first identified as a co-factor for cholera toxin-catalyzed ADP-ribosylation of the heterotrimeric G protein $G_{s\alpha}$ (Kahn and Gilman, 1984, 1986). Human and yeast Arf1 proteins are 74% identical (Sewell and Kahn, 1988). This high degree of conservation has allowed studies on the function of Arf1 in both yeast and higher eukaryotes. Studies in yeast, mammalian cells and *in vitro* systems have implicated Arf1 proteins as crucial regulators of membrane traffic, organelle maintenance and actin cytoskeleton. (reviewed by Donaldson and Jackson, 2000; Randazzo *et al.*, 2000; Spang, 2002; Nie *et al.*, 2003).

In this study, the following nomenclature of Arf proteins is used: ARF1 refers to mammalian ARF1, whereas Arf1p refers to yeast Arf1p. Arf1 refers to Arf1 proteins in general (in both yeast and higher eukaryotes).

Mammalian ARFs are divided into three classes based on primary structure: class I (ARF1, ARF2, and ARF3), class II (ARF4, ARF5) and class III (ARF6). Class I ARFs are involved in trafficking in the Golgi-ER and endosomal systems and their functions have been extensively studied. The class III ARF, ARF6, functions exclusively in the endosomal-plasma membrane system. ARF6 is involved in processes as diverse as endosomal recycling to the plasma membrane, regulated secretion, coordinating actin cytoskeleton at the plasma membrane and F_c-mediated phagocytosis in macrophages. (Altschuler *et al.*, 1999; Millar *et al.*, 1999; Yang and Mueckler, 1999; Zhang *et al.*, 1999). In contrast, virtually nothing is known about the class II ARFs. In the yeast *Saccharomyces cerevisiae*, three Arf proteins fulfill all Arf functions. The class I Arfs Arf1p and Arf2p are functionally interchangeable (96% protein sequence identity), and at least one these proteins is required for viability. Arf1p, though, constitutes 90% of Arf1 activity in yeast cells (Stearns *et al.*, 1990a). Yeast Arf3p probably corresponds to mammalian ARF6.

The effects of Arfs depend on their function as GTP-dependent switches. In analogy to other Ras-like proteins, the conformation of two regions of Arf, switch 1 and switch 2, differ between the GDP- and the GTP-bound forms (Amor *et al.*, 1994; Greasley *et al.*, 1995; Goldberg, 1998; Pasqualato *et al.*, 2002) (Fig. 7A and B). Arf has two additional nucleotide-sensitive regions: the myristoylated N-terminal amphiphatic helix that associates with a hydrophobic cleft in Arf-GDP but is free to associate with lipids and potentially other proteins in Arf-GTP. And lastly, the interswitch domain that is retracted

A

```
  1  MGLFASKLFS NLFGNKEMRI LMVGLDGAGK TTVLYKLKLG EVITTIPTIG
 51  FNVETVQYKN ISFTVWDVGG QDRIRSLWRH YYRNTEGVIF VVDSNDRSRI
101  GEAREVMQRM LNEDELRNAA WLVFANKQDL PEAMSAAEIT EKLGLHSIRN
151  RPWFIQATCA TSGEGLYEGL EWLSNSLKNS T
```

B

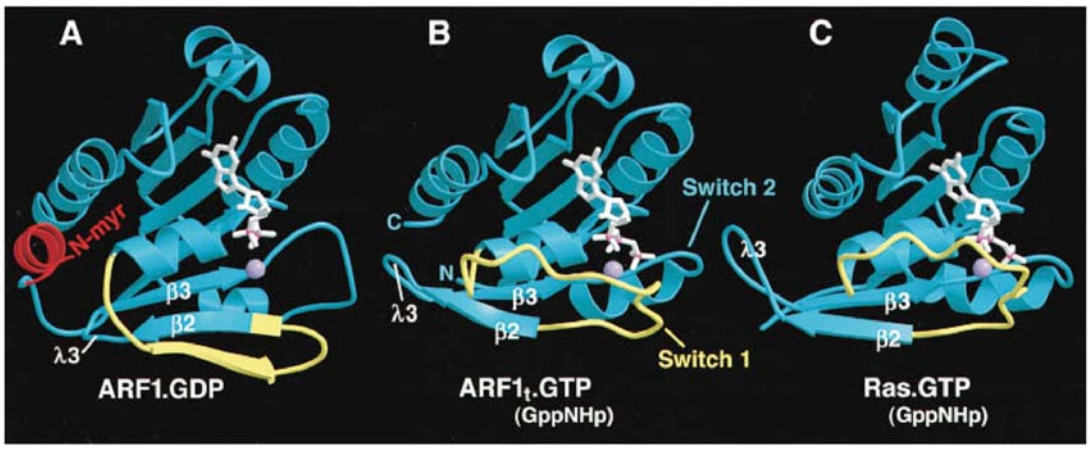

C

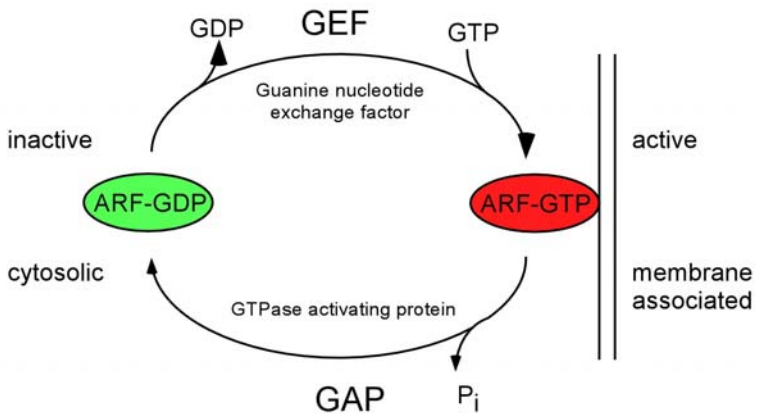

Figure 7: Arf as a nucleotide sensitive switch. **(A)** Primary structure of Arf1p from *Saccharomyces cerevisiae*. The myristoylated N-terminal helix is underlined. The consensus GTP-binding motifs conserved among Ras superfamily GTPases are shown in boxes. Switch 1 is shown in red, switch 2 in green and the α-helix 3 in blue. **(B)** A ribbon representation of crystal structures of human full-length ARF1 bound to GDP, human truncated ARF1 bound to a GTP analog in comparison to GTP-analog-bound Ras (from Goldberg, 1998). The N-terminal helix of ARF1-GDP is colored in red, bound nucleotide is colored white, with phosphorus atoms pink; Mg^{2+} ions are drawn as magenta spheres. **(C)** The GTPase cylce of Arf1.

and forms a pocket to accommodate the myristoylated N-terminal helix in Arf-GDP. These four surfaces on Arf presumably form the interface for nucleotide-dependent association with other proteins. The carboxyl-terminus and the α-helix 3 have also been implicated in protein-protein interactions (Goldberg, 1999; Takeya *et al.*, 2000; Gommel *et al.*, 2001).

As all members of the Ras superfamily of GTPases, Arf1 proteins undergo cycles of activation and inactivation mediated by Arf1-GEFs and Arf1-GAPs (reviewed by Jackson and Casanova, 2000; Randazzo and Hirsch, 2004) (Fig. 7 C). In the GDP-bound state, Arf1 can weakly associate with membranes via the myristoyl moiety of the N-terminus. Upon nucleotide exchange, Arf1 undergoes a conformational change leading to insertion of hydrophobic residues into the membrane and tightly associates with the membrane (Antonny *et al.*, 1997). In the membrane-bound, activated form, Arf1 can interact with downstream effectors until it is inactivated again by GTP hydrolysis. Consistent with the multiple sites of action and range of effects, Arf1-GTP interacts with diverse groups of proteins.

Arf1 has a number of biochemical activities that can be measured *in vitro*. These include the ability to recruit certain coat proteins to membranes (coatomer, AP-1, AP-3, AP-4, GGAs) (Serafini *et al.*, 1991; Donaldson *et al.*, 1992; Palmer *et al.*, 1993; Stamnes and Rothman, 1993; Traub *et al.*, 1993; Ooi *et al.*, 1998; Puertollano *et al.*, 2001). The co-factor activity for bacterial ADP-ribosylating toxins (Kahn and Gilman, 1986; Lee *et al.*, 1991), the activation of phospholipase D (Brown *et al.*, 1993) and the stimulation of phospholipids kinases (Godi *et al.*, 1999; Honda *et al.*, 1999; Jones *et al.*, 2000; Skippen *et al.*, 2002) complement the so far known biochemical activities of Arf1.

The cellular functions of ARF1, however, which can be observed on a phenotypical level in mammalian cells, involve the regulation of many steps of membrane traffic and the regulation of the actin cytoskeleton. In the yeast *Saccharomyces cerevisiae*, Arf1p has been implicated as regulator of a large number of cellular functions including vesicular traffic, mitotic growth, entry into the cell-cycle, maintenance of organelle morphology, sporulation and actin cytoskeleton regulation (Stearns *et al.*, 1990a; Stearns *et al.*, 1990b; Ireland *et al.*, 1994; Kahn *et al.*, 1995; Gaynor *et al.*, 1998; Rudge *et al.*, 1998; Blader *et al.*, 1999; Fucini *et al.*, 2000).

1.6 Interactors of Arf1

The means by which the biochemical activities of Arf1 mediate these diverse cellular functions are not completely understood. The guanine nucleotide-bound state of Arf1 is controlled by GEFs and GAPs. Many proteins regulating Arf1 activity and proteins presumably acting as effectors have been identified and the number is still growing (reviewed by Donaldson and Jackson, 2000; Randazzo *et al.*, 2000; Spang, 2002; Nie *et al.*, 2003). Consistent with the multiple sites of action, diverse groups of proteins have been identified.

1.6.1 Arf1-regulators: Arf1-GEFs and Arf1-GAPs

These regulatory proteins are conserved throughout evolution. Both reside in the cytosol and need to be recruited to the site of action on the membrane.

All Arf-GEFs contain a Sec7 domain comprising the catalytic site (reviewed by Jackson and Casanova, 2000). A subclass of GEFs and GAPs contain a pleckstrin homology domain (PH) which interacts with phosphoinositides in the membrane. In yeast, three Arf1p-GEFs with established functions have been identified: Gea1p, Gea2p and Sec7p. Gea1p and Gea2p have overlapping functions in retrograde transport from the Golgi to the ER, while Sec7p has been implicated in vesicle formation from the trans-Golgi (Franzusoff *et al.*, 1992; Spang *et al.*, 2001). The cellular role of the fourth Sec7-domain containing protein, Syt1p, is still unclear but it might act at the post-Golgi level (Jones *et al.*, 1999c). Which of the GEFs mediates the other Arf1p-dependent transport steps, remains to be established.

The main characteristic of Arf-GAPs is the zinc finger domain which is involved in GTPase activation. Sixteen mammalian ARF-GAPs have been identified thus far as well as several proteins containing the Arf-GAP motif but without demonstrated Arf-GAP activity (reviewed by Randazzo and Hirsch, 2004). Arf-GAPs have been categorized into three groups: Arf-GAP1 type, Git type, and AZAP type. The diversity in domain organization in GAPs in higher eukaryores might allow their recruitment to different sites of action. For example, ARAPs (from the AZAP type) have been shown recently to represent a family of phosphatidylinositol 3,4,5-trisphosphate-dependent ARF-GAPs that regulate ARF-, Rho- and Cdc24-dependent cell activities (Krugmann *et al.*, 2002; Miura *et al.*, 2002). Thus, three small GTPases, which are thought to play roles in maintaining Golgi structure, seem to be regulated via the same family of effectors.

Arf1p-GAPs outnumber the Arf1p-GEFs in *Saccharomyces cerevisiae*. At least six putative Arf1p-GAPs are present in the yeast genome. Three of which are thus far characterized: Gcs1p and Glo3p have overlapping functions in retrograde transport from the Golgi to the ER (Poon *et al.*, 1999). Age2p can be replaced by Gcs1p in the endocytic pathway (Poon *et al.*, 2001). In addition, Gcs1p influences actin polymerization dynamics in yeast (Blader *et al.*, 1999).

1.6.2 Vesicle coat proteins and adaptors

Vesicle coat proteins are central to the models explaining the regulatory role of Arfs in membrane traffic. Arf1-dependent coats include clathrin/AP-1, clathrin/AP-3, clathrin/AP-4, clathrin/GGA1/2/3 and coatomer. In each case, Arf1 binds the coat directly (Donaldson *et al.*, 1992; Palmer *et al.*, 1993; Ooi *et al.*, 1998; Zhu *et al.*, 1999; Boehm *et al.*, 2001). For coatomer, AP-1 and AP-3 binding, the switch 1 domain was mapped as the interaction site by cross-linking studies (Zhao *et al.*, 1999; Austin *et al.*, 2002). For GGA binding, switch 1 and switch 2 have both been implicated by mutational analysis (Puertollano *et al.*, 2001; Jacques *et al.*, 2002).

1.6.3 Proteins interacting with Arf1-GDP

In addition to ARF1-GEFs, ARF1-GDP has been shown to interact with members of the p24 family of transmembrane cargo receptors such as p23. In biochemical studies, a peptide corresponding to the cytosplasmic domain of p23 bound to the carboxy-terminal 22 amino acids of ARF1-GDP but not to ARF1-GTP (Gommel *et al.*, 2001). This is in agreement with studies in live cells using fluorescence resonance energy transfer (Majoul *et al.*, 2001). In one model (Gommel *et al.*, 2001), ARF1-GDP is recruited to membranes by binding p23 prior to activation of ARF1 mediated by ARF1-GEF to a site of relative cargo enrichment. As mentioned before, however, this model cannot provide a universal explanation of Arf activation (Springer *et al.*, 2000).

1.6.4 Phospholipid-metabolizing enzymes

Arf-GTP binds to and activates phosphatidyl-inositol kinases and phospholipase D (PLD), leading to the production of phosphatidylinositol 4,5-bisphosphate (PIP2) and phosphatidic acid (PA), respectively. PIP2 and PA are likely to contribute to the effects of Arfs in both actin and membrane remodeling. Nonetheless, the relationship between Arfs and lipids is first complex and second only poorly understood.

ARF1 can stimulate phospholipase D *in vitro* and *in vivo* in mammalian cells (Brown *et al.*, 1993). PA, produced by ARF1-activated PLD, has first been implicated to be directly involved in the recruitment of coat proteins (Ktistakis *et al.*, 1996; West *et al.*, 1997). However, it is now firmly established that activation of PLD does not serve as the sole mechanism by which ARF1 regulates the recruitment of coat proteins (Stamnes *et al.*, 1998; Jones *et al.*, 1999b; Kuai *et al.*, 2000). In addition, phospholipase D is not activated by Arf1p in yeast (Rudge *et al.*, 1998) and is at least not required for retrograde transport (Spang and Schekman, 1998).

Although a role for PIP2 in membrane traffic is likely, its precise role remains to be determined. Phospholipids have long been known to regulate the actin cytoskeleton (Lassing and Lindberg, 1985). An intriguing concept has been proposed in which Arf1-dependent changes in the actin cytoskeleton are linked to membrane traffic (Lorra and Huttner, 1999).

1.6.5 Other effectors

Arfaptin2 (and related proteins) bind to both the actin cytoskeleton regulator Rac of the Rho family bound to either GDP or GTP as well as to ARF1-GTP. Rac and ARF1-GTP binding are mutually exclusive. It has been proposed that Arfaptin2 acts to sequester Rac until activated ARF1 bind Arfaptin2. The displaced Rac is then free to be activated and to interact with Rac effectors (Tarricone *et al.*, 2001). These results suggest that Rho family and Arf family protein function is coordinated within the cell.

Arfophilin is an example of an effector binding to class II and class III ARFs at the same time. Thus, the same cellular event could be influenced by two different ARF isozymes simultaneously (Shin *et al.*, 2001). However, the function of Arfophilin is unclear.

Some other effectors have been identified, although their significance remains obscure. As mentioned above, Arfs are able to bind to cholera toxin and other bacterial toxins and are required as co-factor for the ADP-ribosylation of G-protein subunits (Kahn and Gilman, 1986; Lee *et al.*, 1991). This feature distinguishes Arf proteins from the closely related Arl proteins (Arf-like proteins). Arf proteins bind to mitotic kinesin-like protein 1 (MKLP1) in a GTP-dependent fashion (Boman *et al.*, 1999). Furthermore, class I Arfs interact with PICK1 (protein interacting with C-kinase) (Takeya *et al.*, 2000).

Although some circumstantial evidence exists for the role of these effectors, the molecular function of these interaction partners is far from being clear.

1.7 Aim of this study

The small GTPase Arf1p is a crucial regulator of vesicle formation in many steps of the secretory pathway in the yeast *Saccharomyces cerevisiae*. In addition, there is growing evidence of Arf1p being involved in actin cytoskeleton rearrangements as well as in lipid metabolism. The variety of already known regulators and effectors of Arf1p is, however, still insufficient to explain the multiple functions of the same molecule at different cellular locations. Furthermore, it is likely that new Arf1p-dependent pathways await discovery in both yeast and mammals which are not necessarily conserved.

It is the aim of this study to identify new interactors of the small GTPase Arf1p in the yeast *Saccharomyces cerevisiae*. The subsequent characterization of the newly identified interactors and the elucidation of the pathways involved should lead to new insights concerning unexpected Arfp-dependent pathways and shed more light on vesicle formation and concomitant cargo protein sorting.

2 Materials and Methods

2.1 Instrumentation

Analytical balance BL310	Sartorius
Axiocam MRm	Zeiss
Axioplan 2 epi-fluorescence microscope	Zeiss
Cooling centrifuge 5417 R	Eppendorf
Cooling centrifuge 5810 R	Eppendorf
Cooling centrifuge RC-5B	Sorvall
Developer machine	Agfa
Dissection scope	Singer
Dynal MPC-S magnetic separation rack	Dynal Biotech
Electrophoresis chamber B1A	Owl
Electrophoresis chamber SE250	Amersham Bioscience
Electroporation Gene Pulser	Biorad
FPLC Äkta Prime	Amersham Bioscience
Fraction collector 2110	Biorad
Gel dryer GD 2000	Amersham Bioscience
Gel shaker 3020	GFL
Heatable magnetic stirrer Ikamag RCT	Ika Labortechnik
Heating block	Grant Boekel
Incubators	Heraeus
Incubators	Memmert
Laboratory blender	Waring
Light microscope Axioskop 2 plus	Zeiss
PCR-machine PTC-100	MJ Research, Inc.
pH-meter pH 330	WTW
Power supply EPS 601	Amersham Bioscience
Power supply Power Pac 200	Biorad
Rotator Labquake	Barnstead/Thermolyne
Rotor 50.2 Ti	Beckman
Rotor GS3	Kendro
Rotor SS34	Kendro
Rotor SW28	Beckman
Rotor SW50.1	Beckman
Semi-dry transfer cell	Biorad
Shaking incubators Innova 4400 / 4430	New Brunswick Scientific
Shaking incubators Unitron	Infors
Sonifier B12	Branson Sonic Power Company
Spectrophotometer DU 640	Beckman
Stratalinker 1800 UV Crosslinker	Stratagene
Thermomixer Compact	Eppendorf
Ultracentrifuge T-2060	Centrikon
UV-transilluminator	MWG-Biotech
Vortexer Vortex Genie 2	Scientific Industries
Water treatment system Milli-Q	Millipore
Waterbath Julabo	Bioblock Scientific
Wet blot tank TE22	Amersham Bioscience

2.2 Chemicals

All standard chemicals were obtained from Sigma, Roth or Merck.

1 kb DNA-Ladder	15615-016	Invitrogen
30% Acrylamide stock solution with 0.8% Bisacrylamid	3029.1	Roth
4',6-Diamidino-2-phenylindole dihydrochloride (DAPI)	D-9542	Sigma
Alkaline phosphatase from calf intestine	713023	Roche
Bacto-Agar granulated	214510	Difco

Bacto-Peptone	211830	Difco
Bacto-Tryptone	211701	Difco
Bacto-Yeast extract	212730	Difco
Bacto-Yeast nitrogen base w/ amino acids and ammonium sulfate	233520	Difco
Bacto-Yeast nitrogen base without amino acids	291920	Difco
Benchmark Protein Ladder Prestained	10748-010	Invitrogen
Benchmark Protein Ladder	10747-012	Invitrogen
Brillant Blue G250	35050	Serva
Brillant Blue R250	35051	Serva
Calcofluor white dye	F-3543	Sigma
Citifluor	R1320	Plano
Complete mini EDTA-free protease inhibitors	1836170	Roche
Desoxynucleosid-5‘-triphosphate (dNTPs) for PCR	1969064	Roche
Dextrose	0155-17-4	Difco
Digoxigenin-11-UTP	1209256	Roche
Dimethylpimelimidate (DMP)	21667	Pierce
DNase I, RNase-free	776785	Roche
ECL advance kit	RPN 2135	Amersham Bioscience
ECL kit	RPN 2106	Amersham Bioscience
ECL+ kit	RPN 2133	Amersham Bioscience
Ficoll 400	17-0400-02	Amersham Bioscience
Guanosine-5‘-diphosphat (GDP)	G-7127	Sigma
Guanosine-5‘-triphosphat (GTP)	G-8877	Sigma
Guanosine-5’-O-(3-thiotriphosphate) (GTPγS)	G-8634	Sigma
Heparin	H-3393	Sigma
Horse serum, heat-inactivated	26050-070	Invitrogen
Leupeptin	L-8511	Sigma
Metaphor agarose	850.184	Biozym
Non-fat dry milk powder		Frema
Nycodenz	D-2158	Sigma
Oligonucleotide-primers		MWG-Biotech
Oligonucleotide-primers		Qiagen
Pellet Paint co-precipitant	69049-3	Merck
Pepstatin A	P-5318	Sigma
Phenol/Chloroform/Isoamylalkohol (PCI)	15593-031	Invitrogen
Protein A magnetic beads	S1425S	NEB
Protein A-sepharose CL-4B	17-0780-01	Amersham Bioscience
Protein G agarose	1243233	Roche
Restriction enzymes		NEB
Restriction enzymes		Roche
Rhodamine-Phalloidine	R415	MoBiTec
RNase A	109142	Roche
RNase	109126	Roche
RNasin	R2511	Promega
RQ1-RNase-free DNase	M6101	Promega
Salmon sperm-DNA	85346022-39	Roche
Seakem LE agarose	840.004	Biozym
Taq DNA polymerase (5U/µl)	1418432	Roche
Yeast tRNA	109495	Roche

2.3 Materials

Centriprep YM-10	4304	Amicon
Dialysis bag Spectrapor 12 – 14.000	132 700	Spectrum
Diethylaminoethane (DEAE) Sephacel	17-0500-01	Amersham Bioscience
Electroporation cuvettes	24704640	Fischer
Gel blotting paper	426 890	Schleicher & Schuell
Hybond N+ nitrocellulose membrane	RPN 203B	Amersham Bioscience
Hyperfilm ECL	RPN 3114K	Amersham Bioscience
N-Hydroxysuccinimide (NHS)-activated Sepharose 4 Fast Flow	17-0906-01	Amersham Bioscience
Nickel-Nitrilotetra-actetic acid agarose (Ni-NTA)	1000632	Qiagen

Nitrocellulose membrane Protran 0.45 µm	10401196	Schleicher & Schuell
Polyvinylidenfluorid (PVDF)-membrane 0.2 µm	162-0177	Biorad
Sephacryl S-100 High Resolution	17-0612-01	Amersham Bioscience
Ultralink Iodacetyl resin	53155	Pierce

2.4 Kits

AlkPhos Direct labeling module	RPN3680	Amersham Bioscience
BCA protein assay kit	23227	Pierce
Biorad DC protein assay reagents	500-0116	Biorad
Biorad protein assay kit	500-0001	Biorad
CDP-Star detection reagent	RPN3682	Amersham Bioscience
Expand High Fidelity PCR system	1732641	Roche
HNPP fluorescent detection kit	1758888	Roche
MEGAscript T7 kit	1334	Ambion
OneStep RT-PCR kit	210210	Qiagen
pET100D-TOPO expression kit	K100-01	Invitrogen
pTrcHis-TOPO TA expression kit	K4410-01	Invitrogen
Qiagen HiSpeed plasmid midi kit	12643	Qiagen
Qiagen plasmid mini kit	12123	Qiagen
QIAquick gel extraction kit	28704	Qiagen
QIAquick PCR purification kit	28106	Qiagen
Rapid DNA ligation kit	1635379	Roche
RNeasy mini kit	74104	Qiagen

2.5 Media

All media were autoclaved at 121°C for 20 min. Water from the Millipore Milli Q water treatment system was used exclusively. Standard yeast media were used (Sherman, 1991).

LBamp:	10 g Bacto-tryptone 5 g yeast-extract 10 g NaCl 20 g Bacto-agar (Difco) ad 1 l with H_2O 1 ml 1000x Ampicillin was added after autoclaving
YPD:	20 g Bacto-peptone 10 g yeast extract 20 g dextrose 20 g Bacto-agar (Difco) ad 1 l H_2O
YPD-G418:	20 g Bacto-peptone 10 g yeast extract 20 g dextrose 20 g Bacto-agar (Difco) ad 1 l H_2O After cooling to approximately 50°C 10 ml 100x G418 was added.

SOC-Medium:	5 g yeast extract 20 g Bacto-peptone 20 g dextrose 10 mM NaCl 2.5 mM KCl 10 mM $MgSO_4$ ad 1 l with H_2O
HC-medium:	6.7 g Yeast nitrogen base without amino acids 10x HC-selection mixture ad 1 l with H_2O after autoclaving, a carbon source was added.
HC-plates:	a) 6.7 g Yeast nitrogen base without amino acids 20 g dextrose 10 ml 10x HC-selection mixture ad 0.5 l with H_2O b) 20 g Bacto-agar (Difco) ad 0.5 l with H_2O a) and b) were mixed after autoclaving
Spo-plates	1% KAc 1x Selection mixture complete 20 g Bacto-agar (Difco) ad 1 l with H_2O
Super Spo-plates	1.5% KAc 1x Selection mixture comlete 0.25% yeast extract 0.05% dextrose 20 g Bacto-agar (Difco) ad 1 l with H_2O
YMP+ plates:	6.3 g Yeast nitrogen base without amino acids and ammonium sulfate 4.5 g yeast extract 9.0 g Bacto-peptone 9.0 g succinic acid 5.4 g NaOH 20 g dextrose 25 g $(NH_4)_2SO_4$ 20 g Bacto-agar (Difco) ad 1 l with H_2O

Calcofluor white plates:	a) 6.7 g Yeast nitrogen base without amino acids 1.0 g yeast extract 20 g dextrose 1x HC-selection mixture ad 0.5 l with H_2O b) 20 g Bacto-agar (Difco) ad 0.4 l with H_2O a) and b) were mixed after autoclaving 100 ml 10 % MES-buffer pH 6.0 were added, Calcofluor white stock solution was added dropwise to 0.1 mg/ml final.
5-FOA-plates:	0.34 g Yeast nitrogen base without amino acids 0.05 g 5-Fluoroorotic acid 1 g dextrose 1x HC-selection mixture 5 ml H_2O filter sterilized mix with 4% Bacto-agar (55°C)

2.6 Commonly used solutions and buffers

H_2O filtered by Millipore Milli Q water treatment system was used exclusively for all solutions and buffers.

1000x ampicillin:	100 mg/ml, filter sterilized
1000x carbenicillin:	100 mg/ml, filter sterilized
150x IPTG:	150 mM, filter sterilized
50x lysozym:	50 mg/ml
250x kanamycin:	10 mg/ml, filter sterilized
Myristic acid:	125 mM Na-myristate Dissolved by heating in the microwave and filter sterilized while still warm.
1000x pepstatin A/leupeptin:	each 1 mg/ml in DMSO
100x PMSF:	0.1 M in isopropanol

10x HC-selection mixture	0.2 mg/ml adenine hemi-sulfate 0.35 mg/ml uracil 0.8 mg/ml L-tryptophan 0.2 mg/ml L-histidine-HCl 0.8 mg/ml L-leucine 1.2 mg/ml L-lysine-HCl 0.2 mg/ml L-methionine 0.6 mg/ml L-tyrosine 0.8 mg/ml L-isoleucine 0.5 mg/ml L-phenylalanine 1.0 mg/ml L-glutamic acid 2.0 mg/ml L-threonine 1.0 mg/ml L-aspartic acid 1.5 mg/ml L-valine 4.0 mg/ml L-serine 0.2 mg/ml L-arginine-HCl autoclaved without the components to select for
6x loading buffer for agarose gel-electrophoresis:	0.25% bromphenolblue 0.25% xylencyanole 30% glycerol
B88-buffer:	20 mM HEPES/KOH pH 6.8 250 mM sorbitol 150 mM KAc 5 mM $Mg(Ac)_2$ filter sterilized
5x Laemmli-buffer:	62.5 mM Tris/HCl pH 6.8 5% β-mercaptoethanol 10% glycerol 2% SDS 0.0025% bromphenolblue
STE-Puffer:	50 mM Tris/HCl pH 8.0 25% sucrose 40 mM EDTA autoclaved
50x TAE-buffer:	2 M Tris/HAc pH 7.7 5 mM EDTA
20x TBS:	60 g Tris/HCl pH 7.4 160 g NaCl 4 g KCl ad 1 l with H_2O

20x PBS	46.6 g $Na_2HPO_4 \cdot 12\ H_2O$ 4.2 g KH_2PO_4 175.2 g NaCl 44.8 g KCl ad 1 l with H_2O
TBST:	TBS with 0.1% Tween-20
TE:	10 mM Tris/HCl pH 8.0 1 mM EDTA
100x G418:	20 mg/ml Geneticin, filter sterilized
Calcofluor white stock:	50 mg/ml NaOH added dropwise to dissolve
50x Denhardt's reagent:	10 g Ficoll type 400 10 g BSA fraction V 10 g polyvinylpyrrolidone ad 1 l with H_2O filter sterilized, stored at –20°C
20x SSC	3 M NaCl 0.3 M Na-citrate/NaOH pH 7.0

2.7 Strains, plasmids, antibodies, oligonucleotide primers

Table 1: Plasmids used

Plasmid	Description	Source
pUG6	loxP-Kanamycin cassette	Johannes Hegemann
pUG27	loxP-HIS5 cassette	Johannes Hegemann
pUG72	loxP-URA3 cassette	Johannes Hegemann
pUG73	loxP-LEU2 cassette	Johannes Hegemann
pSH63	Cre-recombinase, TRP1	Johannes Hegemann
pSH47	Cre-recombinase, URA3	Johannes Hegemann
pBS-3GFP-TRP1	3GFP-TRP1	John Cooper
pYM-3GFP-TRP1	3GFP-TRP1 template	This study
pEG203	Bait two hybrid plasmid	Rainer Duden
pEG203-ΔN17-Arf1-Q71L	Bait two hybrid plasmid	Rainer Duden
pJG4-5	Prey two hybrid plasmid	Rainer Duden
pJG4-5-PAB1	Prey two hybrid plasmid	This study
pJG4-5-PUB1	Prey two hybrid plasmid	This study
pJG4-5-GLO3	Prey two hybrid plasmid	Rainer Duden
pUSE-SEC7-GFP-URA	SEC7-GFP tagging	Ben Glick
pDH3	CFP-KAN template	Yeast Resource Center
pDH5	YFP-HIS5 template	Yeast Resource Center
pRJ-2GFP-TRP1	2GFP tagging	Ralf Jansen
pCY204	YCp50-HO-endonuclease	Andreas Mayer
pUG35	CEN URA3 METprom-GFP	Johannes Hegemann
pU6H3VSV	6His-3VSV template	Dieter Gallwitz
pUGLys2	LoxP-LYS2 cassette	Steven Oliver
pRJ-ASH1-myc9	URA3	Dieter Gallwitz
pYM1 - pYM12	Template tagging plasmide	Elmar Schiebel
pG14-MS2-GFP	GFP-MS2	Pascal Chartrand
YEP lac195-Lz-MS2-ASH1 3‘UTR	ASH1-MS2-binding sites	Pascal Chartrand
YEP lac195-Lz-MS2-ADH II	ADH1-MS2-binding sites	Pascal Chartrand
pRS315	CEN LEU2	Sikorski and Hieter, 1989
pRS425	2µ LEU2	Phil Hieter
pCRP12-CHS3-GFP	CHS3-GFP (CEN HIS3)	Valdivia *et al.*, 2002
pRS426-CHS7	CHS7 (2µ URA3)	Trilla *et al.*, 1999
pRS315-CHS6	CHS6 (CEN LEU2)	This study
pRS425-CHS6	CHS6 (2µ LEU2)	This study
pRS315-BUD7	BUD7 (CEN LEU2)	This study
pRS425-BUD7	BUD7 (2µ LEU2)	This study
pRS315-YMR237w	YMR237w (CEN LEU2)	This study
PRS425-YMR237w	YMR237w (2µ LEU2)	This study
pRS315-YKR027w	YKR027w (CEN LEU2)	This study
PRS425-YKR027w	YKR027w (2µ LEU2)	This study
YEpGFP*-BUD8F	GFP-BUD8 (2µ LEU2)	Schenkman *et al.*, 2002
YEpGFP*-BUD9	GFP-BUD9 (2µ URA3)	Schenkman *et al.*, 2002
pKU76	TAT2-GFP (CEN URA3)	Umebayashi and Nakano, 2003
pUG35-FUS1-GFP	FUS1-GFP (CEN URA3)	This study
p424-GPD	(2 µ TRP1)	Mumberg *et al.*, 1995

Table 2: *E. coli* expression strains

Strain	Plasmid	Source
M15	pREP4; pQE30-ΔN17-Arf1p-Q71L-His_6	Rainer Duden
M15	pREP4; pQE30-ΔN17-Arf1p-T31N-His_6	Rainer Duden
M15	pREP4; ΔN17-wt-Arf1p-His_6	Rainer Duden
BL21 (DE3)	wt-Arf1p; Nmt1p	Richard Kahn
BL21 (DE3) Star	pET100D-His_6-Pab1p	This study
BL21 (DE3) Star	pET100D-His_6-Chs5p	This study
BL21 Codon Plus	pTrc-His-TOPO-Bfr1p	This study

Table 3: Antibodies used.

Antibodies	Dilution (WB)	Source
Rabbit anti-coatomer, polyclonal	1:1.000; IP	Randy Schekman
Rabbit anti-Gea2p, polyclonal	1:1.000	Anne Spang
Rabbit anti-Glo3p, polyclonal	1:1.000	Pak Poon
Rabbit anti-Arf1p, polyclonal	1:1.000; IP	Anne Spang
Rabbit anti-Emp47p, polyclonal	1:1.000	Stefan Schröder-Köhne
Rabbit anti-Bet1p, polyclonal	1:1.000	Randy Schekman
Mouse anti-HA-epitope, monoclonal HA.11	1:1.000; IP	Eurogentec
Mouse anti-HA-epitope, monoclonal HA-7	1:1.000 IF	Sigma
Mouse anti-myc-epitope, monoclonal 9E10	1:1.000 WB; 1:1000 IF	Sigma
Mouse anti-GFP, monoclonal	1:1.000	Abcam
Sheep anti GFP, polyclonal	IP	Michael Knop
Rabbit anti-GFP, polyclonal purified	1:1.000 WB; 1:400 IF; IP	Torrey Pines
Rabbit anti-AU5 epitope, polyclonal purified	1:1.000 WB; IP	Abcam
Mouse anti-Pab1p, monoclonal	1:2.000	Alan Sachs
Goat anti-rabbit-HRP	1:25.000 – 1:100.000	Pierce
Goat anti-mouse-HRP, polyclonal purified	1:25.000 – 1:100.000	Pierce
Rabbit anti-Pab1p, polyclonal, affinity purified	1:250	This study
Rabbit anti-Chs5p, polyclonal,	IP	This study
Rabbit anti-Chs5p, polyclonal, affinity purified	1:500	Robert Gauss
Rabbit anti-Arf1p, polyclonal, affinity purified	1:1.000; IP	This study
Rabbit IgG, purified	IP-control	Dianova
Goat anti-mouse-Cy3	1:400 IF	Jackson ImmunoRes.
Donkey anti-rabbit-FITC	1:200 IF	Jackson ImmunoRes.
Sheep anti-digoxigenin-AP F_{ab}-fragments	1:5.000 *in situ* hybridization	Roche

WB western blot, IF immunofluorescence, IP immunoprecipitation.

Table 4 : Yeast strains used in chapter 3.2

Strain	Genotype	Source
GPY60	*MATα ura3-52 leu2,3-112 his4-579 pep4::ura3 prb1 trp4-579*	R. Schekman
YPH500	*MATα ade2-101 his3-200 leu2-1 lys2-801 trp-63 ura3-52*	P. Hieter
W303-1Aa	*MATα ade2-1 ura3-1 trp1-1 his3-11,15 leu2,3-112 can1-100*	P. Poon
EGY48	*MATα trp1 ura3 his3 6xLexAop-LEU2 pSH18-34 (URA3)*	E. Golemis
YAS321	*MATα ade2-101 his3-200 leu2-1 lys2-801 trp-63 ura3-52 arf1::HIS3MX6*	This study
YAS147	*MATα ade2-101 his3-200 leu2-1 lys2-801 trp-63 ura3-52 pG14-MS2-GFP (LEU2) YEP15-Lz-MS2-ASH1-3'UTR (URA3)*	This study
YAS324	*MATα ade2-101 his3-200 leu2-1 lys2-801 trp-63 ura3-52 arf1::HIS3MX6 pG14-MS2-GFP (LEU2) YEP15-Lz-MS2-ASH1-3'UTR (URA3)*	This study
YAS212	*MATα ade2-101 his3-200 leu2-1 lys2-801 trp-63 ura3-52 ARF1::ARF1-6HA-klTRP1*	This study
YAS225	*MATa ade2-101 his3-200 leu2-1 lys2-801 trp-63 ura3-52 PAB1::PAB1-9myc-klTRP1*	This study
YAS238	*ade2-101 his3-200 leu2-1 lys2-801 trp-63 ura3-52 ARF1::ARF1-6HA-klTRP1 PAB1::PAB1-9myc-klTRP1*	This study
YAS258-A	*ade2-101 his3-200 leu2-1 lys2-801 trp-63 ura3-52 ARF1::ARF1-YFP-HIS3MX6*	This study
YAS258-B	*ade2-101 his3-200 leu2-1 lys2-801 trp-63 ura3-52 ARF1::ARF1-YFP-HIS3MX6 PAB1::PAB1-CFP-KANMX6*	This study
YAS258-C	*ade2-101 his3-200 leu2-1 lys2-801 trp-63 ura3-52 PAB1::PAB1-CFP-KANMX6*	This study
YAS258-D	*ade2-101 his3-200 leu2-1 lys2-801 trp-63 ura3-52*	This study
YAS259-A	*ade2-101 his3-200 leu2-1 lys2-801 trp-63 ura3-52 ARF1::ARF1-CFP-KANMX6 PAB1::PAB1-YFP-HIS3MX6*	This study
YAS259-B	*ade2-101 his3-200 leu2-1 lys2-801 trp-63 ura3-52 ARF1::ARF1-CFP-KANMX6*	This study
YAS259-C	*ade2-101 his3-200 leu2-1 lys2-801 trp-63 ura3-52*	This study
YAS259-D	*ade2-101 his3-200 leu2-1 lys2-801 trp-63 ura3-52 PAB1::PAB1-YFP-HIS3MX6*	This study
NYY0-1	*MATa ade2::ARF1::ADE2 arf1::HIS3 arf2::HIS3 ura3 lys2 trp1 his3 leu2*	A. Nakano
NYY11-1	*MATa ade2::arf1-11::ADE2 arf1::HIS3 arf2::HIS3 ura3 lys2 trp1 his3 leu2*	A. Nakano
NYY17-1	*MATa ade2::arf1-17::ADE2 arf1::HIS3 arf2::HIS3 ura3 lys2 trp1 his3 leu2*	A. Nakano
NYY18-1	*MATa ade2::arf1-18::ADE2 arf1::HIS3 arf2::HIS3 ura3 lys2 trp1 his3 leu2*	A. Nakano
NYY0-1	*MATa ade2::ARF1::ADE2 arf1::HIS3 arf2::HIS3 ura3 lys2 trp1 his3 leu2 MYO4::MYO4-2GFP-KlTRP1*	This study
NYY11-1	*MATa ade2::arf1-11::ADE2 arf1::HIS3 arf2::HIS3 ura3 lys2 trp1 his3 leu2 MYO4::MYO4-2GFP-KlTRP1*	This study
NYY17-1	*MATa ade2::arf1-17::ADE2 arf1::HIS3 arf2::HIS3 ura3 lys2 trp1 his3 leu2 MYO4::MYO4-2GFP-KlTRP1*	This study
NYY18-1	*MATa ade2::arf1-18::ADE2 arf1::HIS3 arf2::HIS3 ura3 lys2 trp1 his3 leu2 MYO4::MYO4-2GFP-KlTRP1*	This study
RSY248	*MATα his4-619*	R. Schekman
RSY271	*MATα his4-619 sec18-1*	R. Schekman
RSY1017	*MATα his3-200 ura3-52 pep4::URA3 sec21-1*	R. Schekman
RSY281	*MATα his4-619 ura3-52 sec23-1*	R. Schekman
RSY1312	*MATa leu2,3-112 trp1 ura3-52 sec27-1*	R. Schekman
sar1-D32G	*MATα ura3 leu2 trp1 his3 ade2 lys2 sar1::HIS3 pep4::ADE2 pMYY3-1(YCp[sar1-D32G TRP1])*	A. Nakano
YAS2314	*MATa ade2 his3 leu2 trp1 ura3 spb8::LEU2 pab1::HIS3*	A. Sachs
RJY585	*MATa ade2-1 his3-11 leu2-3 trp1-1 ura3 HO-ADE2 HO-CAN1 ASH1::HIS3 (S. pombe)*	R. Jansen
BY4741	*MATa his3Δ1 leu2Δ0 met15Δ0 ura3Δ0*	EUROSCARF
Δarf1	*MATa his3Δ1 leu2Δ0 met15Δ0 ura3Δ0 arf1::KanMX4*	EUROSCARF
Δarf2	*MATa his3Δ1 leu2Δ0 met15Δ0 ura3Δ0 arf2::KanMX4*	EUROSCARF
Δbfr1	*MATa his3Δ1 leu2Δ0 met15Δ0 ura3Δ0 bfr1::KanMX4*	EUROSCARF
YAS318-D	*his3Δ1 leu2Δ0 MET15 lys2Δ0 ura3Δ0 arf1::HIS3MX6 bfr1::KanMX4*	This study
Δscp160	*MATa his3Δ1 leu2Δ0 met15Δ0 ura3Δ0 scp160::KanMX4*	EUROSCARF

Table 5: Yeast strains used in chapter 3.3

Designation	Genotype	Reference
YPH499	*MAT a ade2 his3 leu2 lys2 trp1 ura3*	Sikorski and Hieter, 1989
YPH500	*MAT α ade2 his3 leu2 lys2 trp1 ura3*	Sikorski and Hieter, 1989
YPH501	*MAT a/α ade2/ade2 his3/his3 leu2/leu2 lys2/lys2 trp1/trp1 ura3/ura3*	Sikorski and Hieter, 1989
YAS431	*MAT a ade2 his3 leu2 lys2 trp1 ura3 CHS5::LEU2 (K. lactis)*	This study
YAS572	*MAT α ade2 his3 leu2 lys2 trp1 ura3 CHS5:: LEU2 (K. lactis)*	This study
YAS571	*MAT a ade2 his3 leu2 lys2 trp1 ura3 ARF1::HIS3MX6*	This study
YAS321	*MAT α ade2 his3 leu2 lys2 trp1 ura3 ARF1:: HIS3MX6*	This study
YAS525	*MAT α ade2 his3 leu2 lys2 trp1 ura3 CHS6::URA3 (K. lactis) BCH2::KAN (Tn903)*	This study
YAS430	*MAT a ade2 his3 leu2 lys2 trp1 ura3 BUD7::LEU2 (K.lactis) BCH1::HIS5 (S. pombe)*	This study
YAS563-2a	*MAT a ade2 his3 leu2 lys2 trp1 ura3 CHS6::URA3 (K. lactis)*	This study
YAS563-2α	*MAT α ade2 his3 leu2 lys2 trp1 ura3 CHS6::URA3 (K. lactis)*	This study
YAS563-2aMFT	*MAT a ade2 his3 leu2 lys2 trp1 ura3 CHS6::loxP pSH63 (TRP1)*	This study
YAS563-3a	*MAT a ade2 his3 leu2 lys2 trp1 ura3 BUD7::LEU2 (K.lactis)*	This study
YAS563-3α	*MAT α ade2 his3 leu2 lys2 trp1 ura3 BUD7:: URA3 (K. lactis)*	This study
YAS563-4a	*MAT a ade2 his3 leu2 lys2 trp1 ura3 BCH2::KAN (Tn903)*	This study
YAS563-4α	*MAT α ade2 his3 leu2 lys2 trp1 ura3 BCH2::KAN (Tn903)*	This study
YAS563-5a	*MAT a ade2 his3 leu2 lys2 trp1 ura3 BCH1::HIS5 (S. pombe)*	This study
YAS563-5α	*MAT α ade2 his3 leu2 lys2 trp1 ura3 BCH1::HIS5 (S. pombe)*	This study
YAS563-6a	*MAT a ade2 his3 leu2 lys2 trp1 ura3 CHS6::URA3 (K. lactis) BUD7::LEU2 (K.lactis)*	This study
YAS563-6α	*MAT α ade2 his3 leu2 lys2 trp1 ura3 CHS6::URA3 (K. lactis) BUD7::LEU2 (K.lactis)*	This study
YAS563-7a	*MAT a ade2 his3 leu2 lys2 trp1 ura3 CHS6::URA3 (K. lactis) BCH2::KAN (Tn903)*	This study
YAS563-7α	*MAT α ade2 his3 leu2 lys2 trp1 ura3 CHS6::URA3 (K. lactis) BCH2::KAN (Tn903)*	This study
YAS563-8a	*MAT a ade2 his3 leu2 lys2 trp1 ura3 CHS6::URA3 (K. lactis) BCH1::HIS5 (S. pombe)*	This study
YAS563-8α	*MAT α ade2 his3 leu2 lys2 trp1 ura3 CHS6::URA3 (K. lactis) BCH1::HIS5 (S. pombe)*	This study
YAS563-9a	*MAT a ade2 his3 leu2 lys2 trp1 ura3 BUD7::LEU2 (K.lactis) BCH2::KAN (Tn903)*	This study
YAS563-9α	*MAT α ade2 his3 leu2 lys2 trp1 ura3 BUD7::LEU2 (K.lactis) BCH2::KAN (Tn903)*	This study
YAS563-10a	*MAT a ade2 his3 leu2 lys2 trp1 ura3 BUD7::LEU2 (K.lactis) BCH1::HIS5 (S. pombe)*	This study
YAS563-10α	*MAT α ade2 his3 leu2 lys2 trp1 ura3 BUD7:: BCH1::HIS5 (S. pombe)*	This study
YAS563-11a	*MAT a ade2 his3 leu2 lys2 trp1 ura3 BCH2::KAN (Tn903) BCH1::HIS5 (S. pombe)*	This study
YAS563-11α	*MAT α ade2 his3 leu2 lys2 trp1 ura3 BCH2::KAN (Tn903) BCH1::HIS5 (S. pombe)*	This study
YAS563-12a	*MAT a ade2 his3 leu2 lys2 trp1 ura3 CHS6::URA3 (K. lactis) BUD7::LEU2 (K.lactis) BCH2::KAN (Tn903)*	This study
YAS563-12α	*MAT α ade2 his3 leu2 lys2 trp1 ura3 CHS6::URA3 (K. lactis) BUD7::LEU2 (K.lactis) BCH2::KAN (Tn903)*	This study
YAS563-13a	*MAT a ade2 his3 leu2 lys2 trp1 ura3 BUD7::LEU2 (K.lactis) BCH2::KAN (Tn903) BCH1::HIS5 (S. pombe)*	This study
YAS563-13α	*MAT α ade2 his3 leu2 lys2 trp1 ura3 BUD7::LEU2 (K.lactis) BCH2::KAN (Tn903) BCH1::HIS5 (S. pombe)*	This study
YAS563-14a	*MAT a ade2 his3 leu2 lys2 trp1 ura3 CHS6::URA3 (K. lactis) BCH2::KAN (Tn903) BCH1::HIS5 (S. pombe)*	This study

YAS563-14α	*MAT α ade2 his3 leu2 lys2 trp1 ura3 CHS6::URA3 (K. lactis) BCH2::KAN (Tn903) BCH1::HIS5 (S. pombe)*	This study
YAS563-15a	*MAT a ade2 his3 leu2 lys2 trp1 ura3 CHS6::URA3 (K. lactis) BUD7::LEU2 (K.lactis) BCH1::HIS5 (S. pombe)*	This study
YAS563-15α	*MAT α ade2 his3 leu2 lys2 trp1 ura3 CHS6::URA3 (K. lactis) BUD7::LEU2 (K.lactis) BCH1::HIS5 (S. pombe)*	This study
YAS563-16a	*MAT a ade2 his3 leu2 lys2 trp1 ura3 CHS6::URA3 (K. lactis) BUD7::LEU2 (K.lactis) BCH2::KAN (Tn903) BCH1::HIS5 (S. pombe)*	This study
YAS563-16α	*MAT α ade2 his3 leu2 lys2 trp1 ura3 CHS6::URA3 (K. lactis) BUD7::LEU2 (K.lactis) BCH2::KAN (Tn903) BCH1::HIS5 (S. pombe)*	This study
YAS776	*MAT a/α ade2/ade2 his3/his3 leu2/leu2 LYS2/lys2 TRP1/trp1 ura3/ura3 CHS5:: LEU2 (K. lactis)/CHS5:: LEU2 (K. lactis)*	This study
YAS778	*MAT a/α ade2/ade2 his3/his3 leu2/leu2 lys2/lys2 trp1/trp1 ura3/ura3 CHS6::URA3 (K. lactis)/CHS6::URA3 (K. lactis)*	This study
YAS779	*MAT a/α ade2/ade2 his3/his3 leu2/leu2 lys2/lys2 trp1/trp1 ura3/ura3 BUD7::LEU2 (K.lactis)/BUD7:: URA3 (K. lactis)*	This study
YAS780	*MAT a/α ade2/ade2 his3/his3 leu2/leu2 lys2/lys2 trp1/trp1 ura3/ura3 BCH2::KAN (Tn903)/BCH2::KAN (Tn903)*	This study
YAS781	*MAT a/α ade2/ade2 his3/his3 leu2/leu2 lys2/lys2 trp1/trp1 ura3/ura3 BCH1::HIS5 (S. pombe)/BCH1::HIS5 (S. pombe)*	This study
YAS793	*MAT a ade2 his3 leu2 lys2 trp1 ura3 CHS5:: LEU2 (K. lactis) ARF1::HIS3MX6*	This study
YAS794	*MAT a ade2 his3 leu2 lys2 trp1 ura3 CHS6::URA3 (K. lactis) ARF1:: HIS3MX6*	This study
YAS795	*MAT a ade2 his3 leu2 lys2 trp1 ura3 BUD7::LEU2 (K.lactis) ARF1:: HIS3MX6*	This study
YAS796	*MAT a ade2 his3 leu2 lys2 trp1 ura3 BCH2::KAN (Tn903) ARF1:: HIS3MX6*	This study
YAS797	*MAT a ade2 his3 leu2 lys2 trp1 ura3 BCH1::HIS5 (S. pombe) ARF1::KANMX6*	This study
YAS564	*MAT a/α ade2/ade2 his3/his3 leu2/leu2 lys2/lys2 trp1/trp1 ura3/ura3 BUD8::BUD8-6HA-TRP1 (K. lactis)/BUD8::BUD8-6HA-TRP1 (K. lactis)*	This study
YAS785	*MAT a/α ade2/ade2 his3/his3 leu2/leu2 lys2/lys2 trp1/trp1 ura3/ura3 BUD8::BUD8-6HA-TRP1 (K. lactis)/BUD8::BUD8-6HA-TRP1 (K. lactis) BUD7::LEU2 (K.lactis)/BUD7:: URA3 (K. lactis)*	This study
YAS565	*MAT a/α ade2/ade2 his3/his3 leu2/leu2 lys2/lys2 trp1/trp1 ura3/ura3 BUD9::BUD9-6HA-TRP1 (K. lactis)/BUD9::BUD9-6HA-TRP1 (K. lactis)*	This study
YAS789	*MAT a/α ade2/ade2 his3/his3 leu2/leu2 lys2/lys2 trp1/trp1 ura3/ura3 BUD9::BUD9-6HA-TRP1 (K. lactis)/BUD9::BUD9-6HA-TRP1 (K. lactis) BUD7::LEU2 (K.lactis)/BUD7:: URA3 (K. lactis)*	This study
YAS849	*MAT a/α ade2/ade2 his3/his3 leu2/leu2 lys2/lys2 trp1/trp1 ura3/ura3 BUD8::BUD8-3GFP-TRP1 (K. lactis)/BUD8::BUD8-3GFP-TRP1 (K. lactis)*	This study
YAS850	*MAT a/α ade2/ade2 his3/his3 leu2/leu2 lys2/lys2 trp1/trp1 ura3/ura3 BUD8::BUD8-3GFP-TRP1 (K. lactis)/BUD8::BUD8-3GFP-TRP1 (K. lactis) BUD7::LEU2 (K.lactis)/BUD7:: URA3 (K. lactis)*	This study
YAS855	*MAT a/α ade2/ade2 his3/his3 leu2/leu2 lys2/lys2 trp1/trp1 ura3/ura3 BUD9::BUD9-3GFP-TRP1 (K. lactis)/BUD9::BUD9-3GFP-TRP1 (K. lactis)*	This study
YAS856	*MAT a/α ade2/ade2 his3/his3 leu2/leu2 lys2/lys2 trp1/trp1 ura3/ura3 BUD9::BUD9-3GFP-TRP1 (K. lactis)/BUD9::BUD9-3GFP-TRP1 (K. lactis) BUD7::LEU2 (K.lactis)/BUD7:: URA3 (K. lactis)*	This study
YAS823	*MAT a/α ade2/ade2 his3/his3 leu2/leu2 lys2/lys2 trp1/trp1 ura3/ura3 RAX2::RAX2-GFP-KANMX6/ RAX2::RAX2-GFP-KANMX6*	This study
YAS827	*MAT a/α ade2/ade2 his3/his3 leu2/leu2 lys2/lys2 trp1/trp1 ura3/ura3 RAX2::RAX2-GFP-KANMX6/ RAX2::RAX2-GFP-KANMX6 BUD7::LEU2 (K.lactis)/BUD7:: URA3 (K. lactis)*	This study
YAS862	*MAT a ade2 his3 leu2 lys2 trp1 ura3 GAP1::GAP1-GFP (KANMX6)*	This study
YAS863	*MAT a ade2 his3 leu2 lys2 trp1 ura3 BCH1::HIS5 (S. pombe) GAP1::GAP1-GFP (KANMX6)*	This study

Table 6: Yeast strains used in chapter 3.4

Designation	Genotype	Reference
YPH499	*MAT a ade2 his3 leu2 lys2 trp1 ura3*	Sikorski and Hieter, 1989
YPH500	*MAT α ade2 his3 leu2 lys2 trp1 ura3*	Sikorski and Hieter, 1989
YPH501	*MAT a/α ade2/ade2 his3/his3 leu2/leu2 lys2/lys2 trp1/trp1 ura3/ura3*	Sikorski and Hieter, 1989
YAS325	*MAT a ade2 his3 leu2 lys2 trp1 ura3 CHS5::CHS5-6HA-TRP1 (K. lactis)*	Robert Gauss
YAS839	*MAT a ade2 his3 leu2 lys2 trp1 ura3 CHS5::CHS5-6HA-TRP1 (K. lactis) CHS6::URA3 (K. lactis) BUD7::LEU2 (K.lactis) BCH2::KAN (Tn903) BCH1::HIS5 (S. pombe)*	This study
YAS328	*MAT a ade2 his3 leu2 lys2 trp1 ura3 CHS6::CHS6-9myc-TRP1 (K. lactis)*	Robert Gauss
YAS606	*MAT α ade2 his3 leu2 lys2 trp1 ura3 CHS6::CHS6-6HA-TRP1 (K. lactis)*	This study
YAS594	*MAT α ade2 his3 leu2 lys2 trp1 ura3 CHS6::CHS6-Prot A-KanMX6*	This study
YAS595	*MAT α ade2 his3 leu2 lys2 trp1 ura3 CHS6::CHS6-GST-KanMX6*	This study
YAS596	*MAT α ade2 his3 leu2 lys2 trp1 ura3 CHS6::CHS6-yEGFP-KanMX6*	This study
YAS597	*MAT α ade2 his3 leu2 lys2 trp1 ura3 CHS6::CHS6-6His-3VSV-KanMX6*	This study
YAS335	*MAT a ade2 his3 leu2 lys2 trp1 ura3 BUD7::BUD7-9myc-TRP1 (K. lactis)*	Robert Gauss
YAS576	*MAT αade2 his3 leu2 lys2 trp1 ura3BUD7::BUD7-9myc-TRP1 (K. lactis)*	This study
YAS697	*MAT a/α ade2/ade2 his3/his3 leu2/leu2 lys2/lys2 trp1/trp1 ura3/ura3 BUD7::BUD7-9myc-TRP1 (K. lactis)/BUD7::BUD7-9myc-TRP1 (K. lactis)*	This study
YAS339	*MAT a ade2 his3 leu2 lys2 trp1 ura3 BCH1::BCH1-9myc-TRP1 (K. lactis)*	Robert Gauss
YAS844	*MAT α ade2 his3 leu2 lys2 trp1 ura3 BCH1::BCH1-3myc-His3MX6*	This study
YAS861	*MAT a ade2 his3 leu2 lys2 trp1 ura3 BCH1::BCH1-3HA-His3MX6*	This study
YAS598	*MAT α ade2 his3 leu2 lys2 trp1 ura3 BCH1::BCH1-GST-KanMX6*	This study
YAS599	*MAT α ade2 his3 leu2 lys2 trp1 ura3 BCH1::BCH1-yEGFP-KanMX6*	This study
YAS600	*MAT α ade2 his3 leu2 lys2 trp1 ura3 BCH1::BCH1-6His-3VSV-KanMX6*	This study
YAS659	*MAT α ade2 his3 leu2 lys2 trp1 ura3 BCH1::BCH1-2AU5-LEU2 (K. lactis)*	This study
YAS589	*MAT a ade2 his3 leu2 lys2 trp1 ura3 BCH2::BCH2-9myc-TRP1 (K lactis)*	This study
YAS603	*MAT a ade2 his3 leu2 lys2 trp1 ura3 BCH2::BCH2-3HA-His3MX6*	This study
YAS333	*MAT a ade2 his3 leu2 lys2 trp1 ura3 CHS6::CHS6-9myc-TRP1 (K. lactis) CHS5::LEU2 (K. lactis)*	Robert Gauss
YAS379	*MAT a ade2 his3 leu2 lys2 trp1 ura3 BUD7::BUD7-9myc-TRP1 (K. lactis) CHS5::LEU2 (K. lactis)*	Robert Gauss
YAS380	*MAT a ade2 his3 leu2 lys2 trp1 ura3 BCH1::BCH1-9myc-TRP1 (K. lactis) CHS5::LEU2 (K. lactis)*	Robert Gauss
YAS582	*MAT a ade2 his3 leu2 lys2 trp1 ura3 BCH2::BCH2-9myc-TRP1 (K lactis) CHS5::LEU2 (K. lactis)*	This study
YAS653	*MAT a ade2 his3 leu2 lys2 trp1 ura3 CHS6::CHS6-9myc-TRP1 (K. lactis) BUD7::LEU2 (K.lactis) BCH2::KAN (Tn903) BCH1::HIS5 (S. pombe)*	This study

YAS615	*MAT a ade2 his3 leu2 lys2 trp1 ura3 BUD7::BUD7-9myc-TRP1 (K. lactis) ura3 CHS6::URA3 (K. lactis) BCH2::KAN (Tn903) BCH1::HIS5 (S. pombe)*	This study
YAS614	*MAT a ade2 his3 leu2 lys2 trp1 ura3 BCH1::BCH1-9myc-TRP1 (K. lactis) CHS6::URA 3 (K. lactis) BUD7::LEU2 (K.lactis) BCH2::KAN (Tn903)*	This study
YAS654	*MAT a ade2 his3 leu2 lys2 trp1 ura3 BCH2::BCH2-9myc-TRP1 (K lactis) CHS6::URA3 (K. lactis) BUD7::LEU2 (K.lactis) BCH1::HIS5 (S. pombe)*	This study
YAS684	*MAT a ade2 his3 leu2 lys2 trp1 ura3CHS6::CHS6Δc-9myc-TRP1 (K. lactis)*	This study
YAS798	*MAT a ade2 his3 leu2 lys2 trp1 ura3BUD7::BUD7Δc-9myc-TRP1 (K. lactis)*	This study
YAS799	*MAT α ade2 his3 leu2 lys2 trp1 ura3 BUD7::BUD7Δc-9myc-TRP1 (K. lactis)*	This study
YAS802	*MAT a/α ade2/ade2 his3/his3 leu2/leu2 lys2/lys2 trp1/trp1 ura3/ura3 BUD7::BUD7Δc-9myc-TRP1 (K. lactis)/BUD7::BUD7-Δc-9myc-TRP1 (K. lactis)*	This study
YAS698	*MAT a ade2 his3 leu2 lys2 trp1 ura3 BCH1::BCH1Δc-9myc-TRP1 (K. lactis)*	This study
YAS800	*MAT α ade2 his3 leu2 lys2 trp1 ura3 BCH1::BCH1Δc-3HA-His3MX6*	This study
YAS801	*MAT α ade2 his3 leu2 lys2 trp1 ura3 BCH2::BCH2Δc-9myc-TRP1 (K lactis)*	This study
YAS792	*MAT a ade2 his3 leu2 lys2 trp1 ura3 BUD7::BUD7-9myc-TRP1 (K. lactis) CHS6::CHS6-yEGFP-KanMX6 BCH2::BCH2-3HA-HIS3MX6 BCH1::BCH1-2AU5-LEU2 (K. lactis)*	This study
YAS699	*MAT a ade2 his3 leu2 lys2 trp1 ura3BUD7::BUD7-9myc-TRP1 (K. lactis) CHS6::CHS6-yEGFP-KanMX6 BCH2::BCH2-3HA-HIS3MX6*	This study
YAS700	*MAT α ade2 his3 leu2 lys2 trp1 ura3 CHS6::CHS6-yEGFP-KanMX6 BCH1::BCH1-2AU5-LEU2 (K. lactis)*	This study
YAS604	*MAT a ade2 his3 leu2 lys2 trp1 ura3 BUD7::BUD7-9myc-TRP1 (K. lactis) BCH2::BCH2-3HA-His3MX6*	This study
YAS525	*MAT α ade2 his3 leu2 lys2 trp1 ura3 CHS6::URA3 (K. lactis) BCH2::KAN (Tn903)*	This study
YAS563-5a	*MAT a ade2 his3 leu2 lys2 trp1 ura3 BCH1::HIS5 (S. pombe)*	This study
YAS779	*MAT a/α ade2/ade2 his3/his3 leu2/leu2 lys2/lys2 trp1/trp1 ura3/ura3 BUD7::LEU2 (K.lactis)/BUD7:: URA3 (K. lactis)*	This study
YAS381	*MAT a ade2 his3 leu2 lys2 trp1 ura3 CHS5::CHS5-6HA-TRP1 (K. lactis) SEC7::SEC7-GFP-URA3*	Robert Gauss
YAS382	*MAT a ade2 his3 leu2 lys2 trp1 ura3 CHS6::CHS6-9myc-TRP1 (K. lactis) SEC7::SEC7-GFP-URA3*	Robert Gauss
YAS385	*MAT a ade2 his3 leu2 lys2 trp1 ura3 BUD7::BUD7-9myc-TRP1 (K. lactis) SEC7::SEC7-GFP-URA3*	Robert Gauss
YAS386	*MAT a ade2 his3 leu2 lys2 trp1 ura3 BCH1::BCH1-9myc-TRP1 (K. lactis) SEC7::SEC7-GFP-URA3*	Robert Gauss
YAS655	*MAT a ade2 his3 leu2 lys2 trp1 ura3 BCH2::BCH2-9myc-TRP1 (K lactis) SEC7::SEC7-GFP-URA3*	This study
YAS384	*MAT a ade2 his3 leu2 lys2 trp1 ura3 CHS6::CHS6-9myc-TRP1 (K. lactis) CHS5::LEU2 (K. lactis) SEC7::SEC7-GFP-URA3*	Robert Gauss
YAS387	*MAT a ade2 his3 leu2 lys2 trp1 ura3 BUD7::BUD7-9myc-TRP1 (K. lactis) CHS5::LEU2 (K. lactis) SEC7::SEC7-GFP-URA3*	Robert Gauss
YAS388	*MAT a ade2 his3 leu2 lys2 trp1 ura3 BCH1::BCH1-9myc-TRP1 (K. lactis) CHS5::LEU2 (K. lactis) SEC7::SEC7-GFP-URA3*	Robert Gauss
YAS656	*MAT a ade2 his3 leu2 lys2 trp1 ura3 BCH2::BCH2-9myc-TRP1 (K lactis) CHS5::LEU2 (K. lactis) SEC7::SEC7-GFP-URA3*	This study
YAS835	*MAT a ade2 his3 leu2 lys2trp1 ura3CHS6::CHS6Δc-9myc-TRP1 (K. lactis) SEC7::SEC7-GFP-URA3*	This study
YAS836	*MAT a ade2 his3 leu2 lys2 trp1 ura3BUD7::BUD7Δc-9myc-TRP1 (K. lactis) SEC7::SEC7-GFP-URA3*	This study
YAS837	*MAT a ade2 his3 leu2 lys2 trp1 ura3 BCH1::BCH1Δc-9myc-TRP1 (K. lactis) SEC7::SEC7-GFP-URA3*	This study
YAS838	*MAT α ade2 his3 leu2 lys2 trp1 ura3 BCH2::BCH2Δc-9myc-TRP1 (K lactis) SEC7::SEC7-GFP-URA3*	This study

Table 7: Oligonucleotide primers used in chapter 3.2

Designation	Sequence	Purpose
MT-A3	TATGAAGGTTTGGAATGGTTAAGTAACAGTTTGAAAAACTCAACT CGTACGCTGCAGGTCGAC	ARF1-tagging, pYM
MT-A4	TTCATTTAGTTTATACAAGCGTATTTGATCCATATTCTA GAATTT ATCGATGAATTCGAGCTCG	ARF1-tagging, pYM
MT-A16	TATGAAGGTTTGGAATGGTTAAGTAACAGTTTGAAAAACTCAACT GGTCGACGGATCCCCGGG	ARF1-tagging, pDH
MT-A17	TTCATTTAGTTTATACAAGCGTATTTGATCCATATTCTAGAATTT ATCGATGAATTCGAGCTCG	ARF1-tagging, pDH
MT-A26	TATGAGTCTTTCAAAAAGGA GCAAGAACAACAAACTGAGCAAGCT CGTACGCTGCAGGTCGAC	PAB1-tagging, pYM
MT-A27	GATGATAAGTTTGTTGAGTAGGGAAGTAGGTGATTACATAGAGCA ATCGATGAATTCGAGCTCG	PAB1-tagging, pYM
MT-A18	TATGAGTCTTTCAAAAAGGAGCAAGAACAACAAACTGAGCAAGCT GGTCGACGGATCCCCGGG	PAB1-tagging, pDH
MYO4-tag-F	TTAGCTACTGTCAGTAAAATTATAAAATTAGACAGAAAA tcc ggt tct gct gct agt	MYO4-tagging with 2GFP
MYO4-tag-R	ATACATATATACATATATGGGCGTATATTTACTTTGTTC tta cct cga ggc cag aag act	MYO4-tagging with 2GFP
MT-A19	GATGATAAGTTTGTTGAGTAGGGAAGTAGGTGATTACATAGAGCA ATCGATGAATTCGAGCTCG	PAB1-tagging, pDH
MT-A41	GGAAAAGGATGCTGATGGAA	PAB1-tagging control
MT038	CCAGCCCAAATACAAGCAAT	MYO4-tagging control
MT039	GGTCAGAAAAGCCATGTGGT	MYO4-tagging control
MT-A5	TTGAAGGTATAAGAAAGAACTCAAACAGGTTTAATAGAATTAAAA CGTACGCTGCAGGTCGAC	ARF1-deletion
MT-A6	TTCATTTAGTTTATACAAGCGTATTTGATCCATATTCTAGAATTT ATCGATGAATTCGAGCTCG	ARF1-deletion
MT-A7	CGAATTGAGCGTTTCTGACA	ARF1-deletion and tagging control
MT-A8	TTGGCTGGTGATCGTCAATA	ARF1-deletion and tagging control
MT-A12	ATT CCG GAA TTC gct gat att act gat aag aca	Two-hybrid-cloning PAB1
MT-A13	TAT CCG CTC GAG tta agc ttg ctc agt ttg ttg	Two-hybrid-cloning PAB1
MT-A14	ATT CCG GAA TTC tct gaa aat aac gaa gaa caa	Two-hybrid-cloning PUB1
MT-A15	TAT CCG CTC GAG tct tca taa tat tta ttg ttg	Two-hybrid-cloning PUB1
MT-A33	ATGTGTCGCCAATTCTTTCC	ASH1 RT-PCR
MT-A34	TGGTGAATTGCCTGGTGTTA	ASH1 RT-PCR
MT-A35	AGCTTTTGCCAGATGGTGAC	IST2 RT-PCR
MT-A36	TAGTGGCAGCATCGTCTTTG	IST2 RT-PCR
MT-A37	gccctaatgcaaggtcaaaa	SIC1 RT-PCR
MT-A38	gttcgaattgggaggtgcta	SIC1 RT-PCR
MT-A39	aaacgttgatgacaccgtga	ADH1 RT-PCR
MT-A40	gacggtggtgaaggtaagga	ADH1 RT-PCR
MT022	AGAGTTGCCCCAGAAGAACA	ACT1 RT-PCR
MT023	GGCTTGGATGGAAACGTAGA	ACT1 RT-PCR

MT024	ATGGCTTGGGAAGATGTCAG	PFK1 RT-PCR
MT025	GCGTCAATACCTTGCGAAAT	PFK1 RT-PCR
MT026	CTTAACTTCCGGCCACTTGA	GPD1 RT-PCR
MT027	GCAACCACCTTGGCAATAGT	GPD1 RT-PCR
MT030	CCAGCTGAGCTTTTGAATCC	PCK1 RT-PCR
MT031	TCTGGTGTGGCTCTGTCTTG	PCK1 RT-PCR
MT-A31	TTTTCCTATCGCTCCTGTCC	ASH1 *in situ* RNA antisense-probe
MT-A32	TAATACGACTCACTATAGGGAGACTTCGAAATGGG CGAAAATA	ASH1 *in situ* RNA antisense-probe
MT113	TAACACCAGGCAATTCACCA	ASH1-probe Northern blot
MT114	GTGGAGGGAGATGGAGATGA	ASH1-probe Northern blot
MT115	ACGAATCCCACGGTAAGTTG	ADH1-probe Northern blot
MT116	GACAAGCCGACAACCTTGAT	ADH1-probe Northern blot
MT-A22	CACC GCTGATATTACTGATAAGACAGCTGAA	PAB1 pET100-D cloning
MT-A23	AAAAACGTTTGCATTTTGTCA	PAB1 pET100-D cloning

Table 8: General oligonucleotide primers

Designation	Sequence	Purpose
KAN&HIS-Primer	TGGGCCTCCATGTCGCTGG	pYM-tagging control
TRP-Primer	GCTATTCATCCAGCAGGCCTC	pYM-tagging control
1MAT	AGT CAC ATC AAG ATC GTT TAT GG	Mating type PCR
2MAT-alpha	GCA CGG AAT ATG GGA CTA CTT CG	Mating type PCR
3MAT-a	ACT CCA CTT CAA GTA AGA GTT TG	Mating type PCR

Table 9: Oligonucleotide primers used in chapter 3.3

Designation	Sequence	Purpose
RG084	GCGTAGATGCTAAATGTTATCGCGGTTTAGCTTGCATGTTACGTTCCAGCTGAAGCTTCGTACGTGC	CHS5 deletion, pUG
RG085	GCTTGGCGGCTACTGAGTACCCCTCTCAAGAAAATGAAGTGATCGCATAGGCCAACTAGTGGATC	CHS5 deletion, pUG
MT042	TTTCTTAAGCTGTTGGTGCAAAAAAGGATTACATCTATTGCCCTT CAG CTG AAG CTT CGT ACG C	CHS6 deletion, pUG
MT043	TCCAACCGTAGTGGTTATATAATAATACTAAGAGCACCGTTTTGT GCA TAG GCC ACT AGT GGA TCT G	CHS6 deletion, pUG
MT-A9	TGAGC GCAAAAAAAT AAAGAACTAA GGAAGAAGAG C TTCCCTCAG CAG CTG AAG CTT CGT ACG C	BUD7 deletion, pUG
MT-A10	TCGAAACTTTGGTCAGACTCATATCTTGAATAACCACACTTAAAC GCA TAG GCC ACT AGT GGA TCT G	BUD7 deletion, pUG
RG060	CTCAATTCATCTTCTTGAGAGCACTTTCCGCCAGCTGAAGCTTCGTACGTGCAGGT	YMR237w deletion, pUG
RG061	GGGTTATACTCAGTTTCGCTTTACGCGGATCATAGGCCAACTAGTGGATCTGATA	YMR237w deletion, pUG
RG092	GTATAAGTAGTAAAGTACAGTTAACAGATCAATTGGCCTCGAGGAATCCAGCTGAAGCTTCGTACGTGC	YKR027w deletion, pUG
RG093	GGATATTACCCGCGCTAAAGTATTAGCATTATCGCCGTAAATTTGCATAGGCCAACTAGTGGATC	YKR027w deletion, pUG
MT-A5	TTGAAGGTATAAGAAAGAACTCAAACAGGTTTAATAGAATTAAAA CGTACGCTGCAGGTCGAC	ARF1 deletion, pYM
MT-A6	TTCATTTAGTTTATACAAGCGTATTTGATCCATATTCTAGAATTT ATCGATGAATTCGAGCTCG	ARF1 deletion, pYM
RG088	CGGTCGGCCCTTCAAGTTCTCC	CHS5 deletion control
RG089	CGTTTTCGTAGAGCGCGACGG	CHS5 deletion control
RG090	GGTACTCCCTAGCACCCCAAGC	CHS6 deletion control
RG091	CCCTTATCAAGCAGATCTGG	CHS6 deletion control
MT-A11	AGCGTCACGTGAACACATTC	BUD7 deletion control
RG046	AATCGTTCACGCTGGATCAT	BUD7 deletion control
RG078	GCCGGCAGTGGATTAGGAGT	YMR237w deletion control
RG079	GAATTAACGCTGTCGCATCAC	YMR237w deletion control
RG096	GGTTTCCGAGGCATTGTTACACCG	YKR027w deletion control
RG098	GCTAAAGTATTAGCATTATCGCCG	YKR027w deletion control
MT-A7	CGAATTGAGCGTTTCTGACA	ARF1 deletion control
MT-A8	TTGGCTGGTGATCGTCAATA	ARF1 deletion control
MT044	ATGGCCGGTATTGCTATTGGATTTGGTGTGGGTATAACACGTGAA CGTACGCTGCAGGTCGAC	BUD8 tagging, pYM
MT045	AACAGTTTTTTATTTTTTATCCTATTTGATGAATGATACAGTTTC ATCGATGAATTCGAGCTCG	BUD8 tagging, pYM
MT046	TTTGCTAGCATAGGAATAGG ATTTGGTGTGGGAATAATAAGAGAG CGTACGCTGCAGGTCGAC	BUD9 tagging, pYM
MT047	ATAGAGAGTAGCAGGAAATCTTCGACGAGTAAGTCCAGCATGGAG ATCGATGAATTCGAGCTCG	BUD9 tagging, pYM
MT048	GTGGTTCCGGATGTTTTGTC	BUD8 tagging control
MT049	CGCTATGGCCACTGAAAAAT	BUD8 tagging control

MT050	TCCTCAAAGGGTTTGAATGG	BUD9 tagging control
MT051	TCGTGAAATGGGCTAGCTTT	BUD9 tagging control
MT091	GCCGCATTCACAGTTATTTTCAGCTGTGTTCCCGGCCGTCGTGTA CGTACGCTGCAGGTCGAC	RAX1 tagging, pYM
MT092	AATATGCGGTGCACAGGTGTTTTTATAGGGGGGTGATGGATTACA ATCGATGAATTCGAGCTCG	RAX1 tagging, pYM
MT093	GAAATGCTTGATACCGTCCCACCCGAAAAACTTATGAAGTTTGTC CGTACGCTGCAGGTCGAC	RAX2 tagging, pYM
MT094	TGTTCATTATTTTAAGTAGTTATATATTATATAATACAACCCCGA ATCGATGAATTCGAGCTCG	RAX2 tagging, pYM
MT095	CGATCACGTGCCAATGATAC	RAX1 tagging control
MT096	TTCCGCGAGAGGTGATAAGT	RAX1 tagging control
MT097	AACCGCGAATTGATGAGAAT	RAX2 tagging control
MT098	CATTTTTCATGGCTTCACCA	RAX2 tagging control
MT105	ATGGCCACAAAGCCAAGATGGTATAGAATCTGGAATTTCTGGTGT CGTACGCTGCAGGTCGAC	GAP1 tagging, pYM
MT106	TGATTATCTAAAAAATAAAGTCTTTTTTTGTCGTTGTTCGATTCA ATCGATGAATTCGAGCTCG	GAP1 tagging, pYM
MT107	AAGCTTTTCATCCCAGCAGA	GAP1 tagging control
MT108	AATGCGGGGAAATCATATTG	GAP1 tagging control
MT001	TCCC CCC GGG GAAGGACAAGGTGCCAGGTA	CHS6 cloning in pRS315 and 425
MT002	GGA CCG CGG CCTTACCCTCAGTCCATCCA	CHS6 cloning in pRS315 and 425
MT003	TCCC CCC GGG GTGGTTCTCTTGGTCGGGTA	BUD7 cloning in pRS315 and 425
MT004	GGA CCG CGG GAAGCGTATCGCCAATTTTT	BUD7 cloning in pRS315 and 425
MT005	TCCC CCC GGG CCGGCAGTGGATTAGGAGTA	YMR237w cloning in pRS315 and 425
MT006	GGA CCG CGG CCCGTTTCTTGTTAATTGATTTC	YMR237w cloning in pRS315 and 425
MT007	TCCC CCC GGG TTCACAATGGAACCCAACAA	YKR027w cloning in pRS315 and 425
MT008	GGA CCG CGG TCGCCGTAAATTTGTCCATT	YKR027w cloning in pRS315 and 425
MT056	GG ACTAGT TTCCATGGCAAGTTCCTACC	FUS1 cloning in pUG35
MT057	CCC AAGCTT GTCGTATTCTTGGAGACAGTCA	FUS1 cloning in pUG35
MT-A20	CACC TCTTCAGTTGATGTACTGTTAACAGTAGGT	CHS5 pET100-D cloning
MT-A21	GGAACTCATTGAAGGCATCC	CHS5 pET100-D cloning

Table 10: Oligonucleotide-primers used in chapter 3.4

Designation	Sequence	Purpose
RG066	AATAAGAAGAAGAATAAGAAGAATAAGAAGAAA GGGAAAAAGAAACGTACGCTGCAGGTCGAC	Chs5p tagging, pYM
RG067	AAAAAATAAACGTGCGTCGTGGAACTCATTGAAGGCATCCATTAAATCGATGAATTCGAGCTCG	Chs5p tagging, pYM
RG068	GCCATGCTTGCGTGGATAGCCGACCTAGATCACACAGTACAACCTCGTACGCTGCAGGTCGAC	Chs6p tagging, pYM
RG069	TCCAACCGTAGTGGTTATATAATAATACTAAGAGCACCGTTTTGTATCGATGAATTCGAGCTCG	Chs6p tagging, pYM
RG070	TTGCTCAATTTCTTCACTACTTGCACCATTGGATGCTACGATGCACGTACGCTGCAGGTCGAC	Bud7p tagging, pYM
RG071	ATTTTTTTTGGATTATATATACGTATTAATGTCTTTTTATCGTATATCGATGAATTCGAGCTCG	Bud7p tagging, pYM
RG072	ATTCTAAATTTTCTGAAGAATTTCACGAATGACACTTTCGATAATCGTACGCTGCAGGTCGAC	Bch1p tagging, pYM
RG073	TTAATTGATTTCTTTCACCTTTTTATTGATTGTATTCATCTTTTTATCGATGAATTCGAGCTCG	Bch1p tagging, pYM
RG094	CGCCCTCTTCCAGATCTTCCTTCCACTATCAAACCTCTGGCAGACCGTACGCTGCAGGTCGAC	Bch2p tagging, pYM
RG095	CACACACAGTATATATATATAGATTCATTAAATCAATTTGATCAGATCGATGAATTCGAGCTCG	Bch2p tagging, pYM
MT064	GCCATGCTTGCGTGGATAGCCGACCTAGATCACACAGTACAACCT TCC CAC CAC CAT CAT CAT CAC	Chs6p tagging, pU6H3VSV; MT043
MT065	ATTCTAAATTTTCTGAAGAATTTCACGAATGACACTTTCGATAAT CAC CAC CAT CAT CAT CAC	Bch1p tagging, pU6H3VSV
MT066	TTAATTGATTTCTTTCACCTTTTTATTGATTGTATTCATCTTTTT ATA GGG AGA CCG GCA GAT	Bch1p tagging, pU6H3VSV
MT075	ATTCTAAATTTTCTGAAGAATTTCACGAATGACACTTTCGATAAT ACTGATTTTTATCTAAAA GGT ACTGATTTTTATCTAAAA TAA CAG CTG AAG CTT CGT ACG C	Bch1p tagging with 2xAU5; pUG73; MT066
MT077	CAACCTTCCATAGGAGACGAAATCATGGTCATGATCGATGCCATG CGTACGCTGCAGGTCGAC	Chs6p, c-terminal deletion + tagging, pYM
MT078	TGTTCAAGGTTGTACTGTGTGATCTAGGTCGGCTATCCACGCAAG ATCGATGAATTCGAGCTCG	Chs6p, c-terminal deletion + tagging, pYM
MT089	TCAAGATATCCAGAAACTGTTCTCAACTTGGTGCAGGAGAATTTG CGTACGCTGCAGGTCGAC	Bud7p, c-terminal deletion + tagging, pYM
MT090	TTATGCATCGTAGCATCCAATGGTGCAAGTAGTGAAGAAATTGAG ATCGATGAATTCGAGCTCG	Bud7p, c-terminal deletion + tagging, pYM
MT079	TCTAGATTTTCTGACCCAGTAGCCCAATTGATTGACGATAACATT CGTACGCTGCAGGTCGAC	Bch1p, c-terminal deletion + tagging, pYM
MT080	CTAATTATCGAAAGTGTCATTCGTGAAATTCTTCAGAAAATTTAG ATCGATGAATTCGAGCTCG	Bch1p, c-terminal deletion + tagging, pYM
MT087	TCTCCTTACGGGCAAGCTGGCATCACTTCGGTGATAGATTATATG CGTACGCTGCAGGTCGAC	Bch2p, c-terminal deletion + tagging, pYM
MT088	ATAGGCTAGGCAGGCTTCATTCCTATTTTTAGAGAGGCATTCAAG ATCGATGAATTCGAGCTCG	Bch2p, c-terminal deletion + tagging, pYM
RG041	GAGGCCTCTGCTTCTCTTGA	Chs5p tagging control
RG042	CGGCAAAAATAACGGGTAAA	Chs5p tagging control
RG043	CAGCGGATTAGAGTGGGAAC	Chs6p tagging control
RG044	TTTGCGTACCTTTCCCAAAT	Chs6p tagging control
RG045	GCGAGGAAACTGCTGGAATA	Bud7p tagging control
RG046	AATCGTTCACGCTGGATCAT	Bud7p tagging control
RG047	GGGAATTATTCGGCCTTTGT	Bch1p tagging control
RG048	GTTTCGCTTTACGCGGATTA	Bch1p tagging control
RG097	CCCGATGCAGTAGCGTGTCTACG	Bch2p tagging control
RG098	GCTAAAGTATTAGCATTATCGCCG	Bch2p tagging control

2.8 Biochemical Methods

2.8.1 Determination of yeast cell density

1 OD_{600} corresponds to $2.75 \cdot 10^7$ yeast cells per ml on the spectrophotometer DU 640 (Beckman). For OD_{600} measurements, cells were diluted to yield an OD_{600} of no more than 0.5. Unless otherwise indicated, logarithmically growing cells were harvested at an OD_{600} of no more than 0.5.

2.8.2 Preparation of yeast total cell extract

2 OD_{600} of yeast cells were harvested and resuspended in 150 µl 5x Laemmli-buffer (65°C, including 1 mM PMSF). Approximately 120 µl glass beads were added. After vigorous vortexing for 5 min, samples were incubated for 5 min at 65°C followed by 1 min of vortexing. Cell debris and glass beads were sedimented (2 min, 20,000 g, 4°C) and the supernatant was transferred to a fresh reaction tube. For subsequent analysis by SDS-PAGE and immunoblotting, 5 µl of the lysate were used.

For comparison of protein expression levels in different mutants grown at non-permissive temperature, the following procedure was used: 2 OD_{600} cells were resuspended in 150 µl lysis buffer and lysed by vortexing for 10 min at 4°C with roughly 120 µl glass beads. The crude lysate obtained after settling of the beads was centrifuged for 10 min at 20,000 g at 4°C. The supernatant contained soluble proteins. The lysates were normalized to equal total protein concentration using the Biorad protein assay.

Lysis buffer
50 mM Tris/HCl pH 7.5
1 mM EDTA
50 mM DTT
PMSF, Pepstatin A, Leupeptin

2.8.3 Preparation of yeast cytosol

Yeast cytosol was prepared as described before (Spang and Schekman, 1998). Usually, 3 l of mid-logarithmic liquid culture (OD_{600} between 1.0 and 1.5) were harvested (5 min, 5,000 rpm, GS3-rotor, 4°C) and washed once in water. The cell pellet was resuspended in 2 ml B88 and slowly pipetted into liquid nitrogen to allow small beads to form. Cell beads were either stored at –70°C or immediately processed. Lysis of cells occurred under liquid nitrogen in a mortar (placed on dry ice) in which the cells were ground for approximately 30 min. Alternatively, a blender was used for 15 min. The resulting fine powder was

thawed in an ice/water bath and supplemented with the same volume of B88. After a pre-clearing step (10 min, 8,000 rpm, GS3-rotor, 4°C), the lysate was spun at 100,000 g (60 min, 39,000 rpm, Ti 50.2-rotor, 2°C). The supernatant was carefully collected avoiding the lipid layer on top. The protein concentration was measured by Biorad protein assay. Aliquots were frozen in liquid nitrogen and stored at –70°C.

2.8.4 Preparation of enriched Golgi membranes from yeast

For the preparation of enriched Golgi-membranes from yeast (Spang and Schekman, 1998), cells were grown to an OD_{600} of no more than 0.5 (early to mid-logarithmic growth phase). Usually, 3 l of liquid culture were harvested (5 min, 5,000 rpm, GS3-rotor, 4°C) and washed once in water. The cell pellet was resuspended in 2 ml B88 and slowly pipetted into liquid nitrogen to allow small cell beads to form. Cells were either stored at –70°C or immediately processed. Lysis of cells occurred under liquid nitrogen in a mortar (placed on dry ice) in which the cells were ground for approximately 30 min. The resulting fine powder was thawed in an ice/water bath and supplemented with the same volume of B88 (supplemented with 1 mM DTT and 1mM PMSF). The lysate was pre-cleared by centrifugation with 3,000 g (2 min, 5,000 rpm, SS34-rotor, 4°C). The supernatant was collected and centrifuged twice at 27,000 g (15 min, 15,000 rpm, SS34-rotor, 4°C). The ER-free supernatant was loaded on a 60% (w/w) sucrose cushion (in 20 mM HEPES/KOH pH 6.8) and spun at 100,000 g (30 min, 25,000 rpm, SW28-rotor, 4°C). The membranes were carefully collected at the interface and diluted again to the initial volume before ultra-centrifugation in order to wash away cytosolic contaminants. The ultra-centrifugation step was repeated and the enriched Golgi-membranes were collected at the interface. The protein concentration was determined by the Biorad DC protein assay. Aliquots were frozen in liquid nitrogen and stored at –70°C.

2.8.5 Protein determination

The determination of protein concentrations of detergent-free solutions were performed using the Biorad protein assay, which is based on the Bradford method (Bradford, 1976). Bovine γ-globulin served as protein standard. For detergent-containing solutions, the detergent-compatible Biorad DC protein assay was used which is based on the Lowry method (Lowry *et al.*, 1951). In this case, bovine serum albumin served as standard. For relative determination of peptide amounts in order to estimate peptide coupling efficiencies, the BCA-asssay from Piece was used which is based on the BCA-method

(Smith *et al.*, 1985). All determinations were performed according to the manufacturer's recommendations.

2.8.6 Trichloro acetic acid precipitation

TCA-precipitations of proteins were conducted essentially as described (Bensadoun and Weinstein, 1976). 1/10 volume of 100% (w/v) TCA (4°C) was added to the ice-cold protein solution. After incubation on ice for 30 min, the sample was centrifuged for 15 min (14.000 rpm, Eppendorf 5417 R, 4°C). The pellet was washed with 1 ml acetone (-20°C) and sedimented again. After aspiration of the acetone, the pellet was dried for approximately 5 min at 65°C and dissolved in a smaller volume of 100 mM Tris pH 8.0.

2.8.7 SDS-PAGE

For the discontinuous, denaturing SDS-polyacrylamide-gel-electrophoresis (Davis, 1964; Ornstein, 1964; Laemmli, 1970), both mini-gels (8 cm x 6.5 cm x 0.075 cm) as well as large gels (14.5 cm x 10 cm x 0.1 cm with 0.8% agarose used for sealing) were used. In both instances, the stacking gel was 4%. The percentage of the separation gel was chosen according to the analytical problem. The protein samples to be analyzed were complemented by 1/2 volume of 5x Laemmli-buffer, incubated at 65°C for 5 – 10 min and spun shortly. The separation was performed at constant current (25 mA for mini-gels, 50 mA for large gels). Examples of standard gel compositions are given.

Table 11: Composition of 12.5% SDS-mini-gels, sufficient for 13 gels.

	12.5% separation gel	4% stacking gel
Acrylamide 29.2%/Bisacrylamide 0.8%	25 ml	5 ml
1.5 M Tris/HCl pH 8.0	15 ml	---
0.5 M Tris/HCl pH 6.8	---	7,5 ml
10% SDS	300 µl	150 µl
H_2O	19.5 ml	17.1 ml
TEMED	40 µl	36 µl
10% APS	400 µl	240 µl

Table 12: Composition of large 10% SDS-gels, sufficient for 2 gels.

	10% separation gel	4% stacking gel
Acrylamide 29.2%/Bisacrylamide 0.8%	12 ml	1.25 ml
1.5 M Tris/HCl pH 8.0	9 ml	---
0.5 M Tris/HCl pH 6.8	---	1.9 ml
10% SDS	180 µl	37.5 µl
H_2O	14.7 ml	4.3 ml
TEMED	15 µl	9 µl
10% APS	180 µl	60 µl

SDS-PAGE running buffer
25 mM Tris
192 mM glycine
0.1% SDS

2.8.8 Coomassie-Blue staining of polyacrylamide gels

Polyacrylamide gels were routinely stained after electrophoresis for 15 min in Coomassie-staining solution at room temperature (Meyer and Lamberts, 1965). Destaining of the gels was usually performed overnight in destaining solution at 4°C. The gels were equilibrated in water and dried for documentation.

Coomassie-staining solution
7.5% acetic acid
50% methanol
0.25% Serva Brillant Blue R250

Destaining solution
7.5% acetic acid
50% methanol

2.8.9 Colloidal Cooomassie-Blue staining of polyacrylamide gels according to Fairbanks

For improved sensitivity, especially if protein bands were to be cut out for protein identification by mass spectrometry, the polyacrylamide gels were stained using the Fairbanks method (Fairbanks *et al.*, 1971). The gels were agitated gently for 1 h in destaining solution. Staining was performed overnight in solution A. The destaining was accomplished by stepwise incubation for 1 h in solution B, 1 h in solution C and finally by incubation in solution D until the background was completely removed.

Solution A
25% isopropanol
10% acetic acid
0.05% Serva Brillant Blue G250

Solution B
25% isopropanol
10% acetic acid
0.005% Serva Brillant Blue G250

Solution C
10% actetic acid
0.002% Serva Brillant Blue G250

Solution D
10% acetic acid

Destaining solution
7.5% acetic acid
50% methanol

2.8.10 Silver staining of polyacrylamide gels

The staining was performed essentially as described (Blum *et al.*, 1987). The different steps are listed in table 13.

Table 13: Silver staining procedure

Step	Solution*	Time scale
Fixation	70% MetOH, 0,037% HCHO	≥ 10 min
Washing step	H_2O	2 x 5 min
Sensitizing	0,02% $Na_2S_2O_3$	1 min
Washing step	H_2O	2 x 20 s
Silver staining	0.1% $AgNO_3$	≥ 30 min
Washing step	H_2O	2 x 20 s
Developing	3% Na_2CO_3, 0.0004% $Na_2S_2O_3$, 0.037% HCHO	3 – 10 min
Stop	10% HAc	10 min

*except for 70% MetOH, the 2% $Na_2S_2O_3$-stock solution, and the 3% Na_2CO_3, everything was prepared freshly.

2.8.11 Blue Native PAGE

The Blue Native PAGE was performed as described before (Schagger and von Jagow, 1991; Schagger, 2001). The separation of proteins occurred with the aid of 4 – 20.5% large gradient polyacrylamide gels. The gels were cast with the help of a gradient mixer. The compositions of gradient gels and buffers used are given in table 14.

To prepare yeast lysates, 10 OD_{600} of yeast cells were incubated in 2 ml DTT-buffer (10 mM Tris/HCl pH 9.4, 10 mM DTT) for 5 min at 30°C. The buffer was replaced by 2 ml SP-buffer (76% YPD, 0.7 M sorbitol, 10 mM Tris/HCl pH 7.5) and supplemented with 30 µl Zymolyase T-20 (10 mg/ml). The cells were spheroplasted for 40 min at 30°C. The

spheroplasts were sedimented (3 min, 1,000 g) and lysed in 0.5 ml BNP-solubilization buffer. After solublization for 3 min at RT, the lysate was cleared by centrifugation (10 min, 14,000 rpm, Eppendorf 5417 R, 4°C). 25 µl 50% glycerol were added to 100 µl of the supernatant . The samples were immediately loaded onto a 4 – 20.5% Blue Native gradient gel. 20 µl of each sample were loaded and BSA (66 kDa, 132 kDa), Apoferritin (443 kDa) and Thyroglobin (667 kDa) served as molecular weight markers. Electrophoresis was performed initially for 75 min at 100 V/15 mA, and then for further 165 min at 500 V/15 mA (both steps at 4°C). The gel was briefly washed in electrode buffer and the proteins were transferred to a PVDF-membrane using the semi-dry method (at 4°C, 20 V for 150 min or overnight). The membrane was processed as usual for immunoblots except that unspecific binding sites were blocked for at least 12 h in 5% non-fat milk in TBS.

Table 14: Composition of a 4% - 20.5% Blue native polyacrylamide gradient gel.

	Sample gel	Gradient separation gel	
	4% T	4% T	20.5% T
AB-Mix	0.33 ml	0.92 ml	3.75 ml
3x gel buffer	1.33 ml	3.67 ml	3 ml
H_2O	2.33 ml	6.4 ml	-
50% glycerol			2.25 ml
TEMED	40 µl	60 µl	40 µl
10% APS*	4 µl	6 µl	4 µl
	4 ml	11 ml	9 ml

* prepared freshly

AB-Mix (49.5% T, 3% C)
48% (w/v) acrylamide
1.5% (w/v) bisacrylamide
filtered

3x gel buffer
75 mM imidazole/HCl pH7.0
1.5 M 6-aminohexanoic acid

SB cathode buffer
50 mM Tricine
7.5 mM imidazole
(resulting pH is around 7.0)
0.002% Serva blue G250

Electrode buffer (for semi-dry transfer)
25 mM tricine
7.5 mM imidazole
(resulting pH is around 7.0)

Anode buffer
25 mM imidazole/HCl pH 7.0

2.8.12 Immunoblots

Generally, proteins were transferred onto nitrocellulose or PVDF membranes, depending on the analytical problem. The transfer was usually carried out using the wet-blot method (Towbin *et al.*, 1979). Alternatively, for low molecular weight proteins (< 80 kDa), the faster semi-dry method was employed (Kyhse-Andersen, 1984). In either method, a sandwich is assembled consisting of the gel, the membrane and 3 gel blotting papers on each side. The proteins are electro-transferred in transfer buffer (wet-blot: 3 h at RT or overnight at 4°C, 30 V/250 mA; semi-dry: 45 min at RT, 15 V/2 A).

After the transfer, the nitrocellulose was stained in Ponceau S solution for 1 min (optionally). The background was removed by washes in water. Complete destaining was accomplished by incubation in TBS. The PVDF membrane was stained in colloidal Coomassie-solution for 5 min. The background was removed by washes in destain solution. Complete destaining was obtained by incubation in methanol.

Unspecific binding sites were blocked by incubation for 1 h in 5% milk (non-fat milk powder in TBS; 0.02% NaN_3). The membrane was decorated with primary antibodies diluted usually in 5% milk for 1 h at RT or overnight at 4°C. The membrane was washed in TBST (3 x brief washes, 1 x 15 min, 3 x 5 min). The secondary antibody coupled to horseradish-peroxidase was diluted in TBST and incubated for 1 h at RT. After repeated washes in TBST, the signals were detected using either the ECL, ECL+ or ECL advance system (Amersham Bioscience) according to the manufacturer's recommendations. The chemoluminescence was reported on ECL hyperfilms employing different exposure times.

Transfer buffer:
25 mM Tris
192 mM glycine
0.25% SDS
20% methanol

2.8.13 Purification of recombinant Arf1p proteins with His_6-tag from *E. coli*

For the purification of ΔN17-Arf1p, ΔN17-Arf1p-Q71L or ΔN17-Arf1p-T31N, *E. coli* stocks were freshly streaked out. 50 ml of LBamp were inoculated with a single colony and incubated overnight at 37°C. 1.5 l LBamp were inoculated with the overnight culture and after 2 h of growth at 37°C, protein expression was induced by addition of 1 mM IPTG. After incubation for additional 3 h at 37°C, cells were harvested (10 min 6,000 rpm, GS-3 rotor, 4°C) and washed in STE-buffer (10 min, 10,000 rpm, SS34-rotor, 4°C). The cell pellet was frozen in liquid nitrogen and stored at –70°C.

The cell pellet was thawed on ice and resuspended in 20 ml STE-buffer. Lysozyme was added to 1 mg/ml final concentration and the suspension was gently agitated for 15 min at RT. After addition of 8 ml of cold Triton buffer, the cells were sonified with several 15 s pulses and intermittent incubations on ice. The lysis was checked under the microscope and the cell debris was removed by centrifugation (15 min, 20,000 rpm, SS34, 4°C). 2.5 ml of pre-equilibrated Ni-NTA-agarose slurry (30 min in 20 ml binding buffer at RT) were added to the supernatant and agitated for 1 h at 4°C. The Ni-NTA-agarose was sedimented (2 min, 4,000 rpm, Eppendorf 5810 R, 4°C) and washed with 3 x 10 ml binding buffer. The last suspension was transferred to a Polyprep column (Biorad). The proteins were eluted with 10 x 1 ml elution buffer. Fractions were analyzed by SDS-PAGE and Coomasie-blue staining, protein-containing fractions were pooled and dialyzed twice (2.5 l dialysis buffer, at least 6 h each). The protein concentration was determined and aliquots were frozen in liquid nitrogen and stored at –70°C.

Triton buffer
50 mM Tris/HCl pH 8.0
0.2% Triton X-100
100 mM $MgCl_2$

Binding buffer
20 mM HEPES/NaOH pH 7.4
1 mM $MgCl_2$
1 mM DTT
200 mM KCl
20 mM imidazole

Dialysis buffer
20 mM HEPES/NaOH pH 7.4
1 mM EDTA
100 mM NaCl
1 mM DTT
2 mM $MgCl_2$

Elution buffer
20 mM HEPES/NaOH pH 7.4
1 mM $MgCl_2$
1 mM DTT
200 mM KCl
500 mM imidazole

2.8.14 Purification of other recombinant His_6-tagged proteins from *E. coli*

Chs5p and Bfr1p were purified from *E. coli* under denaturing conditions in 8 M urea. The proteins were purified by Ni-NTA (Qiagen) using protocols provided by the manufacturer. Pab1p was purified from *E. coli* under native conditions as described previously (Deardorff and Sachs, 1997).

2.8.15 Purification of recombinant wild-type Arf1p protein from *E. coli*

The purification of recombinant myristoylated Arf1p from *E. coli* was performed as described before with minor modifications (Randazzo *et al.*, 1992). An *E. coli* strain co-transformed with plasmids for Arf1p and Nmt1p (N-myristoyl-transferase 1) was used. The glycerol stock was streaked out on LB 0.5x kan/0.5x carb and grown overnight. 40 ml LBkan/carb were inoculated and grown for 3 – 4 h at 37°C to an OD_{600} of about 0.75. 1.5 l LBkan/carb were inoculated with the pre-culture. After 2 – 3 h at 37°C the culture reached an OD_{600} of about 0.5. At this point, protein expression was induced by 1 mM IPTG and 2.4 ml 125 mM myristic acid were added. After additional incubation for 3 – 5 h at 30°C, cells were harvested at an OD_{600} between 1 and 2 (10 min 6,000 rpm, GS-3 rotor, 4°C), washed in STE-buffer, and sedimented (10 min, 10,000 rpm, SS34-rotor, 4°C). The cell pellet was frozen in liquid nitrogen and stored at –70°C. Subsequently, the cell pellet was thawed on ice and resuspended in 30 ml STE-buffer with protease inhibitors (PMSF, pepstatin A, leupeptin). Lysozyme was added to 1 mg/ml final concentration and the suspension was gently agitated for 15 min at RT. After addition of 12 ml of cold Triton-buffer, the cells were sonified with several 15 s pulses intermittent by incubations on ice.
The lysate was centrifuged at 100,000 g centrifugation (1 h, 39,000 rpm, Ti 50.2-rotor, 2°C). The supernatant was loaded on a 50 ml DEAE-Sephacel ion-exchange chromatography column, which was equilibrated in DEAE-buffer. The column was washed with 50 ml DEAE-buffer. The flow-through was fractionated (110 drops, approximately 3 ml). Five µl of the fractions were added to 200 µl Biorad protein assay reagent on a micro-titer-plate, the protein peak was visualized by the color shift of the Bradford reagent. Protein containing fractions were pooled. The column was regenerated with 50 ml 2 M NaCl, and subsequent washes in H_20. The column was stored in 20% ethanol. Particles in the protein pool were removed by centrifugation at 100,000 g (30 min, 39,000 rpm, Ti 50.2-rotor, 2°C). The supernatant was concentrated using a Centriprep YM-10 (approximately 8 h, 4,000 rpm, Eppendorf 5810 R, 4°C) to less than 10 ml.

The protein solution was loaded on a gel filtration column (230 ml Sephacryl S-100), which was pre-equilibrated with dialysis buffer, and developed with dialysis buffer. Three ml fractions were collected overnight at a flow-rate of 0.4 ml/min. The column was regenerated by 2 column volumes of dialysis buffer. For storage, NaN_3 was added to 0.02%. The fractions of the gel filtration were analyzed by SDS-PAGE and Coomassie-blue staining. Fractions that contained appropriate protein amounts of Arf1p were pooled and concentrated to less than 5 ml using a Centriprep YM-10. After determination of protein concentration, aliquots were frozen in liquid nitrogen and stored at –70°C.

DEAE-Puffer:
20 mM Tris/HCl pH 7.4
50 mM NaCl
1 mM EDTA
1 mM DTT

Triton buffer
50 mM Tris/HCl pH 8.0
0.2% Triton X-100
100 mM $MgCl_2$

Dialysis buffer
20 mM HEPES/NaOH pH 7.4
1 mM EDTA
100 mM NaCl
1 mM DTT
2 mM $MgCl_2$

2.8.16 Preparation of affinity material

Proteins were covalently coupled to column material using NHS-Agarose (Amersham Bioscience). The carboxyl groups of the column material (with aminohexanoic acid as spacer) were activated by N-hydroxysuccinimid and reacted with amino groups of the proteins forming amide bonds. Coupling, blocking of non-reacted groups and washing was performed according to the manufacturer's recommendations. The coupling efficiency was estimated by measuring the protein concentration in the flow-through.

Peptides were covalently coupled to Ultralink Iodacetyl resin (Pierce). The terminal iodacetyl group of a 15 atom spacer reacted with sulfhydryl groups forming a thioether linkage. Coupling, blocking of non-reacted groups and washing was performed according to the manufacturer's recommendations. The coupling efficiency was estimated by measuring the absorbances of the peptides in the BCA-assay before and after coupling.

2.8.17 Differential Arf1p-affinity chromatography

Recombinant ΔN17-Arf1p-Q71L and ΔN17-Arf1p-T31N were expressed in *E. coli*. Fifty mg of each protein were covalently coupled to 1.2 ml NHS-activated sepharose 4 fast flow

(Amersham Bioscience). For the affinity chromatography, the columns were pre-equilibrated with 10 ml NE buffer. The nucleotide exchange was performed in 3 ml NE buffer with 200 µM of the corresponding nucleotide for 1 h at 37°C (GTP for Arf1p-Q71L, GDP for Arf1p-T31N). The control column without protein was treated in the same way as the Arf1p-Q71L-column. The columns were washed with 10 ml NS buffer. Yeast cytosol (125 mg) was allowed to bind for 1 h at 4°C. The columns were washed with 60 ml NS buffer (+ 0.1% Triton X-100) and subsequently with 10 ml pre-warmed exchange buffer containing 10 µM GXP. Proteins were eluted using 4 x 1 ml exchange buffer containing 500 µM GX'P (GDP for Arf1p-Q71L, GTP for Arf1p-T31N). For the first elution, the columns were incubated for 30 min at 37°C, whereas for the following elution steps 10 min were used. The samples were analyzed by SDS-PAGE and silver staining and immunoblotting. For protein identification by mass spectrometry, the elutions were TCA-precipitated and separated on a large 10% SDS-poyacrylamide gel and stained by the Fairbanks method. Protein bands that were clearly enriched in one or the other eluate were cut out and subjected to mass spectrometric analysis.

Nucleotide exchange buffer (NE)	Nucleotide stabilization buffer (NS)
25 mM HEPES pH 7.7	20 mM HEPES pH 7.4
100 mM NaCl	100 mM NaCl
1 mM EDTA	1 mM DTT
0.5 mM $MgCl_2$	1 mM EDTA
0.1 % Na-cholate	2 mM $MgCl_2$
	10 µM GXP

2.8.18 Affinity purification of immunoglobulins

Affinity purifications of immunoglobulins were carried out essentially as described previously (Harlow and Lane, 1988). Although the purification was performed at RT, all solutions were kept on ice. Ten ml of the antiserum were thawed on ice and diluted with 10 ml PBS. The solution was filtered through a 0.2 µm membrane and passed three times over the appropriate affinity column (antigen covalently coupled to the resin). The column was washed with 20 ml Tris/HCl pH 7.5 and 20 ml Tris/HCl pH 7.5, 0.5 M NaCl. The first elution of the antibodies was carried out with 100 mM glycine pH 2.5. 10 x 1 ml fractions were collected in reaction tubes containing 100 mM Tris/HCl pH 8.0. The elution was performed rapidly and care was taken as to immediately neutralize the elutions. The column was washed with 10 ml 100 mM Tris/HCl pH 7.5. The second elution of high-affinity antibodies was carried out with 10 x 1 ml 4.5 M $MgCl_2$. The column was regenerated by washes with TBS and stored at 4°C with 0.02% NaN_3.

Appropriate fractions of the glycine and $MgCl_2$ elutions were pooled separately and dialyzed twice against PBS (2 x 2.5 l, at least 6 h each). The protein concentration was determined. Aliquots were frozen in liquid nitrogen and stored at –70°C. The quality and titers of the affinity purified antibodies were tested in immunoblots, in immunoprecipitations and in immunofluorescence.

2.8.19 In-gel digestion and mass spectrometric identification of proteins

The in-gel digestions were carried out by Jörn Dengjel. Mass spectrometric analysis of the trypric digests were performed by Jörn Dengjel and Markus Schirle. Both are present and past members of the AG Rammensee, University of Tübingen.

In-gel tryptic digestions were performed as described previously (Shevchenko *et al.*, 1996) and modified as outlined below. Briefly, protein bands were excised from gels, fully destained, and digested for 3 h with porcine trypsin (sequencing grade, modified; Promega, Madison, WI) at a concentration of 67 ng/µl in 25 mM ammonium bicarbonate, pH 8.1, at 37°C. Before peptide mass mapping and sequencing of tryptic fragments by tandem mass spectrometry, peptide mixtures were extracted from gels by 1% formic acid followed by two changes of 50% acetonitrile. The combined extracts were vacuum-dried until only 1 – 2 µl was left, and the peptides were purified by ZipTip according to the manufacturer's instructions (Millipore, Bedford, MA). MALDI-time of flight (TOF) analysis from the matrix α-cyano-4-hydroxycinnamic acid/nitrocellulose prepared on the target by using the fast evaporation method (Arnott *et al.*, 1998) was performed on a Bruker Reflex III (Bruker Daltonik, Bremen, Germany) equipped with a N_2 337-nm laser and gridless pulsed ion extraction. Sequence verifications of some fragments were performed by nanoelectrospray tandem mass spectrometry on either a Q-Tof I mass spectrometer (Micromass, Manchester, England) or a QStar Pulsar i Qqoa Tof mass spectrometer (Applied Biosystems-MDS Sciex, Weiterstadt, Germany) equipped with a nanoflow electrospray ionization source. Gold-coated glass capillary nanoflow needles were obtained from Protana (Odense, Denmark) (type medium NanoES spray capillaries). Database searches (NCBInr, nonredundant protein database) were done using the MASCOT software (Perkins *et al.*, 1999).

2.8.20 *In vitro* Golgi-budding assay

2.8.20.1 With purified coat components

The Golgi budding assay was performed as described by Spang and Schekman (1998) with minor modifications. For the Golgi budding reactions, membranes were incubated with 0.1 mM GTP or GTPγS, coatomer (125 µg/ml which was available in the laboratory), and wild-type, myristoylated Arf1p (25 µg/ml) at 30°C for 30 min in a total volume of 400 µl. After chilling on ice for 5 min, the samples were loaded on a Ficoll-sucrose gradient consisting of 0.3 ml 60% (w/w) sucrose, 0.8 ml 7.5 %, 1 ml 5, 4, and 3 % and 0.8 ml 2% (w/w) Ficoll in 15 % (w/w) sucrose in 20 mM HEPES/KOH pH 6.8, 5 mM $Mg(Ac)_2$. The vesicles were separated from the Golgi apparatus by centrifugation for 2 h at 35,000 rpm (SW50.1 rotor, 2°C). Fractions (400 µl) were collected from the top. Fractions 4-6 of the gradient were pooled, mixed with an equal volume of 80% (w/v) Nycodenz in B88*, and overlaid with 600 µl of 35, 25, 20, and 15% and 400 µl 10% (w/v) Nycodenz in B88*. Gradients were centrifuged for 16 h at 40,000 rpm (SW50.1 rotor, 2°C). Fractions (300 µl) were collected from the top, TCA precipitated, and analyzed by immunoblot.

B88
20 mM HEPES/KOH pH 6.8
5 mM $Mg(Ac)_2$
150 mM KAc
250 mM sorbitol

B88*
20 mM HEPES/KOH pH 6.8
5 mM $Mg(Ac)_2$
150 mM KAc

ATP-regeneration system
55 mg ATP
1.31 g creatine phosphate
add cold B88 to near 10 ml
adjust pH to 6.8 with 1 M KOH (~75 µl)
add 20 mg creatine phosphokinase
adjust to 10 ml with B88
aliquot and freeze in liquid N_2, store at –80°C

2.8.20.2 With cytosol

For the Golgi budding reactions using cytosol, 150 µl Golgi membranes were incubated with 0.2 mM GTPγS, 75 µl cytosol and 10 µl ATP-regeneration system at 30°C for 30 min in a total volume of 240 µl. After chilling on ice and dilution with 160 µl B88, the samples were loaded on a Ficoll-sucrose gradient consisting of 0.3 ml 60% (w/w) sucrose, 0.8 ml 7.5 %, 1 ml 5, 4, and 3 % and 0.8 ml 2% (w/w) Ficoll in 15 % (w/w) sucrose in 20 mM HEPES/KOH pH 6.8, 5 mM $Mg(Ac)_2$. Vesicles were separated from the Golgi apparatus by centrifugation for 2 h at 35,000 rpm (SW50.1 rotor, 2°C). Fractions (400 µl) were

collected from the top. Fractions 4-6 of the gradients were pooled, mixed with an equal volume of 80% (w/v) Nycodenz in B88*, and overlaid with 1.6 ml 30%, 0.6 ml 20% and 0.6 ml 10% (w/v) Nycodenz in B88*. The gradients were centrifuged for 16 h at 40,000 rpm (SW50.1 rotor, 2°C). Fractions (300 µl for fractions 1-10 and 1.2 ml for fractions 11 and 12) were collected from the top, precipitated by TCA, resolved on SDS-PAGE and analyzed by immunoblot.

2.8.21 Co-immunoprecipitation

Co-immunoprecipitation experiments were performed essentially as described previously (Harlow and Lane, 1988). To prepare yeast lysates for co-immuno-precipitations, 10 OD_{600} of logarithmically growing yeast cells were incubated in 2 ml DTT-buffer (10 mM Tris/HCl pH 9.4, 10 mM DTT) for 5 min at 30°C. The buffer was replaced by 2 ml SP-buffer (0.76% YPD, 0.7 M sorbitol, 10 mM Tris/HCl pH 7.5), supplemented with 30 µl Zymolyase T-20 (10 mg/ml). Cells were spheroplasted for 40 min at 30°C. The spheroplasts were sedimented (2 min, 1,000 x g) and lysed in B150-TW20. The lysates were cleared by centrifugation (10 min, 16,000 x g, RT).

Immunoprecitpitations were performed using either 10 µg affinity-purified α-Arf1p antibodies or affinity-purified rabbit IgGs, 10 µl α-Chs5p serum or pre-immune serum, 5 µl α-HA.11 (Eurogentec, mouse monoclonal), 5 µl α-Myc (9E10, Sigma, mouse monoclonal), 5 µl α-AU5 (Abcam, rabbit polyclonal) or 5 µl α-GFP (Torrey Pines, rabbit polyclonal) per 1 ml cleared lysate for 1 hr at 4°C. The beads were washed with B150-TW20 (the last wash was in B150 buffer), and resuspended in 50 µl Laemmli-buffer. Aliquots were analyzed by SDS-PAGE and subsequent immunoblotting.

The co-immunoprecipitations probing the Arf1p-Pab1p interactions were performed with 10 µl α-Arf1p serum, 10µl α-Coatomer serum or control serum per 1 ml lysate for 1 hr at 4°C. In other cases, 7 µl α-HA.11 (Eurogentec, mouse monoclonal) or 5 µl α-myc 9E10 (9E10, Sigma, mouse monoclonal) were added to the lysate. The beads were washed, and resuspended in 50 µl Laemmli-buffer. Aliquots were analyzed by SDS-PAGE and subsequent immunoblotting.

For Bfr1p co-immunoprecipitation, the lysate was incubated with 10 µg of affinity purified anti-Arf1p antibody cross-linked to 25 µl ProteinA magnetic beads (NEB) using DMP (Pierce) according to the manufacturer's recommendations. The antibody-protein interaction was severed by elution with 0.2 M glycin pH 2.5.

For RNA digestion experiments, the lysates were treated for 35 min at 4°C with 200 µg RNase A (Roche) or 500 U RNase-free DNase I and centrifuged (10 min, 14,000 rpm, Eppendorf 5417 R, 4°C) before precipitation.

B150-TW20
20 mM HEPES/KOH pH 6.8
150 mM KAc
5 mM $Mg(Ac)_2$
1% Tween-20

B150
20 mM HEPES/KOH pH 6.8
150 mM KAc
5 mM $Mg(Ac)_2$

2.9 Molecular biological methods

Standard techniques for nucleic acid manipulations were used throughout in this study (Sambrook *et al.*, 1989).

2.9.1 Transformation of *E. coli*

Routinely, *E. coli* cells were transformed chemically. Usually, 20 µl chemically competent cells (which were available in the laboratory) were thawed on ice and mixed with 0.3 µl plasmid DNA (or 50 µl cells with 5 µl of a ligation reaction). The cells were heat-shocked for 30 s at 42°C and immediately placed on ice. SOC-medium (240 µl) was added to the cells. The mixture was incubated on a shaker for 30 min at 37°C before the cells were plated out on selection plates. In case a plasmid with ampicillin-resistance was transformed, this last incubation step was not necessary.
Alternatively, *E. coli* cells were transformed by electroporation (Dower *et al.*, 1988). Fifty µl of electrocompetent cells (which were available in the laboratory) were thawed on ice and mixed with DNA. The mixture was pipetted in an electroporation cuvette which had been placed on ice before. The electroporation was performed with 2,500 V, 960 µF and 200 Ω. After the electroporation pulse, 1 ml of SOC-medium was added immediately to the cuvette. The cell suspension was incubated on a shaker at 37°C for 30 – 60 min before the cells were plated out on selection plates.

2.9.2 Plasmid preparation from *E. coli*

Plasmid preparations were performed according to the alkaline lysis method described by Birnboim and Doly (1979) with minor modifications. Routinely, 1.5 ml of an overnight

culture were harvested (5 min, 14,000 rpm, Eppendorf 5417 R, 4°C). Cells were resuspended in 300 µl P1-buffer and 300 µl P2-buffer was added. After incubation for 5 min at RT, 300 µl of buffer P3 were added. The solution was cleared by centrifugation (10 min, 14,000 rpm, Eppendorf 5417 R, 4°C). The plasmid DNA in the supernatant was precipitated by adding 600 µl isopropanol and subsequent centrifugation (10 min, 14,000 rpm, Eppendorf 5417 R, 4°C). The resulting pellet was washed with 1 ml 70% ethanol and spun again (5 min, 14,000 rpm, Eppendorf 5417 R, 4°C). The pellet was dried at 65°C for about 5 min and the DNA was dissolved in 20 µl H_20 and stored at –20°C.
In case the DNA was to be used for sequencing reactions or larger amounts were needed, the Qiagen plasmid mini kit or the Qiagen HiSpeed plasmid midi kit were used according to the supplier's recommendations.

P1-buffer
20 mM Tris/HCl pH 8.0
10 mM EDTA
100 µg/ml RNase

P2-buffer
0.2 M NaOH
1% SDS

P3-buffer
3 M KAc pH 5.5

2.9.3 Determination of nucleic acid concentration

The concentration of nucleic acids was determined using a spectrophotometer (Beckman DU 640). The nucleic acids were diluted in H_2O and the absorption at 260 nm was determined. It was assumed that an absorption of 1.0 at 260 nm corresponds to 50 µg/ml double-stranded DNA or 40 µg/ml single-stranded RNA.

2.9.4 Restriction digest of DNA

Plasmid preperations were analyzed by restriction digest and agarose gel-electrophoresis with subsequent ethidium bromide staining. The guidelines provided the supplier's of restriction endonucleases (NEB or Roche) for enzymatic digests were followed. For purification of restriction digest for cloning purposes or gel-elution of DNA fragments, the purifications kits from Qiagen (PCR purification kit/Gel extraction kit) were used according to the manufacturer's recommendations.

2.9.5 Cloning of DNA

The DNA fragment for (sub-)cloning was obtained by restriction digest of plasmid DNA or by PCR amplification from genomic yeast DNA. In case of PCR amplification, suitable restriction site sequences were included into the primers. If the gene was to be placed under the control of endogenous regulatory sequences, at least 500 bp upstream the start codon were co-amplified. Purified vector DNA and purified DNA insert were ligated using the rapid ligation kit from Roche following the manufacturer's recommendations. Occasionally, 5'-dephosphorylation of the vector was necessary to prevent excessive re-ligation. Alternatively, TOPO cloning kits (Invitrogen) were used according to the manufacturer's recommendation. Positive clones were identified by restriction digest and verified by DNA-sequencing.

2.9.6 Polymerase-chain-reaction (PCR)

To produce DNA fragments for DNA cloning or homologous recombination, polymerase-chain-reaction was used (Mullis *et al.*, 1986). The proof-reading Expand High Fidelity System (Roche) was used for preparative production of DNA. A typical reaction contained 37 µl H_20, 5 µl 10x reaction buffer, 5 µl 2 mM dNTPs, 2 x 1 µl 10 mM oligonucleotide primer and 1 µl template DNA. Usually, 35 cycles were performed for amplification. The annealing temperature was typically between 52°C and 56°C and 1 min/1,000 bp was allowed for elongation.

2.9.7 Reverse-Transcription-PCR (RT-PCR)

For RT-PCR, the beads and the lysates of co-immunoprecipitation experiments were extracted as described by Gonsalvez *et al.* (2003). Briefly, the beads were extracted with RNA-elution buffer (50 mM Tris/HCl, 100 mM NaCl, 10 mM EDTA, 1%SDS) and heating to 65°C for 5 min. Subsequently, RNA was purified by Phenol/Chloroform extraction and precipitated with Pellet Paint (Merck). DNA was digested by RNase free RQ1-DNase (Promega) for 15 min at 37°C in the presence of RNasin (Promega). The RNA was re-extracted, re-precipitated and re-dissolved in 50 µl RNase-free H_2O. RT-PCR was performed on 2 µl aliquots using the One-Step RT-PCR-Kit (Qiagen) for 25 or 30 cycles using primers specific for certain mRNAs and the conditions recommended by the manufacturer. 20 µl of the reactions were analyzed on 3% Metaphor agarose gels.

2.9.8 DNA-sequencing

DNA was sequenced by the dideoxynucleotide method (Sanger *et al.*, 1977) using four fluorescently labeled dideoxynucleotides. The sequencing reaction contained 0.5 µl big dye terminator mix V3.1, 2 µl 5x BDT-reaction buffer, 0.5 µl 10 mM oligonucleotide-primer and 150 – 300 ng plasmid DNA or 5 – 20 ng PCR-product in a final volume of 10 µl. After denaturation for 20 s at 95°C, 28 cycles were carried out: 20 s 96°C, 10 s 50°C, 4 min 60°C. The reaction was stored at –20°C until it was analyzed by capillary electrophoresis by the in house sequencing service (AG Stefan Schuster). The DNA-sequence was analyzed using the Seqman II software (DNASTAR).

2.9.9 Gylcerol stocks

For the preparation of *E. coli* glycerol stocks, 750 µl of an overnight culture were mixed with 500 µl 50% glycerol and stored at –70°C. For the preparation of yeast glycerol stocks, yeast cells streaked out as rectangle were grown on appropriate plates. The plates were incubated until a dense lawn of cells was obtained. The cells were transferred with a sterile glass pipette into 800 µl 15% glycerol and stored at –70°C.

2.9.10 Chromosomal manipulations of yeast cells

To delete or manipulate genes in yeast cells, the methods described by Guldener *et al.* (1996), Knop *et al.* (1999), De Antoni and Gallwitz (2000), and Gueldener *et al.* (2002) were followed. Briefly, preparative PCR was performed on template plasmids with primers having 45 bp 5'-overhangs homologous to the desired target site in the yeast genome. The PCR-product was transformed directly into yeast cells without further purification. Cells were selected for with the corresponding auxotrophy/resistance markers, correct integrations were confirmed by analytical colony-PCR. Wherever possible, the expression was checked by immunoblotting of total yeast lysates. Occasionally, the chromosomal manipulation had to be sequenced. In this case, the PCR product using the proof-reading Expand PCR system (Roche) on genomic yeast DNA was sequenced to confirm the desired manipulation.

2.9.11 Preparation of genomic yeast DNA

Crude yeast DNA was obtained by following the procedure of Hoffman and Winston (1987): Five ml of yeast culture were grown to saturation. The cells were harvested and resuspended in 200 µl buffer A. Approximately 200 µl glass beads and 200 µl

phenol:chloroform:isoamylalcohol 25:24:1 were added. After vigorous vortexing for 5 min, 200 µl H_2O were added. Phase separation was accomplished by centrifugation (5 min, 20,000 g, 4°C). The aqueous phase was transferred to a fresh reaction tube and 1 ml 100% EtOH (RT) was added. The DNA was pelleted by centrifugation for 2 min (20,000 g). The resulting DNA pellet was dried at 65°C for about 5 min and resuspended in 40 µl H_2O.

Buffer A:
10 mM Tris/HCl pH 8.0
100 mM NaCl
1 mM EDTA
2% Triton X-100
1% SDS

2.9.12 Yeast transformation

Yeast cells were transformed by a high-efficiency lithium acetate transformation method (Gietz *et al.*, 1995). Cells were grown overnight in liquid culture to logarithmic phase. Best results were obtained with an OD_{600} of about 0.1. 5 OD_{600} of cells were harvested and washed once in sterile water. The cells were incubated for 5 min at 30°C in 100 mM LiAc. Subsequently, they were resuspended in 360 µl transformation mix and mixed thoroughly for 1 min. A heat-shock was employed for 40 min at 42°C, after which the cells were pelleted (10 s, 13,000 rpm, Eppendorf 5417 R, 4°C). The cell pellet was resuspended in 1 ml sterile water and 200 µl aliquots were plated on appropriate selection plates. Colonies obtained were subjected to a second round of selection.

In case a kanamycin resistance cassette was transformed, cells were first incubated in YPD for 3 h at 30°C before plating on YPD-G418 plates. Fast growing colonies were chosen for the second round of selection. Sometimes, replica plating was necessary to allow for the selection of stable transformants.

Transformation mix
240 µl 50% (w/v) PEG (AMW 3.350)
36 µl 1 M LiAc
50 µl 2 mg/ml single-stranded salmon sperm DNA
(obtained by heating for 5 min at 95°C and fast cooling in an ice/water bath)
5 µl of PCR product or 0.25 µl plasmid DNA
ad 360 µl with H_20

2.9.13 Analytical PCR of yeast colonies

Analytical PCR of yeast colonies was performed to confirm chromosomal manipulations of yeast cells or to determine the mating type after mating or sporulation. The primers were chosen in a way that in either case a PCR product was obtained and that after agarose gel electrophoresis the altered size of the product (as compared to a wild-type colony) confirmed the chromosomal manipulation. A typical reaction contained 18.5 µl H_2O, 2.5 µl 10x reaction buffer, 2.5 µl 2 mM dNTPs, 2x 0.5 µl 10 µM oligonucleotide-primer, 0.3 µl *Taq* DNA-polymerase (Roche) and a small portion of a yeast colony. Usually, the annealing temperature was between 52°C and 56°C, the elongation time was between 3 min and 6 min and 35 – 40 cylces were used for amplification. Routinely, 20 µl of the reaction were analyzed by agarose gel-electrophoresis. For mating type PCRs (Huxley *et al.*, 1990), 10 µl of the reaction were resolved on a 1.2% agarose gel.

2.9.14 Two-hybrid assay

The two-hybrid assay was performed with the LexA two-hybrid system (Estojak *et al.*, 1995; Golemis and Khazak, 1997). The yeast reporter strain EGY48 as well as the bait plasmid pEG202, the prey plasmid pJG4-5 and the reporter plasmid pSH18-34 (Golemis et al., 1996) were used. Bait vector with *ΔN17-ARF1-Q71L* and prey vector with *GLO3* as a positive control were obtained from Rainer Duden (Eugster *et al.*, 2000).

PAB1 and *PUB1* were amplified from genomic yeast DNA by PCR carrying restriction sites for EcoRI and XhoI and cloned into pJG4-5. Constructs were verified by DNA sequencing.

The constructs were co-transformed into the EGY48 reporter strain. Transformants were selected on HC-HIS/-TRP/-URA plates. Four independent transformants were assessed for growth on HC-HIS/-TRP/-URA/-LEU plates containing 2% galactose and 1% raffinose. The strains were incubated for 4 days at 30 °C.

2.9.15 Digoxigenin-labelling of an ASH1-antisense-RNA-probe

A PCR was perfomed on genomic DNA with primers MT-A31 and MT-A32. The PCR-product was purified and an *in vitro*-transcription using Ambion MEGAscript T7 kit was performed. A ratio of 1:5.6 of Dig-11-UTP:UTP was used. The concentration was determined by absorption at 260 nm. The integrity of the probe was checked by conventional agarose gel-electrophoresis. The probe was divided in 0.5 µg aliquots (in DEPC-treated TE), immediately frozen in liquid nitrogen, and stored at –70°C.

2.9.16 Northern Blot analysis

Cells were grown overnight to logarithmic phase. Where necessary, cells were shifted for 1 hour to the non-permissive temperature. Cells were harvested, frozen in liquid nitrogen and stored at –20°C until further analysis. Total RNA was extracted using the RNeasy kit from Qiagen using the glass-bead lysis protocol provided by the manufacturer. RNA was precipitated using pellet paint co-precipitant (Merck) and resuspended in a smaller volume of RNA-buffer. The RNA was resolved on low-formaldehyde 1.2% agarose gels. To cast the gels, 0.6 g agarose were boiled in 43.5 ml H_2O. After cooling to about 60°C, 5 ml 10x MOPS and 1.5 ml 37% formaldehyde (pH >4) were added in the fume-hood. Equal amounts of RNA (25 µg per lane) in up to 5 µl were mixed with 15 µl RNA-sample buffer and heated to 65°C for 15 min. The samples were placed on ice and immediately 20 µl were loaded per lane. The electrophoresis was performed in 1x MOPS at 50 V. After electrophoresis, the gel was washed in H_2O (3 x 5 min) and finally for 15 min in 10x SSC. The RNA was transfered overnight in 10x SSC onto Hybond N+ membrane by capillary blotting as described previously (Sambrook *et al.*, 1989). The RNA was crosslinked to the damp membrane using the Stratalinker 1800 UV Crosslinker in the autocrosslink mode. The membrane was stained with methylene blue stain, washed in water and photographed for documentation. To prepare Northern blot probes, the AlkPhos direct labeling kit (Amersham Bioscience) was used according to the manufacturer's recommendations. Briefly, a heat-stable alkaline phosphatase was directly crosslinked to a heat-denatured PCR-product. After hybridization at 60°C, the alkaline phosphatase activity was detected using CDP-Star substrate (Amersham Bioscience) and the chemoluminescence was reported on ECL Hyperfilm.

RNA-buffer
10 mM Tris/HCl pH 7.4
1 mM EDTA
0.2% SDS

10x MOPS
230 mM MOPS/NaOH pH 7.0
50 mM NaAC
10 mM EDTA

RNA-loading buffer
1 mM EDTA/NaOH pH 8.0
0.25% bromphenol blue
0.25% xylene cyanol
50% glycerol

RNA-sample buffer
5/3 µl 10x MOPS
3 µl 37% formaldehyde
7 µl formamide
10/3 µl RNA-loading buffer

10 x SSC
150 mM Na-citrate/NaOH pH 7.0
1.5 M NaCl

Methylene blue stain
0.5 M NaAc/HAc pH 5.5
0.04% methylene blue

For all solutions, DEPC-treated H_2O was used and recommendations for working with RNA were followed (Sambrook *et al.*, 1989).

2.10 Cell biological methods

2.10.1 Actin cytoskeleton staining

Actin cytoskeleton staining was performed essentially as described previously (Adams and Pringle, 1991). Cells were grown overnight to logarithmic phase and fixed directly in liquid medium by addition of 37% formaldehyde to a final concentration of 4.4% and incubation for 30 min at RT under gentle agitation. The cells were washed twice with PBS containing 1 mg/ml BSA (2 min, 3,000 rpm, Eppendorf 5810 R; 30 s, 13,000 rpm, Eppendorf 5417 R). The cell pellet was resuspended in 25 µl PBS containing 1 mg/ml BSA and 5 µl of rhodamine-phalloidin were added. After incubation for 1 h at RT in the dark, cells were washed three times and resuspended in 500 µl PBS containing 1 mg/ml BSA. An aliquot was allowed to settle for 15 – 30 min on polyethylenimine-treated multi-well slides. The slides were washed briefly in PBS, Citifluor was added and the coverslips were sealed with nail-polish. Slides were stored at –20°C. The rhodamine fluorescence was observed by epi-fluorescence microscopy using the Cy3 channel on an Axioplan 2 fluorescence microscope from Zeiss. Pictures were taken by Axiocam MRm using Axiovision software. Image processing was performed using Adobe Photoshop 7.0.

2.10.2 Indirect immunofluorescence microscopy

Indirect immunofluorescence microscopy was performed essentially as described previously (Pringle *et al.*, 1991). Cells were grown overnight to logarithmic phase and

fixed directly in the growth medium by adding 2 ml 37% formaldehyde to 18 ml culture and incubation for 1 h at RT under gentle agitation. The cells were washed twice with PBS (2 min, 3,000 rpm, Eppendorf 5810 R; 30 s, 13,000 rpm, Eppendorf 5417 R).The cell pellet was resuspended with 1 ml 100 mM KP_i pH 7.0, 1.2 M sorbitol and 2 µl β-mercaptoethanol were added. After incubation for 5 min at RT, the cells were spheroplasted by addition of 10 µl zymolyase T-100 suspension (10 mg/ml) and incubation for 15 min at 37°C. The cells were washed twice with 100 mM KP_i pH 7.0, 1.2 M sorbitol and resuspended in 500 µl of the same buffer. An aliquot was allowed to settle for 15 – 30 min on polyethylenimine-treated multi-well slides. The slides were briefly washed in PBS (5 min). Blocking was carried out by incubation for 30 min in 1% BSA in PBS or in 5% horse serum in 100 mM Tris/HCl pH 7.5, 150 mM NaCl. The primary antibody was diluted in the same solution. After incubation with the primary antibody in a wet chamber for 1 h at RT or overnight at 4°C, the slides were washed with PBS (1 x 15 min, 3 x 5 min). The secondary antibody was incubated for 1 h at RT in the dark in a wet chamber, after which the slides were washed again with PBS. Sometimes, DAPI staining was performed at this stage (5 min in 1 µg/ml DAPI). The slides were briefly washed in water, Citifluor was added and slides were sealed with nail-polish. Slides were stored at –20°C. Epi-fluorecence microscopy was performed on an Axioplan 2 fluorescence microscope from Zeiss. Pictures were taken by Axiocam MRm using Axiovision software. Image processing was performed using Adobe Photoshop 7.0.

2.10.3 Fluorescence microscopy of GFP fusion proteins in living cells

Cells were grown overnight to logarithmic phase in the appropriate selection medium. YPD-medium contained 50 mg/l adenine to suppress cellular autofluorescence. An aliquot was taken from liquid culture (when necessary briefly washed in H_2O) and visualized directly under an Axioplan 2 fluorescence microscope from Zeiss using the FITC-filter. Pictures were taken by Axiocam MRm using Axiovision software. Image processing was performed using Adobe Photoshop 7.0.

2.10.4 *In vivo* RNA-localization assay

For the visualization of ASH1-RNA localization by GFP particles, the reporter system by Bertrand *et al.* (1998), was used. Cells were transformed with the plasmids pG14-MS2-GFP and YEP195-Lz-MS2-ASH1-3'UTR and grown overnight in HC-Leu/-Ura with 2% glucose. They were washed and diluted in HC-Leu/-Ura with 2% raffinose and 3%

galactose and grown for 4 h at 30°C upon which the cultures were divided and one half was shifted for 3 h to 16°C. Cells were immobilized on slides and inspected under the fluorescence microscope (Axioplan 2 fluorescence microscope from Zeiss using the FITC-filter). Pictures were taken by Axiocam MRm using Axiovision software. Image processing was performed using Adobe Photoshop 7.0. For the evaluation, only those cells were taken into account which had a clearly visible green spot corresponding to the ASH1-GFP reporter particle. At least 100 cells per experiment were counted.

2.10.5 Mating of yeast cells

Liquid YPD medium was inoculated with a small amount of cells of both mating types. After incubation for 12 – 24 h, cells were plated out on appropriate selection plates. In cases in which selection was not possible, cells were singled out and the mating type was determined by analytical colony PCR (Huxley *et al.*, 1990). Quantitative mating assays to measure mating efficiency were carried out as described previously (Santos *et al.*, 1997).

2.10.6 Mating type switching

Mating type switching of yeast cells was performed as described previously (Davis, 1997). Cells were transformed with the plasmid pCY204 bearing the HO-endonuclease under its endogenous promoter. The plasmid was subsequently counter-selected for by growth on 5-FOA plates. The mating type of colonies obtained was determined by analytical colony-PCR (Huxley *et al.*, 1990).

2.10.7 Sporulation of yeast cells

Cells from a stationary liquid culture were harvested and plated on Spo- and Super Spo-plates. The plates were incubated at 23°C or 30°C for 5 – 10 days. The sporulation was monitored by examination of a small amount of cells under the light microscope.

2.10.8 Tetrade dissection

A small amount of cells was scraped from a plate with a high sporulation efficiency and resuspended in 100 µl sterile H_2O. The spore wall was digested by addition of 5 µl zymolyase T-20 suspension (2 mg/ml) for 2 – 5 min at RT. Samples were taken during that time and streaked on a YPD plate. The tetrads were dissected using a dissecting scope as described by Sherman and Hicks (1991). The YPD plate was incubated at 30°C until all

colonies reached a size sufficient for replica plating. The genotype was assessed by replica plating on different selection plates and analytical mating type PCR (Huxley *et al.*, 1990).

2.10.9 *In situ* hybridization of ASH1-mRNA

In situ ASH1-RNA hybridization with digoxigenin-labeled ASH1 antisense probe was performed essentially as described previously (Takizawa *et al.*, 1997). Cells were grown overnight to logarithmic phase. When necessary, cells were shifted for 1 hour to the non-permissive temperature. Cells were directly fixed in liquid medium by adding 2 ml 37% formaldehyde to 18 ml culture and incubation for 1 h at RT under gentle agitation. The cells were washed twice in PBS (2 min, 3,000 rpm, Eppendorf 5810 R; 30 s, 13,000 rpm, Eppendorf 5417 R) and resuspended in 1 ml 100 mM KP_i pH 7.0, 1.2 M sorbitol. β-mercaptoethanol (2 µl) was added. After incubation for 5 min at RT, the cells were spheroplasted by addition of 4 µl of zymolyase T-100 suspension (10 mg/ml) for 20 min at 37°C. Cells were washed twice with 100 mM KP_i pH 7.0, 1.2 M sorbitol and resuspended in 500 µl of the same buffer. An aliquot was allowed to settle for 15 – 30 min on polyethylenimine-treated multi-well slides. The slides were washed twice with 50% formamide, 5x SSC for 5 min. Slides were put in a chamber wetted with 50% formamide, 5x SSC. The cells were incubated with hybridization mix without probe for 1 h at RT in the chamber for pre-hybridization. The hybridization mix was replaced by digoxigenin-labelled ASH1-mRNA antisense probe (0.5 µg/ml in hybridization mix) and the slides were incubated at 37°C overnight. Slides were rinsed with 0.2x SSC and incubated with 0.2x SSC for 1 h at RT in a humid chamber. Blocking solution was applied for 30 min at RT. F_{ab}-fragments of antibodies directed against digoxigenin and covalently coupled to alkaline phosphatase were diluted 1:5.000 in blocking solution and applied to the cells for 1 h at 37°C. Slides were rinsed with washing buffer, washed 3 x 5 min in washing buffer, and washed 2 x 5 min in detection buffer. The HNPP/Fast Red TR mix (Roche) was applied for 30 min at RT after which slides were washed with water (1 x 10 min, 3 x 5 min). Citifluor was pipetted onto the slides and they were sealed by nail polish. The slides were stored at –70°C. The Cy3-filter of the Axioplan 2 fluorescence microscope from Zeiss was used. Pictures were taken by Axiocam MRm using Axiovision software. Image processing was performed using Adobe Photoshop 7.0. At least 100 cells were counted for each condition.

Hybridization mix
50% formamide
5x SSC
1 mg/ml yeast tRNA
100 µg/ml heparin
1x Denhardt's reagent
0.1% Tween-20
0.1% Triton X-100
5 mM EDTA

Blocking solution
5% horse serum
100 mM Tris/HCl pH 7.5
150 mM NaCl

Washing buffer
100 mM Tris/HCl pH 7.5
150 mM NaCl
0.05% Tween-20

Detection buffer
100 mM Tris/HCl pH 8.0
100 mM NaCl
10 mM $MgCl_2$

Fast Red TR solution
25 mg/ml in H_2O
prepared freshly

HNPP/Fast Red TR mix
10 µl HNPP (10 mg/ml in DMF)
10 µl Fast Red TR solution
1 ml detection buffer
prepared freshly
filtered through 0.2 µm nylon membrane

2.10.10 Analysis of budding pattern and staining of cell wall chitin

Analysis of the budding pattern and staining of cell wall chitin was carried out as described previously (Lord *et al.*, 2002). A stationary yeast liquid culture was diluted and grown for at least 16 h to logarithmic phase. Cells were fixed directly in growth medium by adding 2 ml 37% formaldehyde to 18 ml culture and incubation for 1 h at RT under gentle agitation. Cells were washed twice in H_2O, resuspended in 250 µl 1 mg/ml calcofluor white solution and incubated for 5 min at RT. The cells were washed twice with H_2O and resuspended in 1 ml H_2O and stored at 4°C (up to several months). For analysis of budding pattern, a small aliquot was squashed between slide and coverslip as to bring the bud scars of one cell into one focal plane and to facilitate microscopy. Cells were observed using DAPI filter under the epi-fluorescence microscope (Axioplan 2 fluorescence microscope from Zeiss. Pictures were taken by Axiocam MRm using Axiovision software. Image processing was performed using Adobe Photoshop 7.0). Only cells were scored with no more than 4 bud scars.

2.10.11 Drop assays

Strains were grown overnight to logarithmic phase. After adjusting to equal cell concentrations, four serial dilutions (1:10) were dropped onto different plates using a

"frogger" stamp (custom-built by the Max Planck workshop). The plates were incubated for two days at 30°C unless indicated otherwise and photographed for documentation.

3 Results and Discussion

3.1 Differential affinity chromatography to idententify new interactors of Arf1p

To identify new interacting proteins for Arf1p, we performed affinity chromatography with dominant active (ΔN17-Arf1Q71Lp) and dominant inactive (ΔN17-Arf1T31Np) forms of Arf1p (Kahn *et al.*, 1995; Christoforidis *et al.*, 1999). We chose an N-terminal truncated form of Arf1p for our experiments because the N-terminus contains a myristoylation site and forms an amphipathic helix. The replacement of this region of the proteins by a His_6-tag should minimize non-specific interactions on the affinity column, and it greatly facilitated the purification (Rein *et al.*, 2002). Equal amounts of ΔN17-Arf1Q71Lp and ΔN17-Arf1T31Np were covalently coupled to NHS-agarose (Fig. 8A). Guanine nucleotide exchange reactions were performed on the immobilized proteins in order to ensure that Arf1Q71Lp and Arf1T31Np were bound to GTP and GDP, respectively. Cytosolic extracts from a wild-type yeast strain were passed over the columns. For the elution, the Arf1Q71Lp column was incubated with an excess of GDP and the Arf1T31Np column with an excess of GTP. Although the restricted mutants are predominantly in either the GTP- or the GDP-bound form, an excess of the other nucleotide was able to elicit a conformational change under conditions that favor spontaneous guanine nucleotide exchange. In this way, proteins were released that bound specifically to the active or inactive form of Arf1p . An NHS-agarose column, which had been mock treated, served as a negative control.

We validated our approach with immunoblots of eluates from the different columns and antibodies directed against known interactors of Arf1p e.g. coatomer, Arf1p-GEFs and the Arf1p-GAP Glo3p. These proteins behaved as predicted by their biological function (Fig. 8B). Coatomer is the heptameric protein complex that forms together with Arf1p the COPI coat. This coat is involved in vesicular transport within the Golgi and from the Golgi to the ER.

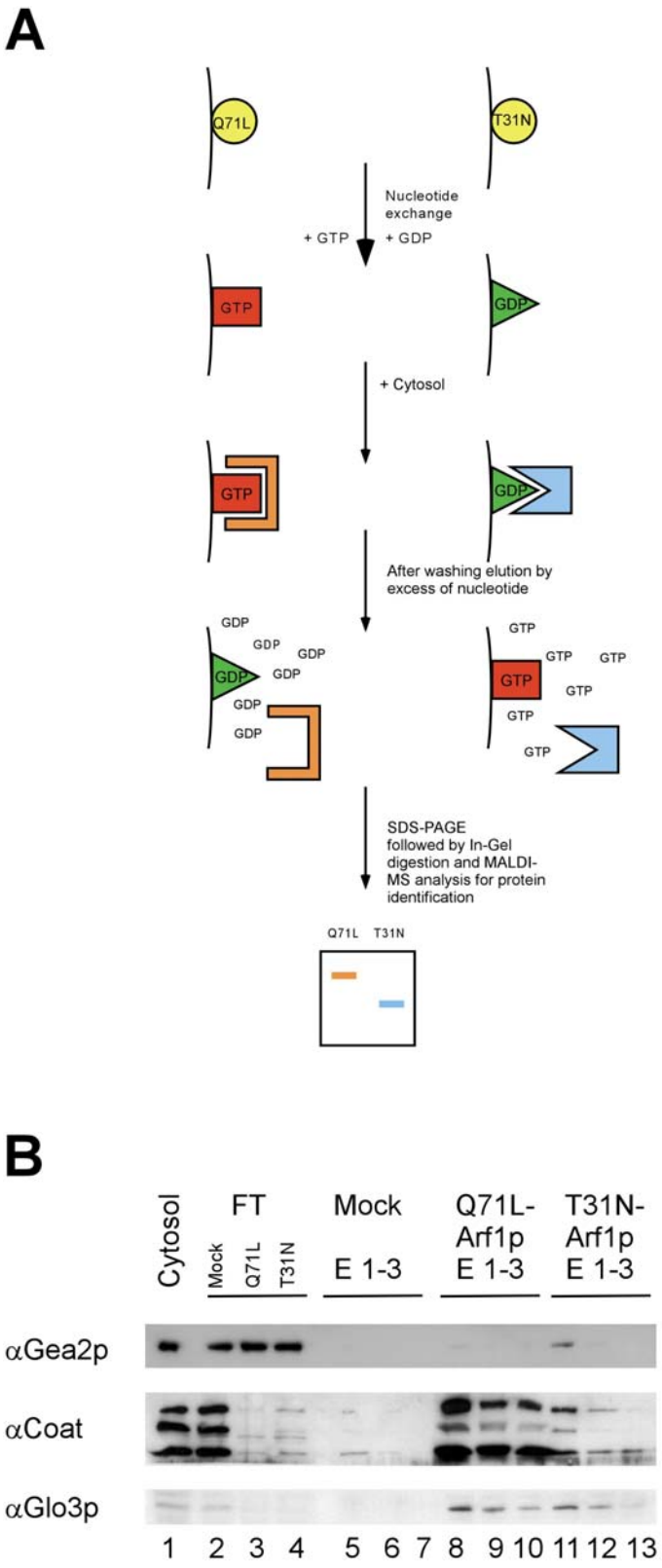

Figure 8: Differential affinity chromatography. Yeast cytosol was incubated with either the Arf1-Q71Lp (Arf1p-GTP) or Arf1-T31Np (Arf1p-GDP) column. After washing, spontaneous nucleotide exchange was elicited resulting in a conformational change on Arf1p and the release of conformation-specific bound proteins. **(A)** Schematic drawing of the procedure. **(B)** The eluates (E1-E3) from a differential Arf1p affinity chromatography experiment were analyzed by immunoblot. FT is the flow-through of unbound protein after incubation of the cytosol with the Arf1p matrix. Beads without Arf1p were mock-treated and served as negative control. The Arf1p-GEF Gea2p is enriched in the Arf1p-GDP column, whereas both the coatomer complex (three subunits are shown) and the Arf1p-GAP Glo3p bind predominately to Arf1p-GTP.

Eluted proteins were precipitated with trichloracetic acid, then separated by SDS-PAGE and stained with Coomassie blue (Fig. 9A). Multiple proteins were eluted from both Arf1p columns. While some proteins appeared in eluates from both Arf1p-columns, a few proteins were at least predominantly present in fractions from only one of the columns. Bands present in the eluates from only one column were excised and analyzed by mass

A

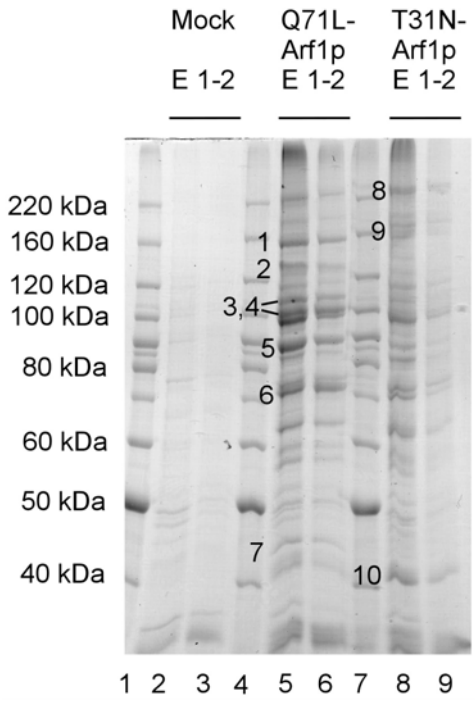

B

Proteins Identified By Mass Spectrometry		
Band	Protein	Description
1	Cop1p	Coatomer alpha-subunit
2	Chs5p	Chitin synthase 5
3	Sec26p	Coatomer beta-subunit
4	Sec27p	Coatomer beta'-subunit
5	Ymr237p	Unknown ORF
6	Pab1p	Poly(A)-binding protein
7	Yhr112p	Unknown ORF
8	Sec7p	ARF-GEF
9	Gea2p	ARF-GEF
10	Gcs1p	ARF-GAP

Figure 9: Identification of new interactors of Arf1p **(A**) The eluates from a differential affinity chromatography experiment were TCA precipitated and separated on an SDS gel. Bands that were enriched in eluates from either the Arf1p-GDP or Arf1p-GTP column were excised and subjected to mass spectrometric analysis. **(B)** Proteins identified by mass spectrometry.

spectrometry. The in-gel digestions were carried out by Jörn Dengjel. Mass spectrometric analysis of the tryptic digests were performed by Jörn Dengjel and Markus Schirle. Both are present and past members of the AG Rammensee, Interfakultäres Institut für Zellbiologie, Abteilung Immunologie, University of Tübingen.

The results of the analysis are summarized in Figure 9B. Six of the analyzed bands corresponded to known Arf1p binding proteins: subunits of the coatomer complex, the ARF-GEFs Gea2p and Sec7p as well as the ARF-GAP Gcs1p. Similar results were obtained using columns with immobilized ΔN17-Arf1p bound to GTP or GDP. Surprisingly, Gcs1p was found in the eluate from the GDP column. However, ARF-GAPs have been shown to fulfill an additional function on recruitment of SNAREs and cargo to

sites of vesicle emergence (Rein *et al.*, 2002). This recruitment does not necessarily require the activated state of Arf1p.

Four interactors have not been decribed in conjunction with Arf1p before, namely Pab1p, Chs5p and the protein products of the unknown ORFs *YMR237w* and *YHR112c*. Although it was possible to confirm the interaction of Yhr112p with Arf1p by co-immunoprecipitation (Robert Gauss, unpublished data), the significance of this interaction remained obscure. Yhr112p is homologous to Cys3p, a cystathion-γ-lyase. Apart from the role of Cys3p in metabolism, a certain role in vesicular transport has been indicated (Matiach and Schroder-Kohne, 2001). The role of Yhr112p has not been analyzed further in this study.

As it turned out during subsequent analyis, Pab1p provided an unexpected link between vesicular traffic and mRNA transport. This is described in Chapter 3.2. Ymr237p belongs to a family of highly homologous proteins in yeast. This family acts in close conjunction with Chs5p in Arf1p-dependent post-Golgi vesicular traffic. The genetic characterization of this family is described in Chapter 3.3, whereas the biochemical analysis follows in Chapter 3.4.

3.2 Arf1p provides an unexpected link between vesicular traffic and mRNA transport in *Saccharomyces cerevisiae*

3.2.1 Results

3.2.1.1 Pab1p binds to a ΔN17-Arf1Q71Lp affinity matrix

One of the new bands that we identified by mass spectrometry corresponded to Pab1p (Fig. 9A, band 6). Pab1p is one of two major polyA-tail binding proteins in yeast. It is localized in the cytoplasm as well as in the nucleus and it is part of the 3'-end RNA processing complex (cleavage factor I). Four RNA recognition domains (RRM) mediate the interaction with the polyA-tail of the mRNA. To confirm the presence of Pab1p, we tested eluates from the affinity columns by immunoblot. Pab1p did not bind to the column material, but was detected in fractions from the ΔN17-Arf1Q71Lp column (Fig. 10A). A small amount of Pab1p was also present in eluates from the ΔN17-Arf1T31Np column. However, Pab1p showed a higher affinity towards the activated form of Arf1p, since the signal from the Arf1T31Np fractions trailed off quickly, while it persisted throughout the eluates from the Arf1Q71Lp matrix. This was consistent with the signal that we observed

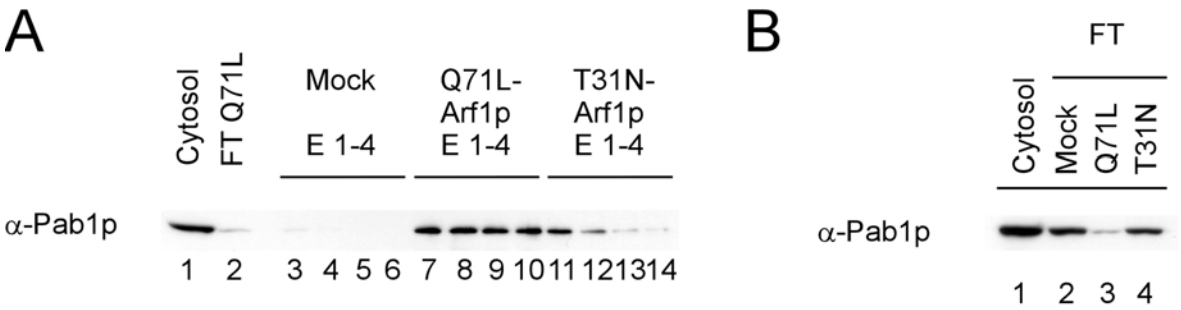

Figure 10: Pab1p binds preferentially to ΔN17Arf1-Q71Lp. **(A)** Fractions from the columns were blotted and incubated with antibodies against Pab1p. Pab1p is highly enriched in eluates from the Arf1p-Q71L column. **(B)** The flow-throughs from the Arf1-Q71Lp column is depleted of Pab1p.The starting cytosol as well as the flow-through from the 3 columns was analyzed for the presence of Pab1p by immunoblot. Pab1p was less abundant in the flow-through of the Arf1p-GTP column compared to the mock-treated and the Arf1p-GDP column.

for coatomer. If the Pab1p-Arf1Q71Lp interaction represents a high affinity contact, one would expect that the cytosol loaded on the column would be at least partially depleted of Pab1p. Therefore, the flow-throughs from different columns were analyzed by immunoblot. While the signal from the control and the ΔN17-Arf1T31Np columns did not alter significantly, the cytosol that had passed through the ΔN17-Arf1Q71Lp matrix contained substantially less Pab1p than the starting material (Fig. 10B).

3.2.1.2 ΔN17-Arf1Q71Lp interacts with Pab1p but not Pub1p

Pab1p is known to bind nonspecifically to many yeast proteins (Gavin *et al.*, 2002). Therefore, to validate the interaction between Arf1p and Pab1p, we performed a two-hybrid assay.

Table 15: The activated form of *ΔN17-ARF1* interacts with *PAB1* but not with *PUB1*. The growth cells on plates lacking leucine is indicated. *GLO3* served as positive, the empty vectors as negative controls. n. d. = not determined

Two Hybrid Assay				
prey / bait	*PAB1*	*PUB1*	*GLO3*	pJG4-5
ΔN17-ARF1-Q71L	+	-	+	-
pEG202	-	n.d.	-	n.d.

We used Δ*N17-ARF1Q71L* as the bait and *PAB1*, *PUB1*, and *GLO3* as preys. Pub1p is the other major polyA-binding protein in the cell and, like Pab1p, localizes to the cytoplasm and the nucleus. We used growth on –LEU plates as the indicator for interactions. While *PAB1* and Δ*N17-ARF1Q71L* showed an interaction in the two-hybrid assay, no growth on –LEU plates could be detected in strains carrying *PUB1* in conjunction with Δ*N17-ARF1Q71L*. *GLO3* served as a positive and the empty vector as a negative control, respectively (Table 15). Eugster *et al.* (2000) have shown that *GLO3* specifically interacts with the active form of Δ*N17-ARF1* but neither with the wild type nor the inactive mutant.

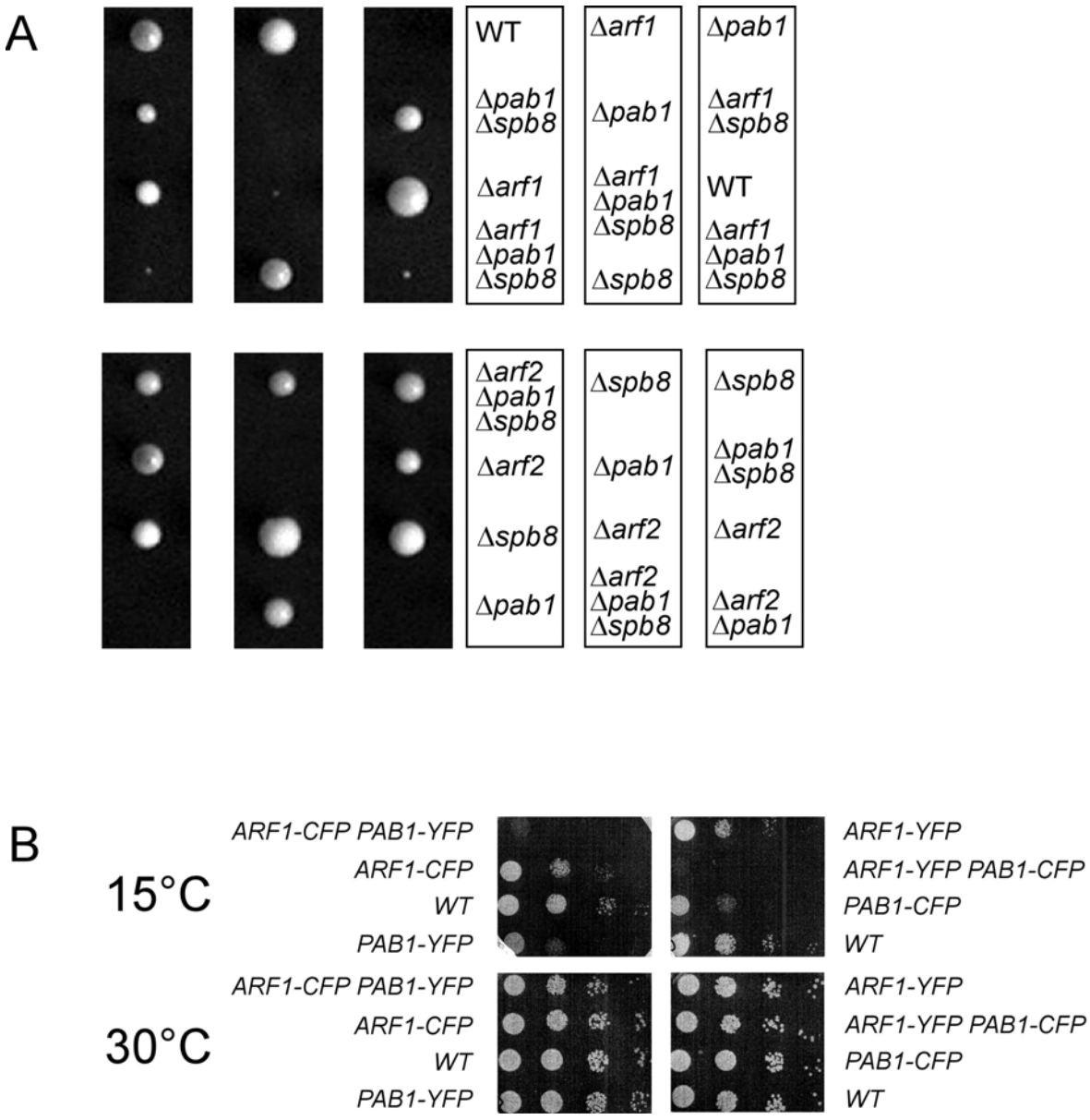

Figure 11: *ARF1* but not *ARF2* interacts genetically with *PAB1*. **(A)** Δ*arf1* or Δ*arf2* haploid strains were crossed with Δ*pab1*Δ*spb8* strains. The resulting diploid strains were sporulated and tetrads dissected. The spores were grown for 2 days at 30°C. **(B)** *ARF1* and *PAB1* were chromosomally appended with either YFP or CFP. The resulting strains were grown to early log phase, and serial dilutions were spotted on YPD plates. The plates were incubated at the indicated temperatures.

Pab1p is essential for cell viability. However, a suppressor mutant has been identified, Δ*spb8*, which allows for survival in the absence of functional Pab1p (Boeck *et al.*, 1998). *ARF1* is not essential, because its homolog *ARF2*, which is 96% identical, can at least partially substitute for *ARF1*. Yet, Arf1p and Arf2p are not fully redundant (Spang *et al.*, 2001). If Arf1p and Pab1p cooperate in an essential pathway, one would predict that a double mutant should show at least an enhanced phenotype compared to the single mutants. Thus, we crossed a Δ*arf1* strain with a Δ*pab1* Δ*spb8* strain (Fig. 11A). While the Δ*pab1* Δ*spb8* mutant had a somewhat reduced growth rate compared to wild type, the Δ*arf1* Δ*pab1* Δ*spb8* spores were very sick and hardly grew at any temperature. In contrast, Δ*arf2* did not show the same phenotype with Δ*pab1*Δ*spb8*, most likely because Arf2p is much less abundant in the cell than Arf1p and Arf1p is still present in Δ*arf2* strains. In addition, we constructed a strain containing chromosomally tagged Arf1p-YFP and Pab1p-CFP, which was cold-sensitive (Fig. 11B). The singly tagged strains do not show this phenotype. Therefore, the cold-sensitivity provides additional evidence for the specific interaction between Arf1p and Pab1p *in vivo*. Taken together, these results are consistent with an interaction of Arf1p and Pab1p *in vivo*.

3.2.1.3 Pab1p and Arf1p form a complex in vivo

As a further test of binding specificity, we performed co-immunoprecipitation experiments. First, we appended chromosomally Arf1p and Pab1p with an HA-tag and a myc-tag, respectively. The resulting strain, YAS238, did not show an altered phenotype when compared to the isogenic wild type (data not shown). Lysates of strain YAS238 were incubated with anti-HA or anti-myc antibodies and Protein G-sepharose. The immunoprecipitates were resolved by SDS-PAGE followed by immunoblot with antibodies against coatomer, the HA- and the myc-tag (Fig. 12A and B). As expected, Pab1p-myc was co-precipitated with Arf1p-HA. This precipitation was dependent on the presence of Arf1p-HA. A similar result was obtained when the Pab1p-myc was precipitated: Arf1p-HA co-sedimented only in the presence of Pab1p-myc (Fig. 12B) Unexpectedly, coatomer was also precipitated with Pab1p-myc. Since coatomer seemed also to be part of an Arf1p-Pab1p complex, we repeated the immunoprecipitation with wild type lysate and anti-coatomer antibodies. Indeed, Pab1p was found in the immunoprecipitate but not in the control (data not shown). Moreover, Pab1p

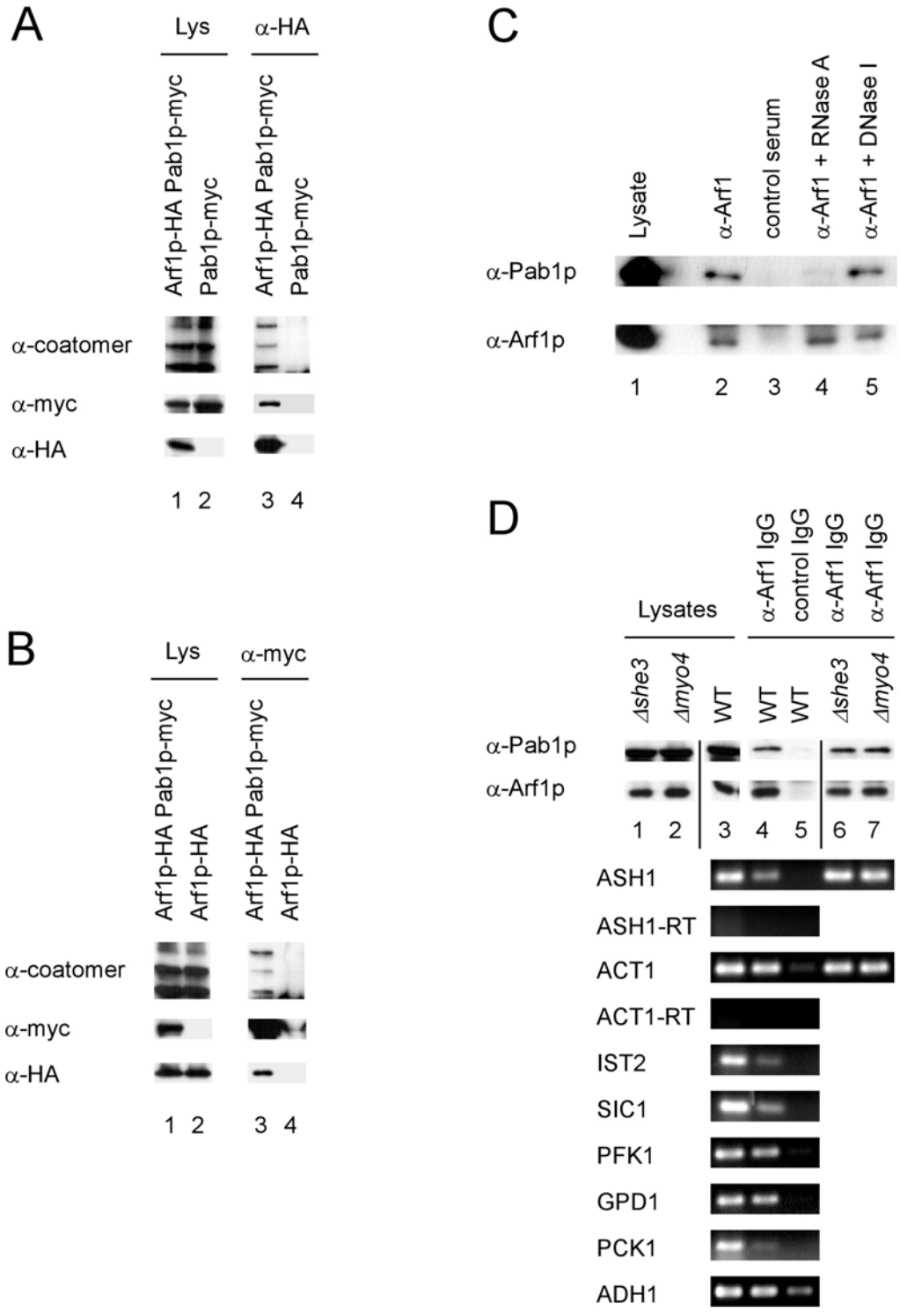

Figure 12: Arf1p and Pab1p are present in a ribonucleotide particle. **(A)** and **(B)** Pab1p and Arf1p co-immunoprecipitate. Pab1p and Arf1p were chromosomally appended with either a myc- or HA-tag. Yeast lysates were prepared from single or double tagged strains and subjected to immunoprecipitation with anti-myc or anti-HA antibodies. The precipitates were analyzed by immunoblot. Lanes 1 and 2 correspond to 1.7 % of the lysate. **(C)** Pab1p-Arf1p interaction depends on mRNA. Yeast lysate from a wild-type strain was incubated with RNAse A, DNAse I or mock treated. After the treatment an immunoprecipitation was performed with anti-Arf1p serum or a control serum and ProteinA-sepharose. The precipitated proteins were detected by immunoblot. In lane 1, 1.7 % of the lysate was loaded. **(D)** ASH1 mRNA is part of the Pab1p-Arf1p ribonucleotide particle even in the absence of the SHE machinery. A co-immunoprecipitation experiment was performed with affinity-purified anti-Arf1p antibodies. RNA was prepared from the precipitate and subjected to RT-PCR with primer specific for the indicated mRNAs. -RT indicates reactions in the absence of reverse transcriptase. In lanes 1 and 2, 1.7 % of the lysate was loaded.

failed to co-immunoprecipitate when antibodies against Sar1p or Sec23p were used (data not shown). Sec23p is the GTPase activating protein of Sar1p, and both are essential for the formation of COPII coated vesicles from the ER. Thus, Pab1p does not associate unspecifically with vesicle coat proteins. Taken together, these results provide further evidence for the existence of an *in vivo* Pab1p-Arf1p interaction and that coatomer is part of this complex.

3.2.1.4 Pab1p is associated with Golgi derived COPI-vesicles

The results presented thus far support an *in vivo* interaction of coatomer, Arf1p and Pab1p. Such an interaction could take place on the Golgi or on COPI vesicles. Pab1p is evenly distributed throughout the cytoplasm (Anderson *et al.*, 1993), making it difficult to assess the place of interaction *in vivo*. Therefore, we employed an *in vitro* Golgi budding assay, in which COPI-coated vesicles are formed from Golgi membranes (Spang and Schekman, 1998). Enriched Golgi membranes that were devoid of ER were incubated in the presence of coatomer, Arf1p and guanine nucleotide. The generated COPI vesicles were separated from the Golgi membranes by velocity centrifugation. The vesicle peak was collected and re-fractionated based on coated membrane buoyant density. Using this purification scheme, vesicles are highly enriched, because contaminating particles would have to show the same behavior on a sedimentation gradient as well as sharing the same buoyant density, which is very unlikely. When GTPγS was used to generate the COPI coated vesicles, the vesicles peaked in fractions 5 and 6 as judged by the presence of the integral membrane cargo Emp47p and the v-SNARE Bos1p (Fig. 13, GTPγS). Pab1p peaked in the same fractions. A strong signal of Pab1p was also observed in the load. This was not surprising since we expected Pab1p to travel piggyback on the COPI vesicles. Thus, some protein if not most was lost during the flotation process. We did not detect any Sec61p, the translocon at the ER, or Pgk1p, a very abundant cytosolic protein in the vesicle fraction (data not shown). The peak changed in appearance when GTP was used instead of GTPγS. In this case, the coat partially disassembled due to GTP hydrolysis, which also resulted in a partial loss of the Pab1p signal in the vesicle fraction. Pab1p was not recovered in the vesicle peak in the absence of coatomer and Arf1p (data not shown). Thus, Pab1p is associated with COPI vesicles generated from Golgi membranes, and this association is lost after the disassembly of the COPI coat.

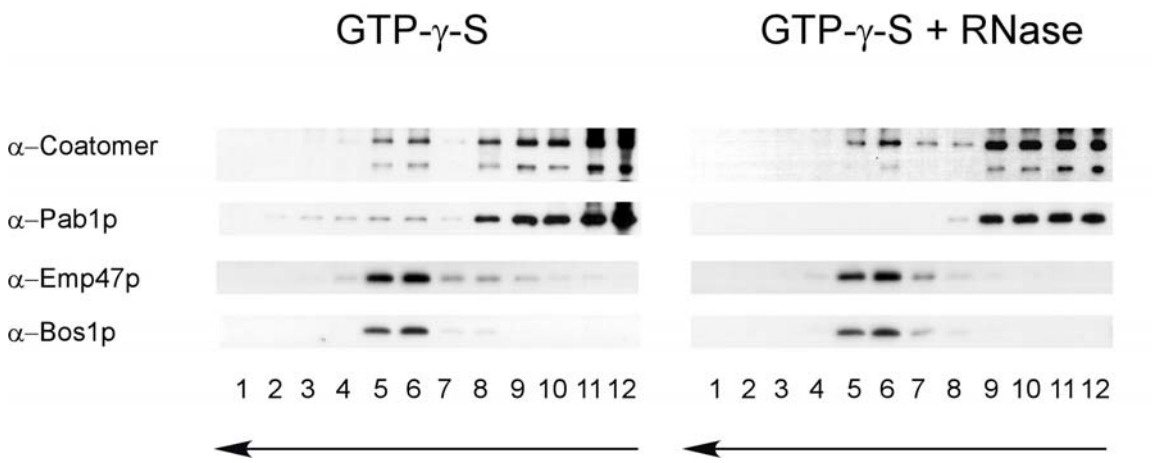

Figure 13: Pab1p association with COPI coated vesicles is dependent on mRNA. COPI vesicles were generated from Golgi membranes in the presence of GTPγS and COPI components. In one experiment RNase (200 µg) was added to the budding reaction. The vesicles were purified over a velocity gradient, and subsequently floated on a Nycodenz gradient. Fractions were collected from the top, separated by SDS-PAGE, and analyzed by immunoblot. The arrows indicate the direction of movement of lipid particles within the gradient. Non-membrane associated proteins remain in the load at the bottom of the gradient. The vesicles peak in fractions 5 and 6.

3.2.1.5 The Pab1p-Arf1p complex is dependent on the presence of mRNA

Pab1p is the major mRNA-binding protein of the cell. Therefore, we wanted to test, if RNA is present in the Pab1p-Arf1p complex and if RNA is required for the stability of the complex. To address these questions, we performed an immunoprecipitation with anti-Arf1p antibodies and digested the lysate with either RNase A or DNase I (Fig. 12C). Pab1p was co-immunoprecipitated with anti-Arf1p antibodies, and did not bind to non-related IgGs (Fig. 12C). Interestingly, the interaction of Arf1p and Pab1p was severed upon addition of RNase A. DNA digestion did not have any influence on the stability of the Pab1p-Arf1p complex. Furthermore, the addition of an excess of purified RNA or DNA did not have any impact on the Pab1p-Arf1p interaction, indicating that binding is not mediated by a nonspecific association of protein and RNA. Thus, Arf1p seems to be part of a ribonucleotide particle. Next, we wondered if Arf1p might be part of special 3'-end RNA processing complexes. Therefore, we performed RT-PCRs on anti-Arf1p immunoprecipitates (Fig. 12D). We tested eight mRNAs that differ in their abundance and that are either symmetrically or asymmetrically localized. In *S. cerevisiae*, at least two asymmetrically localized mRNAs have been identified: ASH1 and IST2. They are transported into the bud along actin cables via the SHE machinery and anchored at the bud tip of a growing cell (Long *et al.*, 1997; Munchow *et al.*, 1999; Takizawa *et al.*, 2000) (Fig. 14). The motor protein Myo4p forms a complex with the RNA binding protein She2p via

She3p (Bohl *et al.*, 2000; Long *et al.*, 2000; Takizawa and Vale, 2000). This complex delivers the mRNA to the bud tip where it is anchored.

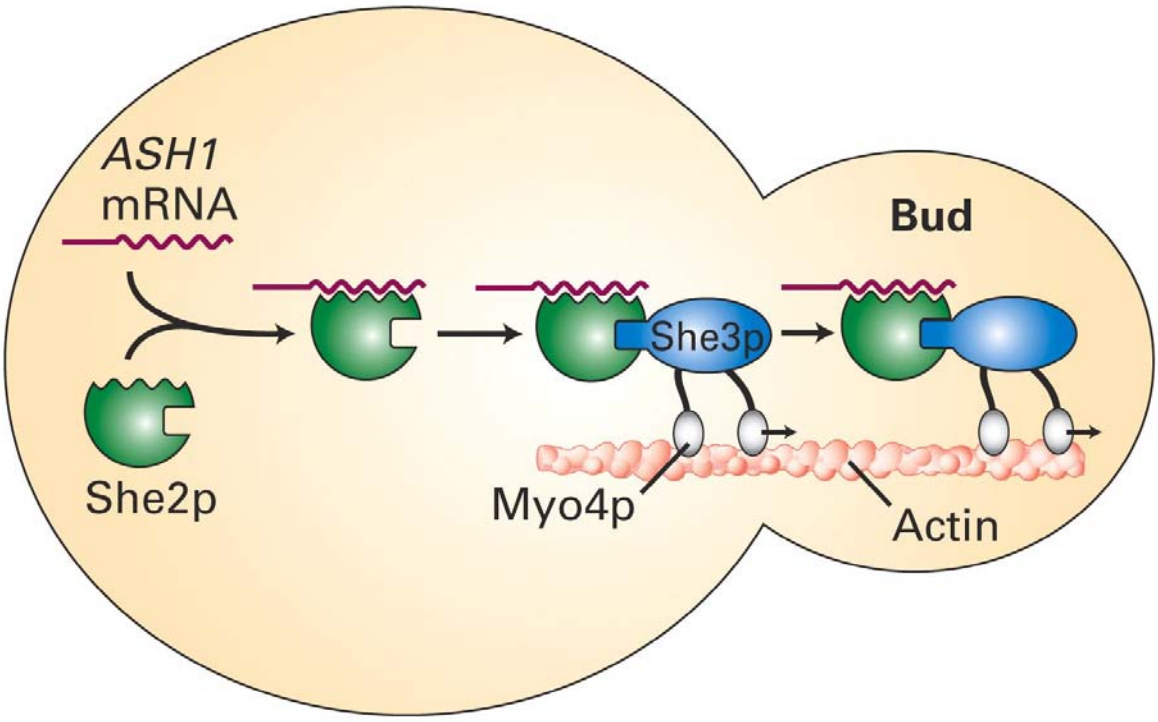

Figure 14: Model for restriction of mating type switching to mother cells in *S. cerevisiae.* ASH1 mRNA is transported by the SHE machinery (including the myosin Myo4p/She1p) along acting cables to the distal bud tip of the daughter cell. Little is known about the anchoring of ASH1 mRNA at this site. Local translation of ASH1 mRNA occurs resulting in an asymmtric Ash1p distribution. Ash1p is a transcriptional repressor of the HO-endonuclease, which is responsible for mating type switching. Thus, even in *S. cerevisiae*, mother and daughter cells have different cell fates. The mother is able to switch its mating type whereas the daughter cannot (adapted from Lodish *et al.*, 2003).

As shown before, Pab1p specifically precipitated with affinity purified anti-Arf1p antibodies and not with control IgGs (Fig. 12D). Using this precipitate as template for the RT-PCR for different mRNAs resulted in a positive signal for all tested mRNAs. These signals were specific since no product was detected in the lanes where a precipitate with control IgGs had been used at 25 cycles. Increasing the cycle number to 30 resulted in a signal also in the control for most of the mRNAs except for ASH1. This result indicates that the Arf1p-Pab1p particles contain a variety of different mRNAs.

Since we also detected the asymmetrically localized ASH1 and IST2 mRNAs in Arf1p-Pab1p ribonucleotide particles, we asked, whether interfering with the SHE machinery would also affect the association of the asymmetrically localized ASH1 mRNA with the COPI vesicles. Therefore, we repeated the Arf1p immunoprecipitation in strains where either *SHE1/MYO4* or *SHE3* had been deleted. As observed in the wild type, Pab1p co-

sedimented with Arf1p (Fig. 12D, compare lane 4 with lanes 6 and 7). Furthermore, the precipitated mRNA contained ASH1 mRNA. Therefore, the association of the asymmetrically localized mRNA ASH1 with the Arf1p-Pab1p complex is independent of its transport by the SHE machinery.

We have established that Pab1p is present on COPI vesicles. Furthermore, ASH1 mRNA was detected on the COPI vesicle fraction of a Golgi budding experiment (data not shown). Yet, does this interaction of Pab1p and Arf1p depend on the presence of mRNA? To address this question, we again performed a Golgi budding experiment (Fig. 13). This time, however, we added RNase during COPI vesicle generation. Treatment of the Golgi membranes with RNase did not affect vesicle generation but the association of Pab1p with the COPI vesicles was completely lost. Therefore, the attachment of Pab1p with Golgi-derived COPI vesicles requires the presence of mRNA.

3.2.1.6 Asymmetric mRNA localization is disturbed in arf1 mutants

The Arf1p-Pab1p ribonucleotide particles contain asymmetrically and symmetrically localized mRNA. Thus, COPI vesicles are likely to contain a wide repertoire of mRNAs. These COPI vesicles are required for intra-Golgi as well as Golgi to ER retrograde transport. Because COPI vesicles are transport carrier, it seemed reasonable to look for a link to mRNA transport. One possible role for the mRNA association with the vesicles could be to bring the mRNA to the ER. The ER is a reticulate structure distributed throughout the cell and we found it hard to study the transport of symmetrically localized mRNAs. Therefore, we investigated an asymmetrically distributed mRNA, ASH1, that was also found on COPI vesicles. First, we tested whether deletion of *ARF1* interferes with the localization of ASH1 mRNA using a GFP-based mRNA-localization assay (Bertrand *et al.*, 1998). GFP is fused to sequences encoding the viral MS2 coat protein, while an ASH1 mRNA reporter construct contains MS2 binding sites. A nuclear localization signal on the GFP containing plasmid restricts GFP to the nucleus. Only after interaction of the MS2 coat protein with MS2 binding sites can GFP exit the nucleus with ASH1 mRNA. We compared the ASH1 mRNA localization of wild type yeast cells to that in a Δ*arf1* strain (Fig. 15). We scored 3 different phenotypes: bud tip (correct localization), bud neck and mother cell. In the wild-type strain over 60% of cells showed the correct localization of ASH1 mRNA in the bud tip at 30°C and 16°C. In contrast, ASH1 mRNA seemed to be mislocalized in Δ*arf1* cells at the permissive temperature and even more severely at the restrictive temperature. Only in about 20% of the Δ*arf1* cells incubated at the restrictive

temperature was the GFP signal confined to the bud tip. The ASH1 mRNA never seemed to reach the bud tip in the remaining 80% of the cells. The GFP particle was either stuck in the bud neck or was randomly localized in the mother cell. This result indicates that Arf1p is required for the correct localization of ASH1 mRNA.

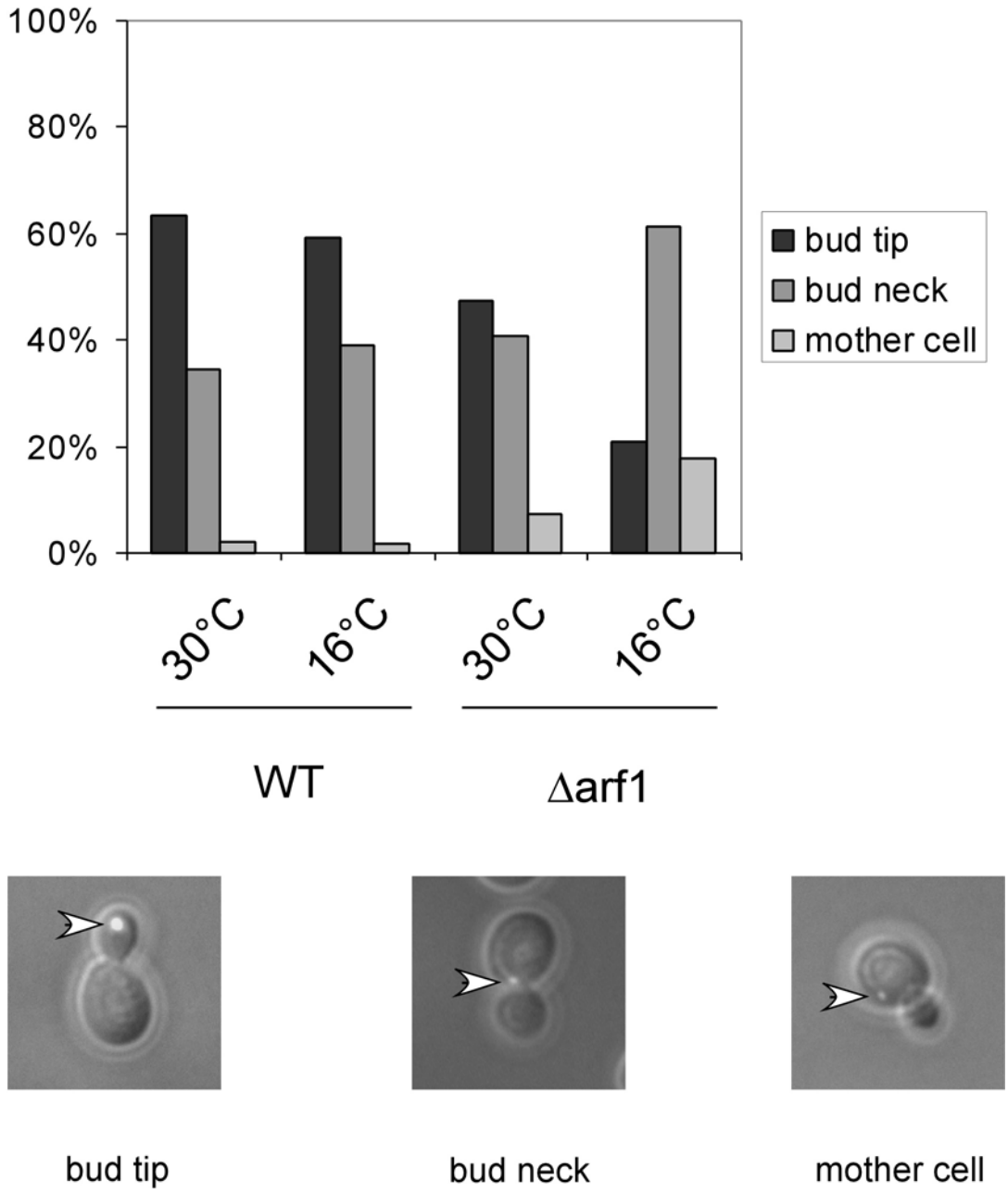

Figure 15: ASH1 mRNA is mislocalized in Δ*arf1* mutant cells. An ASH1 mRNA-GFP reporter system was transformed in either wild type or the isogenic Δ*arf1* strain. Cells were grown to early log phase at 30°C. One half of the cultures were shifted to 16°C for 3 hours. At least 100 cells per strain and temperature were analyzed for the localization of the GFP particle. The scored phenotypes are indicated. The arrowheads point towards the green fluorescent particle.

We extended our results by using temperature-sensitive *arf1* alleles in a Δ*arf2* background generated by Yahara *et al.* (2001). In these strains, ARF function is only provided by the *arf1* ts-allele. In addition, we switched our detection method to fluorescence *in situ* hybridization (FISH). The strains were grown over-night under permissive conditions, shifted for 1 hour to the restrictive temperature and then prepared for FISH analysis. To score the phenotypes as objectively as possible, double-blind experiments were performed. Strain NYY 0-1 corresponds to the 'wild type' in this experiment, since it contains the wild-type allele of *ARF1* in a Δ*arf2* background, while NYY11-1, NYY17-1 and NYY18-1 represent different point mutants (Fig. 16B). NYY11-1 carries three point mutations one of which is in proximity to the switch 1 domain. The other two mutations are towards the C-terminus, which is probably involved in protein-protein interaction. NYY11-1 has a strong defect in Golgi to ER transport. NYY17-1 (mutated in the switch 1 region) seems to be a weaker allele and is a member of a different intragenic complementation group. NYY18-1

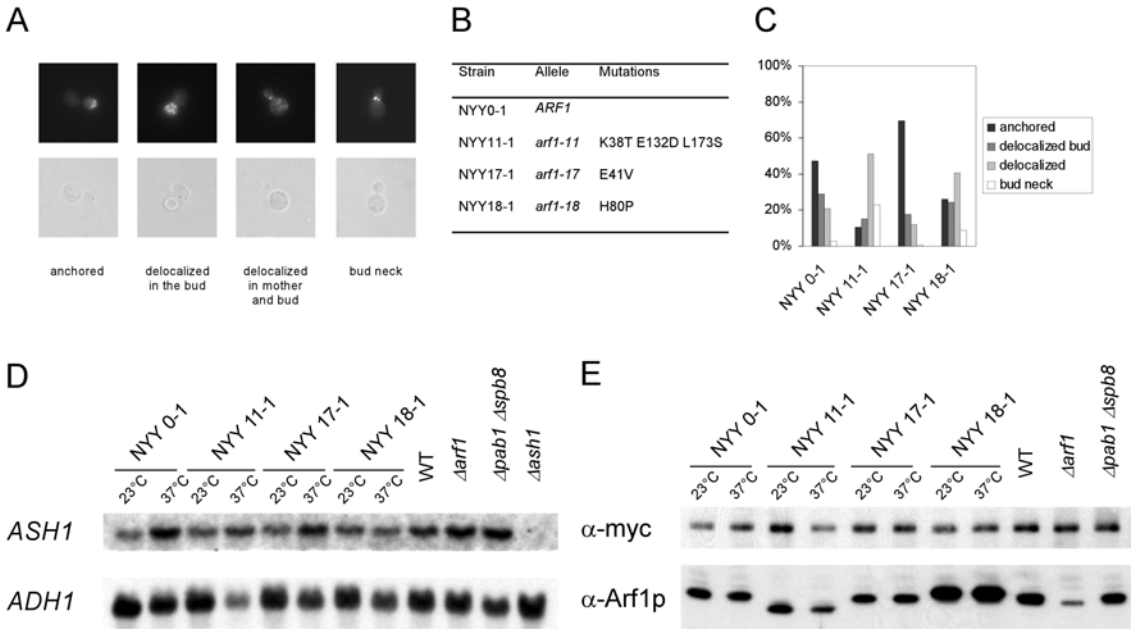

Figure 16: Arf1p and Pab1p are required for ASH1 mRNA localization to the bud tip. **(A)** Overview of scored phenotypes. **(B)** List of mutants used in the analysis in **(C)**. **(C)** The defect in mRNA localization is allele specific. Different mutants in *ARF1* were grown to early log-phase at 23°C and then shifted for 1 hour to 37°C. ASH1 mRNA in the cells was visualized by FISH. At least 100 cells/strain were scored. **(D)** ASH1 mRNA levels are not sensitive to shift to the restrictive temperature. Different mutants in *ARF1* were grown to early log-phase at 23°C and then shifted for 1 hour to 37°C; the deletion mutants in *ARF*1 and *PAB1 SPB8* as well as a wild-type strain were grown at 30°C. Total RNA was extracted from the different strains and analyzed by Northern blot. The blot was incubated with probes for ASH1 mRNA and ADH1 mRNA. Upon temperature-shift, no significant changes in mRNA levels were observed. **(E)** Ash1p levels are not altered in different mutants. The strains were transformed with a CEN plasmid encoding C-terminally myc_9-tagged Ash1p and grown as described in **(D)**. Soluble extracts were prepared and analyzed by immunoblot for the presence of Ash1p-myc and Arf1p. The translation of ASH1 mRNA appeared to be unaffected by shift to restrictive temperature. The Arf-signal in the Δ*arf1* mutant corresponds to Arf2p, which is upregulated in Δ*arf1* strains. Arf2p is 10 times less abundant than Arf1p in wild-type strains.

is supposed to disturb transport at the Golgi and carries a mutation in the switch 2 region (Fig. 16B). At the restrictive temperature, only about 50% of the *ARF1* wild-type showed correct localization of the ASH1 mRNA (Fig. 16C). However, the mutant NYY17-1 was not defective in mRNA localization and showed about 70% correctly anchored ASH1 mRNA. In contrast, the mRNA localization in NYY11-1 and NYY18-1 was severely affected. The predominant defect was delocalized mRNA throughout the cell, indicating that these mutants were either deficient in transport or anchoring of the mRNA in the bud tip. These results indicate that the mRNA mislocalization phenotype displayed by the different mutants is due to a specific involvement of Arf1p in this process.

3.2.1.7 arf1 mutants show no defects in transcription or translation of ASH1

Anchoring of ASH1 mRNA depends at least in part on Ash1 protein translation (Gonzalez *et al.*, 1999). Therefore, the results presented above, although specific for Arf1p, could also be interpreted as a defect in transcription, mRNA instability or down regulation of translation of ASH1. In addition, some mutants of components along the secretory pathway led to a defect in ribosome biosynthesis (Mizuta and Warner, 1994). Moreover, Deloche *et al.* (2004) reported that translation initiation was attenuated very rapidly and protein synthesis was reduced in secretion mutants upon shift to restrictive conditions. To test effects on ASH1 mRNA stability and Ash1p protein synthesis in *arf1* and *pab1* mutant strains before and after shift to the restrictive temperature, we performed Northern and Western blots (Fig. 16D and E). Yet, no significant variations in ASH1 mRNA levels were detected in *arf1* ts-mutant strains upon shift to non-permissive conditions or in strains where *ARF1* or *PAB1* had been deleted (Fig. 16D). Detection of ADH1 mRNA served as internal control. A myc-tagged version of Ash1p is functional and has been used to assess the Ash1p content in cells (Cosma *et al.*, 1999; McBride *et al.*, 2001). Therefore, we used Ash1p-myc expressed from a CEN plasmid (single copy) to determine Ash1p levels in *arf1* and *pab1* mutants. Soluble yeast lysates were analyzed for the presence of Ash1p-myc and Arf1p (Fig. 16E). As observed for the mRNA levels, no significant differences in the Ash1p levels were eminent. Thus, it is unlikely, that transcription or translation of ASH1 is disturbed in the *arf1* mutants and that this would be the cause of the ASH1 mRNA localization defect.

3.2.1.8 Δpab1Δsbp8, Δscp160, and Δbfr1 are defective in ASH1 mRNA localization

Next, we wanted to check, if Pab1p is also required for asymmetric mRNA localization. Cells of a Δ*pab1*Δ*sbp8* strain were grown at 30°C and prepared for FISH as described above. Indeed, a similar phenotype was observed as for a Δ*arf1* mutant (Fig. 17A).

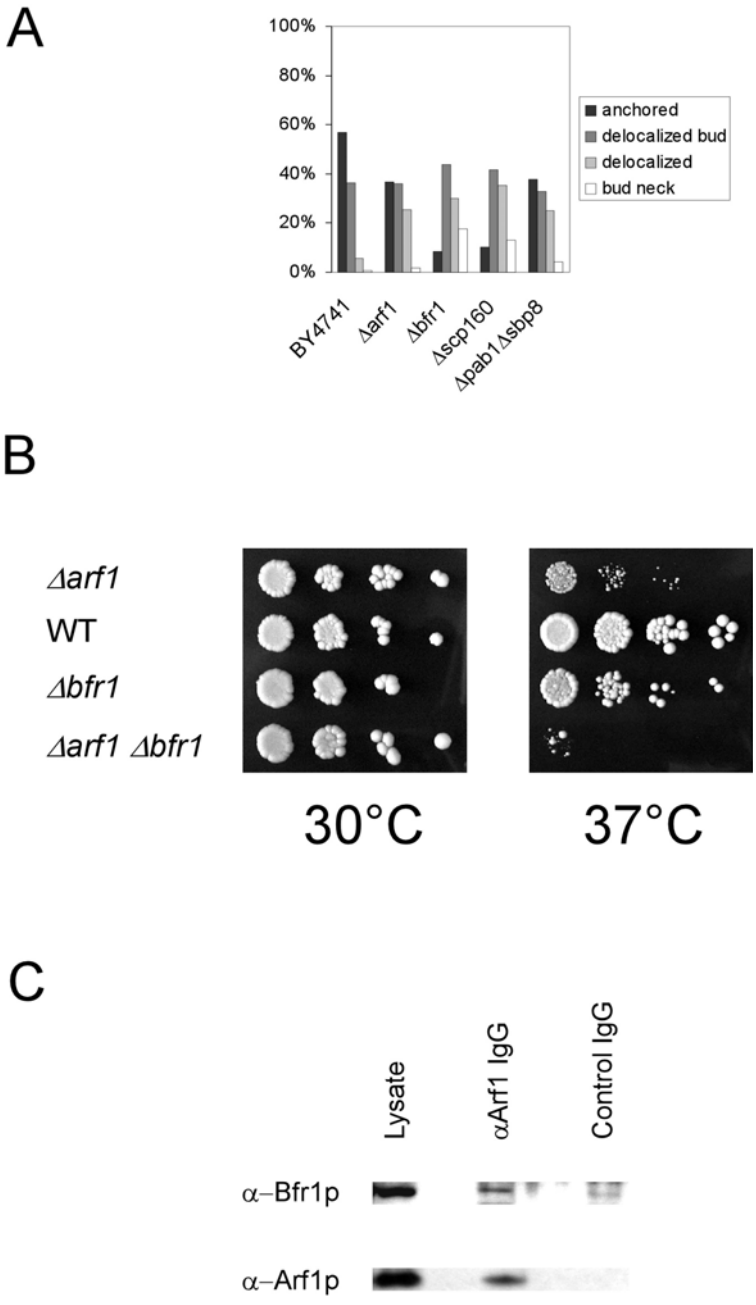

Figure 17: Pab1p binding proteins display abnormal ASH1 mRNA localization. Cells were grown to early log phase at 30°C and FISH for ASH1 mRNA was performed. BY4741 is the corresponding wild type for the strains in **(A)**. At least 100 cells/strain were scored. **(B)** *ARF1* and *BFR1* interact genetically. Single and double mutants in *ARF1* and *BFR1* were grown at 30°C. Serial dilutions were dropped on plates and incubated at the indicated temperatures for 2 days. **(C)** Bfr1p interacts with Arf1p. An immunoprecipitation from yeast lysate was performed with affinity-purified antibodies against Arf1p or control IgGs. Bfr1p was co-precipitated with Arf1p.

In both cases about 60% of the ASH1 mRNA was mislocalized while in the wild-type 60% of the cells the signal was observed anchored in the bud-tip. Pab1p is known to interact with two other proteins, Scp160p and Bfr1p (Lang and Fridovich-Keil, 2000). Moreover, Scp160p has been identified as a multicopy suppressor of a *gea1-4* Δ*gea2* mutant and physically interacts with Gea1p (Peyroche and Jackson, 2001). Gea1p and Gea2p are Arf1p-GEFs that have overlapping functions in retrograde transport from the Golgi to the ER (Peyroche *et al.*, 1996; Spang *et al.*, 2001). Scp160p is a polysome-associated protein that was shown to be defective in anchoring asymmetrically localized mRNA (Irie *et al.*, 2002). Bfr1p is a protein of unknown function that was found in a screen for resistance against brefeldin A (Jackson and Kepes, 1994). Brefeldin A is an un-competitive inhibitor of Arf-GEFs (Peyroche *et al.*, 1999). Bfr1p is required for the association of Scp160p with polysomes but not with Pab1p (Lang *et al.*, 2001). In addition, we found that Δ*bfr1* and Δ*arf1* are synthetically lethal at 37°C (Fig. 17B). Furthermore, Bfr1p co-immunoprecipitates with Arf1p (Fig. 17C). Therefore, at least a part of Arf1p function might be connected to Scp160p and Bfr1p, and it seemed likely that Δ*bfr1* might also be deficient in correct mRNA localization. Indeed, Δ*bfr1* showed the same phenotype as Δ*scp160*, which was stronger than the one observed for Δ*arf1* and Δ*pab1* Δ*sbp8* (Fig. 17A). This is consistent with the probable involvement of Scp160p and Bfr1p in the general translation machinery. In the absence of Arf1p, some mRNA could still get to the ER and interact there with Scp160p or Bfr1p. However, upon deletion of *BFR1* or *SCP160* the translation and thus restriction of mRNA at the ER could be more severely affected.

3.2.1.9 Characterization of the cytoskeleton in the arf1 mutants

So far, we presented evidence that Arf1p is involved in mRNA transport and that the existence of an Arf1p-Pab1p-ASH1 ribonucleotide particle seemed to be independent of the SHE machinery. ASH1 mRNA was mislocalized in *ARF* mutants as determined by two different methods (Fig. 15 and 16C). However, it is known that mutations in *ARF* can also affect the actin cytoskeleton and might also have some effect on microtubules. In order to rule out any general defects in cytoskeletal organization or polarity, we examined the microtubules and actin cytoskeleton in the NYY strains at the permissive and restrictive temperature. All strains showed wild-type microtubules at both temperatures as judged by indirect immunofluorescence (Anne Spang, data not shown). In addition, none of the strains was sensitive towards benomyl, a microtubule depolymerizing drug (Anne Spang, data not shown). Next, we examined the actin localization by staining with rhodamine-

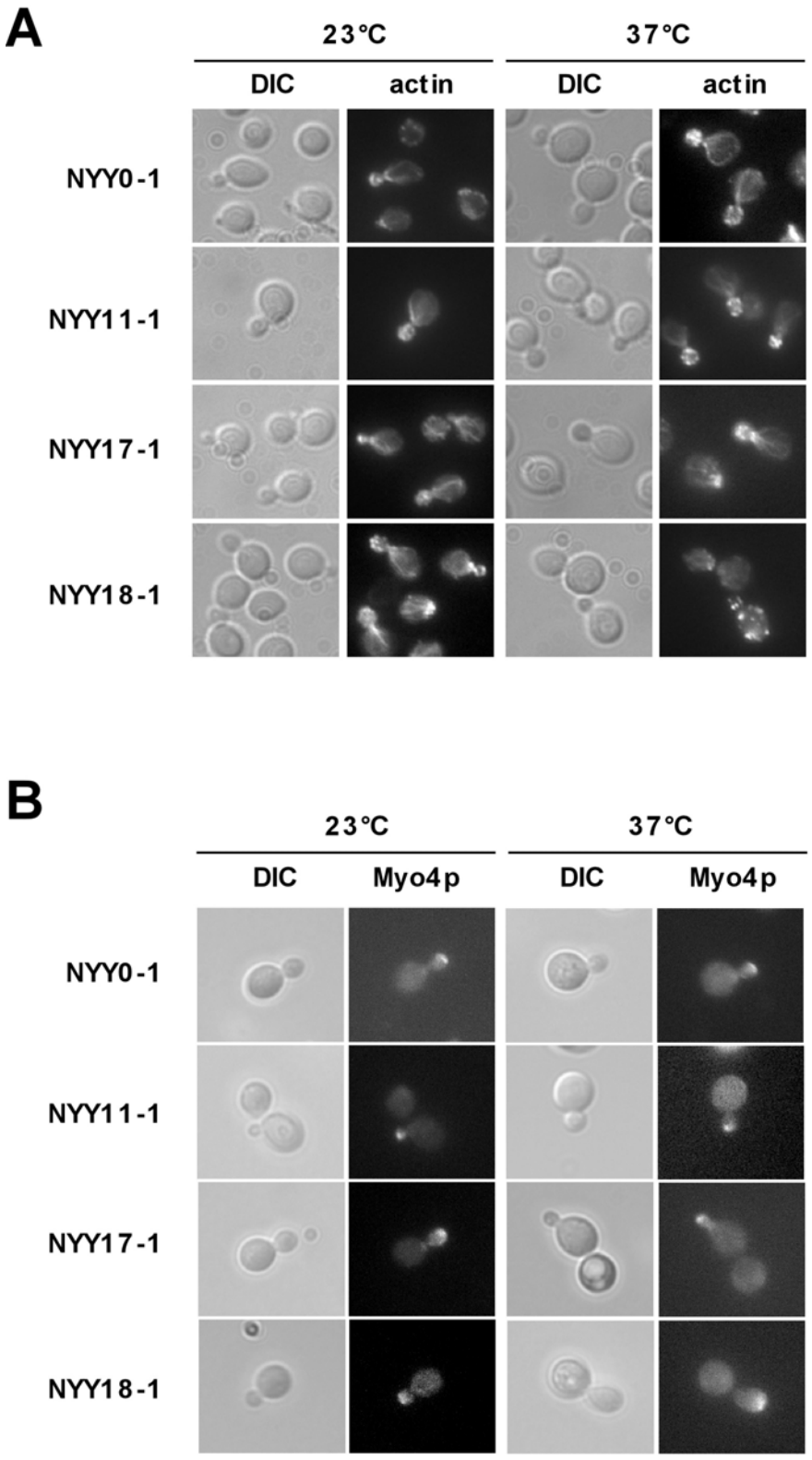

Figure 18: Localization of She1p/Myo4p and actin in *arf1* point mutants. **(A)** The actin cytoskeleton is only disturbed in NYY18-1 at the restrictive temperature. Different mutants in *ARF1* were grown to early log-phase at 23°C and then shifted for 1 hour to 37°C. Cells were fixed and the actin cytoskeleton was stained with rhodamine-phalloidin. **(B)** She1p/Myo4p localizes to the bud tip in *arf1*mutants. *MYO4* was chromosomally appended with 2xGFP. Different mutants in *ARF1* were grown to early log-phase at 23°C and then shifted for 1 hour to 37°C. Cells were examined directly. For the restrictive temperature, a heated stage was mounted onto the microscope to keep the cells at 37°C during the observation. (Fluorescence microscopy was perfomed by Anne Spang.)

phalloidin. NYY0-1, NYY11-1 and NYY17-1 did show correctly polarized actin cables and patches at the permissive and the restrictive temperature (Fig. 18A). In contrast, while NYY18-1 behaved like wild type at 23°C, after the shift to the non-permissive temperature the actin cables were missing and the actin patches were distributed randomly throughout the cell. Thus, the mRNA localization defect in NYY18-1 might be explained by the aberrant actin cytoskeleton. However, the polarity of the cell was not entirely lost, since bud site selection and budding still seemed to be normal as in the other strains tested (Anne Spang, data not shown). The second *arf1* mutant with an ASH1 mRNA localization defect, NYY11-1, behaved like wild type. Thus, the mRNA distribution phenotype in at least NYY11-1 is not caused by general defects in polarity and cytoskeletal organization.

3.2.1.10 She1p/Myo4p localizes correctly to the bud tip in arf1 *mutants*

The actin cytoskeleton was visibly disturbed only in NYY18-1 at the restrictive temperature. Nonetheless, more subtle defects might conceivably prevent the SHE machinery from reaching the bud tip in the *arf* mutants. To test this possibility, we determined the localization of the motor protein She1p/Myo4p in the *arf1* point mutants. The localization of She1p/Myo4p in the bud tip depends on the presence of She2p and She3p (Kruse *et al.*, 2002). Thus, by checking She1p/Myo4p, we can examine the functionality of the entire SHE machinery. *MYO4* was chromosomally appended by 2xGFP in the different NYY strains as described by Kruse *et al.* (2002). At the permissive temperature as well as after a shift to the restrictive temperature for at least 1 hour, Myo4p-GFP localized correctly to the bud tip in the *arf1* point mutants irrespective to their defect in ASH1 mRNA localization (Fig. 18B). Most importantly, Myo4p-GFP was localized correctly at the bud tip in NYY11-1 and NYY18-1 (Fig. 18B). Our data indicate that the SHE machinery is functional in the *arf1* mutants and that Arf1p is most likely involved in retaining ASH1 mRNA in the bud tip after the SHE proteins fulfilled their duty. These results demonstrate, that the involvement of Arf1p in mRNA localization is independent of the SHE machinery. This is in agreement with our findings that the coatomer-Arf1p-Pab1p complex contains also symmetrically localized mRNAs that are not a substrate for the SHE machinery and that the deletion of members of the SHE machinery did not sever the ASH1 mRNA interaction with Pab1p and Arf1p.

3.2.1.11 Components of the early secretory pathway are required for ASH1 mRNA localization

We found that mRNA is associated with COPI coated vesicles that are destined to the ER. Therefore, we wondered if vesicular traffic, especially through COPI transport carriers, might play a role in mRNA localization. To this end, we performed FISH with temperature-sensitive mutants in components of the early secretory pathway. Surprisingly, not only *sec21-1*, a mutant in the γ-subunit of coatomer was defective but also *sec23-1* and *sar1-D32G* (Fig. 19).

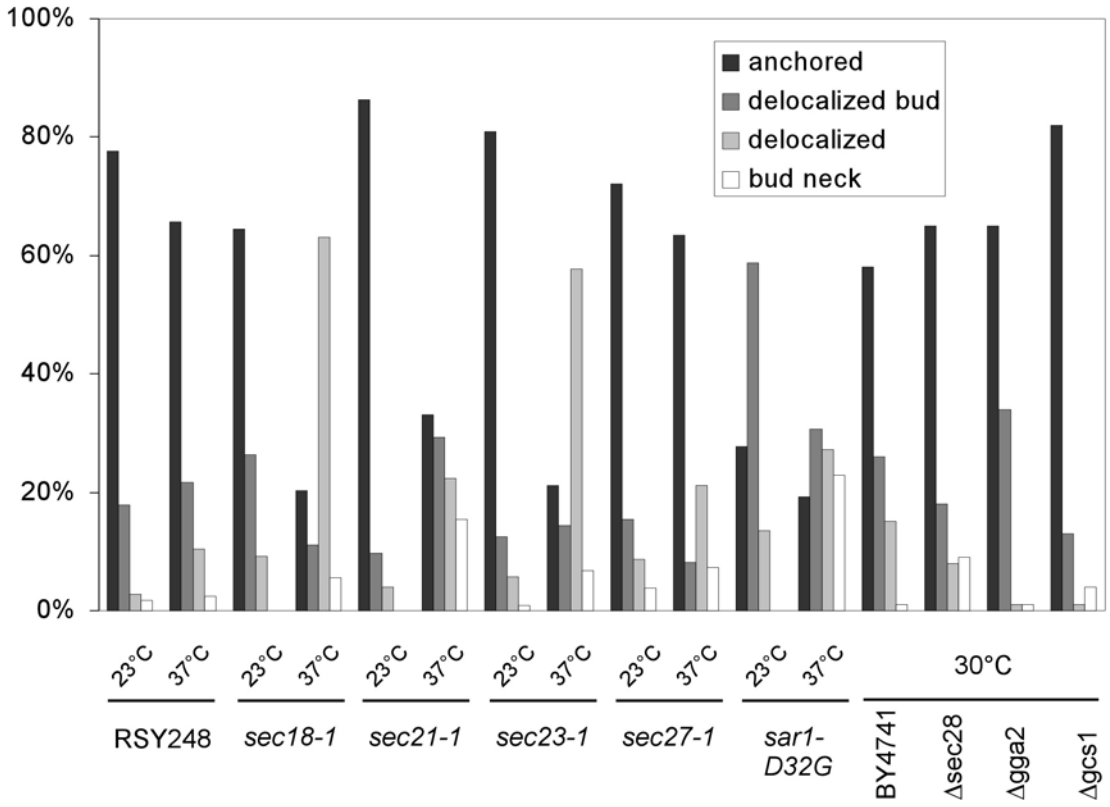

Figure 19: A functional early secretory pathway is necessary for ASH1 mRNA localization. Strains were grown to early log phase at 30°C or 23°C for ts-strains. In case of the ts-strains, one half of the cultures were shifted to 37°C for 1 hour. RSY248 corresponds to the wild-type strain for the ts-mutants and is isogenic to *sec18-1*. BY4741 is the corresponding wild type for the deletion strains. At least 100 cells were scored per strain and condition.

Sar1p is the counterpart of Arf1p in the generation of COPII vesicles, and Sec23p is the GTPase activating protein for Sar1p (Barlowe, 2000). Furthermore, the NEM-sensitive factor Sec18p, which is involved in homotypic and heterotypic membrane fusion (Novick *et al.*, 1981; Graham and Emr, 1991), also seemed to be required for the anchoring of ASH1 mRNA because in about 80% of the cells the FISH signal was mostly distributed all over the cell, and could not be found concentrated in the bud tip. In contrast, two other

mutants in the ß-subunit (*sec27*) and ε-subunit (*sec28*) of coatomer behaved like wild type, indicating that the mRNA localization is a specific event involving coatomer. The phenotype that we detected was not due to a general secretion defect, because mutants in two Arf1p interacting proteins, Gga2p (a GGA protein) and Gcs1p (an Arf1p-GAP), were not defective in ASH1 mRNA localization. Our results indicate, that restricting ASH1 mRNA to the bud tip requires functional ER-Golgi transport.

3.2.1.12 The actin cytoskeleton is not generally disturbed in ER-Golgi transport mutants.
We repeated the actin-phalloidin staining with the temperature-sensitive secretion mutants that were defective in ASH1 mRNA localization (Fig. 20). The mutant strains *sec18-1*, *sec21-1*, and *sar1-D32G* displayed a correctly polarized actin cytoskeleton at the permissive and at the restrictive temperature. In contrast, *sec23-1* cells had a disorganized actin cytoskeleton after one hour shift to the restrictive temperature. Thus, the defect in mRNA localization in these mutants (except for *sec23-1*) is not due to a lack of actin organization in the cell.

Taken together, our results indicate a novel and unexpected role for components of the early secretory pathway in short-range mRNA localization most likely through interaction with Pab1p. This process is independent of the SHE machinery. We have only investigated the localization of the asymmetrically localized mRNA ASH1. However, these results might also reflect a mechanism by which symmetrically localized mRNA is concentrated at the ER.

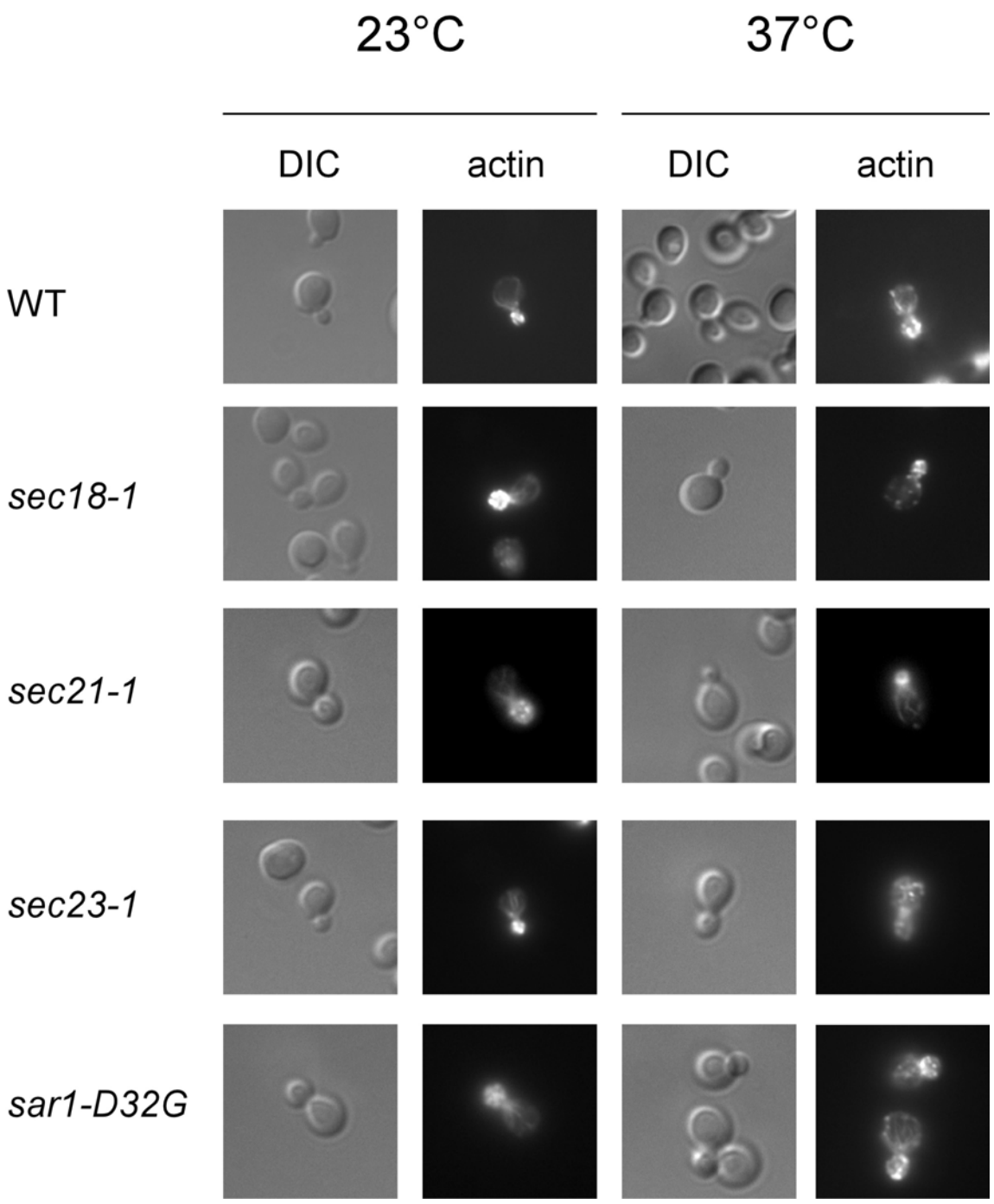

Figure 20: The actin cytoskeleton is not disturbed as a result of a defect in secretion. Secretion mutants that displayed an ASH1 mRNA localization defect were examined for a functional actin cytoskeleton. The strains were grown to early log-phase at 23°C and then shifted for one hour to 37°C. Cells were fixed and actin was stained with rhodamine-phalloidin.

3.2.2 Discussion

We have used a differential affinity chromatography approach to identify new interactors of the small GTPase Arf1p. This approach is valid because known regulators were re-identified. We have identified Pab1p as a new interactor of the small GTPase Arf1p. Pab1p interacts predominantly with the GTP bound form of Arf1p. In a high-throughput protein complex analysis in yeast, Pab1p was found to be one of the major contaminants (Gavin *et al.*, 2002) indicating that Pab1p might interact nonspecifically with many other proteins. Therefore, we confirmed the specificity of interaction by two-hybrid analysis and genetic interaction as well as by mutual co-immunoprecipitation. Furthermore, the interaction between Pab1p and Arf1p is dependent on the presence of mRNA in the complex. Moreover, we found that Pab1p is associated peripherally with COPI vesicles generated from enriched Golgi membranes. Taken together, these results argue strongly that the Arf1p-Pab1p complex is specific. If and how Pab1p is incorporated into the vesicle coat remains elusive at present. Pab1p might not become an intrinsic part of the coat but might be peripherally associated with the vesicles through interactions with Arf1p and coatomer. COPI vesicles still form upon RNase treatment, which prohibits the Pab1p interaction with the coat.

We tested Arf1p immunoprecipitates for the presence of a number of different mRNAs,which varied in their abundance and in their subcellular localization, by RT-PCR. After the immunoprecipitation, essentially all mRNAs were amplified. Thus, no specialized 3'end processing complexes were associated with COPI vesicles. To further investigate the role of Arf1p, Pab1p and the COPI coat in mRNA transport, we concentrated our efforts in studying the asymmetrically distributed ASH1 mRNA. In wild type cells, ASH1 mRNA is asymmetrically localized to the bud tip of a growing yeast cell. However, when we investigated the role of mutants in *ARF1* and *PAB1* in asymmetric mRNA distribution, we found that they mislocalize ASH1 mRNA. Furthermore, using enriched COPI vesicles from the Golgi budding assay, we could detect ASH1 mRNA by RT-PCR.

The fact that the ASH1 mRNA mislocalization phenotype in *arf1* mutants was allele specific indicates that not the whole repertoire of ARF dependent traffic is needed for mRNA localization. Moreover, this finding provides strong evidence that the ASH1 mRNA localization defect is not brought about by a secondary effect. This idea is corroborated by the data showing that some coatomer mutants did show a defect while others did not. Furthermore, the extent of ASH1 mRNA mislocalization was quite variable

in the different mutants of the early secretory pathway. However, other mutants of the early secretory pathway localized ASH1 mRNA correctly to the bud tip. Thus, the asymmetric mRNA distribution phenotype cannot be attributed to a general secretion defect. In addition to mutants in the early secretory pathway, we tested also mutants in late acting components. They either had no effects *(*Δ*gga2*) or the ASH1 mRNA mislocalization phenotype could be related to a defect in the actin cytoskeleton (*sec1-1* and *sec6-4*; Mark Trautwein and Anne Spang, unpublished data). Moreover, the ASH1 mRNA localization defect was not due to defects in the actin cytoskeleton, the microtubules organization or cell polarity. Finally, we ruled out the possibility that ASH1 mRNA stability or translation efficiency were compromised in *arf1* mutants. Ribosome biosynthesis and translation efficiency are affected in secretion mutants (Mizuta and Warner, 1994; Deloche *et al.*, 2004). However, we did not observe this effect in *arf1* and Δ*pab1*Δ*spb8* mutants, which is most likely due to the use of different mutants and different strain backgrounds: the pool of mutants tested in the various studies is non-overlapping. Thus, we are confident that the mRNA localization defect is not due to a secondary effect.

Transport of asymmetrically distributed mRNA into the bud tip was shown to be dependent upon the SHE proteins: She1p/Myo4p is an unconventional myosin that transports She2p, an RNA binding protein. The interaction between these two proteins is mediated by She3p. The role of She4p and She5p/Bni1p in mRNA localization is less well understood, but they seem to be involved in stabilization and polarization of the actin cytoskeleton. They are thought to play a role in anchoring mRNA by a thus far unknown mechanism (Beach and Bloom, 2001). However, Bloom and Beach (1999) speculated that once mRNA reaches the vicinity of its final destination, cytoplasmic flow or passive diffusion may enable mRNA accumulation at that site (the bud tip in yeast). Thus, a mechanism for restricting ASH1 mRNA in the bud is required, which might be independent of the SHE machinery. It further indicates the transport by the SHE machinery is a prerequisite but not sufficient for anchoring ASH1 mRNA at the bud tip. This is in perfect agreement with our finding that the aberrant ASH1 mRNA localization observed could not be correlated with defects in the SHE machinery, because Myo4p-GFP was restricted to the bud tip in *arf1* mutants. Furthermore, deletion of *SHE1/MYO4* or *SHE3* did not disrupt the Arf1p-Pab1p ribonucleotide particle. Therefore, the defects in ASH1 mRNA localization in the early secretion mutants are independent, and most likely downstream, of the SHE machinery. Our data are suggestive of COPI vesicles acting as short-range mRNA transport and localization vehicles: The asymmetric distribution of the

ASH1 mRNA is brought about by the SHE machinery and does not depend on Arf1p and COPI vesicles; they may act only to restrict the mRNA in the bud tip when it is not efficiently anchored. The long-range mRNA transport is dependent on the SHE machinery while the short-range localization might be reliant on COPI vesicles.

We concentrated our efforts on the study of the asymmetrically distributed ASH1 mRNA, because the pathway of ASH1 mRNA localization is well known and more amenable for experiments than symmetrically distributed mRNA. However, since the defects in mRNA localization are independent of the SHE machinery, our observations could also apply to the symmetrically distributed mRNAs. What might be the role then of the early secretory pathway in mRNA localization? We would like to suggest a model in which the mRNA is transported to the ER via the COPI machinery. This mRNA COPI interaction could take place at the Golgi. Pab1p was detected on purified Golgi membranes that we used to generate COPI vesicles *in vitro*. These vesicles contained proteins (e.g. the ER-Golgi v-SNARE Bos1p) that cycle between the Golgi and the ER. Thus, we believe that these COPI vesicles are destined to the ER. Alternatively, the COPI vesicles might be directly loaded on route. This would lead to a fast and efficient way to bring mRNA to the ER. If the mRNA cannot be anchored at the ER and diffuses away, the COPI vesicles destined to the ER might be an efficient transport system for relocation of the mRNA. Thus, COPI vesicles could act as molecular sieve to bring Pab1p containing ribonucleotide particles to the ER. Yet, one other possible explanation for the transport of mRNA on COPI vesicles might be the clearance of the ribosome-free Golgi region from mRNA. Although this might be a likely scenario for mammalian cells, the Golgi in *S. cerevisiae* is scattered throughout the cell and the single different cisternae are surrounded by ribosomes in the cytoplasm. There is no ribosome-free Golgi region in *S. cerevisiae*. Still, we cannot exclude the possibility that there might be an ancient mechanism for mRNA clearance. Alternatively, symmetrically and asymmetrically mRNA transport to the ER might result in an enhancement of membrane-bound ribosome turnover at the ER. At least in mammalian cells, it has been shown, that membrane-bound ribosomes do not distinguish between mRNA substrates and therefore can initiate the translation of any protein, regardless of whether it is cytosolic or destined for translocation/secretion (Potter and Nicchitta, 2000). However, when membrane-bound ribosomes were provided with mRNAs encoding model cytosolic proteins, subsequent translation yielded the release of the ribosome-nascent chain complex from the ER to the cytosol (Potter and Nicchitta, 2000; Potter *et al.*, 2001). Furthermore, mRNAs encoding cytosolic proteins are well represented

in the ER membrane-bound polysome fraction (Diehn *et al.*, 2000; Lerner *et al.*, 2003). Nicchitta (2002) proposed a model suggesting that the exchange of ribosomes on the ER membrane is dependent on and driven by the translation of cytosolic proteins by membrane-bound ribosomes. Our data are in agreement with this hypothesis because COPI vesicles could act as carriers for mRNAs to the ER to allow for the ribosome exchange.
The mutant in the COPII component Sar1p could display such a strong defect for two reasons, which might lead to an additive effect: Since COPII vesicles are no longer formed in these mutants, the lipid and protein composition of the ER membrane is changed. As a result, the mRNA complex might 'adhere' less efficiently at the ER membrane. The mRNA complex diffuses away and cannot be brought back since blocking anterograde COPII transport from the ER to the Golgi immediately abrogates retrograde COPI transport from the Golgi to the ER. Hence, one would observe a stronger phenotype than in the retrograde transport mutants. Although we cannot exclude a direct involvement of COPII components in mRNA localization, Pab1p did not interact with Sar1p or Sec23p. Therefore, we favor an indirect role of the COPII components in mRNA transport.

Taken together, our results provide the first evidence for a role of Pab1p and COPI vesicles in concentrating mRNA at the ER. Because, we tested only 8 different mRNAs, we cannot exclude that not all mRNAs travel on COPI vesicles. Performing a DNA microarray analysis similar to that was used to identify 22 bud-localized transcripts (Shepard *et al.*, 2003) might prove useful in solving this problem.

3.3 Genetic evidence for interaction with a new family of putative cargo receptors at the trans-Golgi in *S. cerevisiae*

3.3.1 Results

3.3.1.1 Chs5p and Ymr237p are new interactors of activated Arf1p

In Chapter 3.1, we described the identification of new interactors of Arf1p by means of a differential Arf1p-affinity chromatography approach with mutant proteins restricted to the either GTP or GDP-bound form of Arf1p. Out of ten protein bands analyzed, six corresponded to already known interactors of Arf1p. Two protein bands corresponded to Chs5p and the protein product of the uncharacterized ORF *YMR237w*. Both proteins were enriched in the Arf1p-GTP affinity eluate. We generated an antiserum against Chs5p and binding to Arf1p-GTP was confirmed by immunoblotting of the Arf1p affinity eluates (Fig. 21). Attempts to raise antisera against full-length Ymr237p or against peptides derived from Ymr237p were unsuccessful. However, the fact that Ymr237p was clearly enriched in the Arf1p-GTP eluate (and therefore chosen for MS analysis) strongly suggests that Ymr237p also interacts predominantly with Arf1p-GTP. Thus, Chs5p and Ymr237p were identified as new interactors of activated Arf1p.

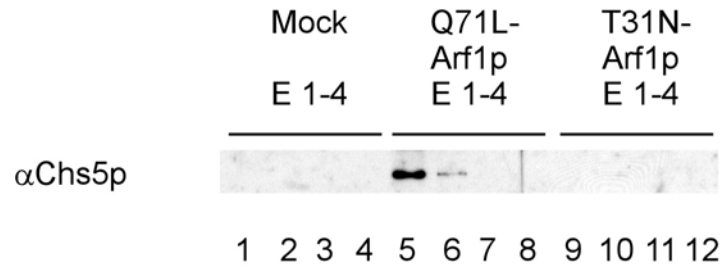

Figure 21: Chs5p binds to Arf1p-GTP. Yeast cytosol was incubated with either Arf1p-Q71L (Arf1p-GTP) or Arf1p-T31N (Arf1p-GDP) column material. After washing, spontaneous nucleotide exchange was elicited resulting in a conformational change on Arf1p and the release of conformation-specific bound proteins. Eluates (E1-E4) from the Arf1p affinity chromatography were analyzed for the presence of Chs5p by immunoblot. Chs5p is highly enriched in eluates from the Arf1p-GTP column. Beads without Arf1p were mock-treated and served as negative control.

3.3.1.2 Chs5p and the Bud7-Chs6 family

Chs5p is a protein that has been implicated in chitin synthesis, cell fusion and mating (Santos *et al.*, 1997). More specifically, it is required for chitin synthase III activity *in vivo* and probably mediates exit of the chitin synthase Chs3p from the trans-Golgi-network (TGN) (Santos and Snyder, 1997). Chs3p is the enzymatic subunit of chitin synthase III complex, which is responsible for formation of a chitin ring at the mother-bud neck at the time of cytokinesis. After cell division, remnants of the chitin rings are still visible as bud

scars. In addition, Chs5p has been shown to be essential for the polarized localization of the cell fusion factor Fus1p to the shmoo tip during mating (Santos and Snyder, 2003). It harbors a Fibronectin type III (FN3) domain, which is found in approximately 2% of all animal proteins. FN3-like domains are also present in bacterial proteins. Another feature of Chs5p is the breast cancer carboxy-terminal domain (BRCT), which is found within many DNA damage repair and cell cycle checkpoint proteins. This domain presumably serves to mediate homo- and hetero-multimer formation. Besides, Chs5p contains small blocks of homology with Sec16p, a COPII vesicle coat protein at the ER (Espenshade *et al.*, 1995). Therefore, Chs5p has been proposed to reside on the outside of Chs3p-containing vesicles (Santos and Snyder, 1997).

Protein sequence alignments suggest that the proteins Ymr237p, Bud7p, Ykr027p and Chs6p are a family of paralogous proteins in *Saccharomyces cerevisiae* (Fig 22). Ymr237p and Bud7p share 54% sequence identity while Ykr027p and Chs6p are slightly less similar (43% sequence identity). Both sub-branches of the family have around 25% sequence identity. Ymr237p is probably the ancestral protein of which Chs6p is derived by gene duplication. Another gene duplication event resulted in Ykr027p and Bud7p. No obvious putative domains within the Bud7-Chs6 family were identified. Orthologous proteins are

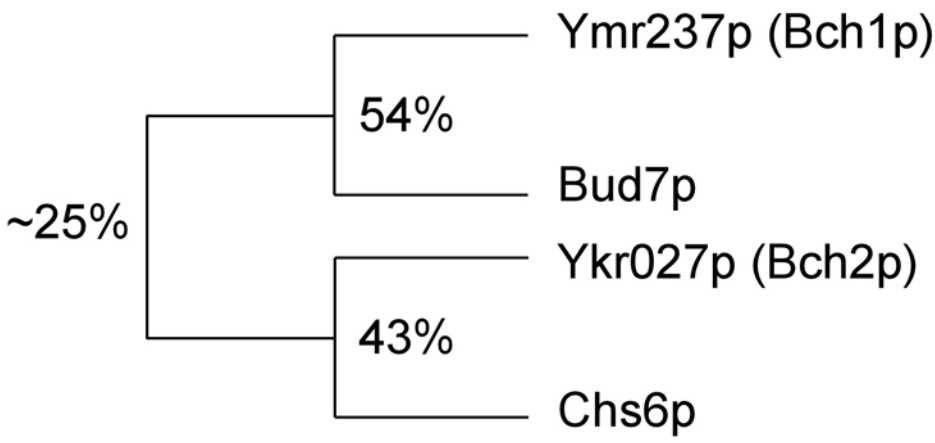

Figure 22: Scheme depicting the relationship of the members of the Bud7-Chs6 family. The percentage of protein sequence identity is given.

only found in fungi, indicating a fungi-specific role for this protein family. Bud7p was identified in a screen for mutants defective in bipolar budding pattern of diploid yeast cells (Zahner *et al.*, 1996). *BUD7* diploid deletion mutants exhibit an axial-like budding pattern (Ni and Snyder, 2001). Depending on the strain background, the pattern appears also often to be random (Ni and Snyder, 2001). In contrast to Bud7p, virtually nothing is known about Ymr237p. Ykr027p was found in the proteome of highly enriched mitochondria

(Sickmann *et al.*, 2003). However, in a genome-wide GFP-localization approach Ykr027p was localized to the Golgi-apparatus (Huh *et al.*, 2003). Chs6p is required for the anterograde transport of Chs3p from internal endosome-like structures ("chitosomes") to the plasma membrane (Ziman *et al.*, 1998; Valdivia *et al.*, 2002). Hence, both Chs5p and Chs6p are required for the transport of the chitin synthase Chs3p to the plasma membrane. This raises the possibility that Chs5p acts not only together with Chs6p on the same pathway but might fulfill an additional role in conjunction with the other three Bud7-Chs6 family members Alternatively, the other three family members might also be implicated in the transport of Chs3p.

We are going to refer to Ymr237p and Ykr027p as Bch1p and Bch2p (for Bud7-Chs6 homologous proteins 1 and 2), respectively.

3.3.1.3 Members of the Bud7-Chs6 family fulfill different functions

In order to study the Bud7-Chs6 family in a systematic manner, we created single deletion strains of the Bud7-Chs6 family members. The single deletion strains were assayed for growth at various temperatures, on different nutrient sources and for growth on plates containing the chitin binding dye calcofluor white (Fig. 23). This dye is toxic to cells with normal chitin levels whereas mutants defective in chitin synthesis or chitin synthase trafficking are unaffected. A deletion of *CHS6* was resistant to the chitin binding dye calcofluor white while *Δbud7*, *Δbch1* or *Δbch2* were sensitive similar to the wild-type (Fig. 23A). From all the deletion strains, only the *Δchs6* strain was temperature-sensitive at 37°C (Fig. 23B). In contrast, a *Δbch1* strain grew slowly at 23°C and was highly sensitive to growth on YMP+ plates (Fig. 23B and C). YMP+ is a rich medium containing elevated levels of ammonium. Deletion of any of the other three members of the Bud7-Chs6 family was no more sensitive than the wild-type towards YMP+. For a *Δbch2* strain we did not observe any obvious defect. As reported before, a homozygous diploid *Δbud7* strain displayed a random budding pattern (Fig. 23D). The *Δbch1* and *Δbch2* homozygous diploid deletions budded in a normal bipolar budding pattern. We were unable to assess the budding pattern of a *Δchs6* homozygous diploid strain due to extremely low staining with calcofluor white, which is used to visualize the bud scars. Instead, sometimes chitin staining was obtained at protrusion of the cell wall. However, it was possible to score the budding pattern in another strain background (BY4743, Robert Gauss, unpublished observation). There, the *CHS6* deletion did not affect the diploid-specific budding pattern.

Another phenotype observed for a *Δbud7* deletion was the fast growth on plates buffered at pH 7.5 (Fig. 2E). The fact that phenotypes observed for specific mutants

are only associated with one member of the Bud7-Chs6 family demonstrates that the proteins of the Bud7-Chs6 family serve different functions in the cell and are not redundant.

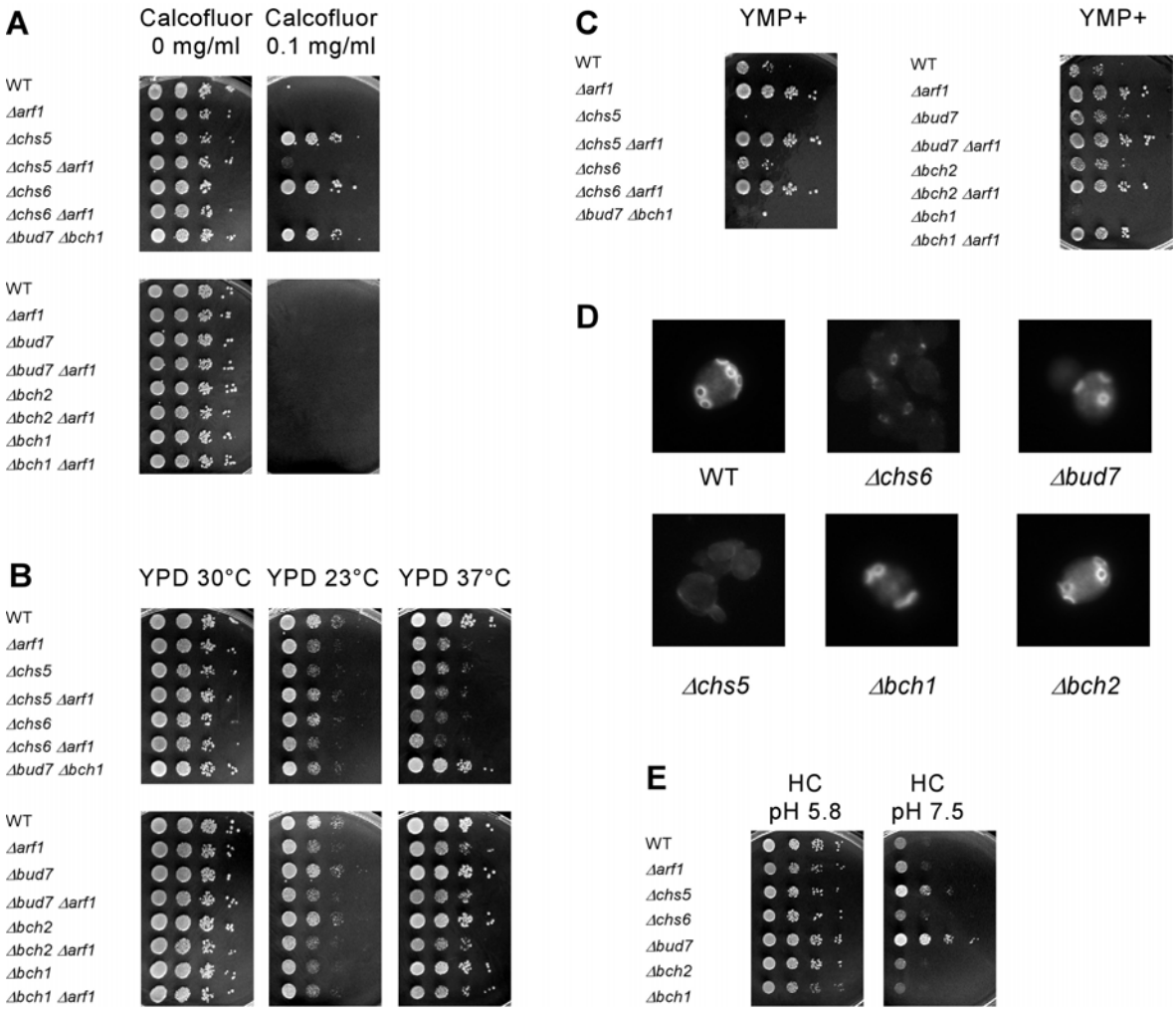

Figure 23: Analysis of single deletion mutants of the Bud7-Chs6 family together with mutants in *CHS5* and *ARF1*. For the drop assays, haploid strains were grown overnight to logarithmic phase in rich medium. After adjusting the cell concentration, serial dilutions (1:10) were dropped onto plates and incubated for two days at 30°C unless indicated otherwise. **(A)** Growth on plates containing the toxic chitin-binding dye calcofluor white. **(B)** Growth at different temperatures. **(C)** Growth on YMP+ plates. These rich medium plates contain an elevated level of ammonium sulfate. **(D)** Analysis of the budding pattern. Diploid yeast strains were grown for at least 16 h to logarithmic phase. After fixation with formaldehyde, the cells were stained with calcofluor white to visualize the bud scars under the fluorescent microscope. **(E)** Growth on minimal medium plates buffered at pH 5.8 and pH 7.5.

Most strikingly, the *Δchs5* deletion strain exhibited all phenotypes observed for the deletion of different members of the Bud7-Chs6 family (Fig. 23), namely resistance to calcofluor white, temperature- and cold-sensitivity, YMP+ sensitive growth, fast growth on plates at pH 7.5, and a random budding pattern in diploid strains (again not scorable in YPH501 but in BY4743, Robert Gauss, unpublished results; also reported by Santos *et al.*, 1997). While the single deletions of the Bud7-Chs6 family resulted in distinct phenotypes typical for a single gene, the *CHS5* deletion combined all the different phenotypes. This indicates that Chs5p is either an upstream regulator or a downstream converging point of Bud7-Chs6 protein family-related pathways.

3.3.1.4 Members of the Bud7-Chs6 family genetically interact with each other and with ARF1

Because we identified Chs5p and Bch1p as interactors of Arf1p-GTP, we wanted to explore the genetic relationship between *ARF1* and the Bud7-Chs6 family or *CHS5*. We therefore created double deletion strains. An *ARF1* deletion restored the calcofluor white sensitivity of both *Δch*s5 and *Δchs6* (Fig. 23 B). The sensitivity to growth on YMP+ plates was abolished for both *Δchs5* and *Δbch1* (Fig. 23 C). Interestingly, a single *ARF1* deletion itself was growing better than the wild-type strain on YMP+ plates. However, the random budding pattern of a diploid *Δbud7* strain was not rescued by an additional *ARF1* deletion (data not shown). Thus, we could demonstrate a genetic interaction between *ARF1* and at least part of the Bud7-Chs6 family and *CHS5*.

All single deletions of the Bud7-Chs6 family resulted in viable strains. We wanted to determine whether there was a genetic relationship between the four paralogs of the Bud7-Chs6 family themselves. Therefore, we created strains of all possible combinations of double, triple and quadruple deletions. As for the single deletions strains, these combinations were assayed for their growth on different plates (Table 16). The calcofluor white resistance of a *CHS6* deletion was not rescued in any deletion combination. However, the temperature-sensitivity was rescued by an additional *BCH1* deletion demonstrating that the calcofluor white resistance and temperature-sensitivity are separable. The sensitivity of a *BCH1* deletion towards YMP+ was not changed in any combination. Surprisingly, a quadruple deletion did not show a deleterious phenotype as could have been anticipated for a family null mutant. Unexpectedly, the *Δbud7 Δbch1* double deletion resulted in a calcofluor white resistant phenotype which was not altered in a *Δchs6 Δbud7 Δbch1* triple deletion (Table 16 and Fig. 23). Furthermore, a double

deletion of *Δchs6* and *Δbch2* was partially sensitive to YMP+. Taken together, members of the Bud7-Chs6 family interact genetically.

Table 16: Phenotypes of strains with combined deletions of Bud7-Chs6 family members.

	Temperature sensitive at 37°C	Calcofluor white resistant	Slow growth at 23°C	YMP+ sensitive
WT	-	-	-	-
Δchs5	+	+	+	+
Δchs6	+	+	-	-
Δbud7	-	-	-	-
Δbch1	-	-	+	+
Δbch2	-	-	-	-
Δchs6 Δbud7	+	+	-	-
Δchs6 Δbch1	-	+	+	+
Δchs6 Δbch2	+	+	+	+/-
Δbud7 Δbch1	-	+	-	+
Δbud7 Δbch2	-	-	-	-
Δbch1 Δbch2	-	-	+	+
Δbud7 Δbch1 Δbch2	+	+	+	+
Δchs6 Δbch1 Δbch2	-	+	+	+
Δchs6 Δbud7 Δbch2	+	+	-	-
Δchs6 Δbud7 Δbch1	-	+	-	+
Δchs6 Δbud7 Δbch1 Δbch2	-	+	+	+

3.3.1.5 The protein expression levels of the Bud7-Chs6 family are tightly regulated

In the single deletion experiments, only *Δchs6* was resistant to calcofluor white. This suggested that from the Bud7-Chs6 family only Chs6p is needed for trafficking of the chitin synthase Chs3p to the cell surface. As reported above, a double deletion of *Δbud7 Δbch1* surprisingly also resulted in calcofluor white resistance. One explanation for that could be that Chs6p is subtracted from Chs3p trafficking events to compensate the loss of Bud7p and Bch1p by fulfilling part of Bud7p/Bch1p functions under these conditions. Hence, Chs6p overexpression (or possibly also overexpression of the closest homolog Bch2p) should restore calcofluor sensitivity in a *Δbud7 Δbch1* strain. Alternatively, Bud7p and Bch1p might both be directly involved in Chs3p transport and therefore

overexpression of Chs6p should not be able to restore calcofluor white sensitivity of a *Δbud7 Δbch1* strain.

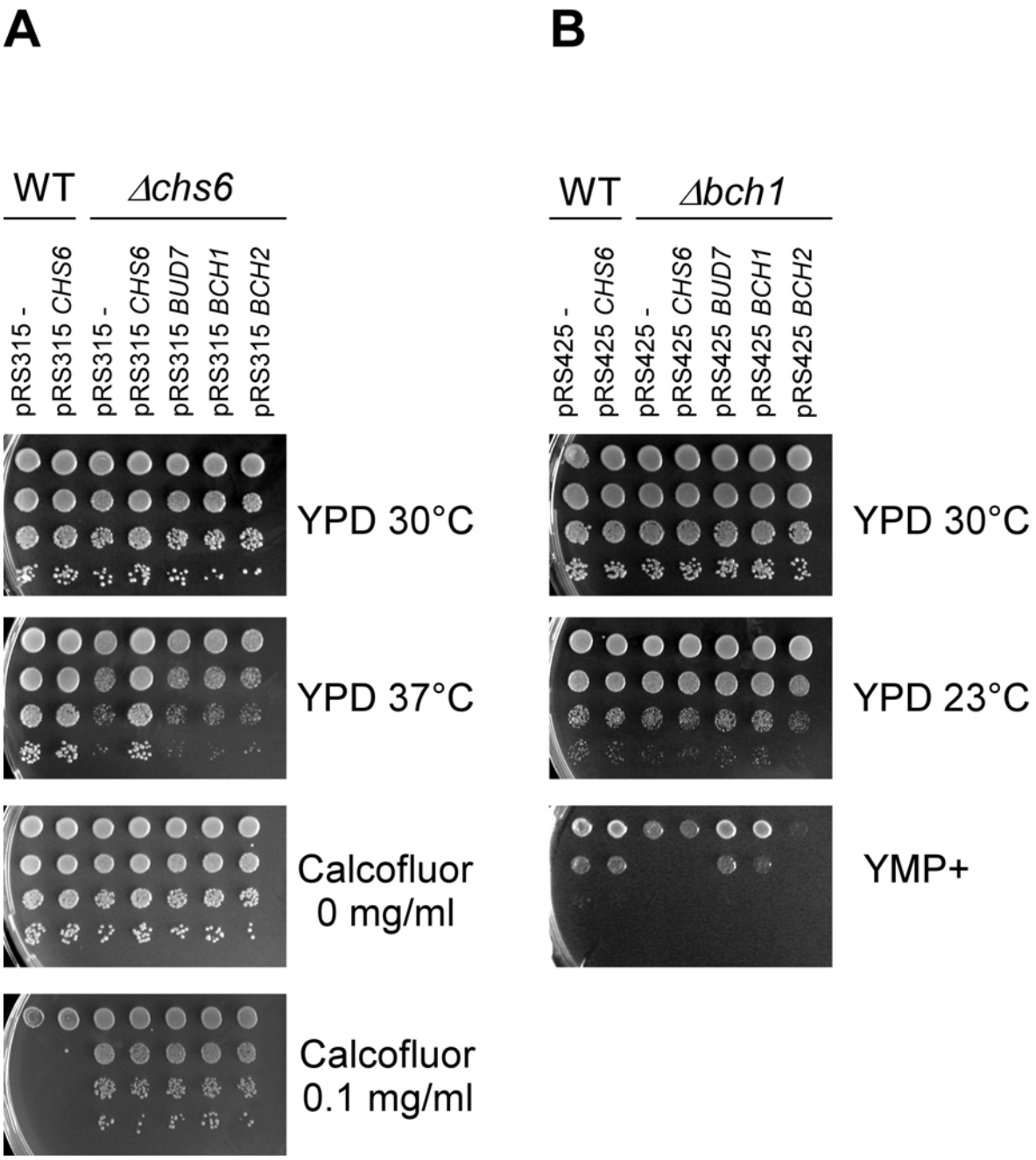

Figure 24: The protein expression levels of the Bud7-Chs6 family are tightly regulated. Haploid yeast cells transformed with different plasmids were grown overnight in selective minimal medium to logarithmic phase. After adjusting the cell concentration, serial dilutions (1:10) were dropped onto plates and incubated for two days at 30°C unless otherwise indicated. **(A)** Rescue of a *CHS6* deletion. Wild-type and *Δchs6* cells transformed with empty vector or low-copy plasmids expressing members of the Bud7-Chs6 family were analyzed for growth at 37°C and on calcofluor white plates **(B)** Rescue of a *BCH1* deletion. Wild-type and *Δbch1* cells transformed with empty vector or high-copy plasmids expressing members of the Bud7-Chs6 family were analyzed for growth at 23°C and on YMP+ plates.

Surprisingly, however, already the rescue of *Δchs6* was problematic. Specifically, the calcofluor white resistance of a *Δchs6* strain could neither be rescued by expression of Chs6p from a low- nor a high-copy plasmid (Fig. 24A and data not shown). Yet, in both cases the temperature-sensitivity of the *Δchs6* strain was rescued which indicated protein expression and provided further evidence for two separable functions of Chs6p. No other member of the Bud7-Chs6 family was competent to restore wild-type growth of *Δchs6* at 37°C. Similarly, the sensitivity of *Δbch1* towards YMP+ was not rescued by expression of Bch1p from a low copy plasmid. When expressed from a high copy plasmid, both Bud7p and Bch1p were able to remedy the phenotype (Fig. 24B and data not shown). In case of the *Δbud7 Δbch1* double deletion, only the sensitivity towards YMP+ (but not the calcofluor white resistance) was rescued by expression of Bud7p or Bch1p from a high copy plasmid (data not shown). These results indicate that simple overexpression is not sufficient to rescue all associated phenotypes. Moreover, the expression of Bud7-Chs6 family members appears to be tightly regulated and needs possibly to be adjusted for each member to a certain level. Alternatively, the expression level of one individual member might depend on other members. Furthermore, Bud7p and Bch1p are more tightly linked than the others since only Bud7p (but not Chs6p or Bch2p) was able to rescue the *BCH1* deletion. The inability of Chs6p to replace Bch1p (and vice versa) under overexpression conditions argues for a direct involvement of Bud7p and Bch1p in the trafficking of Chs3p. Therefore, it is unlikely that Chs6p becomes distracted from Chs3p-trafficking events to compensate loss of Bud7p or Bch1p.

3.3.1.6 Transport of the chitin synthase Chs3p

Since Arf1p is a protein involved in vesicular transport and at least Chs5p and Chs6p have been implicated in trafficking of vesicular cargo, we investigated the transport of known and putative cargo molecules. Given that not only Chs5p and Chs6p but also Bud7p/Bch1p are required for trafficking and sorting of the chitin synthase Chs3p to the bud neck, we analyzed the localization of Chs3p *in vivo* with a system developed by Valdivia *et al.* (2002). In this system, Chs7p (the ER export factor for Chs3p) and Chs3p-GFP are ectopically co-expressed and the localization of Chs3p-GFP is determined by fluorescence microscopy. In wild-type cells, we observed a GFP signal for structures resembling the TGN as well as a more dispersed signal which probably corresponds to chitosomes, similar to the results obtained by Valdivia *et al.* (2002). Occasionally, Chs3p-GFP was present also at the mother-bud neck (Fig. 25). In *Δchs5* and in *Δchs6* cells, the GFP signal was

exclusively in structures corresponding to the TGN. This is consistent with the assumption that Chs5p and Chs6p are required for transport of Chs3p from the TGN to the plasma

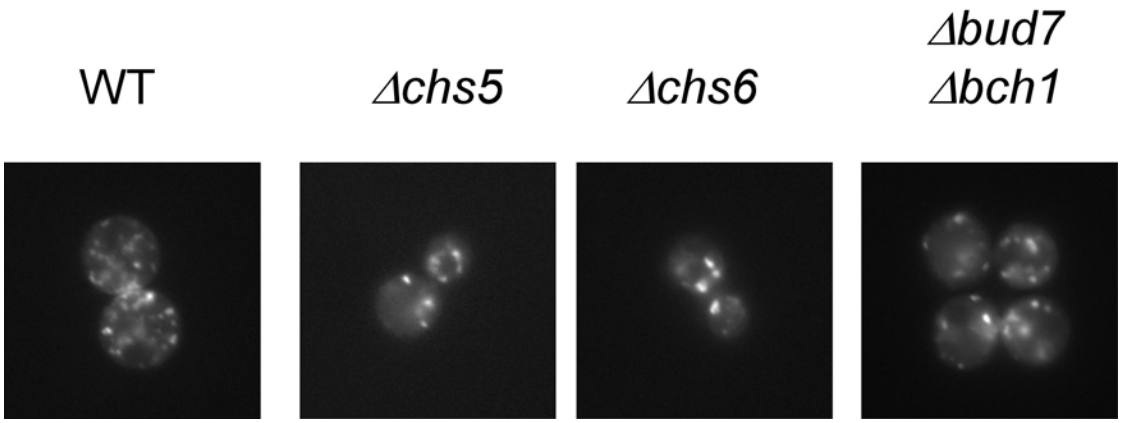

Figure 25: Transport of the chitin synthase Chs3p. Haploid yeast cells co-transformed with Chs3p-GFP and Chs7p were grown overnight in selective medium to logarithmic phase. GFP was visualized by fluorescence microscopy. Pictures were taken from freshly mounted cells. The GFP signal is localized in structures resembling the trans-Golgi-network. A dispersed signal corresponding to the chitosomes is evident only in wild-type cells.

membrane, or more specifically to the bud neck. Chs3p would be a cargo of special vesicles directed to the mother bud neck. Surprisingly, in a *Δbud7 Δbch1* double deletion strain, we observed a mixed population of cells. Few cells looked like wild-type whereas the majority of cells had Chs3p-GFP only in TGN structures. We also stained the deletion strains with calcofluor white in order to assess the chitin levels in the cell wall and to correlate chitin synthesis at the cell wall with Chs3p transport. As expected, in both *Δchs5* and *Δchs6* cells, the cell wall was stained very poorly. This poor staining was remedied by an additional *ARF1* deletion (data not shown). In case of the *Δbud7 Δbch1* double deletion, there was only weak staining of the cell wall. Taken together, this indicates that in the *Δbud7 Δbch1* double deletion strain either Chs3p trafficking was disturbed or Chs3p was not fully active or a combination of both. This was already denoted by the calcofluor white resistance phenotype of this strain. This result implies that Chs6p acts in concert with Bud7p/Bch1p to localize Chs3p to the cell surface and at least the presence of either Bud7p or Bch1p is required.

3.3.1.7 The Bud7-Chs6 family is not required for transport of cell fusion factor Fus1p or of the amino acid permeases Gap1p and Tat2p

It has been reported that Chs5p but not Chs6p is required for mating and more specifically for polarized localization of the cell fusion factor Fus1p to the shmoo tip during mating

(Santos and Snyder, 2003). It seemed obvious to examine whether any other member of the Bud7-Chs6 family apart from Chs6p would be required for mating and Fus1p trafficking. Although we observed a very dramatic mating efficiency defect for *Δchs5* x *Δchs5*, this was not the case for any of the single deletions of the Bud7-Chs6 family. Also, mating of the quadruple deletions resulted only in a minor (if at all) defect in mating efficiency (data not shown). In addition, Fus1p-GFP expressed from a plasmid was correctly localized to the tip of the shmoo and the cell fusion plane in mating cultures of the single deletion strains whereas this was not the case in *Δchs5* mating mixtures (data not shown). Therefore, it is likely that Chs5p is also involved in other pathways apart from the Bud7-Chs6 family-related pathways.

A *Δbch1* strain is sensitive to growth on YMP+ plates. An apparent feature of these plates is the elevated ammonium level. We therefore considered the possibility that Bch1p is involved in nitrogen regulation and might be required for transport of amino acid permeases to the cell surface. The general amino acid permease Gap1p is routed to the cell surface under nitrogen starvation conditions and degraded in the vacuole under non-starvation conditions (Roberg *et al.*, 1997). The tryptophane permease Tat2p is inversely regulated and degraded in the vacuole in nitrogen-starved cells and localized to the cell surface under nutrient-rich conditions (Beck *et al.*, 1999). We examined the localization of Gap1p-GFP and Tat2p-GFP in both wild-type and *Δbch1* strains. However, both Gap1p-GFP and Tat2p-GFP were localized to the cell surface in both wild-type and *Δbch1* strains under appropriate conditions (data not shown). Hence, Bch1p is not required for trafficking of Gap1p or Tat2p.

3.3.1.8 Intracellular localization of the budding pattern landmark proteins Bud8p and Bud9p

A *Δbud7* homozygous diploid strain exhibits a random budding pattern unlike the wild-type bipolar budding pattern. Therefore, we wanted to analyze the localization of the putative landmark proteins for bipolar budding pattern, Bud8p and Bud9p. These proteins are thought to interact with the general bud-site selection machinery, which then in turn establishes cell polarity (Casamayor and Snyder, 2002). Bud8p has been reported to mark the distal cell pole and therefore showing a localization at the distal bud tip (Harkins *et al.*, 2001). The localization of Bud9p is either at the bud side of the bud neck, marking the proximal pole as a true landmark protein (Harkins *et al.*, 2001), or it is also at the distal bud tip and possibly acts there as an inhibitor of Bud8p (Taheri *et al.*, 2000). We

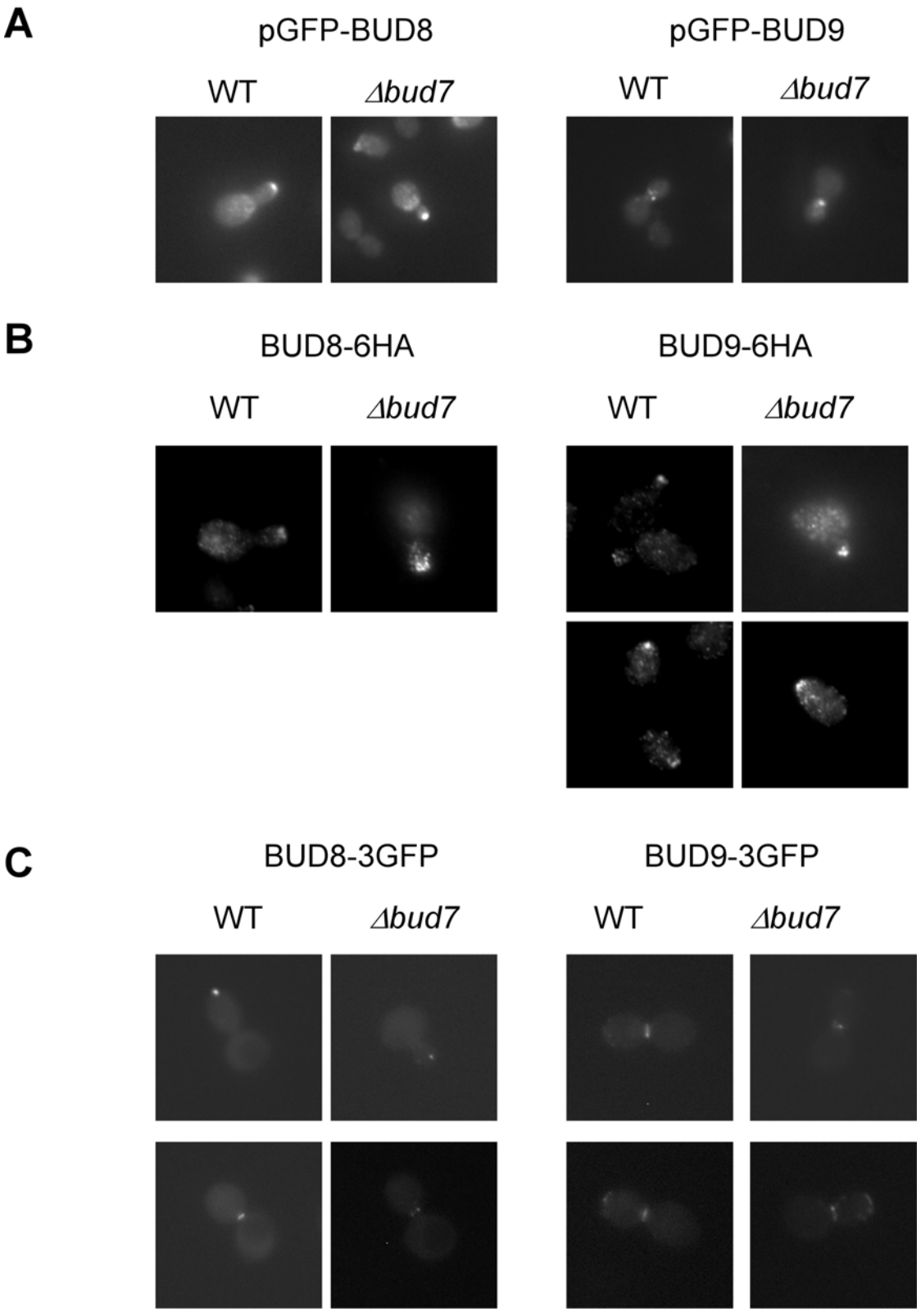

Figure 26: Localization of the bipolar landmark proteins Bud8p and Bud9p is independent of the Bud7-Chs6 family. Diploid wild-type and *Δbud7/Δbud7* yeast strains were grown for at least 16 h to logarithmic phase in either minimal selective medium (ectopic expression) or YPD (chromosomal integrations). YPD medium contained 50 mg/l adenine to suppress cellular autofluorescence associated with the *ade2* mutation. Cells were washed briefly with water and pictures were taken immediately afterwards. **(A)** Ectopic expression of GFP-Bud8p and GFP-Bud9p. Cells were directly visualized under the fluorescent microscope. **(B)** Immunofluorescence of chromosomally tagged Bud8p-6HA and Bud9p-6HA. Cells were fixed in formaldehyde and stained with HA antibodies. The fluorescent dye Cy3 was used for visualization of the proteins. **(C)** Expression of chromosomally tagged Bud8p-3GFP and Bud9p-3GFP.

investigated the localization of Bud8p and Bud9p in wild-type diploid as well as in a homozygous *BUD7* deletion strains. We initially visualized the proteins by ectopic expression of Bud8p-GFP and Bud9p-GFP fusion proteins (Schenkman *et al.*, 2002). For Bud8p, we observed in both wild-type and *BUD7* deletion strains a localization at the distal bud tip (Fig. 26A). Furthermore, we detected Bud9p at the bud side of the mother-bud neck in both wild-type and *Δbud7/Δbud7* strains. However, it has been reported that overexpression of Bud8p was able to partially suppress the budding pattern defect of a *Δbud7/Δbud7* strain (Ni and Snyder, 2001). We were therefore concerned that the overexpression of GFP-Bud8p would veil a mislocalization of this protein under physiological conditions in a *Δbud7/Δbud7* strain. Consequently, we constructed homozygous diploid strains in which Bud8p and Bud9p were C-terminally chromosomally tagged with 6HA in both wild-type and *Δbud7/Δbud7* strains resulting in endogenous expression levels. The wild-type strains exhibited a bipolar budding pattern indicating that the chromosomal fusions were functional. We performed immunofluorescence on these strains and Bud8p-6HA localized in both wild-type and *Δbud7/Δbud7* strains again to the distal bud tip (Fig. 26B). To our surprise, Bud9p-6HA localized also to the distal bud tip and to one pole in unbudded cells in both wild-type and *Δbud7/Δbud7* strains. To resolve this discrepancy, we chromosomally appended Bud8p and Bud9p with 3GFP in order to be able to visualize the proteins directly in living cells at endogenous expression levels. Both Bud8p-3GFP and Bud9p-3GFP homozygous diploid strains showed a bipolar budding pattern indicating functional fusion proteins. Again, Bud8p-3GFP localized to the distal bud tip (Fig. 26C). Additionally, however, a localization at the mother-bud neck junction was observed later in the cell cycle. Bud9p-3GFP localized to the distal bud tip in cells with small and medium size buds and to the mother-bud neck in cells with large buds, similar to the ectopic expression. It seemed that Bud9p-3GFP reached the mother-bud neck earlier than Bud8p-3GFP during the cell cycle. The localization of Bud8p-3GFP and Bud9p-3GFP was indistinguishable from wild-type in *Δbud7/Δbud7* cells. Bud8p-6HA and Bud9p-6HA at the mother-bud junction might be less amenable to antibody staining in immunofluorescence. This might be the reason why only the bud tip was stained in these experiments. Most importantly, however, both Bud8p and Bud9p localizations were unaffected by the deletion of *BUD7* indicating that Bud7p is not involved in the transport of these bipolar landmark proteins.

3.3.1.9 Transport of the inherited protein Rax2p which is required for bipolar budding pattern

Since the bipolar landmark proteins Bud8p and Bud9p were not transported in a Bud7p-dependent fashion, we were searching for genes that resulted in a similar phenotype as a *BUD7* deletion and might therefore be acting on the same pathway. *BUD7* is member of a small class of genes in which mutations exhibit the peculiar axial-like budding pattern phenotype (Ni and Snyder, 2001). It is characteristic for this class of mutants that they neither bud in a bipolar nor in a true axial fashion, which is the normal budding pattern for haploid strains (Fig. 27). However, the budding pattern is distinct from a random budding pattern, which is the predominant phentotype in many mutants. Apparently, it depends on the strain background to which extent the axial-specific markers, which are present in diploids, can take over when bipolar landmarks are missing (Ni and Snyder, 2001). The axial-like phenotype is shifted to a random budding pattern in strain backgrounds in which the influence of the axial-specific markers in diploids is weak. In our strain background, we observed a random budding pattern for homozygous *BUD7* deletions. *ISY1*, *YOR300w, RAX1*, *RAX2*, and *BUD7* are so far the only members of the axial-like budding pattern class (Ni and Snyder, 2001). Isy1p is supposedly a protein involved in transcription and localizes to the nucleus. *YOR300w* overlaps both with the 3'-end of *BUD7* and the promoter of *RAX1*. Therefore, it is likely that this ORF is not expressed as the effects of a deletion can be readily explained by concomitant deletion of the C-terminus of Bud7p (compare Chapter 3.4) and interference with Rax1p expression. Thus, we wanted to investigate the localization of the remaining candidates, Rax1p and Rax2p, in wild-type and *Δbud7/Δbud7* strains. We constructed strains in which the proteins were chromosomally tagged under their endogenous promoters. Although a *RAX2-GFP/RAX2-GFP* strain exhibited a bipolar budding pattern, the C-terminal fusions of Rax1p with 6HA, 9Myc or GFP resulted in nonfunctional proteins because the resulting strains budded randomly. Hence, we were unable to include Rax1p in our analysis. Rax2p-GFP was visible in wild-type cells at the bud neck, older bud scars and occasionally in the distal bud tip (Fig. 28A). In a *Δbud7/Δbud7* strain, Rax2p-GFP still localized to the bud neck, the distal bud tip and to older bud scars (Fig. 28B). However, the older bud scars were randomly distributed in the *Δbud7/Δbud7* strain. This means the localization of this protein to a cellular structure, namely the bud scars, was correct but the structures themselves were mislocalized.

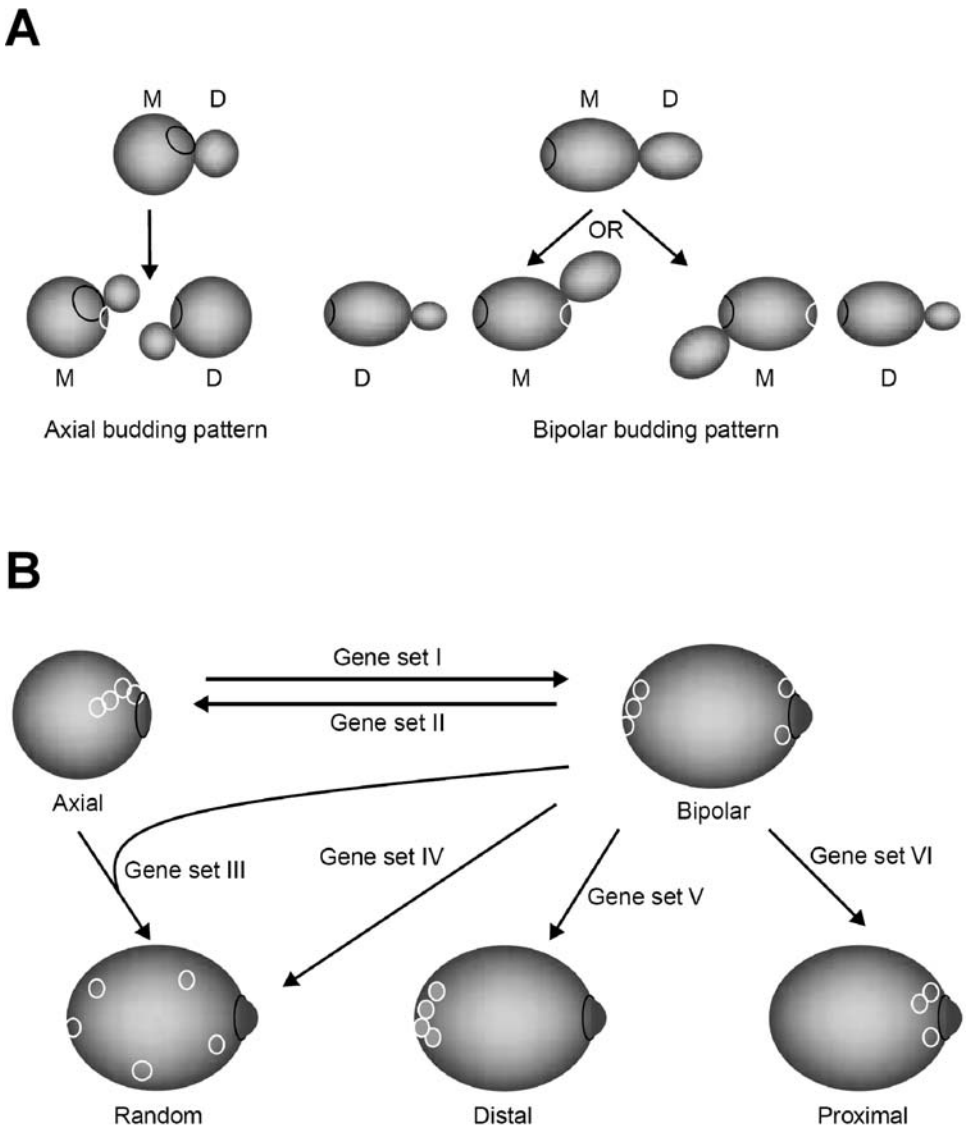

Figure 27: (A) Axial and bipolar budding patterns in yeast cells. Staining with the calcofluor dye permits visualization of two types of scars on the surface of yeast cells. The scar marking the place where the cell was initially attached to its mother cell (M) is called the birth scar. Smaller scars that originated by cytokinesis of the daughter cells (D) are named bud scars. Examination of the pattern of bud and/or birth scars reveals the budding pattern. The axial budding pattern is typically found in haploid cells, and is characterized by adjacent budding to the birth scar in both mother and daughter cells. Diploid cells follow a bipolar budding pattern in which daughter cells usually bud distally (that is, at the opposite pole to the birth scar), and the mother cell buds at either pole. The birth scar is represented by a curved black line, and subsequent bud scars are represented by curved white lines. **(B)** Localization of birth and bud scars denotes wild-type and mutant budding patterns (axial, bipolar, etc.) in yeast cells. The bipolar budding pattern naturally occurs in diploid cells. However, it can also be found in haploid cells mutated in any of the genes included in gene set I. Conversely, a diploid cell containing mutations affecting any gene in gene set II exhibits a preference for the axial budding pattern. Random, distal and proximal budding patterns can be consequences of mutation in any of the genes in gene sets III, IV, V or VI, depending on whether the cell is diploid or haploid (adapted from Casamayor and Snyder, 2002)

Since localization of Rax2p is dependent on Rax1p (Chen *et al.*, 2000; Fujita *et al.*, 2004), it is likely that also Rax1p is correctly localized to the bud scars in *Δbud7/Δbud7* strains. Both *Δrax1/Δrax1* and *Δrax2/Δrax*2 also display random budding patterns and Rax1p has

been shown to be required for Bud8p localization (Ni and Snyder, 2001; Fujita *et al.*, 2004). This places them upstream of the bud site selection process. Rax2p is correctly localized to bud scars (which are themselves mislocalized) in *Δbud7/Δbud7* strains. Bud8p and Bud9p are correctly localized in a *Δbud7/Δbud7* strain, yet the strain shows a random budding pattern. Our results provide evidence that *BUD7* acts in a pathway downstream of *RAX2* but upstream of *BUD8* and *BUD9*.

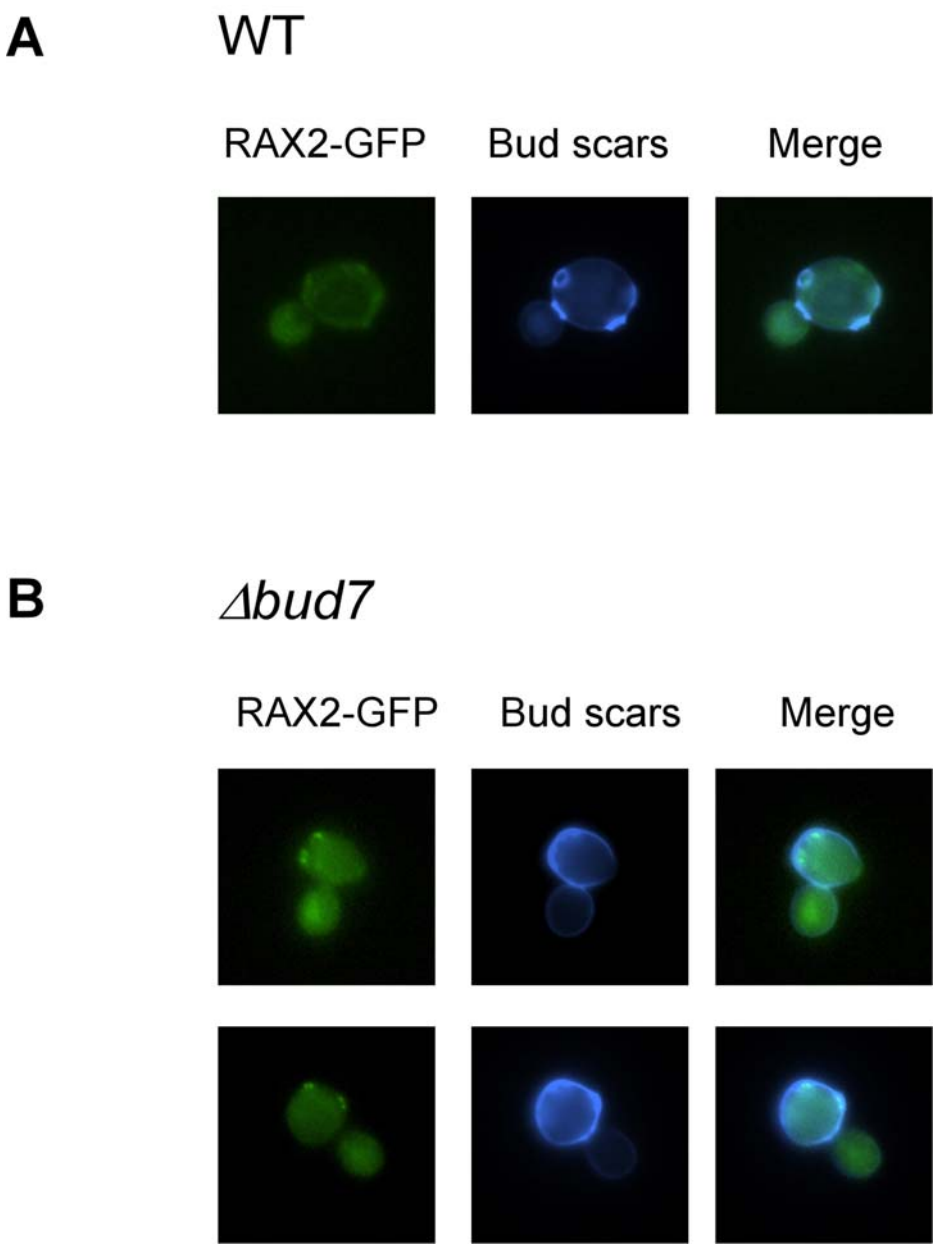

Figure 28: Localization of the inherited protein Rax2p required for maintenance of bipolar budding pattern is independent of the Bud7-Chs6 family. **(A)** Diploid wild-type and **(B)** *Δbud7/Δbud7* yeast cells expressing two chromosomal versions of Rax2p tagged with GFP at the C-terminus were grown in YPD containing 50 mg/l adenine for at least 16 h to logarithmic phase. Cells were briefly washed in water and pictures were taken immediately afterwards using the fluorescence microscope. To correlate the Rax2p-GFP signal (green) with bud scars, living cells were stained with calcofluor white (blue) and the fluorescence of GFP and calcofluor white was compared (merge). In both wild-type and *Δbud7* cells, Rax2p-GFP co-localized with bud scars.

3.3.2 Discussion

Using differential Arf1p affinity chromatography, we were able to identify Chs5p and Ymr237p as new interactors of Arf1p-GTP. Ymr237p (Bch1p) is member of a family of four paralogous proteins in yeast. This family also includes Chs6p, Bud7p and Ykr027p (Bch2p). Both Chs5p and Chs6p have been implicated in the trafficking of the chitin synthase Chs3p to the bud neck (Santos and Snyder, 1997; Ziman *et al.*, 1998). Bud7p is required for bipolar bud-site selection in diploid strains (Zahner *et al.*, 1996; Ni and Snyder, 2001). Little was known about the so far uncharacterized ORFs *YMR237w* and *YKR027*w. Orthologs of Bud7-Chs6 family proteins are only found in fungi indicating a fungi-specific role for this protein family. Chs5p has already been proposed to reside on the outside of vesicles containing Chs3p (Santos and Snyder, 1997). Activated Arf1p is able to recruit different components from the cytosol to the Golgi membrane to initiate vesicle formation. As Chs5p and Bch1p interacted with activated Arf1p, it was tempting to speculate that Arf1p would initiate budding of a special kind of post-Golgi vesicles. It is conceivable that Chs5p could be recruited from the cytosol to the Golgi membrane by Arf1p. Depending on the cell's needs, different cargoes could be selected for incorporation into a vesicle and one or more members of the Bud7-Chs6 family would mediate this cargo selection process. Chs5p and the Bud7-Chs6 family would then serve at the same time as coat proteins and cargo receptors for a specialized kind of vesicles initiated by Arf1p (see also Chapter 3.4).

We examined the phenotypes of different single deletion as well as of multiple deletion strains of the Bud7-Chs6 family in a systematic manner. Except for *BCH2*, we have established testable phenotypes for the different members of the Bud7-Chs6 family as well as for *CHS5*. Phenotypes we observed for a deletion of one member of the family were not observed for a single of any other member indicating that the proteins serve different functions and are not overlapping at a first glance. In contrast, all phenotypes observed for mutants in the Bud7-Chs6 family were also present in a *Δchs5* strain. This indicates that Chs5p is acting upstream the Bud7-Chs6 family or downstream at a converging point.

Chs5p has been shown to be required for polarized secretion of Fus1p to the distal shmoo tip during mating (Santos and Snyder, 2003). Although we observed a very dramatic mating efficiency defect in *Δchs5* strains, this was not the case in a quadruple deletion of the Bud7-Chs6 family. Furthermore, all single deletions were able to localize Fus1p to the distal shmoo tip during mating whereas this was not the case for *Δchs5* cells. This demonstrates an additional role for Chs5p in secretion other than mediating the actions of

the Bud7-Chs6 protein family. These results are consistent with specific functions for each member of the Bud7-Chs6 protein family and a more general function for Chs5p.

It is noteworthy at this point that in case of Fus1p trafficking, the cargo is directed to the distal tip and not to the mother-bud junction. Thus, Chs5p might be responsible for trafficking of cargo to either site; the Bud7-Chs6 family might be required for trafficking only to the mother-bud neck region. Site-specific delivery might be more critical for some cargo proteins than for others.

The calcofluor resistance phenotype of a *Δchs5* and a *Δchs6* strain was rescued by an additional *ARF1* deletion. Valdivia *et al.* (2002) have proposed, that the chitin synthase Chs3p does no longer reach the plasma membrane in these strains and is instead trapped in an endosomal pool and constantly recycled back to the TGN. An additional *ARF1* deletion would then block this recycling step and Chs3p would escape the endosomal pool and reach the plasma membrane, although not in a site-specific manner. This explains the restored calcofluor white sensitivity of the double deletion strains and the restored staining of cell wall chitin. Interestingly, in a *Δbud7 Δarf1* strain, the putative Bud7p cargo would also reach the plasma membrane but at no specific site and thereby the bipolar budding pattern would not be rescued because in this case it is critical that the Bud7p cargo reaches a specific site.

Although Chs6p is present in *Δbud7 Δbch1* cells, Chs3p was mislocalized and the cell wall was only poorly stainable for chitin. This implies that both Chs6p and at least one of the proteins Bud7p or Bch1p are directly required for transport of Chs3p. One explanation for this is that only Chs6p is directly responsible for incorporation of Chs3p. In this case, at least one protein of each sub-branch of the Bud7-Chs6 family could be essential to generate vesicles as such and the specific members could be responsible for the selection of certain cargo. In a *Δchs6* strain, the protein responsible for incorporation of Chs3p would be missing, however, vesicles could be formed. In single deletion strains of either *BUD7* or *BCH1*, one protein could compensate for the loss of the other. This is suggested by the ability of Bud7p to rescue a *BCH1* deletion under overexpression conditions. In the *Δbud7 Δbch1* strain, Chs6p is be present, however, because both members of one Bud7-Chs6 family sub-branch are missing, no vesicles are formed. This model would predict that *CHS6 BCH2* double deletion should exhibit phenotypes associated with a *BUD7* or a *BCH1* deletions. A *Δchs6 Δbch2* strain is indeed at least partially sensitive to YMP+.

Rax1p has been shown to be required for the delivery of Rax2p through the secretory pathway (Chen *et al.*, 2000; Fujita *et al.*, 2004). Both proteins appear to localize to the

distal bud tip as well as the bud neck and to form rings at these sites. Both Rax1p and Rax2p are not required for the establishment but for the maintenance of bipolar budding pattern. They are highly stable and inherited throughout the generations to mark the sites of previous divisions. It has already been proposed that the proteins act upstream of Bud8p and Bud9p and a yet to be identified factor X may accentuate the establishment of Bud8 and Bud9 landmarks (Fujita *et al.*, 2004). The bipolar landmark proteins Bud8p and Bud9p are correctly localized in a *Δbud7/Δbud7* strain. Nevertheless, it exhibits a random budding pattern. Moreover, Rax2p, which is not required for the establishment but for the maintenance of the bipolar budding pattern, is localized correctly. This indicates that Rax2p alone is not sufficient to maintain the bipolar budding pattern and that therefore another factor must be involved. Furthermore, it strongly argues for *BUD7* acting downstream of *RAX2*.

We would like to propose a refined model for the establishment of bipolar budding pattern and postulate that the yet to be identified fidelity factor X is a cargo of Bud7p-dependent vesicles destined to the bud neck (akin to Chs3p). Both Bud8p and Bud9p are landmark proteins which define the budding site and mediate downstream interaction with the general bud-site selection complex resulting in polarity establishment. At the time of cytokinesis, memory rings of Rax1p and Rax2p would form at the distal bud tip and the mother-bud neck thereby marking these cell poles for the next budding events. The fidelity factor X could be brought to the mother-bud neck in Bud7p-dependent vesicles, much in the same way as the chitin synthase Chs3p is brought to the mother-bud neck by vesicles in a Chs6p-dependent manner. There, the factor X might possibly interact with or modulate Bud8p and/or Bud9p function. The Rax1/2 memory rings could help to confine this guidance factor at this site. The factor X would then guide the new landmarks to define new budding sites in close proximity of the memory rings. In *Δbud7/Δbud7*, *Δrax1/Δrax1* and *Δrax2/Δrax2* cells, the fidelity factor X would have no or no clear localization and the guidance for the new landmarks would be missing. This would result in a random budding pattern (or an axial-like if the axial cues are partially used) as is observed for the strains mentioned. This model also predicts a random budding pattern (or an axial-like) for *BUD7 BUD8* or *BUD7 BUD9* double mutant strains, which is indeed the case (Zahner *et al.*, 1996).

In conclusion, we propose that Chs5p in conjunction with the Bud7-Chs6 protein family mediates trafficking of fungi-specific post-Golgi vesicles directed to the mother bud neck.

The chitin synthase Chs3p is one cargo whose incorporation is ensured by Chs6p. A yet to be identified fidelity factor required for the maintenance of bipolar budding pattern might be incorporated by Bud7p and transported to the mother-bud junction. Bch1p would transport a factor required for growth on YMP+ and also Bch2p is likely to transport an unknown factor to this site.

3.4 Biochemical analysis of the Bud7-Chs6 cargo receptor protein family in *Saccharomyces cerevisiae*

3.4.1 Results

3.4.1.1 Chromosomal epitope tagging of the Bud7-Chs6 family members

In Chapter 3.3, we described the characterization of the Bud7-Chs6 family on a genetic level. The involvement of Chs6p and at least either Bud7p or Bch1p in the trafficking of the chitin synthase Chs3p to the mother-bud neck suggested a possible role of the Bud7-Chs6 family as cargo receptors in Arf1p-dependent post-Golgi traffic. In order to be able to analyze the functions of Bud7-Chs6 family proteins on a biochemical level, we decided to epitope tag each family member. Antisera raised against the proteins were problematic due to cross-reactivity between the family members. We were unable to raise specific antisera for a single member. To obtain functional fusion proteins at endogenous expression levels, we chromosomally tagged the proteins at the C-terminus with different epitope tags and tested the resulting fusion proteins for their functionality (Table 17). Strains provided by Robert Gauss are indicated in Chapter 2.7.

Table 17: Analysis of the functionality of C-terminal chromosomal epitope tags of the Bud7-Chs6 family proteins.

Chs6p		Bud7p		Bch1p	
Tag	Phenotype	Tag	Phenotype	Tag	Phenotype
none	-	none	bipolar budding	none	-
9myc	-	9myc	bipolar budding	3myc	-
Prot A	-	6HA	bipolar budding	9myc	not applicable
GST	-			3HA	-
yEGFP	-			2AU5	-
6HA	ts, resistant to calcofluor white			GST	sensitive to YMP+, slow growth at 23°C
3VSV-6His	ts, resistant to calcofluor white			yEGFP	sensitive to YMP+, slow growth at 23°C
				3VSV-6His	sensitive to YMP+, slow growth at 23°C

A *CHS6* deletion renders the yeast cells temperature-sensitive and resistant to calcofluor white (a chitin binding dye). This was also observed for 6HA and 3VSV-6His tags

indicating that these tags lead to non-functional proteins. However, we obtained functional Chs6p fusions for 9myc, Protein A, GST and GFP. The protein expression level was, however, too low for visualization of the GFP fusion by fluorescence microscopy. Homozygous diploid *Δbud7* strains bud in a random fashion unlike wild-type diploid yeast cells which bud in a bipolar manner. Both homozygous diploid strains with Bud7p-6HA and Bud7p-9myc exhibited a bipolar budding pattern suggesting that both of these Bud7p fusions were functional. C-terminal fusions of GST, GFP or 3VSV-6His to Bch1p resulted in strains sensitive to YMP+ and in slow growth at 23°C, which was the same phenotype observed in *BCH1* deletion strains. In contrast, Bch1p fused to 3myc, 3HA or 2AU5 gave no detectable phenotype. The Bch1p-9myc fusion was impossible to score since this construct uses the *K. lactis TRP1* marker. We noticed that the *TRP1*-gene alone was able to rescue both the slow growth and the sensitivity to YMP+, thereby compromising the assessment of the functionality of the fusion protein. The reason for this behavior is unknown, although not without precedence. It has been reported before that *TRP1* and related genes are able to suppress cold-sensitive phenotypes (Hampsey, 1997). However, biochemical data discussed below strongly suggest that also the Bch1p-9myc fusion is functional. A deletion of *BCH2* resulted in no detectable phenotype. Therefore, the functionality of Bch2p fusion was not scorable. In our experiments, we used 9myc (which worked for the other three family members) and also 3HA (which is a rather small tag, minimizing unfavorable effects). In cases in which we employed chromosomally tagged Chs5p, we used Chs5p-6HA. The corresponding strain exhibited no phenotype unlike the *CHS5* deletion, indicating that Chs5p-6HA is functional. In conclusion, we successfully constructed a set of strains with functional epitope tagged proteins expressed at endogenous levels.

3.4.1.2 A short deletion of the C-terminus renders Bud7-Chs6 family proteins non-functional

During the construction of the epitope tagged strains, we obtained two clones of Chs6p-9myc, which were both positive as judged by analytical colony-PCR. To our surprise, one clone behaved like wild-type whereas the other was both temperature-sensitive and calcofluor white resistant, which is identical to the phenotype of a *Δchs6* strain. Hence, we sequenced the C-terminus of *CHS6* in these strains and found that the non-functional fusion clone had a frame-shift resulting in a stop codon just after that frame-shift. The resulting protein had lost the last 13 amino acids at the C-terminus. To exploit the

importance of the C-terminus, we constructed strains in which a short peptide at the C-terminus of the Bud7-Chs6 family proteins is replaced by a 9myc epitope (or the 3HA epitope in case of Bch1p to circumvent the *TRP1* marker problem mentioned above) (Fig. 29A). As expected, the *CHS6Δc-9myc* strain showed the features of a *Δchs6* strain, temperature-sensitivity and calcofluor white resistance (Fig. 29B). The *BCH1Δc-3HA* strain was sensitive to YMP+ and grew slowly at 23°C, both features are hallmarks of a *Δbch1* strain (Fig. 29B). A diploid *BUD7Δc-9myc/BUD7Δc-9myc* strain budded in a random fashion (like a *Δbud7/Δbud7* strain) (Fig. 29C). The C-terminal deleted proteins

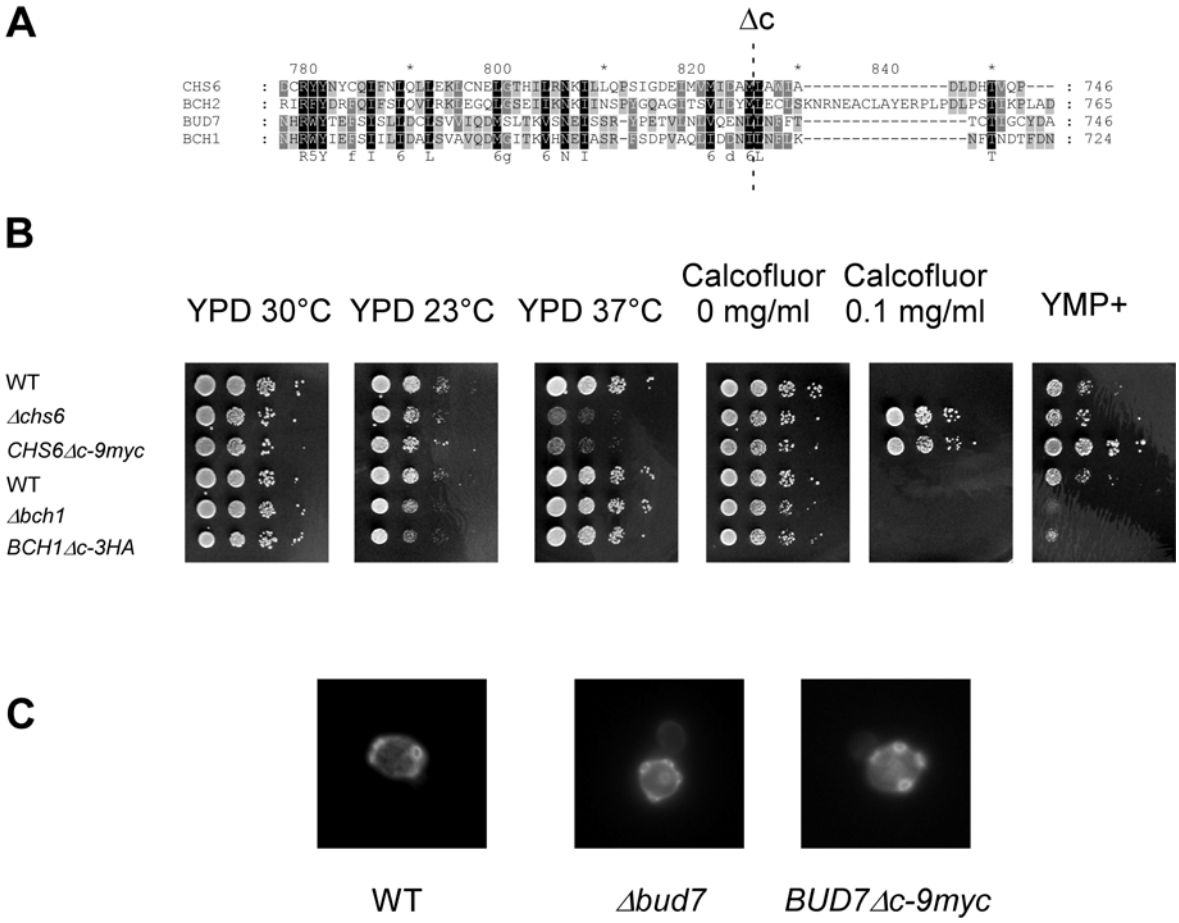

Figure 29: The C-terminus of the Bud7-Chs6 family proteins is essential for their function. **(A)** Protein sequence alignment of the C-terminus of the Bud7-Chs6 family proteins. The last 13 amino acids of Chs6p were deleted and replaced by 9myc. The C-termini of the other three family members were deleted and replaced by epitope tags according to this alignment. A dashed line indicates the site of deletion. **(B)** Growth of the C-terminal deleted strains as compared to wild-type and full-deletions on different plates and different conditions. Haploid strains were grown overnight in rich medium to logarithmic phase. After adjusting the cell concentrations, serial dilutions (1:10) were dropped on various plates and incubated at 30°C for two days unless otherwise indicated. Note that the *CHS6Δc-9myc* strain grew even faster than the wild-type on YMP+ plates because of the concomitantly introduced *TRP1* marker. **(C)** Budding pattern of a homozygous diploid *BUD7Δc-9myc* strain. Diploid yeast strains were grown for at least 16 h to logarithmic phase. After fixation with formaldehyde, the cells were stained with calcofluor white to visualize the bud scars and were observed under the fluorescence microscope.

were expressed and stable since the proteins were still detected with the same efficiency as the epitope-tagged wild-type versions in lysates (Fig. 30 A-D, compare lane 1 and 3). Only in the case of Bch2pΔc-9myc was the protein level lower, most likely because this strain contained the longest deletion (Fig. 29A). This means that short deletions at the C-termini resulted in the same phenotypes as the corresponding complete deletions. The fact that C-terminal truncated versions of Chs6p with and without epitope tag resulted in the corresponding deletion phenotype indicates that the effects are not just due to altered protein structure imposed by the epitope tag. These experiments imply that short sequences at the C-terminus of these proteins are essential for protein function (and in the case of Bch2p also for protein stability). Because the non-functional proteins were still expressed, the C-terminal deleted strains served as valuable tools in the course of further experiments.

3.4.1.3 All Bud7-Chs6 family members interact with Arf1p and Chs5p

We reported that Bch1p interacts physically with the activated form of Arf1p and that both *BCH1* and *CHS6* genetically interact with *ARF1* (Chapter 3.3). Furthermore, the functions of the Bud7-Chs6 family seemed to be strongly linked to *CHS5*. Hence, we wanted to study the interactions between Arf1p, Chs5p and all members of the Bud7-Chs6 family biochemically. To this end, we performed co-immunoprecipitation experiments with affinity-purified αArf1p-IgGs in different strains. As shown in Fig. 30 (A-D, lane 5), Chs6p-9myc, Bud7p-9myc, Bch1p-9myc and Bch2p-9myc were co-immmunoprecipitated with αArf1p-IgGs. Neither the deletion of *CHS5* (Fig. 30, A-D, lane 7) nor the deletion of the three remaining members of the Bud7-Chs6 family (Fig. 30, A-D, lane 9) had an impact on the precipitation efficiency. However, the short deletion of the C-terminus increased the amount of protein which was precipitated in the case of Chs6p, Bud7p, and Bch1p (Fig. 30, A-C, lane 8). As already mentioned, Bch2pΔc-9myc resulted in lower protein concentration, therefore it was prudent not to draw conclusions from this data. Since Bch1p interacted with Arf1p-GTP, it is reasonable to assume that also the other members might preferably interact with the activated Arf1p-form. Most of the cellular Arf1p is present in the inactive GDP-form: this explains why the recovery of Arf1p-GTP associated proteins is so small. In conclusion, all members of the Bud7-Chs6 family interact independently with Arf1p and neither their complete C-terminus nor Chs5p are required for this interaction.

We found previously by genetic means that Chs5p is either an upstream regulator or a downstream converging point of the Bud7-Chs6 family (Chapter 3.3). To study the

physical relationship of Chs5p and the Bud7-Chs6 family, we performed co-immunoprecipitations with Chs5p antiserum (Fig. 30). Again, the four proteins of the Bud7-Chs6 family were co-precipitated (Fig. 30, A-D, lane 10). The deletion of the three remaining members of the Bud7-Chs6 family did not change significantly the precipitation efficiency (Fig. 30, A-D, lane 13). However, Chs6pΔc-9myc and Bch1pΔc-9myc were not co-precipitated (Fig. 30, A-B, lane12). The amount of precipitated Bud7pΔc-9myc was only slightly reduced. As observed before, no clear judgment for Bch2pΔc-9myc could be made because of the low protein level. Most importantly, however, these experiments provide evidence that the members of the Bud7-Chs6 family bind independently from each

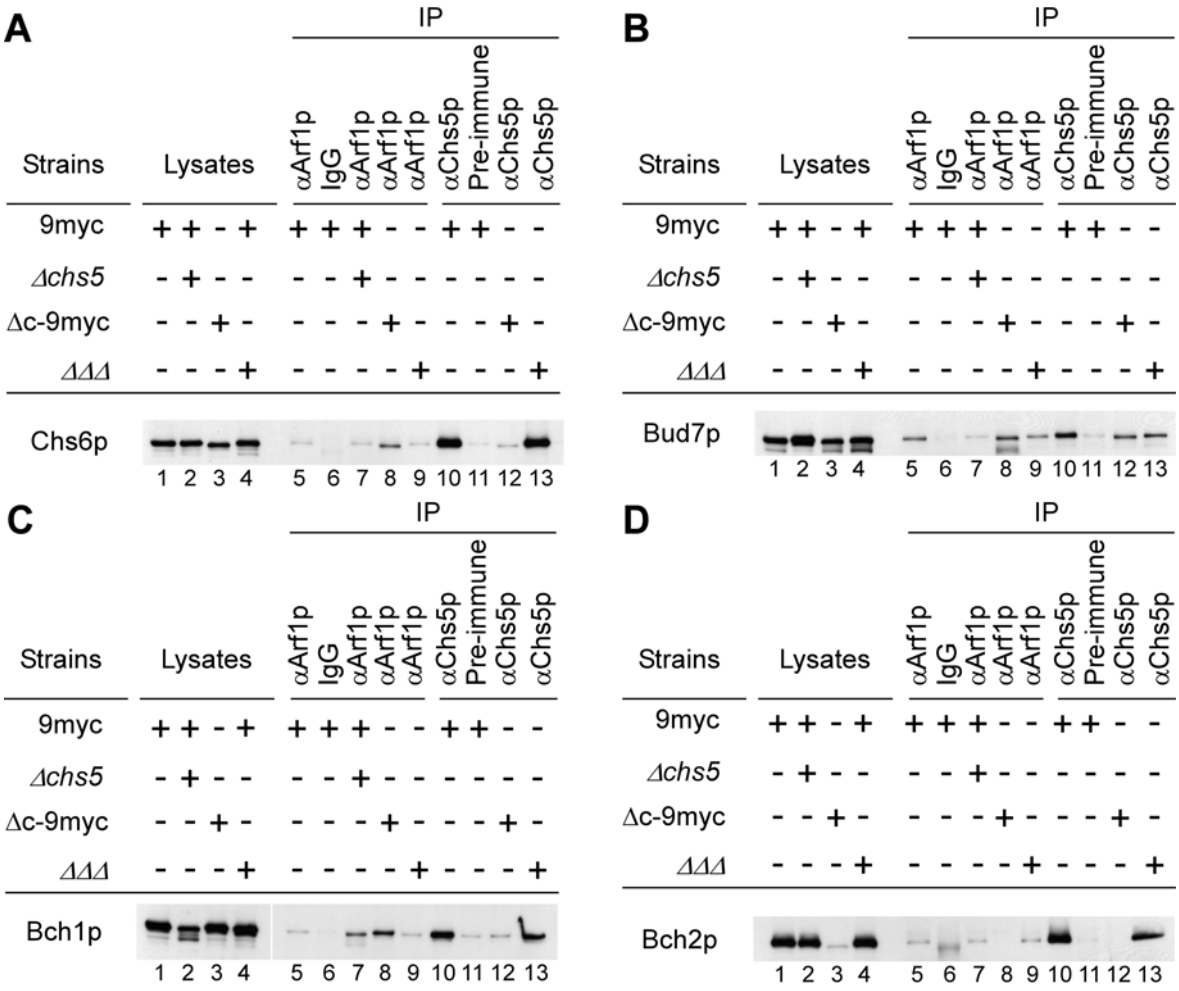

Figure 30: The Bud7-Chs6 family proteins interact with Arf1p and Chs5p. Co-immunoprecipitation experiments were performed using strains in which the Bud7-Chs6 family proteins were chromosomally tagged with 9myc. In addition to wild-type and *Δchs5*, we analyzed strains in which the C-terminus of the proteins was replaced by 9myc (Δc-9myc) and strains in which the remaining members of the Bud7-Chs6 family were deleted (ΔΔΔ). The lysates were treated with either affinity purified αArf1p-IgGs or αChs5p antiserum and Protein A-Sepharose. The precipitate was analyzed by SDS-PAGE and immunoblotted with antibodies directed against the myc epitope. Analysis of myc tagged strains of *CHS6*, *BUD7*, *BCH1*, and *BCH2* in **(A)**, **(B)**, **(C),** and **(D)**, respectively. 1.7% of the lysates used for immunoprecipitations was loaded in lane 1.

other to Chs5p and that their C-terminus is required for this interaction. Furthermore, the fact that a short deletion of the C-terminus leads to non-functional proteins can now be related to the inability to interact with Chs5p.

3.4.1.4 The Bud7-Chs6 family members interact with each other

The co-immunoprecipitation experiments could be interpreted in a way that both Arf1p and Chs5p form individual complexes with each member of the Bud7-Chs6 family. However, we had also found genetic interactions within the Bud7-Chs6 family. Furthermore, the protein expression levels within the family seemed tightly regulated (Chapter 3.3). For instance, simple overexpression of Chs6p was not able to restore calcofluor white sensitivity of a *Δchs6* strain. In addition, both Chs6p as well as either Bud7p or Bch1p were essential for trafficking of the chitin synthase Chs3p to the plasma membrane in the mother-bud neck. We therefore also considered the possibility that members of the Bud7-Chs6 family interact with each other.

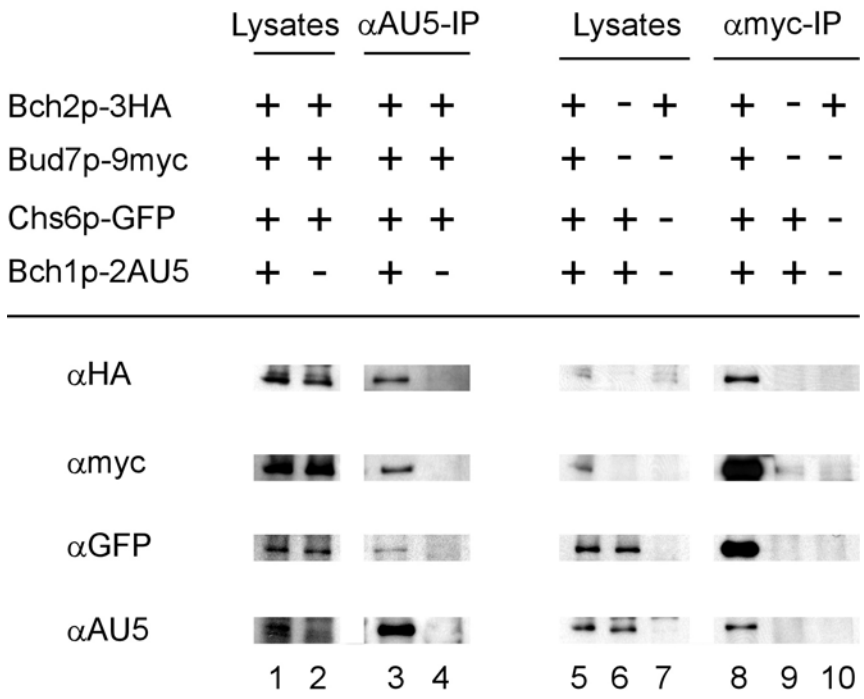

Figure 31: The Bud7-Chs6 family proteins interact with each other. A quadruply tagged strain along with control strains were subjected to immunoprecipitation. The precipitates were analyzed by SDS-PAGE and immunoblotted with antibodies directed against all four different epitope tags. Precipitation with αAU5 and with αmyc-IgGs are shown. 1.7% of the lysates used for immunoprecipiations were loaded in lanes 1, 2, and 5 – 7.

To test this possibility, we constructed a quadruply tagged strain. Chs6p was fused to GFP, Bud7p appended with 9myc, Bch1p carried a double AU5 epitope and Bch2p was tagged with 3HA. The resulting strain behaved like the corresponding wild-type strain again indicating that all chromosomal fusions were functional. Again, co-immunoprecipitation experiments were performed. When polyclonal AU5 antibodies were used for precipitation, all the three other members of the Bud7-Chs6 family could be detected (Fig. 31, lane 3). This was not the case in control strains lacking the AU5 tag (Fig. 31, lane 4). A similar result was obtained when Bud7p-9myc was precipitated with monoclonal myc antibodies (Fig. 31). Again, Bch2p, Chs6p and Bch1p were detected in the precipitate by the use of their epitope tags (Fig. 31, lane 7). The signals were absent when control lysates lacking the myc-epitope were used (Fig. 31, lane 8 and 9). Similar results were obtained for co-immunoprecipitations with monoclonal HA antibodies and polyclonal GFP antibodies (data not shown). The intensities of the signals of the precipitations suggest that the Bud7-Chs6 family proteins form complexes with variable stoichiometries. In conlcusion, these experiments demonstrate that the four members of the Bud7-Chs6 family are not only able to interact with Arf1p and Chs5p but also with each other.

3.4.1.5 Analysis of native complexes by Blue Native PAGE

We have established previously that apart from Chs6p, the presence of either Bud7p or Bch1p is required for transport of Chs3p to the plasma membrane. We had therefore proposed that the Bud7-Chs6 family might act as cargo receptors. For the p24 cargo receptor family, it has been shown that their members are able to form homo- and heteromers and that the oligomerization state might contribute to cargo sorting function (Gommel *et al.*, 1999). Because the members of the Bud7-Chs6 family were able to interact not only with Arf1p and Chs5p but also with each other, we wondered if a similar mode of action might also apply to the Bud7-Chs6 family.

One suitable way to look at native protein complexes is Blue Native PAGE (Schagger, 2001). This technique is used to separate native protein complexes according to their apparent molecular weight. In order to study the native complexes of the Bud7-Chs6 family, we prepared lysates from different strains in which the individual members of the Bud7-Chs6 family were tagged with 9myc. These lysates were subjected to Blue Native PAGE and analyzed by immunoblot (Fig. 32). The strongest signal for Chs6p was detected in a form migrating with an apparent molecular weight of approximately 150 kDa which could represent either the monomeric or dimeric form of Chs6p (Fig. 32A). In addition,

Chs6p was present in a complex of high apparent molecular weight of around 400-500 kDa, visible as a smear. Upon deletion of *CHS5*, all Chs6p was converted to the low molecular weight species. A similar result was obtained when the C-terminus was deleted. Yet, a high molecular weight smear persisted that migrated faster than in wild-type. However, deletion of the three other Bud7-Chs6 family members resulted in a behavior comparable to that from wild-type lysate. A similar pattern was observed for Bch2p (Fig. 32B). Bch2p was present in both a high- and low molecular weight forms. The deletion of

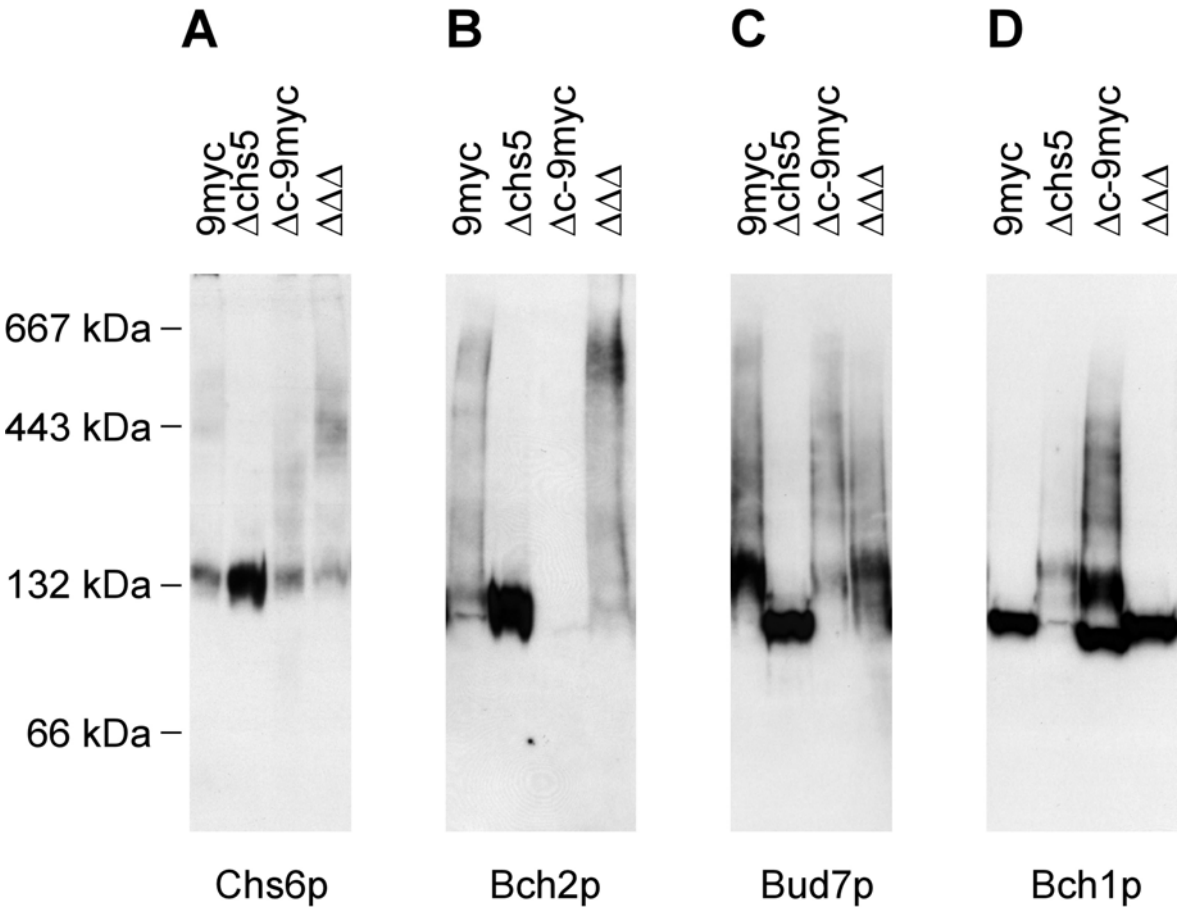

Figure 32: The members of the Bud7-Chs6 family form lower and higher molecular weight complexes. Lysates were prepared from different strains in which the Bud7-Chs6 family proteins were chromosomally tagged with 9myc. In addition to wild-type and *Δchs5*, we analyzed strains in which the C-terminus of the proteins was replaced by 9myc (Δc-9myc) and strains in which the remaining members of the Bud7-Chs6 family were deleted (ΔΔΔ). The lysates were separated by Blue-Native-PAGE and the protein complexes were blotted onto a PVDF-membrane which was decorated with antibodies directed against the myc epitope. Analysis of myc tagged strains of *CHS6*, *BCH2*, *BUD7*, and *BCH1* are shown in **(A)**, **(B)**, **(C)** and **(D)**, respectively.

CHS5 converted all Bch2p to the low molecular weight species. Because of the low protein level in the *BCH2Δc-9myc* strain, no protein signal was detected. Triple deletion of the remaining Bud7-Chs6 family members did not change mobilities as compared to wild-type lysates. Bud7p was present in low-, medium and high molecular weight species (Fig. 32C).

Only the deletion of *CHS5* had a major impact on electrophoretic mobility. In this case, Bud7p was converted to a fast migrating species. Bch1p, in contrast, displayed different characteristics (Fig. 32D). Here, in wild-type cells and in cells in which the other members of the Bud7-Chs6 family were deleted, only a fast migrating species was evident. Surprisingly, this was altered upon deletion of *CHS5* which decreased electrophoretic mobility. This was even reinforced in a *BCH1Δc-9myc* strain in which Bch1p migrated also in a high-molecular weight complex.

In conclusion, Chs6p, Bud7p, and Bch2p are present in low-molecular weight forms and high-molecular weight complexes at steady-state in cells grown under standard conditions. The electrophoretic mobility of these high molecular weight forms is consistent with a complex of at least three additional members of the Bud7-Chs6 family. The unaltered mobilities in triple deletion strains are an indication that the complexes do not represent obligate hetero-multimers. This is dramatically changed in *Δchs5* strains, in which Chs6p, Bud7p, and Bch2p are only present in low-molecular weight species indicating that Chs5p is required for complex formation or stability. The inability of a single member of Chs6p, Bud7p, and Bch2p to bind to Chs5p does not prevent complex formation and interation with other proteins as is evident from analysis of the C-terminal deleted strains.

In contrast to that, most of Bch1p is present in a low-molecular weight form. This indicates that most of Bch1p is not part of a multimeric complex in wild-type cells under standard conditions. However, deletion of *CHS5* or the C-terminus of Bch1p drive complex formation. This was particularly noticeable in the C-terminal deletion. These complexes looked very reminiscent to those of Bud7p. Strikingly, the complexes of the Bud7-Chs6 family had different molecular weights reflecting the possibility that the members might interact with different cargo molecules.

3.4.1.6 Intracellular distribution of the Bud7-Chs6 family is dependent on Chs5p

We wanted to determine if the interactions we detected biochemically would be also reflected in the intracellular distribution of the Bud7-Chs6 family. It has been reported that activated Arf1p resides on Golgi membranes (Stearns *et al.*, 1990b). Furthermore, it has been shown that Chs5p is associated with the TGN (Santos and Snyder, 1997). As the whole Bud7-Chs6 family is able to interact with Chs5p and (activated) Arf1p, we expected the Bud7-Chs6 family also to localize to the Golgi. To investigate the localization of the members of the Bud7-Chs6 family, we performed immunofluorescence on strains in which the members of the Bud7-Chs6 family were tagged with 9myc. For comparison, these

strains also contained a chromosomal *SEC7-GFP*, which was used as a marker of the TGN. As expected, both Chs6p and Bud7p localized to the TGN (co-localization with Sec7p-GFP) as well as to punctate structures in wild-type cells (Fig. 33). In contrast, Bch1p exhibited a very diffuse staining throughout the cytoplasm and only Bch2p was exclusively localized to the TGN. Whereas Chs6p, Bud7p and Bch2p appeared to be expressed to about the same level, Bch1p was expressed noticeably higher. This was evident from immunofluorescence (the exposure time was much shorter for Bch1p) as well as from earlier results of immoblots of the lysates (data not shown). However, all members of the Bud7-Chs6 family were at least partially localized to the TGN (Fig. 33, merge).

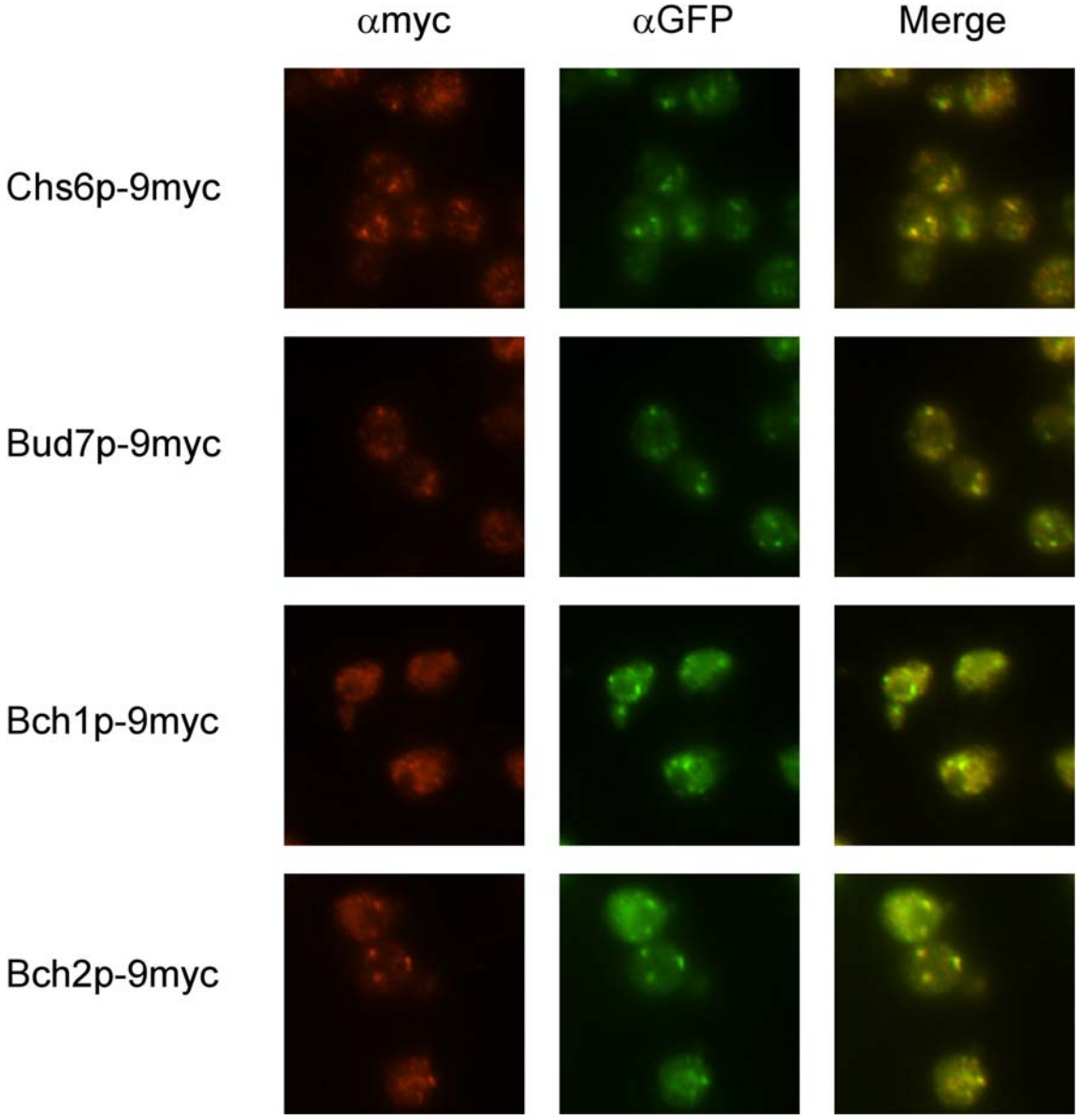

Figure 33: All Bud7-Chs6 family members are at least partially localized to the TGN. The Bud7-Chs6 family members were chromosomally tagged with 9myc and Sec7p with GFP. Strains were grown overnight in rich medium in logarithmic phase. Cells were fixed in formaldehyde and stained with anti-myc and anti-GFP antibodies. The fluorescent dye Cy3 was used for visualization of myc-tagged proteins (first column), whereas Sec7p was visualized by fluorescein (second column). The merge of the two fluorecence channels is shown in the third column.

Since the interaction of the members of the Bud7-Chs6 family with Chs5p is essential for protein function, we analyzed the distribution in suitable deletion strains. The deletion of *CHS5* had a dramatic impact on both expression levels as well as localization of the Bud7-Chs6 family members. In *Δchs5* strains, Bud7p is up- and Bch1p downregulated, both evident in immunofluorescence (Fig. 34A, first column) and immunoblots (Fig. 30B and C, lanes 1 and 2). Chs6p, Bud7p and Bch2p lost their partial or complete TGN-localization and showed a diffuse staining. As expected, the deletion of the C-terminus of the Bud7-Chs6 family proteins had a similar effect like the *CHS5* deletion for Chs6p, Bud7p and Bch2p (Fig. 34A, second column). The impact on the localization of Bch1p was generally hard to score because of the already very diffuse staining of this protein in wild-type cells. These experiments provide further evidence that Chs5p as well as the C-terminus of the Bud7-Chs6 family proteins is required for either recruitment to or stabilization of the Bud7-Chs6 family at the TGN. Localization to the TGN might therefore be a prerequisite for protein function.

We next investigated the influence of the Bud7-Chs6 family on the localization of each other by performing immunofluorescence in triple deletion strains (Fig. 34A, third column). The most dramatic effect was observed for Chs6p, which showed a punctate staining. The TGN-localization was not completely lost for Bud7p and Bch2p retained TGN-staining. Generally, the localization of the Bud7-Chs6 family members was less dependent on each other than on Chs5p and the C-terminus of the proteins.

In contrast, the Bud7-Chs6 family has no effect on the localization of Chs5p. In Fig. 34B, we show an immunofluorescence of Chs5p-6HA cells. Chs5p displayed a localization corresponding to the TGN. The deletion of the whole Bud7-Chs6 family did not affect the localization of Chs5p to any greater extent (Fig. 34B). This demonstrates that Chs5p localizes to the TGN independently of the Bud7-Chs6 family.

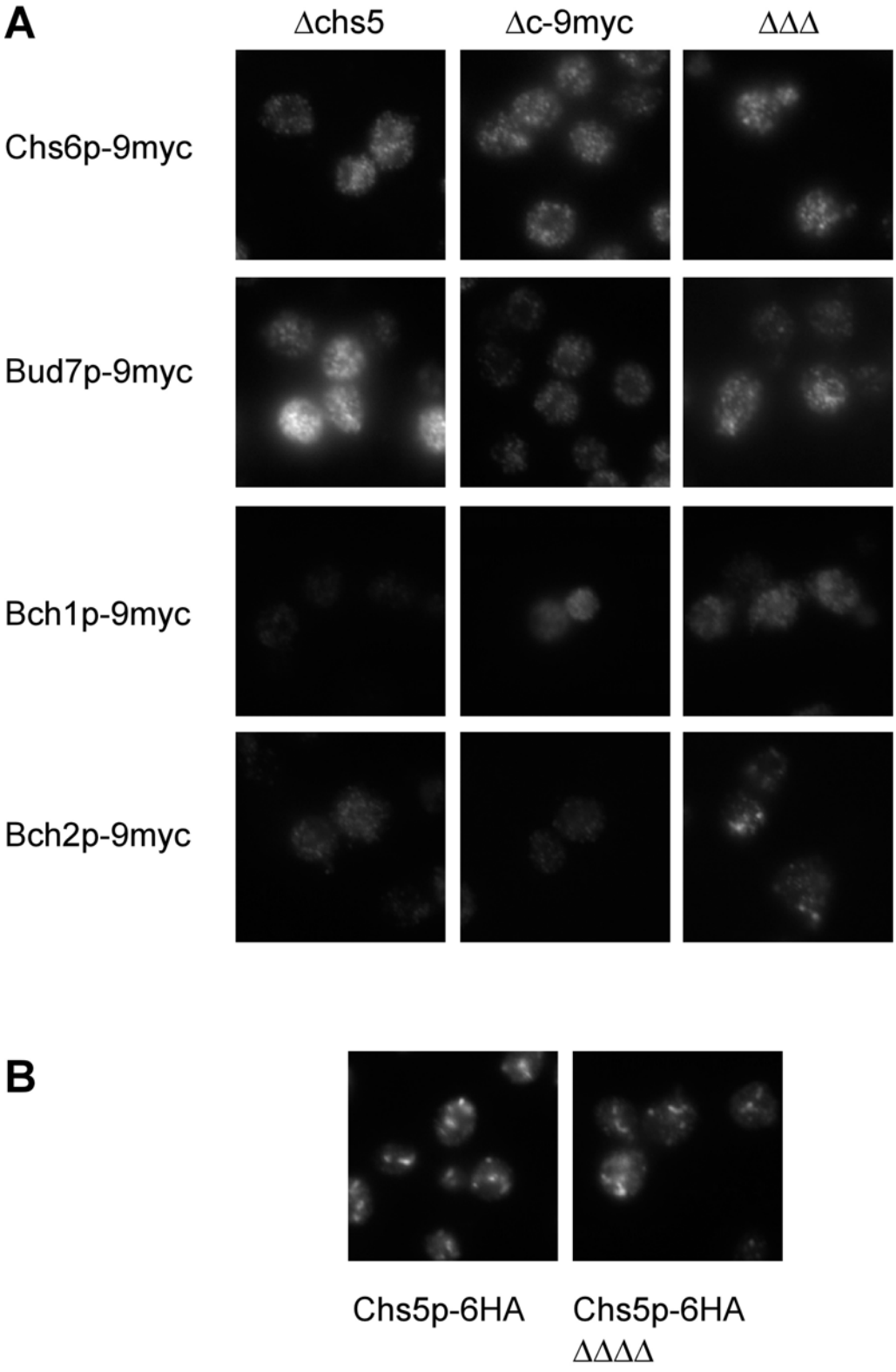

Figure 34: Changes in intracellular distribution of the Bud7-Chs6 family proteins and Chs5p as determined by immunofluorescence. The strains were grown overnight in rich medium into logarithmic phase. Cells were fixed in formaldehyde and incubated with HA or myc antibodies. The fluorescent dye Cy3 coupled to a secondary antibody was used for visualization of the proteins. The same exposure time as in Figure 33 was used for each protein within one row. **(A)** Immunofluorescence of *CHS5*-deleted strains in which the Bud7-Chs6 family proteins were chromosomally tagged with 9myc (first column). The second column shows strains in which the C-terminus of the proteins were replaced by 9myc (Δc-9myc). The third column shows strains in which the remaining members of the Bud7-Chs6 family were deleted (ΔΔΔ). **(B)** Chs5p-6HA staining in wild-type cells and in cells in which the whole Bud7-Chs6 family was deleted (ΔΔΔΔ).

3.4.1.7 Vesicle association

The Bud7-Chs6 family members and the p24 family members have been proposed to act as cargo receptors (Chapter 3.3; Belden and Barlowe, 1996). The latter ones are cycling between ER and Golgi and are an integral part of COPI- and COPII- coated vesicles. A direct interaction with cargo proteins was demonstrated in later studies (Muniz *et al.*, 2000). All members of the Bud7-Chs6 family are soluble proteins but for each of them a membrane-associated pool exists and they are all at least partially localized at the TGN. Therefore, a "cycling" could be achieved by membrane association and dissociation events. Similar to the p24-family, the Bud7-Chs6 family proteins are able to associate into higher molecular weight complexes. An important consideration is whether the Bud7-Chs6 family proteins become associated with vesicles. To address this issue, we employed a Golgi-budding assay. This *in vitro* assay has been used successfully in the studies of COPI-coated vesicle generation (Spang and Schekman, 1998). Enriched Golgi membranes were incubated with cytosol, GTPγS and an energy regeneration system. By this procedure, COPI-coated and other vesicles were formed. These vesicles can be separated from the Golgi membranes by a sedimentation centrifugation. The vesicle peak was collected and further enriched by a flotation based on coated membrane buoyant density. Using this purification scheme, vesicles were highly enriched, because contaminating particles would have to show the same behavior on a sedimentation gradient as well as sharing the same buoyant density. The result of such an experiment is shown in Fig. 35. Golgi membranes and cytosol from a strain containing only tagged members of the Bud7-Chs6 family were used. The fractions of the flotation step were analyzed by immunoblot. As observed before, this procedure resulted in COPI-coated vesicles which are marked by the vesicular transmembrane cargo Emp47 peaking in fractions 4 – 7. Bud7p-9myc and Bch2p-3HA were detected in fractions 3 – 5. This is a strong indication for vesicle association since only proteins associated with lipids are able to float in this gradient during the centrifugation. Most of the signal remained in the load of the gradient, which is expected for peripherally associated proteins. For Chs6p-GFP and Bch1p-2AU5, we obtained a signal only in the fractions corresponding to the load of the gradient (data not shown). However, this might be due to detection problems and does not formally exclude the possibility that these proteins were associated with vesicles. This experiment demonstrates that at least Bud7p and Bch2p, both members of different sub-branches of the Bud7-Chs6 family, are associated with vesicles derived from Golgi membranes. Moreover, these vesicles are distinct from COPI-coated vesicles, which peak in denser fractions.

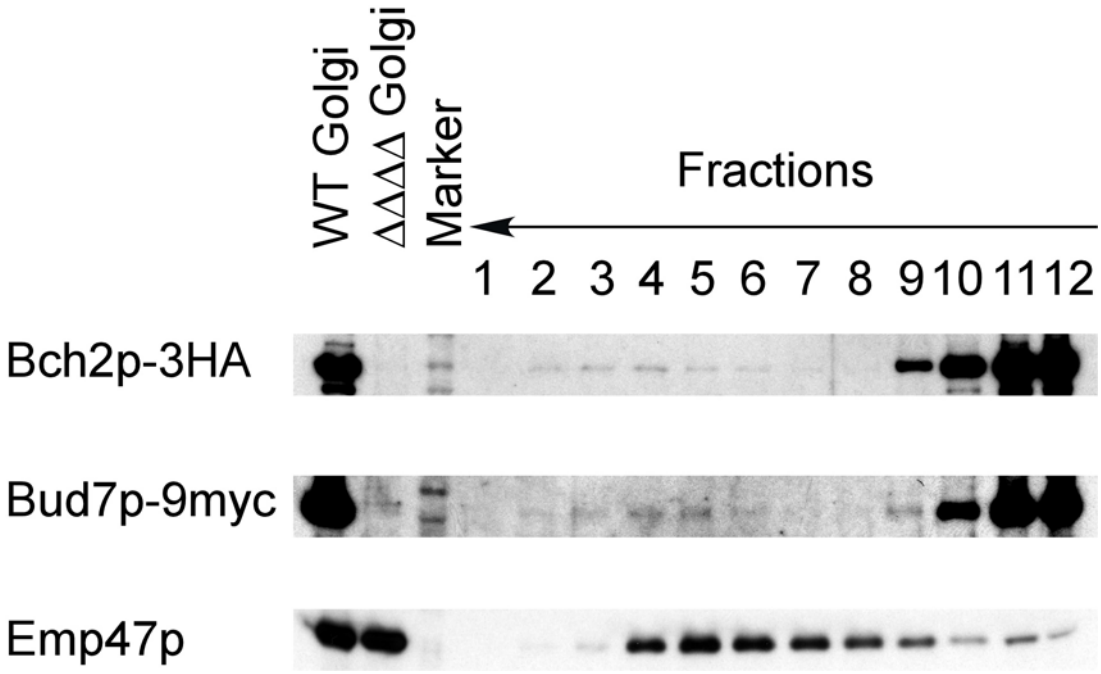

Figure 35: Bud7p and Bch2p are present on Golgi derived vesicles. Golgi membranes and cytosol were prepared from a strain in which all members of the Bud7-Chs6 were chromosomally tagged with different epitopes. Vesicles were generated from these Golgi membranes in the presence of GTPγS and cytosol. The vesicles were separated from the Golgi membranes and subsequently further purified by flotation on a Nycodenz gradient. Fractions were collected from the top, separated by SDS-PAGE, and analyzed by immunoblot. The arrows indicate the direction of movement of lipid particles within the gradient. Non-membrane associated proteins remain in the load at the bottom of the gradient. The COPI-vesicle cargo protein Emp47p peaks in fractions 4 – 7, whereas both Bud7p and Bch2p peak in fractions 3 – 5. For comparison, Golgi membranes derived from wild-type and a strain in which the whole Bud7-Chs6 family is deleted was also loaded on the gel.

3.4.2 Discussion

The finding that Chs5p and Bch1p both interacted with the activated form of Arf1p was the starting point for a series of experiments investigating the function of the Bud7-Chs6 family both on a genetic as well as a biochemical level. We showed that *ARF1* genetically interacts with members of the Bud7-Chs6 family and also with *CHS5*. *CHS5* acts as an upstream regulator or a downstream converging point of the Bud7-Chs6 family as determined by genetics. We had proposed that the Bud7-Chs6 family proteins are involved in Arf1p-dependent post-Golgi transport steps of fungi-specific cargo molecules like the chitin synthase Chs3p to the mother-bud neck (Chapter 3.3). In this chapter, we tried to corroborate the notion that the Bud7-Chs6 family proteins act as cargo receptors .

To study the Bud7-Chs6 family proteins biochemically we decided to construct a set of strains in which the Bud7-Chs6 family members are chromosomally tagged. This was necessary because raising antisera against individual members of the Bud7-Chs6 family were unsuccessful since the antisera cross-reacted due to the high similarity of these proteins (unpublished observation). We paid particular attention not to interfere with the physiological function of the proteins. Therefore, all protein fusions were tagged at the C-terminus on the chromosome in order to keep endogenous protein expression levels. Moreover, all protein fusions strains were tested intensively for functionality and compared to wild-type and deletion strains.

In the course of these experiments we realized that a short deletion at the C-terminus of the proteins renders the Bud7-Chs6 family proteins non-functional. This was of particular interest since the proteins were still present at wild-type levels (except for Bch2pΔc). The strains exhibited the same phenotype as the complete deletion independent of an additional epitope tag. This implies that a short sequence at the C-terminus is required for protein function (and in the case of Bch2pΔc also for protein stability).

We were able to show a physical interaction of all Bud7-Chs6 family members with Arf1p by co-immunoprecipitation experiments. At least for Bch1p, it was shown that it predominantly interacts with Arf1p-GTP. Based on this fact, it is a reasonable assumption that also the other members of the Bud7-Chs6 family might interact with activated Arf1p, which is localizes to the Golgi apparatus (Stearns *et al.*, 1990b). This is consistent with the observation that all Bud7-Chs6 family members are at least partially localized to the TGN. The interaction of one specific member of the Bud7-Chs6 family with Arf1p was independent on the presence of Chs5p or the any other family members. In addition, the C-terminal sequence was not required for binding to Arf1p. On the contrary, the interaction

with Arf1p was even more pronounced in this case. These results would point to a regulatory function of the C-terminal sequence. Alternatively, the amount of precipitable protein might have been increased because some other protein-protein interaction was abolished.

All Bud7-Chs6 family members interacted physically with Chs5p. The interaction of one specific Bud7-Chs6 family member was again not dependent on the presence of any other member. Most importantly, the C-terminuis was required for binding to Chs5p, which was clearly evident for at least Chs6p and Bch1p. The fact that strains with short deletions of the C-terminus behaved like the complete deletion can now be related to the inability to interact with Chs5p. A *CHS5* deletion combines all the phenotypes so far described for the single deletion of the Bud7-Chs6 family. This means that Chs5p binding is essential for mediating the function of each single Bud7-Chs6 family member.

We already realized during the genetic analysis of the Bud7-Chs6 family that some genes are more tightly linked than others. For instance, Bud7p and Bch1p were able to substitute for each other under overexpression conditions whereas this was not the case for Chs6p and Bch2p. In addition, a *CHS6* deletion was calcofluor white resistant, a phenotype we did not observe for the single deletions of *BUD7* and *BCH1*. Unexpectedly, the double deletion of *BUD7 BCH1* was also calcofluor resistant. We therefore considered the possibility that the Bud7-Chs6 family proteins would act in (facultative) pairs: Bud7p-Bch1p would be one pair and Chs6p-Bch2p would be the other pair. These two pairs correspond to the two sub-branches of the Bud7-Chs6 family. Hence, we tested for a physical interaction of the Bud7-Chs6 family proteins which each other. Co-immunoprecipiation experiments suggested that all four members are able to physically interact with each other. These results are consistent with data obtained by Blue Native PAGE analysis which showed that the Bud7-Chs6 family proteins exist in high molecular weight complexes. Whether in all cases all four proteins are involved remains unclear. One possibility might be that a complex is formed containing at least one member of each sub-family. This would mean that not in all complexes all members of the Bud7-Chs6 family are taking part. Rather, the precise constitution of the complex could be adjusted to the cell's needs.

Arf1p and Chs5p have been shown to localize to the Golgi-apparatus. We were able to show by immunofluorescence that Chs5p is still localized to the TGN in the absence of the whole Bud7-Chs6 family. This was not unexpected since Chs5p is also involved in other trafficking events apart from Bud7-Chs6 family related pathways: for instance, the

polarized localization of the cell fusion factor Fus1p during mating (Chapter 3.3; Santos and Snyder, 2003). Based on the results from the co-immunoprecipitation, one could expect that the Bud7-Chs6 family proteins would localize to the TGN. However, this was not the case. Bch2p was the only member with an exclusive TGN localization and, in contrast, Bch1p showed a very diffuse staining. Chs6p and Bud7p localized to the TGN but additionally displayed a punctate staining. This punctate staining might correspond to e.g. chitosomes, a specialized endosomal compartment, through which the chitin synthase Chs3p is traveling in a Chs6p dependent manner. This might be an indication that Chs6p and Bud7p are also needed for a second transport step at this site of the cell or that the Bch1p and Bch2p have a faster dynamics. However, all four Bud7-Chs6 family members exhibited at least partial TGN localization. Upon deletion of *CHS5* or deletion of the C-terminus required for binding to Chs5p, the Bud7-Chs6 family proteins lost their localization at the TGN (although not evident for Bch1p). This demonstrates that Chs5p is required for recruitment and/or stabilization of the Bud7-Chs6 family proteins at the TGN. These results are consistent with the analysis of protein complexes by Blue Native PAGE. In wild-type cells, the Chs6p, Bud7p and Bch2p are present in low- and high molecular weight forms. The high molecular weight form might correspond to a “priming complex” forming at the TGN. Deletion of *CHS5* converts the high-molecular weight species to low-molecular weight species. This would indicate that Chs5p is needed for the formation or stability of this priming complex. Deletion of the C-terminus results in preservation or a slight shift in the high-molecular weight species (Bud7p and Chs6p). Although the ability to interact with Chs5p is lost, other members interacting with the C-terminal deleted form might help to stabilize the priming complex.

Bch1p seems to be an exception - every family has its black sheep. Whereas Chs6p, Bud7p and Bch2p are expressed to about the same level, Bch1p is expressed to much higher extent. The intracellular distribution also differs; it is the only member of the Bud7-Chs6 family showing a very diffuse staining. Also, most of Bch1p is not part of a “priming complex” as determined by Blue Native PAGE but is present as low-molecular weight form. Surprisingly, this changes upon deletion of *CHS5* or the C-terminus of Bch1p. This could mean that Bch1p is for the most part under the conditions tested not involved in generating vesicles but only included according to the cell’s needs. A deletion of *CHS5* might provoke compensation of the cell and the distribution and interaction of the Bud7-Chs6 family proteins might be changed accordingly. Alternatively, Chs5p might have a negatively regulatory role for the incorporation of Bch1p into complexes.

We also tested if the Bud7-Chs6 family proteins would become part of vesicles derived from the Golgi-apparatus. We were able to show a vesicle association for at least Bud7p and Bch2p. The corresponding vesicles have a lower density than COPI-coated vesicles, which were visualized by the cargo molecule Emp47p. We did not detect Bch1p or Chs6p on these vesicles. However, this might be a detection problem and does not exclude that these proteins are also vesicle-associated. Alternatively, they could associate with other kinds of vesicles that were not revealed in this specific experiment. Further experiments are required to resolve this issue.

We speculate that activated Arf1p is recruiting Chs5p and the Bud7-Chs6 family members to the TGN. There, Chs5p is needed for stabilization of the Bud7-Chs6 family proteins. Such a complex would be consistent with the priming complex model proposed by Springer *et al.* (1999), in which coat proteins and cargo receptors are together in one complex. It has already been proposed that Chs5p might act as a coat protein (Santos and Snyder, 1997). This would happen for Bud7-Chs6 family-dependent (like Chs3p) and -independent vesicular traffic (like Fus1p). In case Chs5p is the coat protein, a deletion of *CHS5* would result in no vesicle production. The Bud7-Chs6 family proteins might serve as cargo receptors. Thus, in the absence of one specific member of the Bud7-Chs6 family vesicles would be formed but certain cargo molecules like the chitin synthase Chs3p would not be incorporated. These cargo receptors complexes could be of a modular nature. Depending on the cell's needs, different amounts of cargo receptors would be recruited for vesicle formation. It is conceivable that one protein of the Bud7-Chs6 family is not sufficient but it might require the assistance of other members of the Bud7-Chs6 family members to efficiently recruit cargo molecules. This is of course speculative and other modes of actions of the Bud7-Chs6 family proteins are also conceivable.

We proposed that the Bud7-Chs6 family proteins act as cargo receptors. This notion is corroborated by the following observations: (i) the Bud7-Chs6 family proteins interact with Arf1p. In case of Bch1p, it was shown that it predominantly interacts with activated Arf1p. Arf1p is itself required for the formation of different post-Golgi vesicles. (ii) the Bud7-Chs6 family proteins interact with Chs5p which has been suggested to reside on the outside of vesicles. The interaction with Chs5p is required for protein funtion. Chs5p also interacts with activated Arf1p. (iii) the Bud7-Chs6 family proteins at least partially localize to the TGN. At least Bud7p and Bch2p become associated with vesicles derived from Golgi membranes. (iv) the Bud7-Chs6 family proteins interact with each other. They are able to form higher molecular weight complexes, a feature which is also observed for the

p24 family of cargo receptors (v) the Bud7-Chs6 family proteins seem to be required for trafficking of specific cargo molecules. It has been shown that Chs6p is required for trafficking of Chs3p but not of the closely related Chs1p (Ziman *et al.*, 1998). (vi) the Bud7-Chs6 family proteins exist in membrane-bound and soluble pools. A "cycling" as cargo receptors could be achieved by membrane association and dissociation events. The coatomer complex (recruited by Arf1p) as well as Sec24p (recruited by Sar1p) are examples of soluble cargo receptors for COPI and COPII vesicles, respectively (vii) the knockout of the whole Bud7-Chs6 family does not display a deleterious phenotype. Similarly, the complete knockout of the whole p24 family in yeast displays a rather subtle phenotype (Springer *et al.*, 2000).

This work described here implicates the members of the Bud7-Chs6 family as vesicluar cargo receptors. Valuable tools have been generated that will facilitate more extensive exploration of the molecular involvement of Chs5p and the Bud7-Chs6 family proteins in vesicle generation and cargo-recruitment in the future.

4 Summary

The small GTPase Arf1 is a crucial regulator of vesicle formation at many steps of the secretory pathway in the yeast *Saccharomyces cerevisiae* as well as in higher eukaryotes. Currently best understood is the role of Arf1 in the formation of COPI-coated vesicles at different levels of the Golgi apparatus. In addition, there is growing evidence of Arf1 being involved in actin cytoskeleton rearrangements as well as in lipid metabolism. The variety of already known regulators and effectors of Arf1 is, however, still insufficient to explain the multiple functions of the same molecule at different cellular locations. Furthermore, it is likely that new Arf1-dependent pathways await discovery in both yeast and mammals.

In this study, a differential affinity chromatography approach was used to identify new interactors of Arf1p from *Saccharomyces cerevisiae* cytosol. One of the new interactors of activated Arf1p that was identified was the polyA-binding protein Pab1p, which binds to the polyA-tail of mRNA. Pab1p was found to associate with purified COPI-coated vesicles generated from Golgi membranes *in vitro*. The stability of the Arf1p-Pab1p complex depends on the presence of mRNA. Both symmetrically distributed mRNAs as well as the asymmetrically distributed ASH1 mRNA are found in association with Arf1p. Remarkably, Arf1p and Pab1p are both required to restrict ASH1 mRNA to the bud tip. Arf1p and coatomer play an unexpected role in localizing mRNA independent and downstream of the SHE machinery. Hereby acts the SHE machinery in long-range mRNA transport while COPI vesicles could act as short-range localization vehicles. The ER-Golgi shuttle might be involved in concentrating mRNA at the ER.

Other interactors of activated Arf1p identified were Chs5p and Bch1p, a member of the Bud7-Chs6 family. In this study, I showed that all members of this new and previously uncharacterized fungi-specific protein family physically interact with Arf1p and Chs5p. Moreover, the Bud7-Chs6 family proteins interact with one another and form higher molecular weight complexes. In addition, they are all at least partially localized to the trans-Golgi network. Most importantly, at least Bud7p and Bch2p are found on vesicles generated from Golgi membranes *in vitro*. The Bud7-Chs6 family is required for trafficking of specific cargo molecules like the chitin synthase Chs3p from the trans-Golgi-network to the mother-bud neck and plays a role in bud-site selection. These functions of the Bud7-Chs6 family proteins converge in Chs5p. Finally, I propose that the Bud7-Chs6 family proteins act as cargo receptors and are involved in Arf1p-dependent post-Golgi transport steps of fungi-specific cargo molecules directed to the mother-bud neck.

5 Zusammenfassung

Die kleine GTPase Arf1 ist ein entscheidender Regulator bei der Vesikelbildung an vielen Stellen des sekretorischen Wegs in der Hefe *S. cerevisiae* und ebenso in höheren Eukaryoten. Momentan ist die Funktion von Arf1 bei der Bildung von COPI-Vesikeln am besten charakterisiert. Es gibt aber auch immer mehr Hinweise darauf, dass Arf1 an der Umbildung des Actin-Cytoskeletts beteiligt ist und ebenso den Lipid-Metabolismus beeinflusst. Die große Vielfalt an schon bekannten Interaktoren von Arf1 ist jedoch immer noch nicht ausreichend, um die multiplen Funktionen ein und desselben Moleküls an verschiedenen zellulären Orten zu erklären. Es ist außerdem wahrscheinlich, dass weitere Arf1-abhängige Wege in Hefen und höheren Eukaryoten noch gar nicht entdeckt wurden.

In dieser Arbeit wurde eine differenzielle Affinitätschromatographie durchgeführt, um neue cytosolische Interaktoren von Arf1p aus *S. cerevsiae* zu identifizieren. Einer der neu gefundenen Interaktoren von aktiviertem Arf1p war das PolyA-bindende Protein Pab1p. Es wurde gefunden, dass Pab1p mit aufgereinigten COPI-Vesikeln assoziiert ist, die aus Golgi Membranen *in vitro* hergestellt wurden. Die Stabilität des Arf1p-Pab1p Komplexes war ab hängig von mRNA. Sowohl symmetrische mRNAs als auch die asymmetrisch verteilte ASH1 mRNA waren mit Arf1p assoziiert. Bemerkenswerterweise waren sowohl Arf1p als auch Pab1p nötig, um ASH1 mRNA auf die Knospungspitze zu beschränken. Arf1p und Coatomer spielen eine unerwartete Rolle in der Lokalisierung von mRNA. Diese ist unabhängig von der SHE Maschinerie und ihr nachgeschaltet. Die SHE Maschinerie agiert hier als Langstrecken-Transportsystem, während COPI-Vesikel kurze Strecken überbrücken könnten. Der ER-Golgi Pendelverkehr könnte daran beteiligt sein, mRNA am ER zu konzentrieren.

Weitere neue Interaktoren waren Chs5p und Bch1p, ein Mitglied der Bud7-Chs6 Familie. In dieser Arbeit wurde gezeigt, dass alle Mitglieder dieser pilzspezifischen Proteinfamilie physikalisch mit Arf1p und Chs5p wechselwirken. Darüber hinaus interagieren die Proteine der Bud7-Chs6 Familie miteinander und bilden höhermolekulare Komplexe. Alle sind zumindest teilweise am trans-Golgi Netzwerk lokalisiert und außerdem sind Bud7p und Bch2p auf Vesikeln zu finden. Die Bud7-Chs6 Familie ist nötig für den Transport von spezieller Proteinfracht wie etwa der Chitin Synthase Chs3p vom trans-Golgi-Netzwerk zum Knospungshals und spielt eine Rolle bei der Auswahl der Knospungsstellen. Diese Funktionen der Bud7-Chs6 Familie konvergieren in Chs5p. Es wird vorgeschlagen, dass die Mitglieder der Bud7-Chs6 Familie als neuartige Fracht-Rezeptoren fungieren und beteiligt sind an Arf1p-abhängigen post-Golgi Transportschritten hin zum Knospungshals.

6 References

Adams, A.E., and Pringle, J.R. (1991). Staining of actin with fluorochrome-conjugated phalloidin. Methods Enzymol *194*, 729-731.

Aguilar, R.C., Boehm, M., Gorshkova, I., Crouch, R.J., Tomita, K., Saito, T., Ohno, H., and Bonifacino, J.S. (2001). Signal-binding specificity of the mu4 subunit of the adaptor protein complex AP-4. J Biol Chem *276*, 13145-13152.

Altschuler, Y., Liu, S., Katz, L., Tang, K., Hardy, S., Brodsky, F., Apodaca, G., and Mostov, K. (1999). ADP-ribosylation factor 6 and endocytosis at the apical surface of Madin-Darby canine kidney cells. J Cell Biol *147*, 7-12.

Amor, J.C., Harrison, D.H., Kahn, R.A., and Ringe, D. (1994). Structure of the human ADP-ribosylation factor 1 complexed with GDP. Nature *372*, 704-708.

Anderson, J.T., Paddy, M.R., and Swanson, M.S. (1993). PUB1 is a major nuclear and cytoplasmic polyadenylated RNA-binding protein in Saccharomyces cerevisiae. Mol Cell Biol *13*, 6102-6113.

Antonny, B., Beraud-Dufour, S., Chardin, P., and Chabre, M. (1997). N-terminal hydrophobic residues of the G-protein ADP-ribosylation factor-1 insert into membrane phospholipids upon GDP to GTP exchange. Biochemistry *36*, 4675-4684.

Antonny, B., Gounon, P., Schekman, R., and Orci, L. (2003). Self-assembly of minimal COPII cages. EMBO Rep *4*, 419-424.

Aoe, T., Huber, I., Vasudevan, C., Watkins, S.C., Romero, G., Cassel, D., and Hsu, V.W. (1999). The KDEL receptor regulates a GTPase-activating protein for ADP-ribosylation factor 1 by interacting with its non-catalytic domain. J Biol Chem *274*, 20545-20549.

Arnott, D., O'Connell, K.L., King, K.L., and Stults, J.T. (1998). An integrated approach to proteome analysis: identification of proteins associated with cardiac hypertrophy. Anal Biochem *258*, 1-18.

Austin, C., Boehm, M., and Tooze, S.A. (2002). Site-specific cross-linking reveals a differential direct interaction of class 1, 2, and 3 ADP-ribosylation factors with adaptor protein complexes 1 and 3. Biochemistry *41*, 4669-4677.

Baggett, J.J., and Wendland, B. (2001). Clathrin function in yeast endocytosis. Traffic *2*, 297-302.

Barlowe, C. (2000). Traffic COPs of the early secretory pathway. Traffic *1*, 371-377.

Barlowe, C. (2003). Signals for COPII-dependent export from the ER: what's the ticket out? Trends Cell Biol *13*, 295-300.

Barlowe, C., d'Enfert, C., and Schekman, R. (1993). Purification and characterization of SAR1p, a small GTP-binding protein required for transport vesicle formation from the endoplasmic reticulum. J Biol Chem *268*, 873-879.

Barlowe, C., Orci, L., Yeung, T., Hosobuchi, M., Hamamoto, S., Salama, N., Rexach, M.F., Ravazzola, M., Amherdt, M., and Schekman, R. (1994). COPII: a membrane coat formed by Sec proteins that drive vesicle budding from the endoplasmic reticulum. Cell *77*, 895-907.

Barlowe, C., and Schekman, R. (1993). SEC12 encodes a guanine-nucleotide-exchange factor essential for transport vesicle budding from the ER. Nature *365*, 347-349.

Beach, D.L., and Bloom, K. (2001). ASH1 mRNA localization in three acts. Mol Biol Cell *12*, 2567-2577.

Beck, T., Schmidt, A., and Hall, M.N. (1999). Starvation induces vacuolar targeting and degradation of the tryptophan permease in yeast. J Cell Biol *146*, 1227-1238.

Belden, W.J., and Barlowe, C. (1996). Erv25p, a component of COPII-coated vesicles, forms a complex with Emp24p that is required for efficient endoplasmic reticulum to Golgi transport. J Biol Chem *271*, 26939-26946.

Bensadoun, A., and Weinstein, D. (1976). Assay of proteins in the presence of interfering materials. Anal Biochem *70*, 241-250.

Bertrand, E., Chartrand, P., Schaefer, M., Shenoy, S.M., Singer, R.H., and Long, R.M. (1998). Localization of ASH1 mRNA particles in living yeast. Mol Cell *2*, 437-445.

Bi, X., Corpina, R.A., and Goldberg, J. (2002). Structure of the Sec23/24-Sar1 pre-budding complex of the COPII vesicle coat. Nature *419*, 271-277.

Bigay, J., Gounon, P., Robineau, S., and Antonny, B. (2003). Lipid packing sensed by ArfGAP1 couples COPI coat disassembly to membrane bilayer curvature. Nature *426*, 563-566.

Birnboim, H.C., and Doly, J. (1979). A rapid alkaline extraction procedure for screening recombinant plasmid DNA. Nucleic Acids Res *7*, 1513-1523.

Blader, I.J., Cope, M.J., Jackson, T.R., Profit, A.A., Greenwood, A.F., Drubin, D.G., Prestwich, G.D., and Theibert, A.B. (1999). GCS1, an Arf guanosine triphosphatase-activating protein in Saccharomyces cerevisiae, is required for normal actin cytoskeletal organization in vivo and stimulates actin polymerization in vitro. Mol Biol Cell *10*, 581-596.

Blum, H., Beier, H., and Gross, H.J. (1987). Improved silver staining of plant-proteins, RNA and DNA in polyacrylamide gels. Electrophoresis *8*, 93-99.

Boeck, R., Lapeyre, B., Brown, C.E., and Sachs, A.B. (1998). Capped mRNA degradation intermediates accumulate in the yeast spb8-2 mutant. Mol Cell Biol *18*, 5062-5072.

Boehm, M., Aguilar, R.C., and Bonifacino, J.S. (2001). Functional and physical interactions of the adaptor protein complex AP-4 with ADP-ribosylation factors (ARFs). Embo J *20*, 6265-6276.

Boehm, M., and Bonifacino, J.S. (2002). Genetic analyses of adaptin function from yeast to mammals. Gene *286*, 175-186.

Bohl, F., Kruse, C., Frank, A., Ferring, D., and Jansen, R.P. (2000). She2p, a novel RNA-binding protein tethers ASH1 mRNA to the Myo4p myosin motor via She3p. Embo J *19*, 5514-5524.

Boman, A.L. (2001). GGA proteins: new players in the sorting game. J Cell Sci *114*, 3413-3418.

Boman, A.L., Kuai, J., Zhu, X., Chen, J., Kuriyama, R., and Kahn, R.A. (1999). Arf proteins bind to mitotic kinesin-like protein 1 (MKLP1) in a GTP-dependent fashion. Cell Motil Cytoskeleton *44*, 119-132.

Boman, A.L., Salo, P.D., Hauglund, M.J., Strand, N.L., Rensink, S.J., and Zhdankina, O. (2002). ADP-ribosylation factor (ARF) interaction is not sufficient for yeast GGA protein function or localization. Mol Biol Cell *13*, 3078-3095.

Bonifacino, J.S. (2004). The GGA proteins: adaptors on the move. Nat Rev Mol Cell Biol *5*, 23-32.

Bonifacino, J.S., and Glick, B.S. (2004). The mechanisms of vesicle budding and fusion. Cell *116*, 153-166.

Bonifacino, J.S., and Traub, L.M. (2003). Signals for sorting of transmembrane proteins to endosomes and lysosomes. Annu Rev Biochem *72*, 395-447.

Bradford, M.M. (1976). A rapid and sensitive method for the quantitation of microgram quantities of protein utilizing the principle of protein-dye binding. Anal Biochem *72*, 248-254.

Bremser, M., Nickel, W., Schweikert, M., Ravazzola, M., Amherdt, M., Hughes, C.A., Sollner, T.H., Rothman, J.E., and Wieland, F.T. (1999). Coupling of coat assembly and vesicle budding to packaging of putative cargo receptors. Cell *96*, 495-506.

Brown, H.A., Gutowski, S., Moomaw, C.R., Slaughter, C., and Sternweis, P.C. (1993). ADP-ribosylation factor, a small GTP-dependent regulatory protein, stimulates phospholipase D activity. Cell *75*, 1137-1144.

Casamayor, A., and Snyder, M. (2002). Bud-site selection and cell polarity in budding yeast. Curr Opin Microbiol *5*, 179-186.

Chardin, P., Paris, S., Antonny, B., Robineau, S., Beraud-Dufour, S., Jackson, C.L., and Chabre, M. (1996). A human exchange factor for ARF contains Sec7- and pleckstrin-homology domains. Nature *384*, 481-484.

Chen, T., Hiroko, T., Chaudhuri, A., Inose, F., Lord, M., Tanaka, S., Chant, J., and Fujita, A. (2000). Multigenerational cortical inheritance of the Rax2 protein in orienting polarity and division in yeast. Science *290*, 1975-1978.

Christoforidis, S., McBride, H.M., Burgoyne, R.D., and Zerial, M. (1999). The Rab5 effector EEA1 is a core component of endosome docking. Nature *397*, 621-625.

Cosma, M.P., Tanaka, T., and Nasmyth, K. (1999). Ordered recruitment of transcription and chromatin remodeling factors to a cell cycle- and developmentally regulated promoter. Cell *97*, 299-311.

Cosson, P., and Letourneur, F. (1994). Coatomer interaction with di-lysine endoplasmic reticulum retention motifs. Science *263*, 1629-1631.

Cowles, C.R., Odorizzi, G., Payne, G.S., and Emr, S.D. (1997). The AP-3 adaptor complex is essential for cargo-selective transport to the yeast vacuole. Cell *91*, 109-118.

Crottet, P., Meyer, D.M., Rohrer, J., and Spiess, M. (2002). ARF1.GTP, tyrosine-based signals, and phosphatidylinositol 4,5-bisphosphate constitute a minimal machinery to recruit the AP-1 clathrin adaptor to membranes. Mol Biol Cell *13*, 3672-3682.

Davis, B.J. (1964). Disc Electrophoresis. Ii. Method and Application to Human Serum Proteins. Ann N Y Acad Sci *121*, 404-427.

Davis, C.G., Lehrman, M.A., Russell, D.W., Anderson, R.G., Brown, M.S., and Goldstein, J.L. (1986). The J.D. mutation in familial hypercholesterolemia: amino acid substitution in cytoplasmic domain impedes internalization of LDL receptors. Cell *45*, 15-24.

Davis, D. (1997). Manipulating Cell Types. In: Methods in Yeast Genetics, eds. A.E. Adams, D. Gottschling, C. Kaiser, and e. al., Cold Spring Harbor, USA: Cold Spring Harbor Laboratory.

De Antoni, A., and Gallwitz, D. (2000). A novel multi-purpose cassette for repeated integrative epitope tagging of genes in Saccharomyces cerevisiae. Gene *246*, 179-185.

Deardorff, J.A., and Sachs, A.B. (1997). Differential effects of aromatic and charged residue substitutions in the RNA binding domains of the yeast poly(A)-binding protein. J Mol Biol *269*, 67-81.

Dell'Angelica, E.C., Mullins, C., and Bonifacino, J.S. (1999). AP-4, a novel protein complex related to clathrin adaptors. J Biol Chem *274*, 7278-7285.

Deloche, O., de la Cruz, J., Kressler, D., Doere, M., and Linder, P. (2004). A membrane transport defect leads to a rapid attenuation of translation initiation in Saccharomyces cerevisiae. Mol Cell *13*, 357-366.

Diehn, M., Eisen, M.B., Botstein, D., and Brown, P.O. (2000). Large-scale identification of secreted and membrane-associated gene products using DNA microarrays. Nat Genet *25*, 58-62.

Dominguez, M., Dejgaard, K., Fullekrug, J., Dahan, S., Fazel, A., Paccaud, J.P., Thomas, D.Y., Bergeron, J.J., and Nilsson, T. (1998). gp25L/emp24/p24 protein family members of the cis-Golgi network bind both COP I and II coatomer. J Cell Biol *140*, 751-765.

Donaldson, J.G., Cassel, D., Kahn, R.A., and Klausner, R.D. (1992). ADP-ribosylation factor, a small GTP-binding protein, is required for binding of the coatomer protein beta-COP to Golgi membranes. Proc Natl Acad Sci U S A *89*, 6408-6412.

Donaldson, J.G., and Jackson, C.L. (2000). Regulators and effectors of the ARF GTPases. Curr Opin Cell Biol *12*, 475-482.

Dower, W.J., Miller, J.F., and Ragsdale, C.W. (1988). High efficiency transformation of E. coli by high voltage electroporation. Nucleic Acids Res *16*, 6127-6145.

Drake, M.T., Zhu, Y., and Kornfeld, S. (2000). The assembly of AP-3 adaptor complex-containing clathrin-coated vesicles on synthetic liposomes. Mol Biol Cell *11*, 3723-3736.

Espenshade, P., Gimeno, R.E., Holzmacher, E., Teung, P., and Kaiser, C.A. (1995). Yeast SEC16 gene encodes a multidomain vesicle coat protein that interacts with Sec23p. J Cell Biol *131*, 311-324.

Estojak, J., Brent, R., and Golemis, E.A. (1995). Correlation of two-hybrid affinity data with in vitro measurements. Mol Cell Biol *15*, 5820-5829.

Eugster, A., Frigerio, G., Dale, M., and Duden, R. (2000). COP I domains required for coatomer integrity, and novel interactions with ARF and ARF-GAP. Embo J *19*, 3905-3917.

Fairbanks, G., Steck, T.L., and Wallach, D.F. (1971). Electrophoretic analysis of the major polypeptides of the human erythrocyte membrane. Biochemistry *10*, 2606-2617.

Franzusoff, A., Lauze, E., and Howell, K.E. (1992). Immuno-isolation of Sec7p-coated transport vesicles from the yeast secretory pathway. Nature *355*, 173-175.

Fucini, R.V., Navarrete, A., Vadakkan, C., Lacomis, L., Erdjument-Bromage, H., Tempst, P., and Stamnes, M. (2000). Activated ADP-ribosylation factor assembles distinct pools of actin on golgi membranes. J Biol Chem *275*, 18824-18829.

Fujita, A., Lord, M., Hiroko, T., Hiroko, F., Chen, T., Oka, C., Misumi, Y., and Chant, J. (2004). Rax1, a protein required for the establishment of the bipolar budding pattern in yeast. Gene *327*, 161-169.

Fullekrug, J., Suganuma, T., Tang, B.L., Hong, W., Storrie, B., and Nilsson, T. (1999). Localization and recycling of gp27 (hp24gamma3): complex formation with other p24 family members. Mol Biol Cell *10*, 1939-1955.

Gavin, A.C., Bosche, M., Krause, R., Grandi, P., Marzioch, M., Bauer, A., Schultz, J., Rick, J.M., Michon, A.M., Cruciat, C.M., Remor, M., Hofert, C., Schelder, M., Brajenovic, M., Ruffner, H., Merino, A., Klein, K., Hudak, M., Dickson, D., Rudi, T., Gnau, V., Bauch, A., Bastuck, S., Huhse, B., Leutwein, C., Heurtier, M.A., Copley, R.R., Edelmann, A., Querfurth, E., Rybin, V., Drewes, G., Raida, M., Bouwmeester, T., Bork, P., Seraphin, B., Kuster, B., Neubauer, G., and Superti-Furga, G. (2002). Functional organization of the yeast proteome by systematic analysis of protein complexes. Nature *415*, 141-147.

Gaynor, E.C., Chen, C.Y., Emr, S.D., and Graham, T.R. (1998). ARF is required for maintenance of yeast Golgi and endosome structure and function. Mol Biol Cell *9*, 653-670.

Gietz, R.D., Schiestl, R.H., Willems, A.R., and Woods, R.A. (1995). Studies on the transformation of intact yeast cells by the LiAc/SS-DNA/PEG procedure. Yeast *11*, 355-360.

Godi, A., Pertile, P., Meyers, R., Marra, P., Di Tullio, G., Iurisci, C., Luini, A., Corda, D., and De Matteis, M.A. (1999). ARF mediates recruitment of PtdIns-4-OH kinase-beta and stimulates synthesis of PtdIns(4,5)P2 on the Golgi complex. Nat Cell Biol *1*, 280-287.

Goldberg, J. (1998). Structural basis for activation of ARF GTPase: mechanisms of guanine nucleotide exchange and GTP-myristoyl switching. Cell *95*, 237-248.

Goldberg, J. (1999). Structural and functional analysis of the ARF1-ARFGAP complex reveals a role for coatomer in GTP hydrolysis. Cell *96*, 893-902.

Goldberg, J. (2000). Decoding of sorting signals by coatomer through a GTPase switch in the COPI coat complex. Cell *100*, 671-679.

Golemis, E.A., and Khazak, V. (1997). Alternative yeast two-hybrid systems. The interaction trap and interaction mating. Methods Mol Biol *63*, 197-218.

Gommel, D., Orci, L., Emig, E.M., Hannah, M.J., Ravazzola, M., Nickel, W., Helms, J.B., Wieland, F.T., and Sohn, K. (1999). p24 and p23, the major transmembrane proteins of COPI-coated transport vesicles, form hetero-oligomeric complexes and cycle between the organelles of the early secretory pathway. FEBS Lett *447*, 179-185.

Gommel, D.U., Memon, A.R., Heiss, A., Lottspeich, F., Pfannstiel, J., Lechner, J., Reinhard, C., Helms, J.B., Nickel, W., and Wieland, F.T. (2001). Recruitment to Golgi membranes of ADP-ribosylation factor 1 is mediated by the cytoplasmic domain of p23. Embo J *20*, 6751-6760.

Gonsalvez, G.B., Lehmann, K.A., Ho, D.K., Stanitsa, E.S., Williamson, J.R., and Long, R.M. (2003). RNA-protein interactions promote asymmetric sorting of the ASH1 mRNA ribonucleoprotein complex. RNA *9*, 1383-1399.

Gonzalez, I., Buonomo, S.B., Nasmyth, K., and von Ahsen, U. (1999). ASH1 mRNA localization in yeast involves multiple secondary structural elements and Ash1 protein translation. Curr Biol *9*, 337-340.

Graham, T.R., and Emr, S.D. (1991). Compartmental organization of Golgi-specific protein modification and vacuolar protein sorting events defined in a yeast sec18 (NSF) mutant. J Cell Biol *114*, 207-218.

Greasley, S.E., Jhoti, H., Teahan, C., Solari, R., Fensome, A., Thomas, G.M., Cockcroft, S., and Bax, B. (1995). The structure of rat ADP-ribosylation factor-1 (ARF-1) complexed to GDP determined from two different crystal forms. Nat Struct Biol *2*, 797-806.

Gruenberg, J. (2001). The endocytic pathway: a mosaic of domains. Nat Rev Mol Cell Biol *2*, 721-730.

Gueldener, U., Heinisch, J., Koehler, G.J., Voss, D., and Hegemann, J.H. (2002). A second set of loxP marker cassettes for Cre-mediated multiple gene knockouts in budding yeast. Nucleic Acids Res *30*, e23.

Guldener, U., Heck, S., Fielder, T., Beinhauer, J., and Hegemann, J.H. (1996). A new efficient gene disruption cassette for repeated use in budding yeast. Nucleic Acids Res *24*, 2519-2524.

Hampsey, M. (1997). A review of phenotypes in Saccharomyces cerevisiae. Yeast *13*, 1099-1133.

Hara-Kuge, S., Kuge, O., Orci, L., Amherdt, M., Ravazzola, M., Wieland, F.T., and Rothman, J.E. (1994). En bloc incorporation of coatomer subunits during the assembly of COP-coated vesicles. J Cell Biol *124*, 883-892.

Harkins, H.A., Page, N., Schenkman, L.R., De Virgilio, C., Shaw, S., Bussey, H., and Pringle, J.R. (2001). Bud8p and Bud9p, proteins that may mark the sites for bipolar budding in yeast. Mol Biol Cell *12*, 2497-2518.

Harlow, E., and Lane, D. (1988). Antibodies: A Laboratory Manual. Cold Spring Harbor Laboratory.

Harter, C., Pavel, J., Coccia, F., Draken, E., Wegehingel, S., Tschochner, H., and Wieland, F. (1996). Nonclathrin coat protein gamma, a subunit of coatomer, binds to the cytoplasmic dilysine motif of membrane proteins of the early secretory pathway. Proc Natl Acad Sci U S A *93*, 1902-1906.

Hirst, J., Bright, N.A., Rous, B., and Robinson, M.S. (1999). Characterization of a fourth adaptor-related protein complex. Mol Biol Cell *10*, 2787-2802.

Hoffman, C.S., and Winston, F. (1987). A ten-minute DNA preparation from yeast efficiently releases autonomous plasmids for transformation of Escherichia coli. Gene *57*, 267-272.

Honda, A., Nogami, M., Yokozeki, T., Yamazaki, M., Nakamura, H., Watanabe, H., Kawamoto, K., Nakayama, K., Morris, A.J., Frohman, M.A., and Kanaho, Y. (1999). Phosphatidylinositol 4-phosphate 5-kinase alpha is a downstream effector of the small G protein ARF6 in membrane ruffle formation. Cell *99*, 521-532.

Huh, W.K., Falvo, J.V., Gerke, L.C., Carroll, A.S., Howson, R.W., Weissman, J.S., and O'Shea, E.K. (2003). Global analysis of protein localization in budding yeast. Nature *425*, 686-691.

Huxley, C., Green, E.D., and Dunham, I. (1990). Rapid assessment of S. cerevisiae mating type by PCR. Trends Genet *6*, 236.

Ireland, L.S., Johnston, G.C., Drebot, M.A., Dhillon, N., DeMaggio, A.J., Hoekstra, M.F., and Singer, R.A. (1994). A member of a novel family of yeast 'zn-finger' proteins mediates the transition from stationary phase to cell proliferation. Embo J *13*, 3812-3821.

Irie, K., Tadauchi, T., Takizawa, P.A., Vale, R.D., Matsumoto, K., and Herskowitz, I. (2002). The Khd1 protein, which has three KH RNA-binding motifs, is required for proper localization of ASH1 mRNA in yeast. Embo J *21*, 1158-1167.

IUPAC-IUB Joint Commission on Biochemical Nomenclature (JCBN) (1984). Nomenclature and symbolism for amino acids and peptides. Recommendations 1983 [published erratum appears in Eur J Biochem 1993 Apr 1;213(1):2]. Eur J Biochem *138*, 9-37.

Jackson, C.L., and Casanova, J.E. (2000). Turning on ARF: the Sec7 family of guanine-nucleotide-exchange factors. Trends Cell Biol *10*, 60-67.

Jackson, C.L., and Kepes, F. (1994). BFR1, a multicopy suppressor of brefeldin A-induced lethality, is implicated in secretion and nuclear segregation in Saccharomyces cerevisiae. Genetics *137*, 423-437.

Jacques, K.M., Nie, Z., Stauffer, S., Hirsch, D.S., Chen, L.X., Stanley, K.T., and Randazzo, P.A. (2002). Arf1 dissociates from the clathrin adaptor GGA prior to being inactivated by Arf GTPase-activating proteins. J Biol Chem *277*, 47235-47241.

Jahn, R., Lang, T., and Sudhof, T.C. (2003). Membrane fusion. Cell *112*, 519-533.

Jenne, N., Frey, K., Brugger, B., and Wieland, F.T. (2002). Oligomeric state and stoichiometry of p24 proteins in the early secretory pathway. J Biol Chem *277*, 46504-46511.

Jones, A.T., Spiro, D.J., Kirchhausen, T., Melancon, P., and Wessling-Resnick, M. (1999a). Studies on the inhibition of endosome fusion by GTPgammaS-bound ARF. J Cell Sci *112 (Pt 20)*, 3477-3485.

Jones, D.H., Bax, B., Fensome, A., and Cockcroft, S. (1999b). ADP ribosylation factor 1 mutants identify a phospholipase D effector region and reveal that phospholipase D participates in lysosomal secretion but is not sufficient for recruitment of coatomer I. Biochem J *341 (Pt 1)*, 185-192.

Jones, D.H., Morris, J.B., Morgan, C.P., Kondo, H., Irvine, R.F., and Cockcroft, S. (2000). Type I phosphatidylinositol 4-phosphate 5-kinase directly interacts with ADP-ribosylation factor 1 and is responsible for phosphatidylinositol 4,5-bisphosphate synthesis in the golgi compartment. J Biol Chem *275*, 13962-13966.

Jones, S., Jedd, G., Kahn, R.A., Franzusoff, A., Bartolini, F., and Segev, N. (1999c). Genetic interactions in yeast between Ypt GTPases and Arf guanine nucleotide exchangers. Genetics *152*, 1543-1556.

Kahn, R.A., Clark, J., Rulka, C., Stearns, T., Zhang, C.J., Randazzo, P.A., Terui, T., and Cavenagh, M. (1995). Mutational analysis of Saccharomyces cerevisiae ARF1. J Biol Chem *270*, 143-150.

Kahn, R.A., and Gilman, A.G. (1984). Purification of a protein cofactor required for ADP-ribosylation of the stimulatory regulatory component of adenylate cyclase by cholera toxin. J Biol Chem *259*, 6228-6234.

Kahn, R.A., and Gilman, A.G. (1986). The protein cofactor necessary for ADP-ribosylation of Gs by cholera toxin is itself a GTP binding protein. J Biol Chem *261*, 7906-7911.

Kaiser, C. (2000). Thinking about p24 proteins and how transport vesicles select their cargo. Proc Natl Acad Sci U S A *97*, 3783-3785.

Katzmann, D.J., Odorizzi, G., and Emr, S.D. (2002). Receptor downregulation and multivesicular-body sorting. Nat Rev Mol Cell Biol *3*, 893-905.

Kirchhausen, T. (2000). Three ways to make a vesicle. Nat Rev Mol Cell Biol *1*, 187-198.

Kirchhausen, T., and Harrison, S.C. (1981). Protein organization in clathrin trimers. Cell *23*, 755-761.

Kleijmeer, M., Ramm, G., Schuurhuis, D., Griffith, J., Rescigno, M., Ricciardi-Castagnoli, P., Rudensky, A.Y., Ossendorp, F., Melief, C.J., Stoorvogel, W., and Geuze, H.J. (2001). Reorganization of multivesicular bodies regulates MHC class II antigen presentation by dendritic cells. J Cell Biol *155*, 53-63.

Knop, M., Siegers, K., Pereira, G., Zachariae, W., Winsor, B., Nasmyth, K., and Schiebel, E. (1999). Epitope tagging of yeast genes using a PCR-based strategy: more tags and improved practical routines. Yeast *15*, 963-972.

Krugmann, S., Anderson, K.E., Ridley, S.H., Risso, N., McGregor, A., Coadwell, J., Davidson, K., Eguinoa, A., Ellson, C.D., Lipp, P., Manifava, M., Ktistakis, N., Painter, G., Thuring, J.W., Cooper, M.A., Lim, Z.Y., Holmes, A.B., Dove, S.K., Michell, R.H., Grewal, A., Nazarian, A., Erdjument-Bromage, H., Tempst, P., Stephens, L.R., and Hawkins, P.T. (2002). Identification of ARAP3, a novel PI3K effector regulating both Arf and Rho GTPases, by selective capture on phosphoinositide affinity matrices. Mol Cell *9*, 95-108.

Kruse, C., Jaedicke, A., Beaudouin, J., Bohl, F., Ferring, D., Guttler, T., Ellenberg, J., and Jansen, R.P. (2002). Ribonucleoprotein-dependent localization of the yeast class V myosin Myo4p. J Cell Biol *159*, 971-982.

Ktistakis, N.T., Brown, H.A., Waters, M.G., Sternweis, P.C., and Roth, M.G. (1996). Evidence that phospholipase D mediates ADP ribosylation factor-dependent formation of Golgi coated vesicles. J Cell Biol *134*, 295-306.

Kuai, J., Boman, A.L., Arnold, R.S., Zhu, X., and Kahn, R.A. (2000). Effects of activated ADP-ribosylation factors on Golgi morphology require neither activation of phospholipase D1 nor recruitment of coatomer. J Biol Chem *275*, 4022-4032.

Kyhse-Andersen, J. (1984). Electroblotting of multiple gels: a simple apparatus without buffer tank for rapid transfer of proteins from polyacrylamide to nitrocellulose. J Biochem Biophys Methods *10*, 203-209.

Laemmli, U.K. (1970). Cleavage of structural proteins during the assembly of the head of bacteriophage T4. Nature *227*, 680-685.

Lang, B.D., and Fridovich-Keil, J.L. (2000). Scp160p, a multiple KH-domain protein, is a component of mRNP complexes in yeast. Nucleic Acids Res *28*, 1576-1584.

Lang, B.D., Li, A., Black-Brewster, H.D., and Fridovich-Keil, J.L. (2001). The brefeldin A resistance protein Bfr1p is a component of polyribosome-associated mRNP complexes in yeast. Nucleic Acids Res *29*, 2567-2574.

Lanoix, J., Ouwendijk, J., Lin, C.C., Stark, A., Love, H.D., Ostermann, J., and Nilsson, T. (1999). GTP hydrolysis by arf-1 mediates sorting and concentration of Golgi resident enzymes into functional COP I vesicles. Embo J *18*, 4935-4948.

Lassing, I., and Lindberg, U. (1985). Specific interaction between phosphatidylinositol 4,5-bisphosphate and profilactin. Nature *314*, 472-474.

Lederkremer, G.Z., Cheng, Y., Petre, B.M., Vogan, E., Springer, S., Schekman, R., Walz, T., and Kirchhausen, T. (2001). Structure of the Sec23p/24p and Sec13p/31p complexes of COPII. Proc Natl Acad Sci U S A *98*, 10704-10709.

Lee, C.M., Chang, P.P., Tsai, S.C., Adamik, R., Price, S.R., Kunz, B.C., Moss, J., Twiddy, E.M., and Holmes, R.K. (1991). Activation of Escherichia coli heat-labile enterotoxins by native and recombinant adenosine diphosphate-ribosylation factors, 20-kD guanine nucleotide-binding proteins. J Clin Invest *87*, 1780-1786.

Lerner, R.S., Seiser, R.M., Zheng, T., Lager, P.J., Reedy, M.C., Keene, J.D., and Nicchitta, C.V. (2003). Partitioning and translation of mRNAs encoding soluble proteins on membrane-bound ribosomes. Rna *9*, 1123-1137.

Lewis, S.M., Poon, P.P., Singer, R.A., Johnston, G.C., and Spang, A. (2004). The ArfGAP Glo3 Is Required for the Generation of COPI Vesicles. Mol Biol Cell.

Lodish, H., Berk, A., Matsudeira, P., Kaiser, C.A., Krieger, M., Scott, P.M., Zipursky, S.L., and Darnell, J. (2003). Molecular Cell Biology. W. H. Freeman and Company.

Long, R.M., Gu, W., Lorimer, E., Singer, R.H., and Chartrand, P. (2000). She2p is a novel RNA-binding protein that recruits the Myo4p-She3p complex to ASH1 mRNA. Embo J *19*, 6592-6601.

Long, R.M., Singer, R.H., Meng, X., Gonzalez, I., Nasmyth, K., and Jansen, R.P. (1997). Mating type switching in yeast controlled by asymmetric localization of ASH1 mRNA. Science *277*, 383-387.

Lord, M., Chen, T., Fujita, A., and Chant, J. (2002). Analysis of budding patterns. Methods Enzymol *350*, 131-141.

Lorra, C., and Huttner, W.B. (1999). The mesh hypothesis of Golgi dynamics. Nat Cell Biol *1*, E113-115.

Lowry, O.H., Rosebrough, N.J., Farr, A.L., and Randall, R.J. (1951). Protein measurement with the Folin phenol reagent. J Biol Chem *193*, 265-275.

Majoul, I., Straub, M., Hell, S.W., Duden, R., and Soling, H.D. (2001). KDEL-cargo regulates interactions between proteins involved in COPI vesicle traffic: measurements in living cells using FRET. Dev Cell *1*, 139-153.

Malsam, J., Gommel, D., Wieland, F.T., and Nickel, W. (1999). A role for ADP ribosylation factor in the control of cargo uptake during COPI-coated vesicle biogenesis. FEBS Lett *462*, 267-272.

Marzioch, M., Henthorn, D.C., Herrmann, J.M., Wilson, R., Thomas, D.Y., Bergeron, J.J., Solari, R.C., and Rowley, A. (1999). Erp1p and Erp2p, partners for Emp24p and Erv25p in a yeast p24 complex. Mol Biol Cell *10*, 1923-1938.

Matiach, A., and Schroder-Kohne, S. (2001). Yeast cys3 and gsh1 mutant cells display overlapping but non-identical symptoms of oxidative stress with regard to subcellular protein localization and CDP-DAG metabolism. Mol Genet Genomics *266*, 481-496.

Matsuoka, K., Orci, L., Amherdt, M., Bednarek, S.Y., Hamamoto, S., Schekman, R., and Yeung, T. (1998). COPII-coated vesicle formation reconstituted with purified coat proteins and chemically defined liposomes. Cell *93*, 263-275.

McBride, H.J., Sil, A., Measday, V., Yu, Y., Moffat, J., Maxon, M.E., Herskowitz, I., Andrews, B., and Stillman, D.J. (2001). The protein kinase Pho85 is required for asymmetric accumulation of the Ash1 protein in Saccharomyces cerevisiae. Mol Microbiol *42*, 345-353.

Meyer, T.S., and Lamberts, B.L. (1965). Use of coomassie brilliant blue R250 for the electrophoresis of microgram quantities of parotid saliva proteins on acrylamide-gel strips. Biochim Biophys Acta *107*, 144-145.

Millar, C.A., Powell, K.A., Hickson, G.R., Bader, M.F., and Gould, G.W. (1999). Evidence for a role for ADP-ribosylation factor 6 in insulin-stimulated glucose transporter-4 (GLUT4) trafficking in 3T3-L1 adipocytes. J Biol Chem *274*, 17619-17625.

Miller, E.A., Beilharz, T.H., Malkus, P.N., Lee, M.C., Hamamoto, S., Orci, L., and Schekman, R. (2003). Multiple cargo binding sites on the COPII subunit Sec24p ensure capture of diverse membrane proteins into transport vesicles. Cell *114*, 497-509.

Miura, K., Jacques, K.M., Stauffer, S., Kubosaki, A., Zhu, K., Hirsch, D.S., Resau, J., Zheng, Y., and Randazzo, P.A. (2002). ARAP1: a point of convergence for Arf and Rho signaling. Mol Cell *9*, 109-119.

Mizuta, K., and Warner, J.R. (1994). Continued functioning of the secretory pathway is essential for ribosome synthesis. Mol Cell Biol *14*, 2493-2502.

Morinaga, N., Tsai, S.C., Moss, J., and Vaughan, M. (1996). Isolation of a brefeldin A-inhibited guanine nucleotide-exchange protein for ADP ribosylation factor (ARF) 1 and ARF3 that contains a Sec7-like domain. Proc Natl Acad Sci U S A *93*, 12856-12860.

Mossessova, E., Bickford, L.C., and Goldberg, J. (2003). SNARE selectivity of the COPII coat. Cell *114*, 483-495.

Mullis, K., Faloona, F., Scharf, S., Saiki, R., Horn, G., and Erlich, H. (1986). Specific enzymatic amplification of DNA in vitro: the polymerase chain reaction. Cold Spring Harb Symp Quant Biol *51 Pt 1*, 263-273.

Mumberg, D., Muller, R., and Funk, M. (1995). Yeast vectors for the controlled expression of heterologous proteins in different genetic backgrounds. Gene *156*, 119-122.

Munchow, S., Sauter, C., and Jansen, R.P. (1999). Association of the class V myosin Myo4p with a localised messenger RNA in budding yeast depends on She proteins. J Cell Sci *112 (Pt 10)*, 1511-1518.

Muniz, M., Nuoffer, C., Hauri, H.P., and Riezman, H. (2000). The Emp24 complex recruits a specific cargo molecule into endoplasmic reticulum-derived vesicles. J Cell Biol *148*, 925-930.

Ni, L., and Snyder, M. (2001). A genomic study of the bipolar bud site selection pattern in Saccharomyces cerevisiae. Mol Biol Cell *12*, 2147-2170.

Nicchitta, C.V. (2002). A platform for compartmentalized protein synthesis: protein translation and translocation in the ER. Curr Opin Cell Biol *14*, 412-416.

Nickel, W., Malsam, J., Gorgas, K., Ravazzola, M., Jenne, N., Helms, J.B., and Wieland, F.T. (1998). Uptake by COPI-coated vesicles of both anterograde and retrograde cargo is inhibited by GTPgammaS in vitro. J Cell Sci *111 (Pt 20)*, 3081-3090.

Nie, Z., Hirsch, D.S., and Randazzo, P.A. (2003). Arf and its many interactors. Curr Opin Cell Biol *15*, 396-404.

Novick, P., Ferro, S., and Schekman, R. (1981). Order of events in the yeast secretory pathway. Cell *25*, 461-469.

Novick, P., Field, C., and Schekman, R. (1980). Identification of 23 complementation groups required for post-translational events in the yeast secretory pathway. Cell *21*, 205-215.

Ooi, C.E., Dell'Angelica, E.C., and Bonifacino, J.S. (1998). ADP-Ribosylation factor 1 (ARF1) regulates recruitment of the AP-3 adaptor complex to membranes. J Cell Biol *142*, 391-402.

Ornstein, L. (1964). Disc Electrophoresis. I. Background and Theory. Ann N Y Acad Sci *121*, 321-349.

Palade, G. (1975). Intracellular aspects of the process of protein synthesis. Science *189*, 347-358.

Palmer, D.J., Helms, J.B., Beckers, C.J., Orci, L., and Rothman, J.E. (1993). Binding of coatomer to Golgi membranes requires ADP-ribosylation factor. J Biol Chem *268*, 12083-12089.

Pasqualato, S., Renault, L., and Cherfils, J. (2002). Arf, Arl, Arp and Sar proteins: a family of GTP-binding proteins with a structural device for 'front-back' communication. EMBO Rep *3*, 1035-1041.

Payne, G.S., Baker, D., van Tuinen, E., and Schekman, R. (1988). Protein transport to the vacuole and receptor-mediated endocytosis by clathrin heavy chain-deficient yeast. J Cell Biol *106*, 1453-1461.

Pearse, B.M. (1975). Coated vesicles from pig brain: purification and biochemical characterization. J Mol Biol *97*, 93-98.

Pelham, H.R. (2001). Traffic through the Golgi apparatus. J Cell Biol *155*, 1099-1101.

Pelham, H.R. (2002). Insights from yeast endosomes. Curr Opin Cell Biol *14*, 454-462.

Perkins, D.N., Pappin, D.J., Creasy, D.M., and Cottrell, J.S. (1999). Probability-based protein identification by searching sequence databases using mass spectrometry data. Electrophoresis *20*, 3551-3567.

Peyroche, A., Antonny, B., Robineau, S., Acker, J., Cherfils, J., and Jackson, C.L. (1999). Brefeldin A acts to stabilize an abortive ARF-GDP-Sec7 domain protein complex: involvement of specific residues of the Sec7 domain. Mol Cell *3*, 275-285.

Peyroche, A., and Jackson, C.L. (2001). Functional analysis of ADP-ribosylation factor (ARF) guanine nucleotide exchange factors Gea1p and Gea2p in yeast. Methods Enzymol *329*, 290-300.

Peyroche, A., Paris, S., and Jackson, C.L. (1996). Nucleotide exchange on ARF mediated by yeast Gea1 protein. Nature *384*, 479-481.

Pfeffer, S.R. (2001). Membrane transport: retromer to the rescue. Curr Biol *11*, R109-111.

Poon, P.P., Cassel, D., Spang, A., Rotman, M., Pick, E., Singer, R.A., and Johnston, G.C. (1999). Retrograde transport from the yeast Golgi is mediated by two ARF GAP proteins with overlapping function. Embo J *18*, 555-564.

Poon, P.P., Nothwehr, S.F., Singer, R.A., and Johnston, G.C. (2001). The Gcs1 and Age2 ArfGAP proteins provide overlapping essential function for transport from the yeast trans-Golgi network. J Cell Biol *155*, 1239-1250.

Potter, M.D., and Nicchitta, C.V. (2000). Regulation of ribosome detachment from the mammalian endoplasmic reticulum membrane. J Biol Chem *275*, 33828-33835.

Potter, M.D., Seiser, R.M., and Nicchitta, C.V. (2001). Ribosome exchange revisited: a mechanism for translation-coupled ribosome detachment from the ER membrane. Trends Cell Biol *11*, 112-115.

Pratchett, T., Stewart, I., and Cohen, J. (2002). The Science of Discworld. Ebury Press.

Pringle, J.R., Adams, A.E., Drubin, D.G., and Haarer, B.K. (1991). Immunofluorescence methods for yeast. Methods Enzymol *194*, 565-602.

Puertollano, R., Randazzo, P.A., Presley, J.F., Hartnell, L.M., and Bonifacino, J.S. (2001). The GGAs promote ARF-dependent recruitment of clathrin to the TGN. Cell *105*, 93-102.

Rad, M.R., Phan, H.L., Kirchrath, L., Tan, P.K., Kirchhausen, T., Hollenberg, C.P., and Payne, G.S. (1995). Saccharomyces cerevisiae Apl2p, a homologue of the mammalian clathrin AP beta subunit, plays a role in clathrin-dependent Golgi functions. J Cell Sci *108 (Pt 4)*, 1605-1615.

Randazzo, P.A., and Hirsch, D.S. (2004). Arf GAPs: multifunctional proteins that regulate membrane traffic and actin remodelling. Cell Signal *16*, 401-413.

Randazzo, P.A., Nie, Z., Miura, K., and Hsu, V.W. (2000). Molecular aspects of the cellular activities of ADP-ribosylation factors. Sci STKE *2000*, RE1.

Randazzo, P.A., Weiss, O., and Kahn, R.A. (1992). Preparation of recombinant ADP-ribosylation factor. Methods Enzymol *219*, 362-369.

Rein, U., Andag, U., Duden, R., Schmitt, H.D., and Spang, A. (2002). ARF-GAP-mediated interaction between the ER-Golgi v-SNAREs and the COPI coat. J Cell Biol *157*, 395-404.

Reinhard, C., Schweikert, M., Wieland, F.T., and Nickel, W. (2003). Functional reconstitution of COPI coat assembly and disassembly using chemically defined components. Proc Natl Acad Sci U S A *100*, 8253-8257.

Roberg, K.J., Crotwell, M., Espenshade, P., Gimeno, R., and Kaiser, C.A. (1999). LST1 is a SEC24 homologue used for selective export of the plasma membrane ATPase from the endoplasmic reticulum. J Cell Biol *145*, 659-672.

Roberg, K.J., Rowley, N., and Kaiser, C.A. (1997). Physiological regulation of membrane protein sorting late in the secretory pathway of Saccharomyces cerevisiae. J Cell Biol *137*, 1469-1482.

Robinson, M.S., and Bonifacino, J.S. (2001). Adaptor-related proteins. Curr Opin Cell Biol *13*, 444-453.

Roth, T.F., and Porter, K.R. (1964). Yolk Protein Uptake in the Oocyte of the Mosquito Aedes Aegypti. L. J Cell Biol *20*, 313-332.

Rothman, J.E., and Schmid, S.L. (1986). Enzymatic recycling of clathrin from coated vesicles. Cell *46*, 5-9.

Rudge, S.A., Cavenagh, M.M., Kamath, R., Sciorra, V.A., Morris, A.J., Kahn, R.A., and Engebrecht, J. (1998). ADP-Ribosylation factors do not activate yeast phospholipase Ds but are required for sporulation. Mol Biol Cell *9*, 2025-2036.

Sambrook, J., Fritsch, E.F., and Maniatis, T. (1989). Molecular cloning: A Laboratory Manual. Second Edition. Cold Spring Habor Laboratory Press.

Sandmann, T., Herrmann, J.M., Dengjel, J., Schwarz, H., and Spang, A. (2003). Suppression of coatomer mutants by a new protein family with COPI and COPII binding motifs in Saccharomyces cerevisiae. Mol Biol Cell *14*, 3097-3113.

Sandvig, K., and van Deurs, B. (2002). Transport of protein toxins into cells: pathways used by ricin, cholera toxin and Shiga toxin. FEBS Lett *529*, 49-53.

Sanger, F., Nicklen, S., and Coulson, A.R. (1977). DNA sequencing with chain-terminating inhibitors. Proc Natl Acad Sci U S A *74*, 5463-5467.

Santos, B., Duran, A., and Valdivieso, M.H. (1997). CHS5, a gene involved in chitin synthesis and mating in Saccharomyces cerevisiae. Mol Cell Biol *17*, 2485-2496.

Santos, B., and Snyder, M. (1997). Targeting of chitin synthase 3 to polarized growth sites in yeast requires Chs5p and Myo2p. J Cell Biol *136*, 95-110.

Santos, B., and Snyder, M. (2003). Specific protein targeting during cell differentiation: polarized localization of Fus1p during mating depends on Chs5p in Saccharomyces cerevisiae. Eukaryot Cell *2*, 821-825.

Schagger, H. (2001). Blue-native gels to isolate protein complexes from mitochondria. Methods Cell Biol *65*, 231-244.

Schagger, H., and von Jagow, G. (1991). Blue native electrophoresis for isolation of membrane protein complexes in enzymatically active form. Anal Biochem *199*, 223-231.

Schenkman, L.R., Caruso, C., Page, N., and Pringle, J.R. (2002). The role of cell cycle-regulated expression in the localization of spatial landmark proteins in yeast. J Cell Biol *156*, 829-841.

Schimmoller, F., Singer-Kruger, B., Schroder, S., Kruger, U., Barlowe, C., and Riezman, H. (1995). The absence of Emp24p, a component of ER-derived COPII-coated vesicles, causes a defect in transport of selected proteins to the Golgi. Embo J *14*, 1329-1339.

Serafini, T., Orci, L., Amherdt, M., Brunner, M., Kahn, R.A., and Rothman, J.E. (1991). ADP-ribosylation factor is a subunit of the coat of Golgi-derived COP-coated vesicles: a novel role for a GTP-binding protein. Cell *67*, 239-253.

Sever, S. (2002). Dynamin and endocytosis. Curr Opin Cell Biol *14*, 463-467.

Sewell, J.L., and Kahn, R.A. (1988). Sequences of the bovine and yeast ADP-ribosylation factor and comparison to other GTP-binding proteins. Proc Natl Acad Sci U S A *85*, 4620-4624.

Shepard, K.A., Gerber, A.P., Jambhekar, A., Takizawa, P.A., Brown, P.O., Herschlag, D., DeRisi, J.L., and Vale, R.D. (2003). Widespread cytoplasmic mRNA transport in yeast: identification of 22 bud-localized transcripts using DNA microarray analysis. Proc Natl Acad Sci U S A *100*, 11429-11434.

Sherman, F. (1991). Getting started with yeast. Methods Enzymol *194*, 3-21.

Sherman, F., and Hicks, J. (1991). Micromanipulation and dissection of asci. Methods Enzymol *194*, 21-37.

Shevchenko, A., Wilm, M., Vorm, O., and Mann, M. (1996). Mass spectrometric sequencing of proteins silver-stained polyacrylamide gels. Anal Chem *68*, 850-858.

Shimoni, Y., Kurihara, T., Ravazzola, M., Amherdt, M., Orci, L., and Schekman, R. (2000). Lst1p and Sec24p cooperate in sorting of the plasma membrane ATPase into COPII vesicles in Saccharomyces cerevisiae. J Cell Biol *151*, 973-984.

Shin, O.H., Couvillon, A.D., and Exton, J.H. (2001). Arfophilin is a common target of both class II and class III ADP-ribosylation factors. Biochemistry *40*, 10846-10852.

Sickmann, A., Reinders, J., Wagner, Y., Joppich, C., Zahedi, R., Meyer, H.E., Schonfisch, B., Perschil, I., Chacinska, A., Guiard, B., Rehling, P., Pfanner, N., and Meisinger, C. (2003). The proteome of Saccharomyces cerevisiae mitochondria. Proc Natl Acad Sci U S A *100*, 13207-13212.

Sikorski, R.S., and Hieter, P. (1989). A system of shuttle vectors and yeast host strains designed for efficient manipulation of DNA in Saccharomyces cerevisiae. Genetics *122*, 19-27.

Skippen, A., Jones, D.H., Morgan, C.P., Li, M., and Cockcroft, S. (2002). Mechanism of ADP ribosylation factor-stimulated phosphatidylinositol 4,5-bisphosphate synthesis in HL60 cells. J Biol Chem *277*, 5823-5831.

Smith, A.E., and Helenius, A. (2004). How viruses enter animal cells. Science *304*, 237-242.

Smith, P.K., Krohn, R.I., Hermanson, G.T., Mallia, A.K., Gartner, F.H., Provenzano, M.D., Fujimoto, E.K., Goeke, N.M., Olson, B.J., and Klenk, D.C. (1985). Measurement of protein using bicinchoninic acid. Anal Biochem *150*, 76-85.

Sohn, K., Orci, L., Ravazzola, M., Amherdt, M., Bremser, M., Lottspeich, F., Fiedler, K., Helms, J.B., and Wieland, F.T. (1996). A major transmembrane protein of Golgi-derived COPI-coated vesicles involved in coatomer binding. J Cell Biol *135*, 1239-1248.

Spang, A. (2002). ARF1 regulatory factors and COPI vesicle formation. Curr Opin Cell Biol *14*, 423-427.

Spang, A., Herrmann, J.M., Hamamoto, S., and Schekman, R. (2001). The ADP ribosylation factor-nucleotide exchange factors Gea1p and Gea2p have overlapping, but not redundant functions in retrograde transport from the Golgi to the endoplasmic reticulum. Mol Biol Cell *12*, 1035-1045.

Spang, A., Matsuoka, K., Hamamoto, S., Schekman, R., and Orci, L. (1998). Coatomer, Arf1p, and nucleotide are required to bud coat protein complex I-coated vesicles from large synthetic liposomes. Proc Natl Acad Sci U S A *95*, 11199-11204.

Spang, A., and Schekman, R. (1998). Reconstitution of retrograde transport from the Golgi to the ER in vitro. J Cell Biol *143*, 589-599.

Springer, S., Chen, E., Duden, R., Marzioch, M., Rowley, A., Hamamoto, S., Merchant, S., and Schekman, R. (2000). The p24 proteins are not essential for vesicular transport in Saccharomyces cerevisiae. Proc Natl Acad Sci U S A *97*, 4034-4039.

Springer, S., and Schekman, R. (1998). Nucleation of COPII vesicular coat complex by endoplasmic reticulum to Golgi vesicle SNAREs. Science *281*, 698-700.

Springer, S., Spang, A., and Schekman, R. (1999). A primer on vesicle budding. Cell *97*, 145-148.

Stamnes, M., Schiavo, G., Stenbeck, G., Sollner, T.H., and Rothman, J.E. (1998). ADP-ribosylation factor and phosphatidic acid levels in Golgi membranes during budding of coatomer-coated vesicles. Proc Natl Acad Sci U S A *95*, 13676-13680.

Stamnes, M.A., Craighead, M.W., Hoe, M.H., Lampen, N., Geromanos, S., Tempst, P., and Rothman, J.E. (1995). An integral membrane component of coatomer-coated transport vesicles defines a family of proteins involved in budding. Proc Natl Acad Sci U S A *92*, 8011-8015.

Stamnes, M.A., and Rothman, J.E. (1993). The binding of AP-1 clathrin adaptor particles to Golgi membranes requires ADP-ribosylation factor, a small GTP-binding protein. Cell *73*, 999-1005.

Stearns, T., Kahn, R.A., Botstein, D., and Hoyt, M.A. (1990a). ADP ribosylation factor is an essential protein in Saccharomyces cerevisiae and is encoded by two genes. Mol Cell Biol *10*, 6690-6699.

Stearns, T., Willingham, M.C., Botstein, D., and Kahn, R.A. (1990b). ADP-ribosylation factor is functionally and physically associated with the Golgi complex. Proc Natl Acad Sci U S A *87*, 1238-1242.

Supek, F., Madden, D.T., Hamamoto, S., Orci, L., and Schekman, R. (2002). Sec16p potentiates the action of COPII proteins to bud transport vesicles. J Cell Biol *158*, 1029-1038.

Szafer, E., Pick, E., Rotman, M., Zuck, S., Huber, I., and Cassel, D. (2000). Role of coatomer and phospholipids in GTPase-activating protein-dependent hydrolysis of GTP by ADP-ribosylation factor-1. J Biol Chem *275*, 23615-23619.

Taheri, N., Kohler, T., Braus, G.H., and Mosch, H.U. (2000). Asymmetrically localized Bud8p and Bud9p proteins control yeast cell polarity and development. Embo J *19*, 6686-6696.

Takeya, R., Takeshige, K., and Sumimoto, H. (2000). Interaction of the PDZ domain of human PICK1 with class I ADP-ribosylation factors. Biochem Biophys Res Commun *267*, 149-155.

Takizawa, P.A., DeRisi, J.L., Wilhelm, J.E., and Vale, R.D. (2000). Plasma membrane compartmentalization in yeast by messenger RNA transport and a septin diffusion barrier. Science *290*, 341-344.

Takizawa, P.A., Sil, A., Swedlow, J.R., Herskowitz, I., and Vale, R.D. (1997). Actin-dependent localization of an RNA encoding a cell-fate determinant in yeast. Nature *389*, 90-93.

Takizawa, P.A., and Vale, R.D. (2000). The myosin motor, Myo4p, binds Ash1 mRNA via the adapter protein, She3p. Proc Natl Acad Sci U S A *97*, 5273-5278.

Tan, P.K., Davis, N.G., Sprague, G.F., and Payne, G.S. (1993). Clathrin facilitates the internalization of seven transmembrane segment receptors for mating pheromones in yeast. J Cell Biol *123*, 1707-1716.

Tanigawa, G., Orci, L., Amherdt, M., Ravazzola, M., Helms, J.B., and Rothman, J.E. (1993). Hydrolysis of bound GTP by ARF protein triggers uncoating of Golgi-derived COP-coated vesicles. J Cell Biol *123*, 1365-1371.

Tarricone, C., Xiao, B., Justin, N., Walker, P.A., Rittinger, K., Gamblin, S.J., and Smerdon, S.J. (2001). The structural basis of Arfaptin-mediated cross-talk between Rac and Arf signalling pathways. Nature *411*, 215-219.

Towbin, H., Staehelin, T., and Gordon, J. (1979). Electrophoretic transfer of proteins from polyacrylamide gels to nitrocellulose sheets: procedure and some applications. Proc Natl Acad Sci U S A *76*, 4350-4354.

Traub, L.M., Ostrom, J.A., and Kornfeld, S. (1993). Biochemical dissection of AP-1 recruitment onto Golgi membranes. J Cell Biol *123*, 561-573.

Trilla, J.A., Duran, A., and Roncero, C. (1999). Chs7p, a new protein involved in the control of protein export from the endoplasmic reticulum that is specifically engaged in the regulation of chitin synthesis in Saccharomyces cerevisiae. J Cell Biol *145*, 1153-1163.

Umebayashi, K., and Nakano, A. (2003). Ergosterol is required for targeting of tryptophan permease to the yeast plasma membrane. J Cell Biol *161*, 1117-1131.

Ungewickell, E., and Branton, D. (1981). Assembly units of clathrin coats. Nature *289*, 420-422.

Ungewickell, E., Ungewickell, H., Holstein, S.E., Lindner, R., Prasad, K., Barouch, W., Martin, B., Greene, L.E., and Eisenberg, E. (1995). Role of auxilin in uncoating clathrin-coated vesicles. Nature *378*, 632-635.

Valdivia, R.H., Baggott, D., Chuang, J.S., and Schekman, R.W. (2002). The yeast clathrin adaptor protein complex 1 is required for the efficient retention of a subset of late Golgi membrane proteins. Dev Cell *2*, 283-294.

Weiss, M., and Nilsson, T. (2003). A kinetic proof-reading mechanism for protein sorting. Traffic *4*, 65-73.

West, M.A., Bright, N.A., and Robinson, M.S. (1997). The role of ADP-ribosylation factor and phospholipase D in adaptor recruitment. J Cell Biol *138*, 1239-1254.

Wieland, F., and Harter, C. (1999). Mechanisms of vesicle formation: insights from the COP system. Curr Opin Cell Biol *11*, 440-446.

Yahara, N., Ueda, T., Sato, K., and Nakano, A. (2001). Multiple roles of Arf1 GTPase in the yeast exocytic and endocytic pathways. Mol Biol Cell *12*, 221-238.

Yang, C.Z., and Mueckler, M. (1999). ADP-ribosylation factor 6 (ARF6) defines two insulin-regulated secretory pathways in adipocytes. J Biol Chem *274*, 25297-25300.

Yang, J.S., Lee, S.Y., Gao, M., Bourgoin, S., Randazzo, P.A., Premont, R.T., and Hsu, V.W. (2002). ARFGAP1 promotes the formation of COPI vesicles, suggesting function as a component of the coat. J Cell Biol *159*, 69-78.

Yoshihisa, T., Barlowe, C., and Schekman, R. (1993). Requirement for a GTPase-activating protein in vesicle budding from the endoplasmic reticulum. Science *259*, 1466-1468.

Zahner, J.E., Harkins, H.A., and Pringle, J.R. (1996). Genetic analysis of the bipolar pattern of bud site selection in the yeast Saccharomyces cerevisiae. Mol Cell Biol *16*, 1857-1870.

Zerial, M., and McBride, H. (2001). Rab proteins as membrane organizers. Nat Rev Mol Cell Biol *2*, 107-117.

Zhang, Q., Calafat, J., Janssen, H., and Greenberg, S. (1999). ARF6 is required for growth factor- and rac-mediated membrane ruffling in macrophages at a stage distal to rac membrane targeting. Mol Cell Biol *19*, 8158-8168.

Zhao, L., Helms, J.B., Brunner, J., and Wieland, F.T. (1999). GTP-dependent binding of ADP-ribosylation factor to coatomer in close proximity to the binding site for dilysine retrieval motifs and p23. J Biol Chem *274*, 14198-14203.

Zhu, Y., Drake, M.T., and Kornfeld, S. (1999). ADP-ribosylation factor 1 dependent clathrin-coat assembly on synthetic liposomes. Proc Natl Acad Sci U S A *96*, 5013-5018.

Ziman, M., Chuang, J.S., Tsung, M., Hamamoto, S., and Schekman, R. (1998). Chs6p-dependent anterograde transport of Chs3p from the chitosome to the plasma membrane in Saccharomyces cerevisiae. Mol Biol Cell *9*, 1565-1576.

Zitvogel, L., Regnault, A., Lozier, A., Wolfers, J., Flament, C., Tenza, D., Ricciardi-Castagnoli, P., Raposo, G., and Amigorena, S. (1998). Eradication of established murine tumors using a novel cell-free vaccine: dendritic cell-derived exosomes. Nat Med *4*, 594-600.

7 Abbreviations

Ac	Acetate
AP	Adaptor protein
AP	Alkaline phosphatase
ATP	Adenosine-5’-triphosphate
BNP	Blue Native PAGE
bp	Base pairs
BSA	Bovine serum albumine
CFP	Cyan fluorescent protein
COP	Coat protein
DAPI	4',6-Diamidino-2-phenylindole dihydrochloride
DEAE	Diethylaminoethane
DMF	N,N-Dimethyleformamide
DMP	Dimethylpimelimidate
DMPC	L-α-Dimyristoylphosphatidylcholine
DMSO	Dimethylsulfoxide
DNA	Deoxyribose nucleic acid
DNase	Deoxyribonuclease
dNTPs	Deoxyribonucleotides
DTT	DL-Dithiothreitol
E. coli	*Escherichia coli*
ECL	Enhanced chemoluminesence
EDTA	Ethylenediaminetetraacetic acid
ER	Endoplasmic Reticulum
EtOH	Ethanol
FITC	Fluoresceine-isothiocyanate
5-FOA	5-Fluoro orotic acid
GAP	GTPase activating protein
GDP	Guanosine-5‘-diphosphate
GEF	Guanine nucleotide exchange factor
GFP	Green fluorescent protein
GMP-PNP	Guanosine-5'-(β,γ-imido)triphosphate
GPI	Glycosylphosphatidylinositol

GTP	Guanosine-5‘-triphosphate
GTPase	GTP hydrolase
GTPγS	Guanosine-5’-O-(3-thiotriphosphate)
HEPES	N-[2-Hydroxyethyl]piperazine-N‘-[2-ethanesulfonic acid]
HRP	Horseradish peroxidase
IPTG	Isopropyl-β-D-thiogalactopyranoside
K. lactis	*Kluyveromyces lactis*
KP_i	Potassium phosphate buffer
LB	Luria-Bertani
LDL	Low-density lipoprotein
MALDI	Matrix-assisted Laserionization/Desorption
MetOH	Methanol
MHC	Major Histocompatibility Complex
MIIC	MHC class II compartment
MOPS	3-(N-Morpholino)propanesulfonic acid
mRNA	Messenger RNA
MS	Mass spectrometry
MVB	Multi-vesicular body
NEM	N-Ethylmaleimide
NHS	N-Hydroxysuccinimide
Ni-NTA	Nickel-Nitrilotetraessigsäure
NSF	NEM-sensitive fusion factor
OD	Optical density
ORF	Open reading frame
PA	Phosphatidic acid
PAGE	Polyacrylamide-Gel-Electrophoresis
PBS	Phosphate-buffered saline
PCR	Polymerase Chain Reaction
PEG	Polyethylene glycol
PIP2	Phosphatidylinositol-bisphosphate
PLD	Phospholipase D
PMSF	Phenylmethylsulfonylfluoride
PVDF	Polyvinylidenfluoride

RNA	Ribonucleic acid
RNase	Ribonuclease
RT	Room temperature
RT-PCR	Reverse Transcription Polymerase Chain Reaction
S. cerevisiae	*Saccharomyces cerevisiae*
S. pombe	*Saccharomyces pombe*
SDS	Sodium Dodecylsulfate
SNARE	soluble NSF attachment receptor
TBS	Tris-buffered saline
TCA	Trichloro acetic acid
TEMED	N,N,N‘,N‘-Tetramethylethylenediamin
TGN	*trans*-Golgi-network
Tris	Tris(hydroxymethylaminomethane)
tRNA	transfer RNA
t-SNARE	target-SNARE
UTP	Uridine-5'-Triphosphate
v-SNARE	vesicle-SNARE
YFP	Yellow fluorescent protein

According to the suggestions of the IUPAC-IUB-commission for biological nomeclature (1984), the One-Letter- or Three-Letter code was used for amino acids .

8 Danksagung

an Dr. Anne Spang für ihre außergewöhnlich gute Betreuung meiner Arbeit an der armen kleinen GTPase. Neben ihrer Bereitschaft zur Diskussion war sie nie müde, sich auch mit Problemen an der Bench auseinander zusetzen. Ohne ihre Vision in vielerlei Hinsicht wäre diese Arbeit nicht zustande gekommen. Ihre Ratschläge, die auch über den Rahmen dieser Arbeit hinausgingen, waren immer von großer Bedeutung für mich. Ich hoffe, sie wird nicht wirklich zum Elch.

an Prof. Dr. Hans-Georg Rammensee für sein großes Interesse, seine freundliche Betreuung und die Vertretung meiner Arbeit vor der Fakultät.

an Prof. Dr. Frank Madeo für seine unkomplizierte Bereitwilligkeit, ein Zweitgutachten zu erstellen.

an Prof. Dr. Gabriele Dodt, Prof. Dr. Günter Gauglitz und PD Dr. Stefan Stevanović für ihre Bereitschaft, mich der Disputationsprüfung zu unterziehen.

an Robert-„Ich hasse Hefen“-Gauss für seine Zusammenarbeit, die sich auch auf andere Projekte erstreckte.

an Jörn Dengjel und Dr. Markus Schirle für ihre kompetenten Protein-Verdaus und massenspektrometrische Analysen.

an Mirjam Mayer für ihre exzellente Hilfe bei der Bearbeitung der vier Freunde.

an Silke Wahl für ihre große Hilfe bei den FISH-assays, nicht nur freitags.

an Rebecca Dale und Florian Seiler für unzählige Minis, Trafos, PCRs, ... und nicht zuletzt die ausgezeichneten Golgi Membranen!

an Julia Stevens und nochmals Silke Wahl, die uns allen viel Arbeit und Pflichten im Routine-Laborbetrieb abgenommen haben.

an Rahmiye Kürkçü und Christa Baradoy für ihren unermüdlichen Einsatz bei der Erfüllung unserer Wunschliste, der auch bei den ausgefallensten Platten nicht erlahmte.

an Anja Apel für ihre Southerns, die zu Northerns wurden.

an Dr. Heinz Schwarz, der mir einen Einblick in die Elektronenmikroskopie vermittelte.

An das gesamte Spang-Labor: Rebecca Dale, Melanie Diefenbacher, Robert Gauss, Faustin Kamena, Constantin Kappel, Bernd Mayer, Mirjam Mayer, Peter Nickel, Dmitry Poteryaev, Thomas Sandmann, Christina Schindler, Cornelia Schmutz, Florian Seiler, Julia Stevens, Silke Wahl.
Danke für Eure große Hilfe, Eure Diskussionsbereitschaft und das gute Laborklima!

an Prof. Dr. Enno Hartmann für seine große Diskussionsbereitschaft und seine vielen Myceten.

I would like to thank Prof. Dr. Ian G. Macara for his critical reading of our manuscripts and his attempts to teach ‚Me write pretty one dae'.

I am grateful to Prof. Dr. John Pringle for our discussions about the four friends.

I acknowledge all our collaborators for plasmids, strains and reagents: P. P. Poon, M. Swanson, R. Duden, A. Sachs, A. Nakano, K. Bloom, R. Singer, R. P. Jansen, R. Schekman, J. Pringle, M. Knop, J. Hegemann, C. Roncero, J. Cooper, and B. Glick. Without them, this thesis would have been impossible.

an meine Eltern, die mir das Biochemie-Studium ermöglicht haben.

an Claudia, für so Vieles ...

9 Akademische Lehrer

Meine akademischen Lehrer waren die Professoren und Privatdozenten:

Anatomie	K. Reutter
Analytische Chemie	S. Gaskell*
Anorganische Biochemie	U. Weser
Anorganische Chemie	K. Flower*, E. Lindner, J. Strähle
Biotechnologie	J. Gardiner*
Botanik	W.-E. Mayer
Immunologie	H.-G. Rammensee, P. Overath, S. Stevanović, H.-J. Schild, L. Stitz
Organische Chemie	G. Häfelinger, H.-P. Hagenmaier, M. Hanack, G. Jung, D. Taylor*
Mathematik	H. Pommer
Mikrobiologie	K. Poralla, W. Wohlleben
Molekularbiologie	J. Voigt
Pflanzenphysiologie	K. Wegmann
Physik	P. Grabmayer, W. Nakel
Physikalische Biochemie	K. Albert, H. Bauer, W. Voelter, S. Stoeva
Physikalische Chemie	D. Christen, G. Gauglitz, W. Göpel, H.-G. Mack, H. Oberhammer, A. Offenhäuser, U. Weimar, C. Ziegler
Physiologische Chemie	H. Bisswanger, S. Bröer, P. Bohley, R. Dringen, K. Eisele, K.-U. Fröhlich, R. Gebhardt, B. Hamprecht, W. Hoch, F. Madeo, D. Mecke, H. Probst, U. Weber, H. Wiesinger, K.-H. Wiesmüller
Zoologie	W. Pfeiffer

* während meines Studiums an der *University of Science and Technology* (UMIST), Manchester, Großbritannien

10 Publikationen

Vincent, F., Openshaw, M., **Trautwein, M.**, Gaskell, S.J., Kohn, H., and Widger, W.R.
"Rho transcription factor: symmetry and binding of bicyclomycin."
Biochemistry (2000) *39*, 9077-9083.

Trautwein, M., Gauss, R., Dengjel, J., Schirle, M., and Spang, A.
"The identification of Chs5p, Ymr237p and Yhr112p as new interactors of Arf1p."
Yeast (2003) *20* (S1), S32.

Trautwein, M., Dengjel, J., Schirle, M., and Spang, A.
"Arf1p Provides an Unexpected Link between COPI Vesicles and mRNA in *Saccharomyces cerevisiae*."
Molecular Biology of the Cell (2004) *15*, 5021-5037

Gauss, R.*, **Trautwein, M.***, Sommer, T., and Spang, A.
"New modules for the repeated internal and N-terminal epitope tagging of genes in *Saccharomyces cerevisiae*."
Yeast. Im Druck. *geteilte Autorenschaft

Trautwein, M., Gauss, R., Hartmann, E., and Spang, A.
"Evidence for involvement of the ChAPs in transport from the TGN in *Saccharomyces cerevisiae*."
Manuskript eingereicht.

Trautwein, M., Gauss, R., Dengjel, J., and Spang, A.
"Arf1p, Chs5p, and the ChAPs are required for export of specialized cargo from the Golgi."
Manuskript eingereicht.